The Syntheses, NMR and Photochromic Properties of Modified Dimehtyldihydropyrenes

Rui Zhang

B.Sc. University of Science and Technology of China, China, 1993
M.Sc. Nanyang Technological University, Singapore, 2001

A Dissertation Submitted in Partial Fulfillment of the
Requirements for the Degree of

DOCTOR OF PHILOSOPHY

in the Department of Chemistry

The Syntheses, NMR and Photochromic Properties of Modified Dimehtyldihydropyrenes

Rui Zhang

B.Sc. University of Science and Technology of China, China, 1993
M.Sc. Nanyang Technological University, Singapore, 2001

Supervisory Committee

Dr. Reginald H. Mitchell, Supervisor

(Department of Chemistry)

Dr. David J. Berg, Departmental Member

(Department of Chemistry)

Dr. Cornelia Bohne, Departmental Member

(Department of Chemistry)

Dr. Stephen V. Evans, Outside Member

(Department of biochemistry and Microbiology)

Dr. Michael O. Wolf, External Examiner

(University of British Columbia, Department of Chemistry)

Supervisory Committee

Dr. Reginald H. Mitchell, Supervisor

(Department of Chemistry)

Dr. David J. Berg, Departmental Member

(Department of Chemistry)

Dr. Cornelia Bohne, Departmental Member

(Department of Chemistry)

Dr. Stephen V. Evans, Outside Member

(Department of Biochemistry and Microbiology)

Dr. Michael O. Wolf, External Examiner

(University of British Columbia, Department of Chemistry)

ABSTRACT

The cyclopentadienone-fused dihydropyrenes **46** and **47** were synthesized. The internal methyl resonances, the coupling constants, NICS calculations and X-ray results confirmed that the cyclopentadienone displays antiaromatic character resulting in bond localization in the annulene ring consistent with a $4n$-π fused system. The ring current of the dihydropyrene fragment is reduced by fusion of the antiaromatic system by about 80% of that caused by benzene.

The syntheses of the methylfulvene fused dihydropyrene **56** and the phenylfulvene fused dihydropyrene **58** have been accomplished. The calculated and experimental NMR data and NICS calculations all demonstrated that the fulvenes had weak diatropic ring currents and caused bond localizations in the DHP rings, in which phenyl fulvene has a larger effect than that of methyl fulvene.

A number of bis-dihydropyrene systems, bis-dihydropyrene ketone **117**, bis-benzo[*e*]dihydropyrene ketone **119**, benzo[*e*]dihydropyrene dihydropyrene ketone **122,** bis-benzo[*e*]dihydropyrene methylene **124** and the benzo[*e*]dihydropyrene-dihydropyrene acetylene **130**, have been synthesized, in which **117, 119** and **124** are homo-systems and **122** and **130** are hetero-systems. The multiple photoswitching properties study found that all of these systems except **130** showed multi-states during the photo opening and photo closing processes, which means that each end of the DHP units photo opens or closes separately rather than synchronously. In the homo switches **117**, **119** and **124**, the two DHP units act independently, but the relative differentiation is not very significant. On the other hand, the hetero-switch **122** showed fully differentiated photo opening process and almost a pure open-closed intermediate **122'** could be achieved. This is the first example which clearly showed four states in the UV closing process.

The relative photo opening and closing rates compared to benzoDHP **36** have also been studied. It was found that while the carbonyl linker largely increased the relative photo opening rate (**117, 119** and **122**), the methylene linker only increased it slightly (**124**). The photo closing processes were always fast as usual. The studies of the thermal return reactions of these systems showed that while the carbonyl linker

substantially slowed down the thermal return reactions of the DHP units (**117, 119** and **122**), the methylene linker speeded it up slightly (**124**).

The mono-iron tricarbonyl benzo[*e*]dihydropyrene complex **152,** the bis-iron tricarbonyl benzo[*e*]dihydropyrene complex **153** and the iron tetracarbonyl dihydropyrene complex **151** were synthesized**.** The structures of **152** and **153** were determined by X-ray crystallography. The coordinations of iron tricarbonyl moieties to the DHP rings caused a distortion of ca. 30 degree away from the central DHP plane. Coordination also increased bond alternation and reduced ring currents in the DHP rings. ^{1}H-NMR and X-ray studies showed that **152** showed a weak paratropic ring current in the DHP ring. Iron coordination of the DHP completely stopped the photochromic properties of the dihydropyrenes.

Table of Contents

Title Page	i
Supervisory Committee	ii
Abstract	iii
Table of Contents	vi
List of Tables	xii
List of Figures	xiv
List of Schemes	xvii
List of Abbreviations	xx
List of Numbered Compounds	xxii
Acknowledgements	xxxii
Dedication	xxxiii

Chapter One

Estimating the antiaromaticity of cyclopentadienone and the weak aromaticity of fulvenes

1.1	**Introduction**	2
	1.1.1 Aromaticity	2
	1.1.2 History and theory of aromaticity	3
	1.1.3 The classification of aromatic compounds	5

1.1.3.1 Annulenes 5

1.1.3.2 Aromatic ions 6

1.1.3.3 Heterocycles 7

1.1.3.4 Polycyclic systems 8

1.1.4 Annulenones and fulvenes 9

1.1.5 Criteria for Aromaticity 11

1.1.6 Ring currents and NMR spectroscopy 13

1.1.7 Mitchell's method to estimate ring currents and hence resonance energies or aromaticities 16

1.2 Objectives 20

1.3 Syntheses 21

1.3.1 Synthesis of 2,7-di-*t*-butyl-*trans*-10b,10c-dimethyl-10b,10c-dihydropyrene **35** 21

1.3.2 Syntheses of the cyclopentanone-fused dihydropyrene **43** and cyclopentadiene-fused dihydropyrene **45** 22

1.3.3 Synthesis of cyclopentadienone-fused dihydropyrenes **46** and chloro derivative **47** 23

1.3.3.1 Dehydrogenation of cyclopentanone-fused dihydropyrene 23

1.3.3.2 Intramolecular *trans* Friedel-Crafts cyclization 26

1.3.4 Fulvane and fulvene fused DHP systems 29

1.3.4.1 Fulvane fused DHP **54** 29

1.3.4.2 Methylfulvene fused dihydropyrene **56** 31

1.3.4.3 Phenylfulvene fused dihydropyrene **58** 33

1.3.4.4 Attempts to synthesize the fulvene fused dihydropyrene **59** 35

1.3.4.5 Attempts to synthesize dimethyl and diphenylfulvene fused dihydropyrenes 37

1.4 Results and discusion 37

1.4.1 Estimating antiaromaticity in cyclopentadienone-fused dihydropyrenes 37

1.4.1.1 Introduction 37

1.4.1.2 Relative antiaromaticity 39

1.4.1.3 The paratropic ring current of cyclopentadienone 41

1.4.1.4 Computational studies 43

1.4.1.5 The crystal structure of **43** 46

1.4.1.6 The crystal structure of **46** 50

1.4.2 Investigation of the weak aromaticity of fulvenes 54

1.4.2.1 Introduction 54

1.4.2.2 The weak aromaticity of fulvenes 55

1.4.2.3 Computational studies 58

1.5 Conclusions 63

Chapter Two

Multi-state photoswitches based on bis-dihydropyrenes

2.1 Introduction 65

2.1.1 Photochromism 65

2.1.2 Types of organic photochromes 66

2.1.3 Dimethyldihydropyrenes (DHPs) 69

2.1.4 Multiple photoswitches 75

2.1.4.1 Multiple photoswitches based on dihydropyrenes (DHPs) 76

2.1.4.2 Other multiple systems 80

2.2 Objectives 81

2.3 Syntheses 82

2.3.1 Dihydropyrene starting materials: Syntheses of benzoDHP **36** and bromo-benzoDHP **111** 82

2.3.2 Synthesis of **112** by formylation of **35** 83

2.3.3 Linked DHP systems with a carbonyl as spacer 84

2.3.3.1 Syntheses of carbonyl linked homo switches **117** and **119** 84

2.3.3.2 Synthesis of carbonyl linked hetero switch **122** 90

2.3.4 Linked DHP systems with a methylene group as spacer 93

2.3.4.1 Synthesis of the methylene linked homo-switch **123** 93

2.3.4.2 Synthesis of the methylene linked homo-switch **124** 95

2.3.5 Linked DHP system with an enthynyl as spacer **130** 96

2.4 Results and discussion 98

2.4.1 Photochromism of 2-formyl-7-*tert*-butyl dihydropyrene **112** 98

2.4.2 Multiple photoswitching properties of bis-DHP systems 104

2.4.2.1 Bis-DHP systems linked by a carbonyl group 105

2.4.2.1.1 Homo bis-switch **117** 105

2.4.2.1.2 Homo bis-switch **119** 109

2.4.2.1.3 Hetero bis-switch **122** 113

2.4.2.2 Bis-DHP systems linked by non-conjugated spacers 120

2.4.2.2.1 DHP-C(OH)-DHP **116** and DHP-CH_2-DHP **123** 120

2.4.2.2.2 BDHP-CH_2-BDHP **124** 121

2.4.2.3 Ethynyl spacer linked bis-DHP system **130** 125

2.4.3 Study of the relative photo opening and closing rates 126

2.4.4 Thermal return reactions 128

2.5 Conclusions 134

Chapter Three

Iron Complexes of dihydropyrene

3.1 Introduction 137

3.1.1 Metal complexes of dihydropyrene 137

3.1.2 Annulene iron carbonyl complexes 140

3.2 Objectives 141

3.3 Syntheses 141

3.4 Results and discussion 145

3.4.1 Ring current effects and structures 145

3.4.2 The crystal structure of **152** 148

3.4.3 The crystal structure of **153** 153

3.4.4 Bond localization effects 156

3.4.5 Photoswitching properties 157

3.5 Conclusions 158

Chapter Four Experimental Section

4.1 General Experimental Conditions and Instrumentation 161

4.2 Syntheses 164

References

203

Appendices

214

List of Tables

Table 1.1 Comparison of experimentally estimated values of BLE from Δδ(Ar)/ Δδ(Bz) with Dewar resonance energies values. 19

Table 1.2 NMR data (in $CDCl_3$) for comparison of ring currents. 41

Table 1.3 NICS values for compounds **35**,[54b] **36**,[54b] **43** and **46**. 44

Table 1.4 Summary of crystallographic data of **43** and **46**. 48

Table 1.5 Selected bond lengths [Å] and angles [°] for **43**. 49

Table 1.6 Selected bond lengths [Å] and angles [°] for **46**. 51

Table 1.7 Periphery bond length for **36**, **43** and **46**. 53

Table 1.8 Chemical shifts (ppm) of internal methyl protons in the annelated DHPs. 57

Table 1.9 Chemical shifts (ppm) of selected arene protons in the annelated DHPs. 57

Table 1.10 NICS values for compounds **35**,[54b] **36**,[54b] **54** and **59**. 59

Table 1.11 Calculated and experimental ^{1}H chemical shifts for **56** and **58**. 61

Table 1.12 Calculated and experimental ^{13}C chemical shifts for **56** and **58**. 62

Table 2.1 The thermal decay rate constants and half-lives at 30 °C. 102

Table 2.2 Relative pseudo 1^{st} order photo opening rate constants (vis-open) of some DHP systems compared to benzoDHP **36** at room temperature and relative photo closing rate constants (UV-close) of their photoisomers compared to benzoDHP **36'**. 128

Table 2.3 Rate constants and half-lives at 46 °C. 130

Table 2.4 Thermal return data derived from kinetic results. 131

Table 3.1 Summary of crystallographic data for **152** and **153**. 151

Table 3.2 Selected experimental (exp) and calculated [DFT B3LYP/6-31G*][111] (calcd) bond[a] lengths (Å) for complexes **36**,[54b] **152** and **153**. 152

Table 3.3 Selected bond angles (deg) for complexes **152** and **153**. 153

List of Figures

Figure 1.1	Overlapping p orbitals in benzene.	3
Figure 1.2	The induced ring current and magnetic field in benzene.	13
Figure 1.3	Numbering scheme and location of the NICS points for DHPs nuclei. (NICS points are shown in bold type.)	44
Figure 1.4	An ORTEP3 drawing[63] of complex **43** (30% probability thermal ellipsoids. Hydrogen atoms have been removed for clarity.)	47
Figure 1.5	An ORTEP3 drawing[63] of complex **46** (30% probability thermal ellipsoids. Hydrogen atoms have been removed for clarity.)	52
Figure 1.6	Carbon numbering for bond length comparison.	54
Figure 1.7	Numbering scheme and location of the NICS points for DHPs nuclei. (NICS points are shown in bold type.)	59
Figure 1.8	Numbering scheme for the NMR calculations of **56** and **58**.	60
Figure 2.1	The sequential UV-Vis spectra of photo opening of **112**.	99
Figure 2.2	^{1}H NMR spectra of **112(C)** (top) and **112'(O)** (bottom).	100
Figure 2.3	UV-vis spectra of **117**(**C-C**) and **117"**(**O-O**).	105
Figure 2.4	Proton NMR spectra of **117**(**C-C**) (top) and **117"**(**O-O**) (bottom).	106
Figure 2.5	Sequential partial NMR spectra for the visible light opening (left) of **117** with wavelength > 490 nm light and UV closing (right) of **117"** with 254 nm light.	108
Figure 2.6	Sketches of expected C-C, O-C and O-O isomer concentration changes in the photo opening and closing processes	109

Figure 2.7	UV-Vis spectra of **119**(**C-C**) and **119”**(**O-O**).	110
Figure 2.8	Proton NMR spectra of **119**(**C-C**) (top) and **119”**(**O-O**)(bottom).	110
Figure 2.9	Sequential partial NMR spectra for the visible light opening (left) of **119** with wavelength > 490 nm light and UV closing (right) of **119”** with 254 nm light.	111
Figure 2.10	UV-vis spectra of **122**(C-C) and **122”**(O-O).	113
Figure 2.11	Proton NMR spectra of **122**(C-C) (top) and **122”**(O-O)(bottom).	114
Figure 2.12	Comparison of UV-Vis spectra of **117**, **119** and **122.**	116
Figure 2.13	Comparison of UV-Vis spectrum of **122** and the digital combination spectrum of **117** and **119.**	116
Figure 2.14	Sequential partial NMR spectra for the visible light opening of **122** first with 550-600 nm light and then with > 490 nm light.	117
Figure 2.15	Sequential partial NMR spectra for the UV (254 nm) closing of **122”**.	119
Figure 2.16	UV-Vis spectra of **124** (C-C) and **124”**(O-O).	121
Figure 2.17	Proton NMR spectra of **124**(C-C) (top) and **124”**(O-O) (bottom).	122
Figure 2.18	Sequential partial NMR spectra for the visible light opening (left) of **124** with wavelength > 490 nm light and UV closing (right) of **124”** with 254 nm light.	124
Figure 2.19	Proton NMR spectra of **130**(C-C) (top) and **130’**(O-C) (bottom).	126
Figure 3.1	An ORTEP3 drawing[63] of complex **152** (30% probability thermal ellipsoids). Hydrogen atoms have been removed for clarity.	149

Figure 3.2 An ORTEP3 drawing[63] of complex **153** (30% probability thermal ellipsoids). Hydrogen atoms have been removed for clarity. 154

List of Schemes

Scheme 1.1	The general formula for annulenones and fulvenes.	9
Scheme 1.2	Resonance structures for cyclopropenone and tropone.	10
Scheme 1.3	Resonance structure of cyclopentadienone.	10
Scheme 1.4	Resonance structure of pentafulvene and heptafulvene.	11
Scheme 1.5	Mitchell's method to determine relative aromaticity.	17
Scheme 1.6	Synthesis of DHP **35**.	21
Scheme 1.7	Syntheses of cyclopentanone fused DHP **43** and CpDHP **45**.	22
Scheme 1.8	Retrosynthetic strategy for **46**.	23
Scheme 1.9	Syntheses of **47** and **48**.	24
Scheme 1.10	Synthesis of **46**.	25
Scheme 1.11	Intramolecular *trans* Friedel-Crafts cyclization.	27
Scheme 1.12	The mechanism of intramolecular Friedel-Craft cyclization.	28
Scheme 1.13	Syntheses of indenones by cyclization.	29
Scheme 1.14	Synthesis of fulvane fused DHP **54** and its rearrangement.	31
Scheme 1.15	Olefination of **46**	31
Scheme 1.16	Synthesis of methylfulvene fused DHP **56**.	33
Scheme 1.17	Synthesis of phenylfulvene fused DHP **58**.	34
Scheme 1.18	Attempts to synthesize fulvene fused DHP **59**.	36
Scheme 1.19	Resonance structures of **46**.	39
Scheme 1.20	The bond alternation of $(4n + 2)$-π and $(4n)$-π fused DHP.	43
Scheme 2.1	The two states of a photochromic compound and their conversion	65
Scheme 2.2	The *cis-trans* isomerization for stilbene and azo-benzene.	67

Scheme 2.3	Feringa's photochromes.	67
Scheme 2.4	Pericyclic reaction types of photochromic compounds.	68
Scehme 2.5	Photocyclization of stilbene.	68
Scheme 2.6	Examples of intramolecular hydrogen and group transfer.	69
Scheme 2.7	Examples of cycloaddition and bond cleavage photochromes.	69
Scheme 2.8	Isomerization between **11** and **11'**.	70
Scheme 2.9	Examples of [a]-annelated dihydropyrenes.	72
Scheme 2.10	Examples of [e]-annelated dihydropyrenes.	73
Scheme 2.11	Syntheses of benzo[e]DHP **36** and monobromination product **111**	82
Scheme 2.12	The formylation reaction of **35**.	83
Scheme 2.13	Syntheses of **116** and **118**.	85
Scheme 2.14	Four isomers of **116**.	86
Scheme 2.15	The oxidation of alcohols **116** and **118**.	87
Scheme 2.16	Synthesis of **117** using triphosgene.	87
Scheme 2.17	Two isomers of **117**.	88
Scheme 2.18	Synthesis of **119**.	89
Scheme 2.19	Syntheses of **120** and **121**.	90
Scheme 2.20	Synthesis of **119**.	92
Scheme 2.21	The reduction of alcohol **116**.	93
Scheme 2.22	Two isomers of **123**.	94
Scheme 2.23	Synthesis of **124**.	95
Scheme 2.24	Two isomers of **124**.	96
Scheme 2.25	Syntheses of **130**.	97

Scheme 2.26 Isomerization between **112** and **112'**. 100

Scheme 2.27 Oxygen adducts of dihydropyrenes. 103

Scheme 2.28 Example of the addition of singlet oxygen to an aromatic compound. 103

Scheme 2.29 The stepwise opening of **122**. 117

Scheme 2.30 The stepwise closing of **122"** 118

Scheme 2.31 General thermal closing process for bis-switches. 130

Scheme 2.32 The thermal return rate constants k_1 and k_2**.** 133

Scheme 3.1 Isomerization of **36** and **36'** 158

List of Abbreviations

Ar	arene
BLE	bond localization energy
CI	chemical ionization
CPD	metacyclophanediene
CpDHP	cyclopentadiene-fused dihydropyrene
CTAB	cetyltrimethylammonium bromide
δ	chemical shift in ppm from standard
dec.	decomposition
DFT	density functional theory
DHP	dimethyldihydropyrene
DMF	dimethylformamide
EtOAc	ethyl acetate
EI	electron impact
Eq.	equation
h	hour
HF	Hartree-Fock
HRMS	high resolution mass spectrum
IR	infrared
KO^{t}Bu	potassium *t*-butoxide
LSIMS	liquid secondary ion mass spectrometry
Me	methyl

MeOH	methanol
min	minute
mp	melting point
MS	mass spectrum
NBS	N-bromosuccinimide
NICS	nucleus independent chemical shifts
NMR	nuclear magnetic resonance
bs	broad singlet
s	second, singlet
d	doublet
dd	doublet of doublet
m	multiplet
ppm	parts per million
RE	resonance energy
t	tertiary group
THF	tetrahydrofuran
Univ.	university
UV-vis	ultraviolet and visible

List of Numbered Compounds

1

2

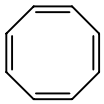

3

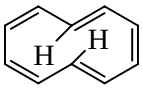

4

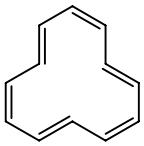

5

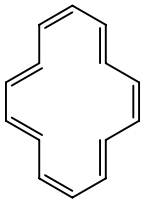

6

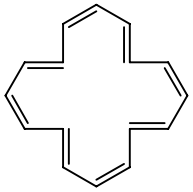

7

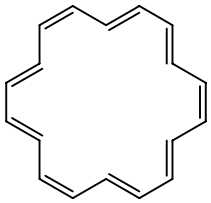

8

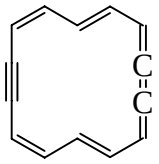

9

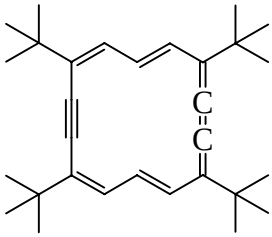

10

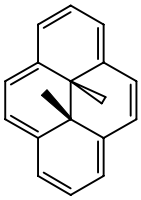

11

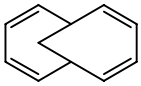

12

13

14

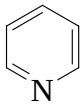

15

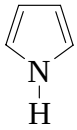

16

17

18

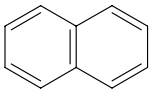

19

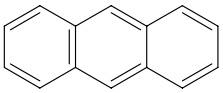

20

21

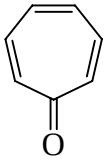

22

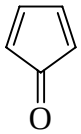

23

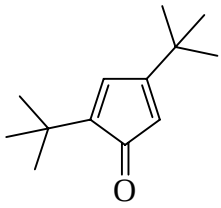

24

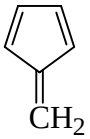

25

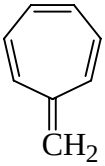

26

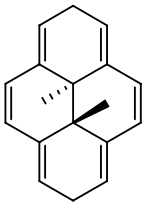

27

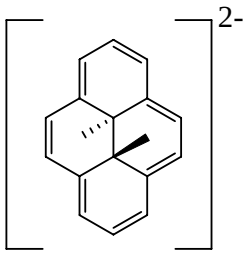

28

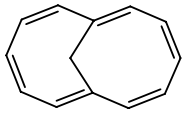

29

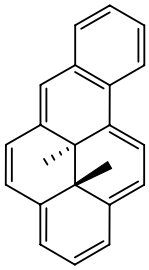

30

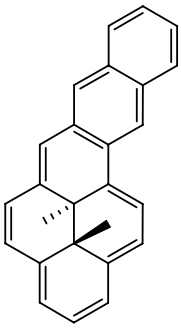

31

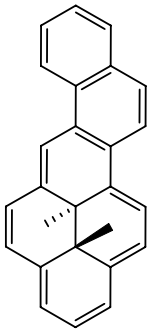

32

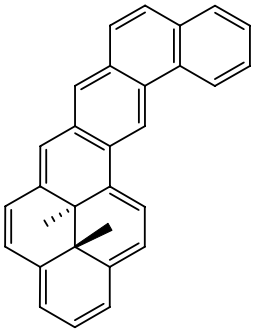

33

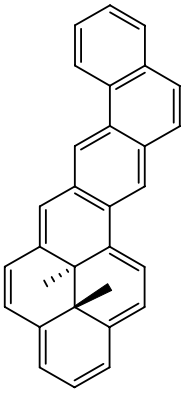

34

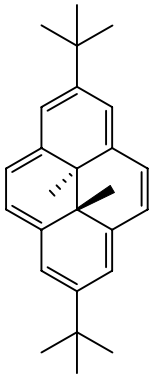

35

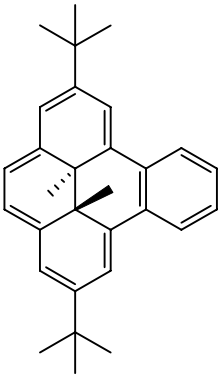

36

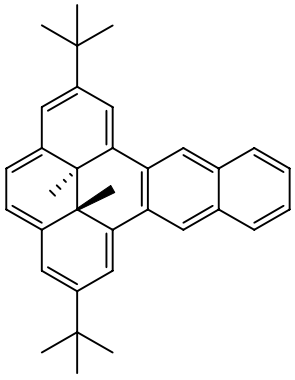

37

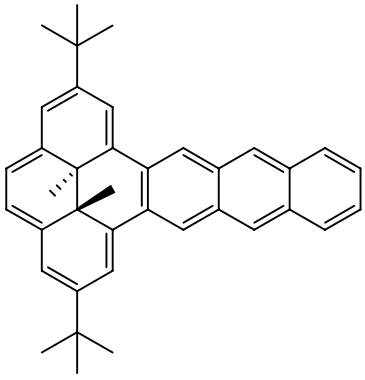

38

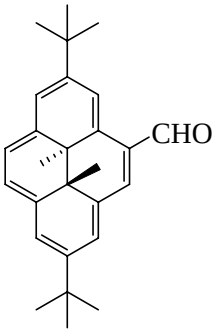

39

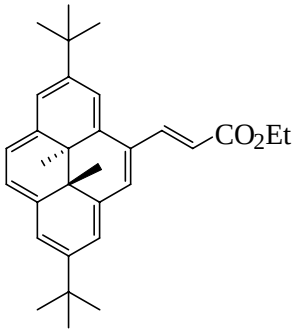

40

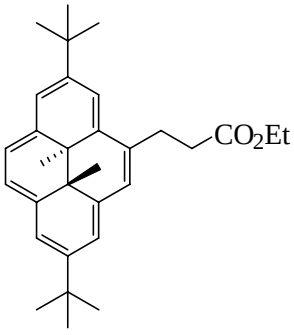

41

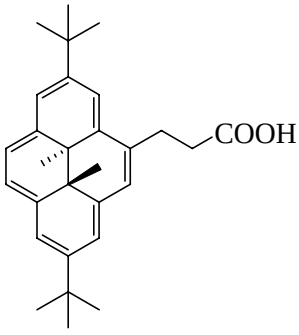

42

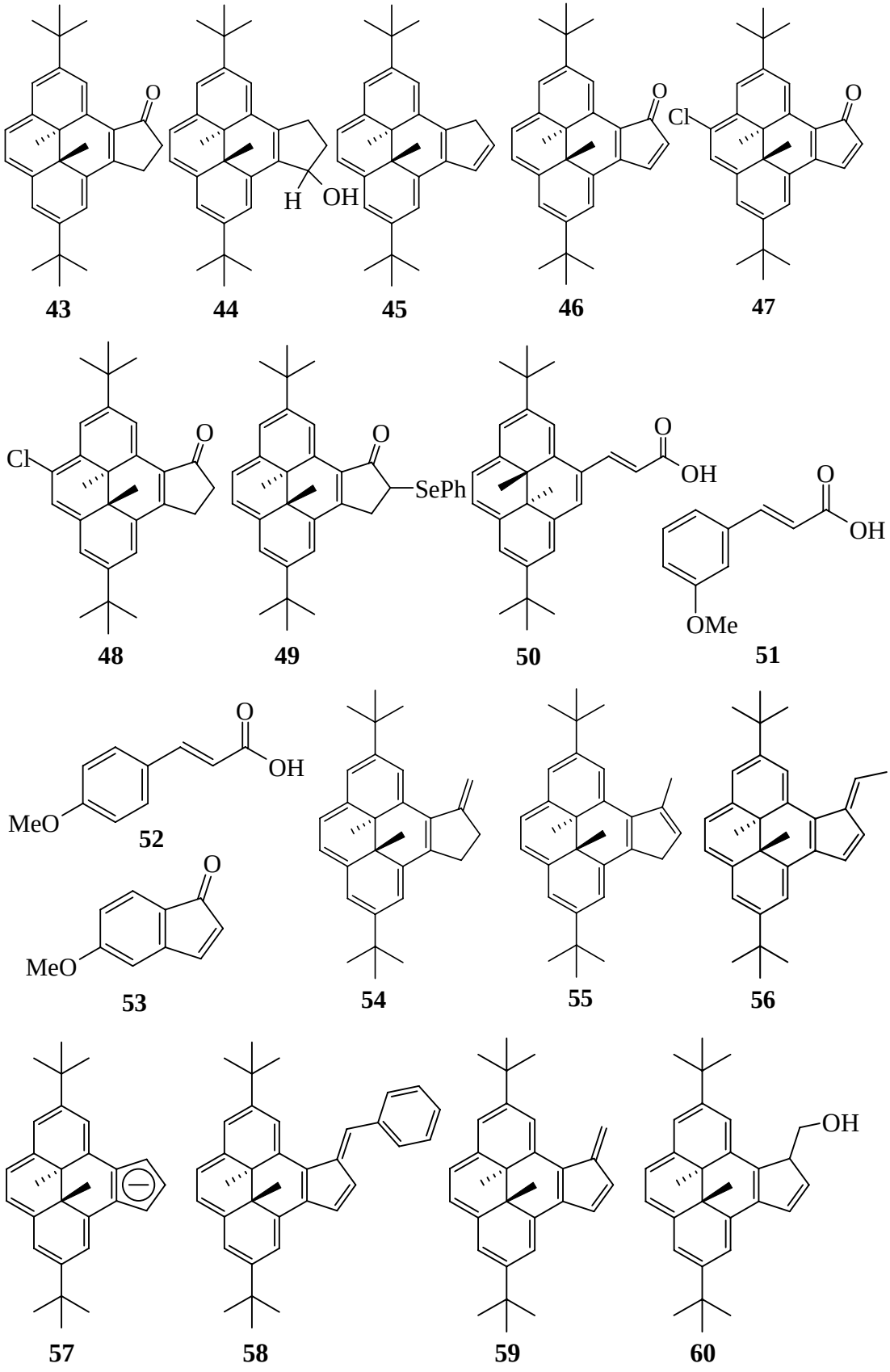

43 **44** **45** **46** **47**

48 **49** **50** **51**

52 **53** **54** **55** **56**

57 **58** **59** **60**

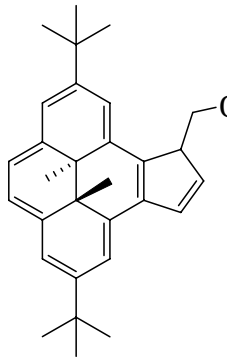

61

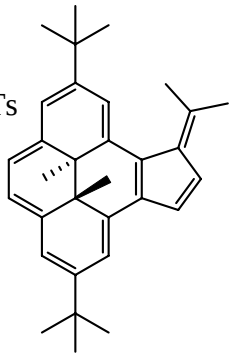

62

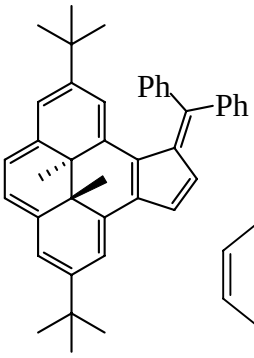

63

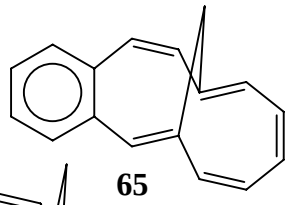

65

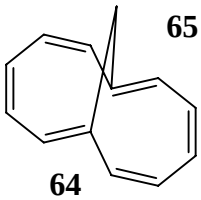

64

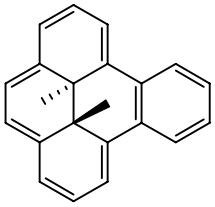

66

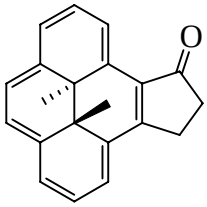

67

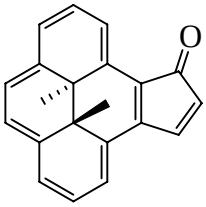

68

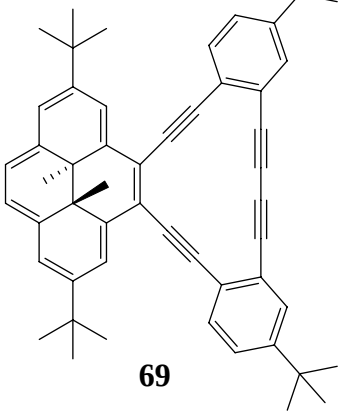

69

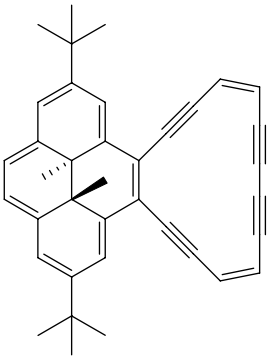

70

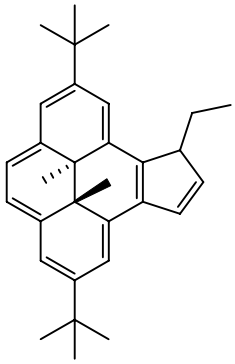

71

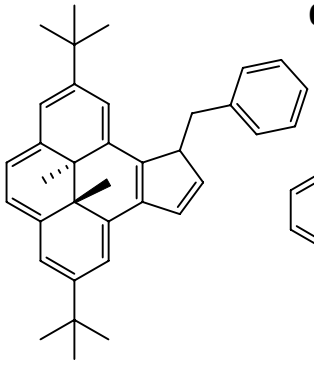

72

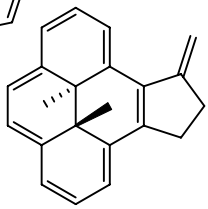

73

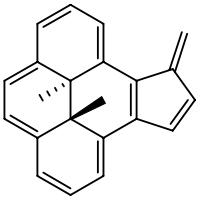

74

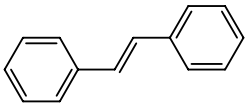

75

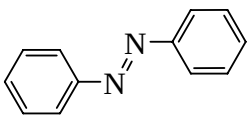

76

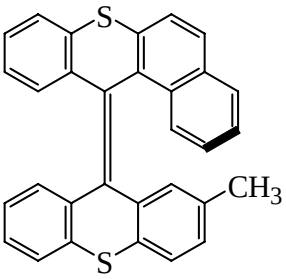

77

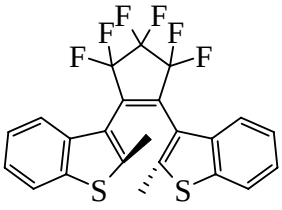

78

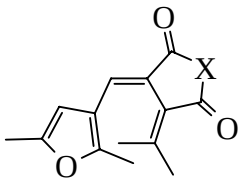

79

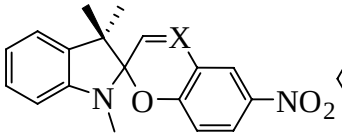

80

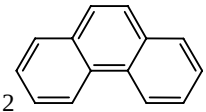

81

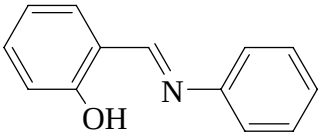

82

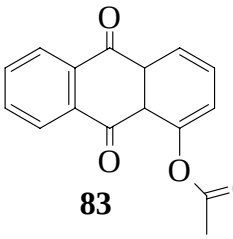

83

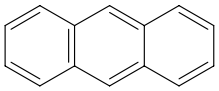

84

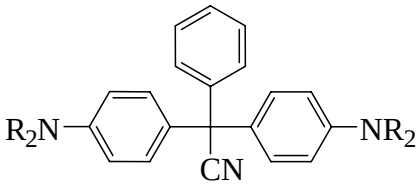

85

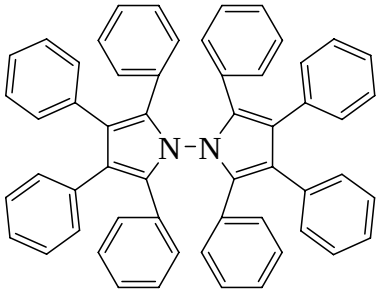

86

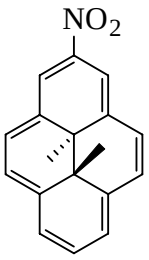

87

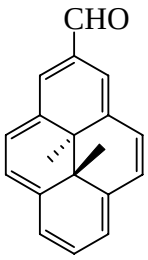

88

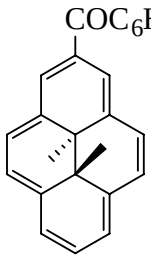

89

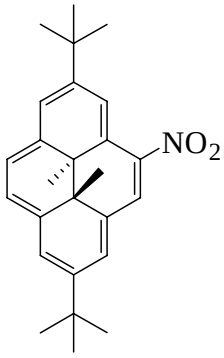

90

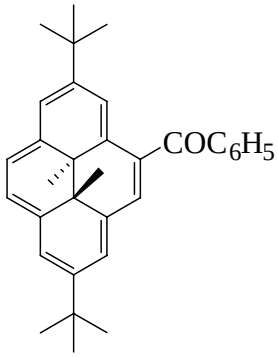

91

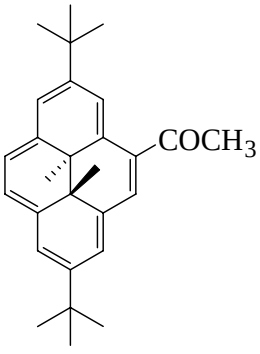

92

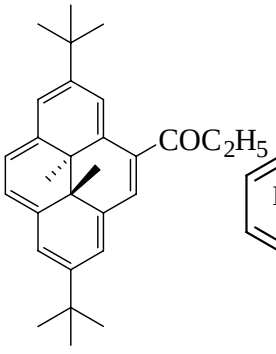

93

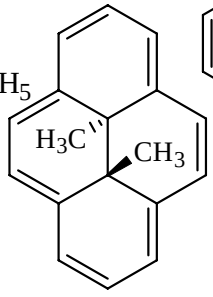

94

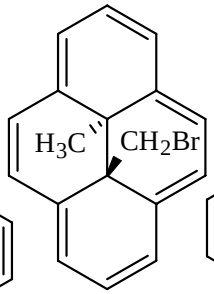

95

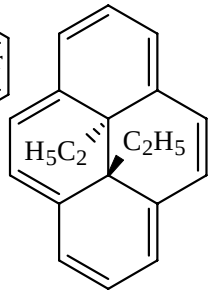

96

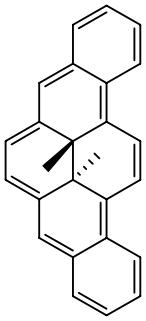

97

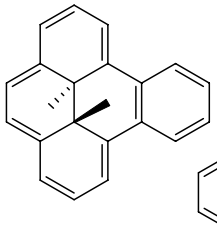

98

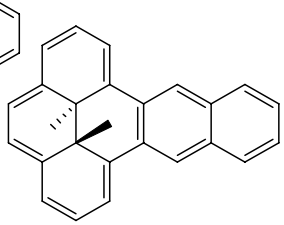

99

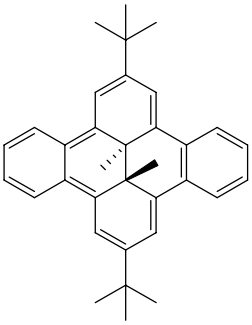

100

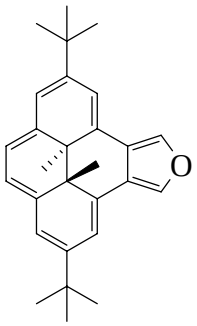

101

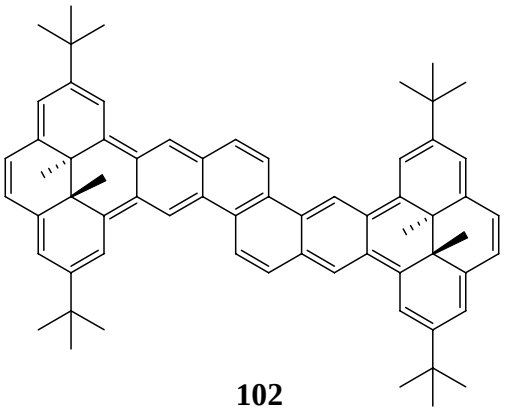

102

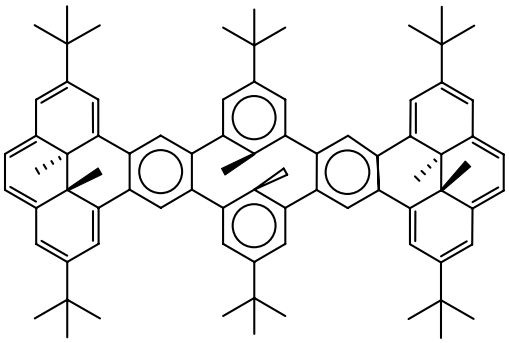

103

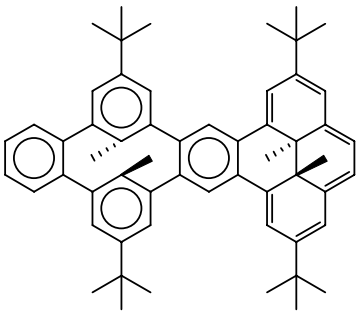

104

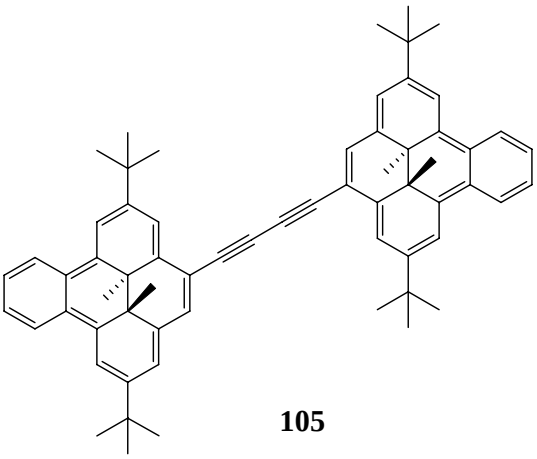

105

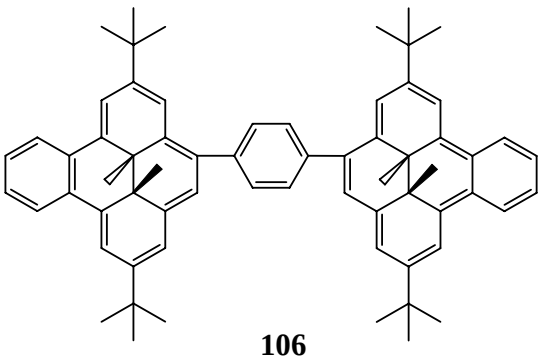

106

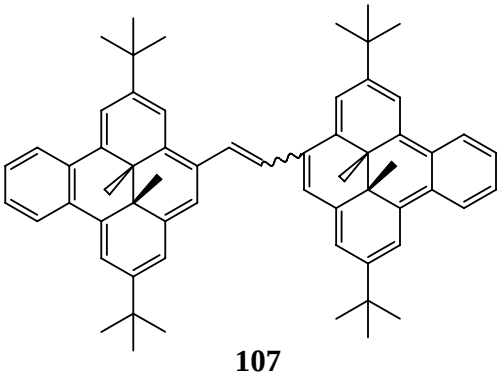

107

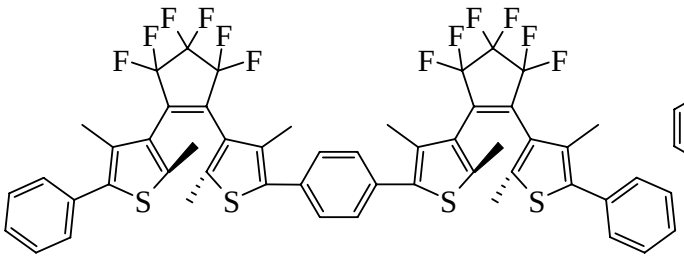

108

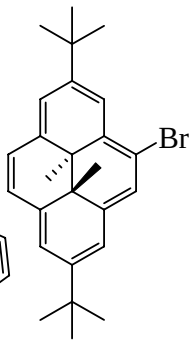

109

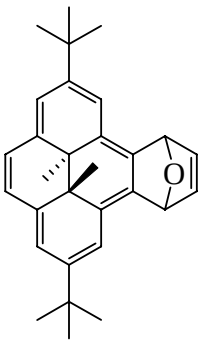

110

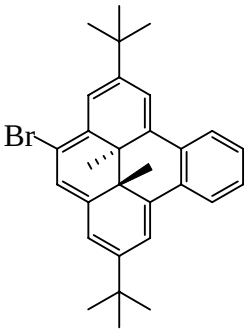

111

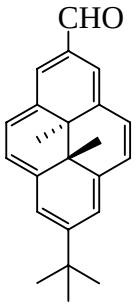

112

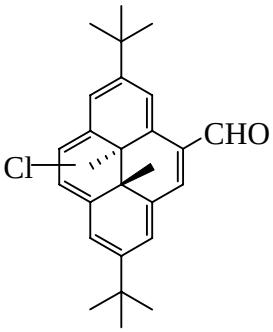

113

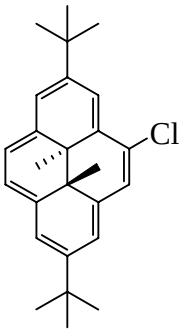

114

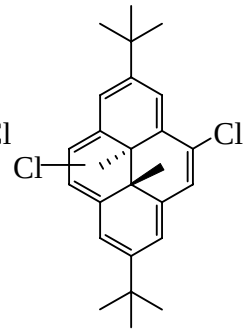

115

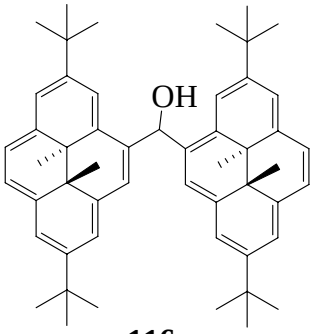

116

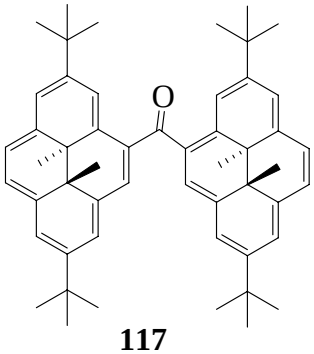

117

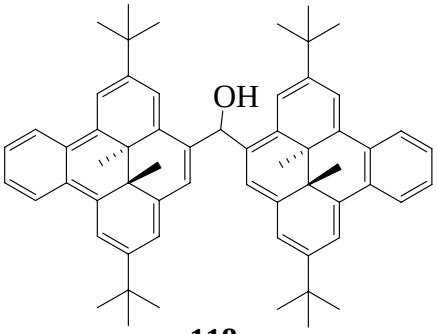

118

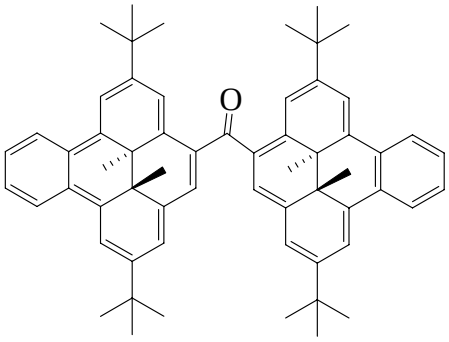

119

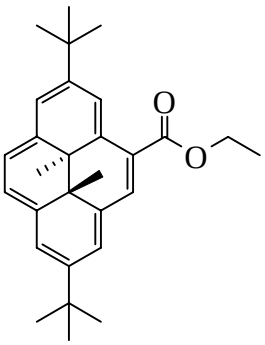

120

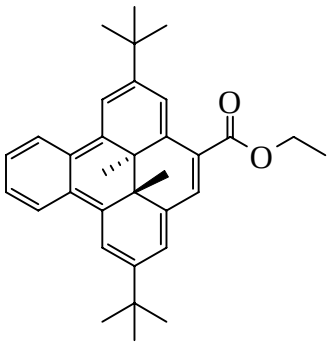

121

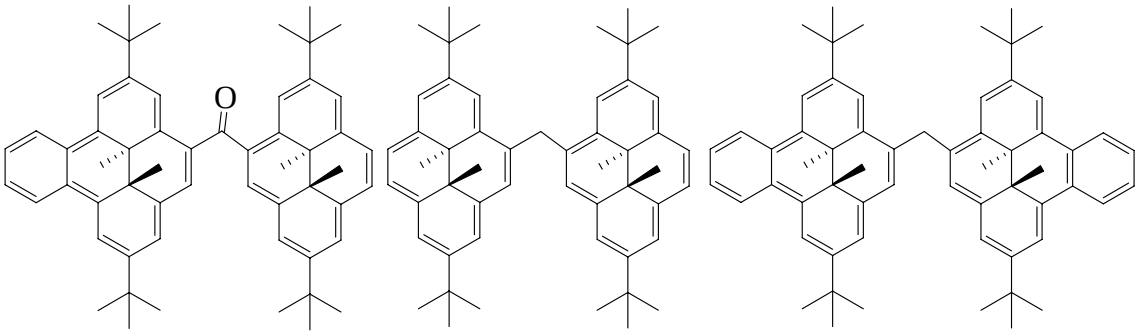

122 **123** **124**

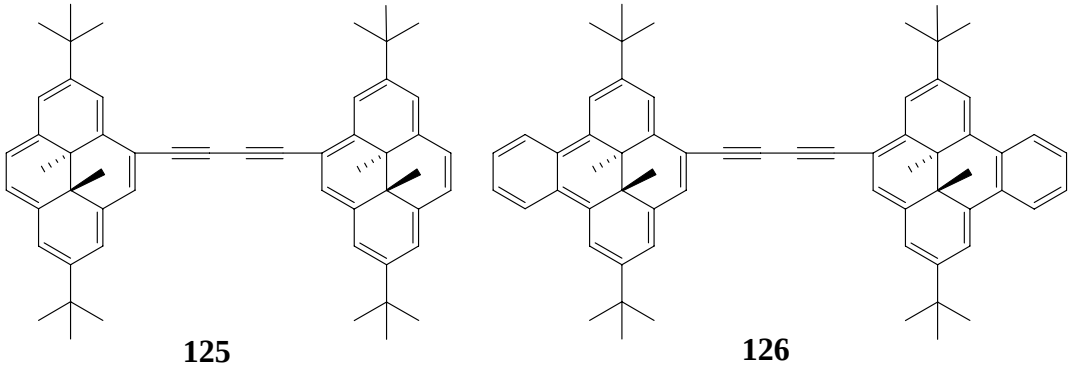

125 **126**

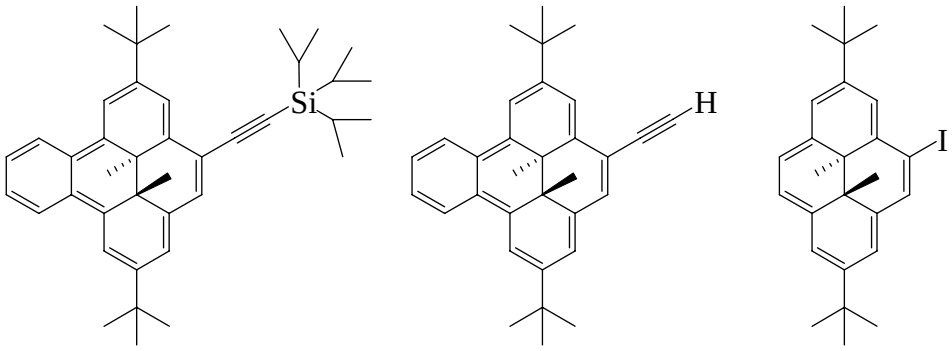

127 **128** **129**

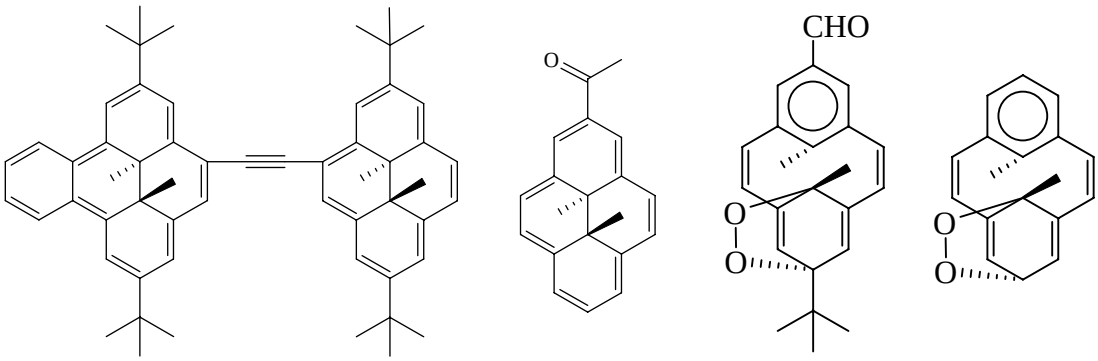

130 **131** **132** **133**

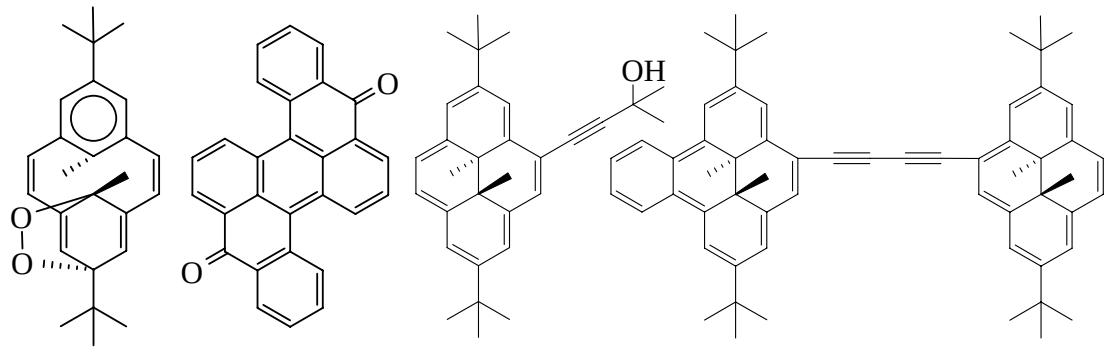

134 **135** **136** **137**

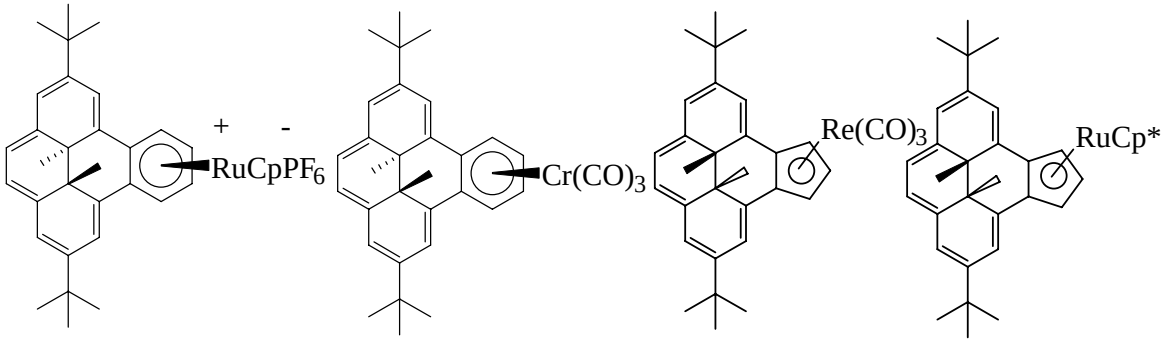

138 **139** **140** **141**

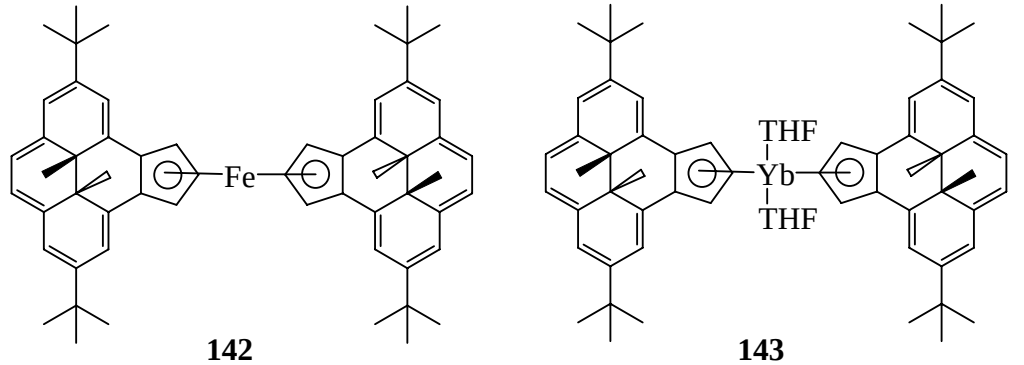

142 **143**

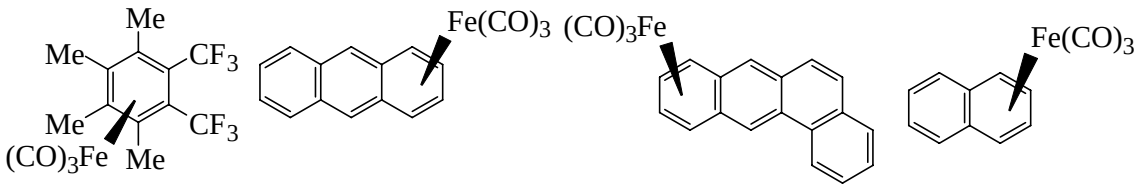

144 **145** **146** **147**

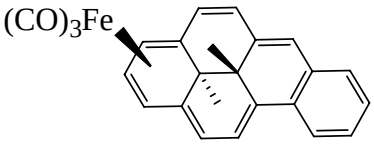

148

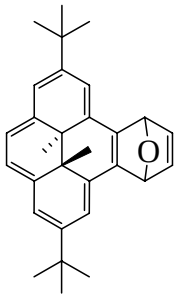

149

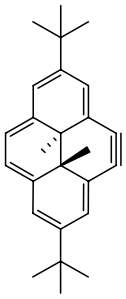

150

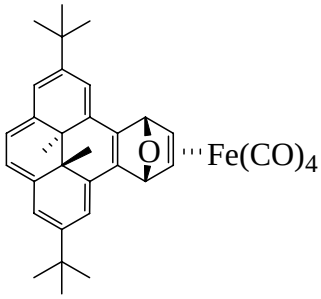

151

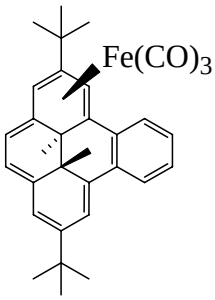

152

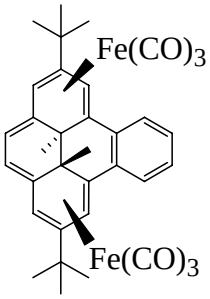

153

Acknowledgements

I wish to express my deep appreciation to Dr. Reginald H. Mitchell for his guidance and constant encouragement during the course of this work. I especially appreciate his patience in the correction of this thesis, both Chemistry and English.

I also wish to express my deep appreciation to Dr. David J. Berg for much help during this work.

I also would like to thank Mrs. Christine Greenwood for recording NMR spectra, Dr. David McGillivary for mass spectrometric analysis and Dr Brenda Twamley, University of Idaho, for single crystal diffraction analysis.

Finally, financial support from the University of Victoria and from the Natural Sciences and Engineering Research Council of Canada is greatly appreciated.

To my wife, Wei Fan and my daughters, Sasa and Rose

Chapter One

Estimating the antiaromaticity of cyclopentadienone and the weak aromaticity of fulvenes

Part of the research presented in this chapter is reproduced with permission from [Mitchell, R. H.; Zhang, R.; Fan, W.; and Berg. D. J. "Measuring Antiaromaticity by an Analysis of Ring Current and Coupling Constant changes in a Cyclopentadienone-Fused Dihydropyrene." *J. Am. Chem. Soc.* **2005**, *127(46)*, 16251-16254.] Copyright 2006, American Chemical Society.

The NICS and NMR calculations in this chapter were performed by Dr. R. V. Williams in the Department of Chemistry, University of Idaho.

1.1 Introduction

1.1.1 Aromaticity

All carbon compounds can be classified as either aromatic or aliphatic, and about 50% of known organic compounds contain an aromatic ring. Loosely, an aromatic means "contains one or more rings with cyclically delocalized π-electrons, where the number of electrons is usually (4n+2)". Many biological molecules contain aromatic rings. Some of these are heterocyclic, i.e. contain atoms such as nitrogen replacing carbon. Many important pharmaceuticals have aromatic or/and heteroaromatic rings, too. Aromatic structures are also important in advanced materials, such as fullerenes and carbon nanotubes, and in environmental chemistry as PAH's (polycyclic aromatic hydrocarbons).

During the period 2000-2005, ISI's web of Science database yields 42,500 papers in which the word "aromatic" is used in titles, keywords or abstracts, and another 1,600 papers using "aromaticity".

1.1.2 History and theory of aromaticity

The idea of aromaticity arose after Faraday[1] discovered benzene from the condensate of compressed illuminating gas in 1825. He determined its composition as CH. In 1833, Mitscherlich[2] prepared benzene from benzoic acid by dry distillation with lime, and also determined the molecular formula of benzene to be C_6H_6. Kekulé[3] suggested the well-known hexagon structure of benzene in 1865. In his structure, the six carbon atoms are in a plane and have alternate single and double bonds, as we would draw cyclohexatriene. Kekulé also called benzene and its derivatives "aromatic compounds" because of their odor. He pointed out that aromatic compounds have special properties, unique to that ring system.

Later, in order to explain that *ortho* and *meta* disubstituted derivatives exist only as one isomer, he further proposed that benzene has a kind of dynamic structure in which two forms of benzene A and B are in state of "equilibrium". This "equilibrium" is so fast that it is impossible to isolate the two forms. However, this did not explain the special stability of benzene, which unlike cyclohexene is not subject to easy oxidation or addition.

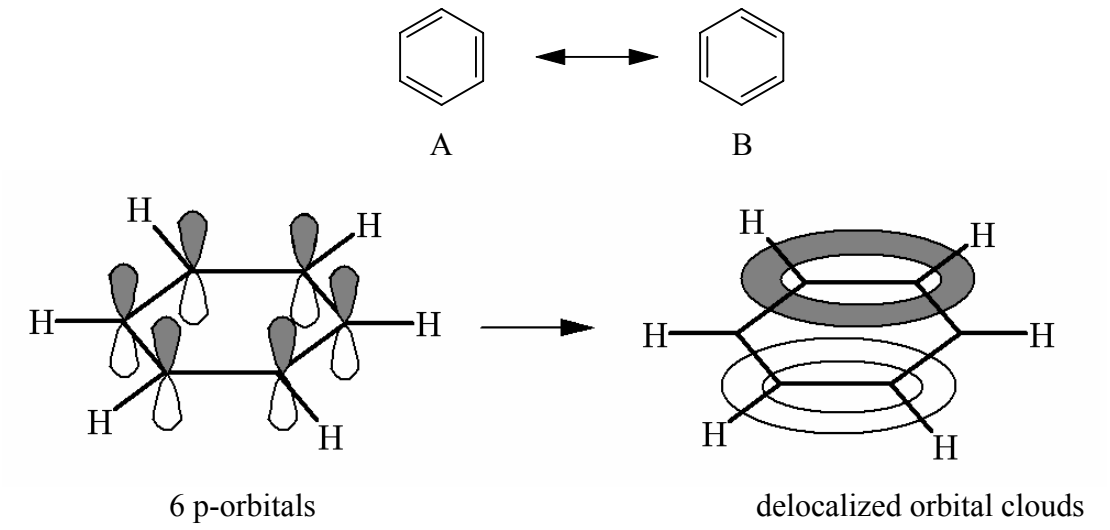

Figure 1.1 Overlapping p orbitals in benzene

It was not until the development of modern chemistry in the 1920s that the behavior of benzene was better understood. All six carbons in benzene are described to be sp^2 hybridized. Two of the three sp^2 orbitals on each carbon form the C-C sigma bonds, and so form a planar ring. The third sp^2 orbital forms the C-H bond. Then each C atom has one remaining p-orbital, with one electron each, which is out of the plane of the ring. When the ring is planar, the p-orbitals are aligned and are close enough to overlap effectively with each other to form a delocalized π system. All the π-orbitals are distributed above and below the plane of the ring (**Figure 1.1**).

In 1931, the German scientist Erich Hückel[4] carried out a series of calculations on the energy levels of the π-electrons of monocyclic conjugated polyolefins using molecular orbit theory (HMO). From there came his famous rule, which states that amongst fully conjugated, planar, monocyclic polyolefins, only those possessing (4n+2, n is an integer or zero) π-electrons have aromatic properties.

From the above discussion, the requirements of aromaticity are:

1) The molecule must be cyclic and this cycle must be fully conjugated;

2) The cycle must be planar so that the p orbitals can overlap in a parallel fashion;

3) The conjugated cycle must satisfy Hückel's rule, namely contain (4n+2) π-electrons, where n = 0,1,2,3,4,.....

In contrast, Breslow[5] describes antiaromatic compounds to be conjugated cyclic planar cyclic systems with 4n π-electrons. Antiaromatics exhibit localized π-electrons and have high reactivity. The prime example of an aromatic compound is benzene, **1**, and of an antiaromatic compound is cyclobutadiene, **2**. The first is very stable; the latter

rapidly dimerizes, and was not made until 1965, by decomposition of a cyclobutadiene-iron tricarbonyl complex in the presence of ceric ions by Pettit[6].

1.1.3 The classification of aromatic compounds

1.1.3.1 Annulenes

Annulenes are monocyclic conjugated polyolefins that can be represented by structures having alternating single and double bonds. Hückel's rule was ratified by observation of the properties of such annulenes. When Hückel's rule was first presented, the only annulenes known were benzene, **1**, and cyclooctatraene, **3**. Benzene has 6 π-electrons and it is aromatic. Cyclooctatraene, **3**, contains 8 (4n where n=2) π-electrons, and is non-aromatic principally because it has a tub shape and is not planar. Cyclooctatraene probably distorts by bending (or folding) into a tub in order to avoid unfavorable delocalization.

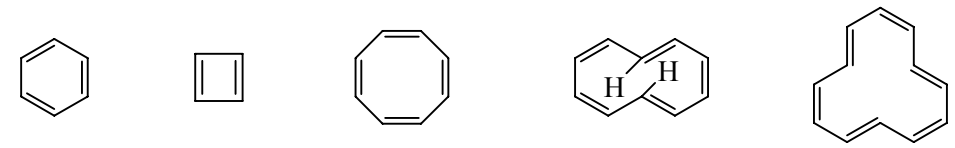

1 **2** **3** **4** **5**

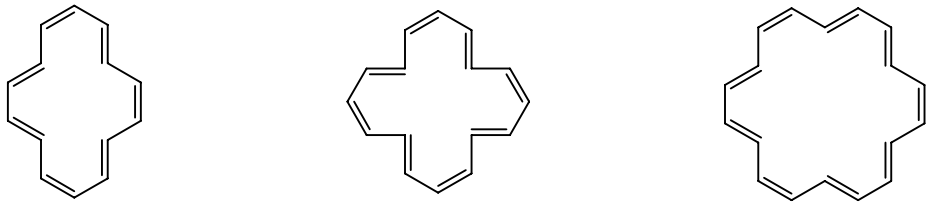

6 **7** **8**

It was not until the 1950s and 1960s, that a number of large-ring annulenes were synthesized, mostly by Franz Sondheimer,[7a] and the predictions of Hückel's rule could be verified. Examples are **4** to **8**. Of these, the [12]annulene **5** and the [16]annulene **7** are

predicted by Hückel's rule not to be aromatic. (They are antiaromatic which will be discussed below). The [14]annulene **6** and the [18]annulene **8** were predicted to be and are aromatic. The [10]annulene **4** would be expected to be aromatic on the basis of electron count, but the ring is not planar because of the steric congestion of the internal protons. In fact, many of the larger rings could not maintain ring planarity which is required for aromaticity. Two successful approaches have been developed to solve this problem. The first approach was to use rigid acetylenic bonds by Sondheimer (compound **9**)[7b] and Nakagawa (compound **10**).[8] The second approach was to use internal bridging groups to hold the ring planar, developed by Boekelheide (compound **11**)[9] and Vogel (compound **12**).[10] In the second approach, the internal groups introduced can also be used as an aromaticity probe for instrumental detection, by nuclear magnetic resonance (NMR) spectroscopy.

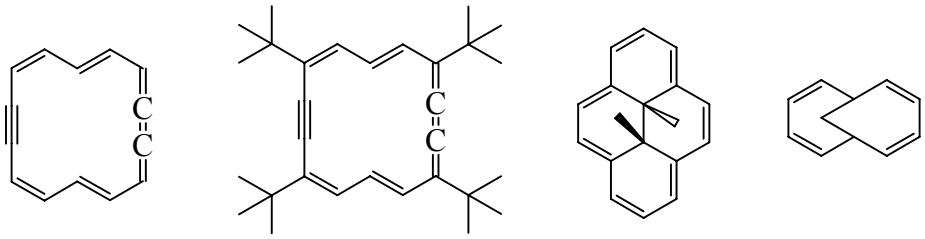

9 **10** **11** **12**

1.1.3.2 Aromatic ions

In addition to the neutral molecules that are discussed above, there are a number of charged monocyclic species known. Some of these show unexpected stabilities. They are also called aromatic. Two examples are the cyclopentadienyl anion (**13**) and cycloheptatrienyl cation (**14**).

Cyclopentadiene is not aromatic because not only does it not have the proper number of π-electrons, but also because the π-electrons can not be delocalized about the entire ring. The intervening sp^3-hybridized CH_2 group has no available *p* orbital. On the other hand, if the CH_2 loses a proton, the carbon atom becomes sp^2 hybridized and there are two electrons in the new *p* orbital. Now the cyclopentadienyl anion, which has five *p* orbitals and six electrons, is an aromatic anion. Similarly, if a hydride ion is abstracted from cycloheptatriene, the cycloheptatrienyl cation has seven *p* orbitals and six electrons and it is an aromatic cation. Indeed, NMR spectroscopy shows that all five hydrogen atoms in the cyclopentadienyl anion are equivalent and that all seven hydrogen atoms in the cycloheptatrienyl cation are equivalent. Both of them show unusual stability.

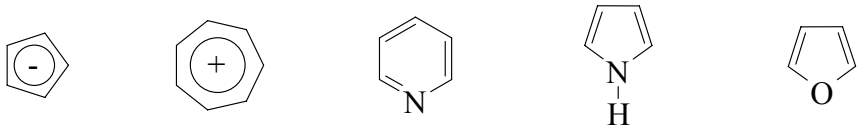

13 **14** **15** **16** **17**

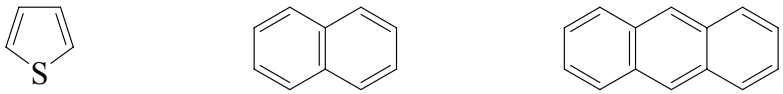

18 **19** **20**

1.1.3.3 Heterocycles

Streitweiser[11] extended Hückel's rule to conjugated heterocycles and helped explain their properties. In heterocycles, one or more of the carbon atoms in the aromatic ring are an other element such as nitrogen, oxygen, or sulfur. Examples are pyridine (**15**), pyrrole (**16**), furan (**17**) and thiophene (**18**). In all these heterocycles, the heteroatoms N, O and S are sp^2 hybridized. For pyridine, since it is a six membered ring, the *p* orbital on nitrogen has one electron. So the ring has six π-electrons, which satisfies Hückel's rule. The lone

pair on nitrogen occupies one of the sp^2 orbitals and is in the plane of ring. This gives pyridine basic character. For pyrrole, the lone pair is in a *p* orbital and is used to supply the necessary six π-electrons for aromaticity. In the cases of furan and thiophene, one lone pair is in the π system and the other in the plane of the ring (analogous to C-H bond on the other positions). There are 6 π-electrons and so furan and thiophene are aromatic. However, neither of these nor pyrrole is as aromatic as benzene. As a consequence, they are more reactive. Such heterocycles are important in life science and pharmaceutical chemistry.

1.1.3.4 Polycyclic systems

Polycyclic aromatics are molecules containing two or more aromatic rings fused along a common side, e.g. naphthalene (**19**) and anthracene (**20**). Three types of bicyclic aromatics are possible: 1) molecules formed by the fusion of two (4n+2) π-electrons rings; 2) molecules formed by the fusion of two (4n) π-electrons rings; 3) molecules formed by fusion of a (4n) and a (4n+2) π-electrons ring. Then prediction of resultant aromaticity is not easy. Counting the total π-electrons on the periphery and simply applying Hückel's rule, is generally not so reliable. Randic introduced his circuit theory[12] to specifically predict the aromaticity of such systems.

Polycyclic aromatic compounds are interesting because they have practical applications in advanced materials. There are two more attractive areas. The first one was the discovery of $C_{60,}$ which now has grown into the area called "fullerene chemistry". The second is carbon nanotubes. Chemical syntheses of fullerenes or carbon nanotubes now attract much attention. Pioneering work in this area were Diederich's[13] precursors to $C_{60,}$ and Scott's[14] bowl shaped polyarenes to mimic the surface of C_{60}, and Vogtle's[15]

cyclophane-based cage compound to mimic the cavity of fullerenes and Tobe's[16] cyclopolyynes to mimic carbon nanotubes.

1.1.4 Annulenones and fulvenes

Annulenones and fulvenes are cyclic polyenes with odd-membered rings. There is an exocyclic double bond on the "odd" carbon atom. It is a carbon-oxygen double bond in annulenones and a carbon-carbon double bond in fulvenes. The general formula for annulenones and fulvenes are shown in **Scheme 1.1**.

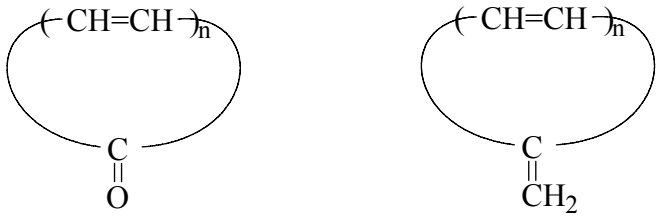

annulenones fulvenes

Scheme 1.1 The general formula for annulenones and fulvenes

The oxygen is electronegative and is strongly electron withdrawing. There is then partial positive charge on the odd carbon atom and negative charge on oxygen in annulenones. The simplest example is cyclopropenone (**21**) which was reported in 1967.[17] It shows high thermal stability and it has a large dipole moment.[18] Its derivatives have a high partial charge on oxygen as indicated by ^{17}O NMR spectroscopy.[19] These suggest that cyclopropenone has the 2 π-electron contributor **21b** (**Scheme 1.2)**, and is aromatic.

Tropone (**22**) is also a stable compound with a conjugated seven-membered ring system. The ^{1}H NMR chemical shifts indicate that it has a diamagnetic ring current.[20]

Tropone (**22**) has significant aromaticity due to the contribution of resonance form **22b** (**Scheme 1.2**).

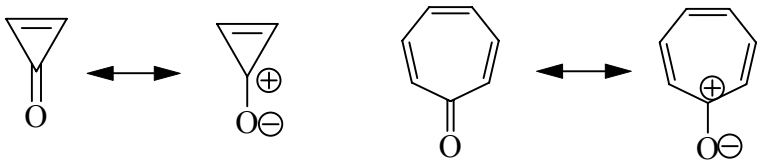

21a **21b** **22a** **22b**

Scheme 1.2 Resonance structure for cyclopropenone and tropone.

In contrast to cyclopropenone (**21**) and tropone (**22**), cyclopentadienone (**23**) is highly reactive and only exists in the form of its dimer. The high reactivity of cyclopentadienone indicates that the electronegativity of oxygen atom leads to the dominance of the very unstable 4π-electron antiaromatic resonance structure **23b** (**Scheme 1.3**). The sterically hindered cyclopentadienone (**24**) was prepared by Garbish and Sprecher,[21] and in its NMR spectrum, the signals for H-3 and H-5 protons were at δ 6.50 and 4.93 respectively.[21] These values are considerably upfield from those expected for the α and β protons of an unsaturated ketone, which suggests a paratropic ring current.

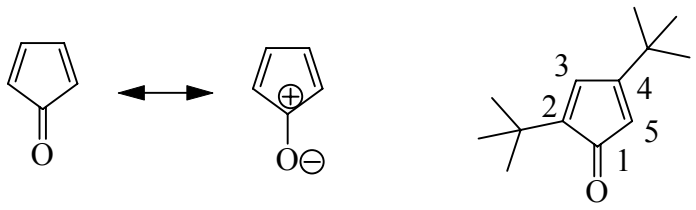

23a **23b** **24**

Scheme 1.3. Resonance structure of cyclopentadienone.

Fulvenes are related to annulenones, where the exocyclic carbonyl group has been replaced by an exocyclic methylene group. Fulvenes, such as pentafulvene (**25**) and

heptafulvene (**26**) are considered generally to be nonaromatic compounds, though some properties suggest they may be weakly aromatic.

Experimentally, fulvenes have a dipole moment on the exocyclic methylene group even though formally there is no electronegative difference between the two carbons. The dipole moment of pentafulvene (**25**) is 0.424 D,[22] which indicates very modest negative charge in the five-membered ring which then has a small degree of 6π-electron character (**25b**, **Scheme 1.4**). Electron donor substituents on the exocyclic methylene of pentafulvene enhance conjugation and aromaticity of this species.[23] Heptafulvene (**26**) has a modest dipole moment of 0.48 D[24, 22c] indicating a small contribution by the dipolar resonance structure **26b** (**Scheme 1.4**). The dipole moment of heptafulvene has the opposite polarization compared to pentafulvene (**25**). This behavior should not be surprising if the aromatic characters of cyclopentadienide and cycloheptatrienyl cation, which both possess six π-electrons, are considered.

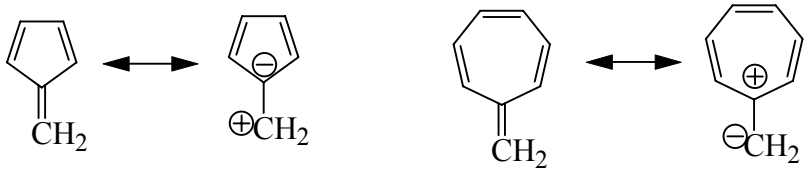

25a **25b** **26a** **26b**

Scheme 1.4 Resonance structure of pentafulvene and heptafulvene

1.1.5 Criteria for aromaticity

Various criteria for aromaticity have been discussed even though a precise definition of aromaticity is difficult.

The classical criterion for aromaticity is chemical evidence in relation to benzene. "Benzene like" properties are: 1) thermal stability; 2) electrophilic substitution reactions,

rather than addition reactions; and 3) resistance to the oxidation. However, there is a problem with criteria based on chemical properties. For example, anthracene, which is usually regarded to be aromatic, often undergoes addition reactions to give 9, 10 addition products under mild conditions rather than substitution reactions.

The π-electrons of aromatic molecules are delocalized throughout the aromatic system. These delocalized π-electrons have a greater bonding energy than they would have if they had been isolated in localized double bonds. This energy difference is called the resonance energy (RE). So theoretically, it can be used as an aromatic criterion. However, there are problems in that the value of resonance energy calculated depends on the methods used and the reference system chosen.

Another criterion is the geometry criterion, which refers to the C-C bond length. In particular the bond lengths of aromatic rings are equalized by π-delocalization. Leroy[25] suggested that a molecule is aromatic if its C-C bonds are between 1.36 and 1.43 Å in length, while the molecule is a polyene if it has alternating bond lengths of 1.34 to 1.356 Å for the double bonds and 1.44 to 1.475 Å for the single bonds. However, this criterion obviously does not easily apply to heterocyclic and polycyclic systems, since the C-C bond lengths in thiophene are 1.352 and 1.455 Å. As well the X-ray data needed to apply this criterion are sometimes difficult to obtain. When X-ray data are not available, it is possible to estimate bond orders from coupling constants of proton NMR spectra,[26,27] however, this is not as good as having a bond length.

Now, the best method to describe whether a compound is aromatic is to use NMR spectroscopy to estimate ring currents.

1.1.6 Ring currents and NMR spectroscopy

We discussed above that the *p* orbitals of an aromatic compound are cyclically overlapped, so that the π-electrons are delocalized over the entire ring. In 1936, Pauling[28] proposed his "ring current theory". The induced ring current produces a secondary magnetic field which is opposed to the applied field inside the ring and reinforced outside the ring (**Figure 1.2**). The induced magnetic field reinforces the applied field outside the ring and thus the external protons of the ring are more deshielded than an analogous alkene. In contrast, the induced magnetic field opposes the applied field inside the ring and thus the inner protons of the ring are more shielded. The induced ring current is responsible for the large diamagnetic anisotropy exhibited by aromatic molecules. Elvidge and Jackman even defined an aromatic compound as "a compound which will sustain an induced ring current".[29]

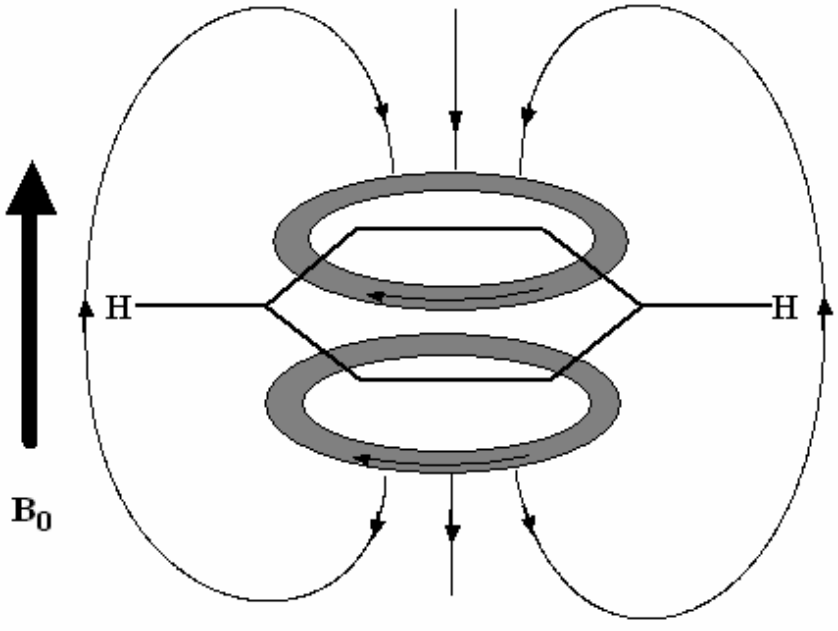

Figure 1.2 The induced ring current and magnetic field in benzene.

The induced ring currents can be detected experimentally by a proton NMR spectrum. The proton chemical shifts in a NMR spectrum can be related to the diatropicity and paratropicity of the system. Aromatic systems with (4n + 2) π-electrons are diatropic and thus protons outside the ring appear downfield and those inside the ring upfield. In contrast, 4n π-electron systems are called paratropic and they have the opposite effect, namely, protons outside the ring appear upfield and those inside the ring downfield.

There is no direct evidence to prove that ring currents exist at the molecular level. However, the ring current model is supported by a large amount of ^{1}H NMR data of annulenes. Benzene itself is a good example. It shows its proton chemical shift at δ 7.27,[30] which is about 1.5 ppm downfield from a typical vinylic proton. This extra deshielding is caused by the induced ring current.

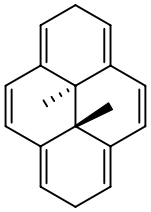

27

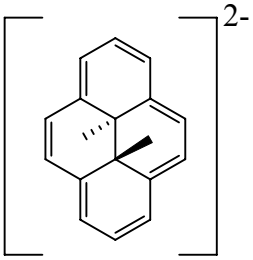

28

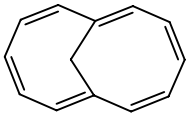

29

The bridged [14] annulene dimethyldihydropyrene **11** is another good example to show the diatropicity and paratropicity of (4n+2) and (4n) π-electron systems respectively. The proton NMR spectrum of **11** shows the deshielded external protons at δ 8.67-7.95, and the internal methyl protons shielded to δ -4.25.[9] This is about 5.2 ppm upfield compared to the noncyclically-delocalized model compound **27**. In contrast, the dianion **28** has 16 π-electrons, and is thus antiaromatic. The dianion **28**, shows a strong paratropic ring current in which the internal methyl protons are deshielded to δ 21 and

the external protons are shielded to δ -3.2 to -4.0.[31] Compound **29** also shows paratropic ring current effects. It is nearly planar and shows the bridge methano proton at δ 6.06.[32] These are strongly deshielded from typical allylic methylene signals at around δ 2.

In real molecules, various other factors as well as ring current can influence proton chemical shifts. Vogler[33] uses **Eq. 1.1** which takes into account of ring current and various other factors.

$$\sigma = \sigma^{RC} + \sigma^{LA} + \sigma_{\mu}^{0} + \sigma_{v}^{q} \qquad \textbf{Eq. 1.1}$$

Where

σ = the total chemical shift

σ^{RC} = shift due to ring current

σ^{LA} = shift due to local anisotropy

σ_{μ}^{0} = zero of chemical shift scale

σ_{v}^{q} = shift due to excess π-electron density

In charged systems and heterocycles, shielding from local anisotropy and from perturbations in the π-electron density can be equally important as ring current.[34]

The chemical shift of the protons of the cyclopentadienyl anion (**3**) is δ 5.6.[35] This is close to that of a typical alkene because the negative charge shields the protons by almost same amount that the aromatic ring current deshields them. In contrast, the positive charge in tropylium ion (**4**) has an additional deshielding effect resulting in a shift to δ 9.2,[32] which is about 3.4 ppm downfield from a typical alkene.

The charge effect can also be seen in heterocycles and is complicated. The proton chemical shifts of pyridine (**15**) are at δ 8.50-7.46.[36] The nitrogen atom in pyridine replaces a carbon atom in benzene. The electronegativity of the nitrogen atom is larger

than that of a carbon atom, and thus the nitrogen atom withdraws electrons from the carbons, which has a deshielding effect. This is proved by the dipole moment of **15** which is polarized towards the nitrogen. In pyrrole (**16**), the nitrogen atom contributes two electrons to the aromatic π system. The ring is thus more electron rich than in pyridine, and the proton chemical shifts (7.7 – 6.05)[36] are upfield of those of pyridine (8.50-7.46).

In 1978, Haddon[37] proposed that the ring current of an annulene relates to its resonance energy (**Eq. 1.2**).

$$RE = \pi^2 RC/3S \qquad \textbf{Eq. 1.2}$$

Where RE is resonance energy; RC is ring current; and S is the area of the ring.

1.1.7 Mitchell's method to estimate ring currents and hence resonance energies or aromaticities

There is no doubt that NMR is the most popular way to study diamagnetic compounds. Proton chemical shifts can be related to the diatropicity or paratropicity of the system, and thus are used to determine whether a molecule is aromatic or antiaromatic. However, determining the degree of aromaticity is more difficult because the chemical shift is affected by factors other than the ring current alone.[33]

In annelated anulenes, the relative contribution of the ring currents of the fused fragments to the overall ring current depends on the resonance energies of the fragments.[12, 37, 38] In another words, an annelating ring determines the delocalization in the other rings in fused aromatic systems. Thus we can estimate this effect by observing the effects of the ring current in each ring. Based on this and the fact that coupling constants are propotional to the bond orders, Günther[39] used benzene as a probe to estimate aromaticity of several annulenes fused to benzene. He used an HMO calculation

of the ratio of the adjacent bond orders. However, it is not that easy to analyze the AA′BB′ set of coupling constants in the benzene ring.

A simple method, involving only chemical shifts to estimate the relative aromaticity was developed by Mitchell[41] using dimethyldihydropyrene (DHP, **11**) as the probe. The DHP **11**, which was originally reported by Boekelheide[9], is a good probe of aromaticity. It is a fully delocalized, planar molecule, in which the internal methyl groups are rigidly held above and below, almost at the center of the molecule and the π-cloud.[41] The internal methyl protons are strongly shielded to δ -4.25. This chemical shift is not affected much by substituents (<0.3 ppm). However, it is remarkably affected by fusion of an aromatic ring on the side. The through space magnetic effect of the annelating ring on these internal protons is also small (<0.1ppm).[42]

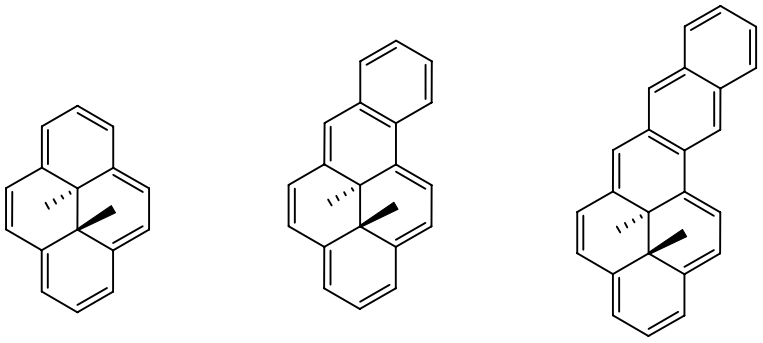

11 **30** **31**

δ(Me) -4.25 -1.62 -0.44

$$\frac{\text{RE(Naphthalene)}}{\text{RE(benzene)}} = \frac{\Delta\delta(\text{Naphth})}{\Delta\delta(\text{Benz})} = \frac{4.25\text{-}0.44}{4.25\text{-}1.62} = 1.45$$

Scheme 1.5 Mitchell's method to determine relative aromaticity

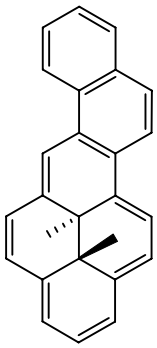

32

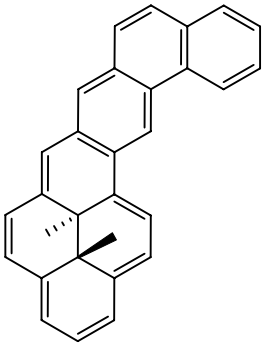

33

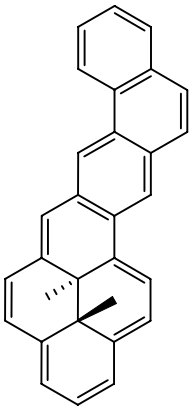

34

Mitchell has shown that the change in chemical shift of the internal methyl protons from that in **11** is proportional to the resonance energy (or more strictly, the bond localization energy, BLE) of the annelating aromatic ring. Then, if different aromatic moieties other than benzene are fused to DHP, and the internal methyl proton chemical shifts are compared to those when benzene is fused, the resonance energy (or more strictly, the bond localization energy, BLE) of the fused ring can be estimated relative to that of benzene (**Scheme 1.5**).[42] **Table 1.1** gives some calculated relative resonance energies determined by this method. They correlate well with Dewar resonance energies.

Mitchell derives the **Eq. 1.3**.[42]

$$BLE = [4.18 + \delta(Me)]/2.59 \qquad \textbf{Eq. 1.3}$$

Where: $\delta(Me)$ is the average chemical shift of the internal methyl protons

BLE is the Dewar bond localization energy of the annelating aromatic (Ar) relative to benzene (BLE of benzene is 1.00 = 0.869 eV).

Table 1.1. Comparison of experimentally estimated values of BLE from ((Ar)/(Bz)) with Dewar resonance energies values

compound	Annelating arene	((Ar)/(Bz))	Dewar value
30	benzene	1	1
31	2,3-naphthalene	1.45	1.52
32	1,2-naphthalene	0.56	0.52
33	2,3-phenanthrene	1.28	1.22
34	2,3-phenanthrene	1.27	1.22

We have discussed above that the Mitchell method worked well on the [a]-fused series. The method can be used in the [e]-fused series, too. The [e]-fused aromatics **35-38** was studied and there is a near linear relationship between BLE (Dewar) and the internal methyl proton chemical shift ((Me) (**Eq. 1.4**).[43]

$$BLE = [3.39 + \delta(Me)]/2.24 \qquad \textbf{Eq. 1.4}$$

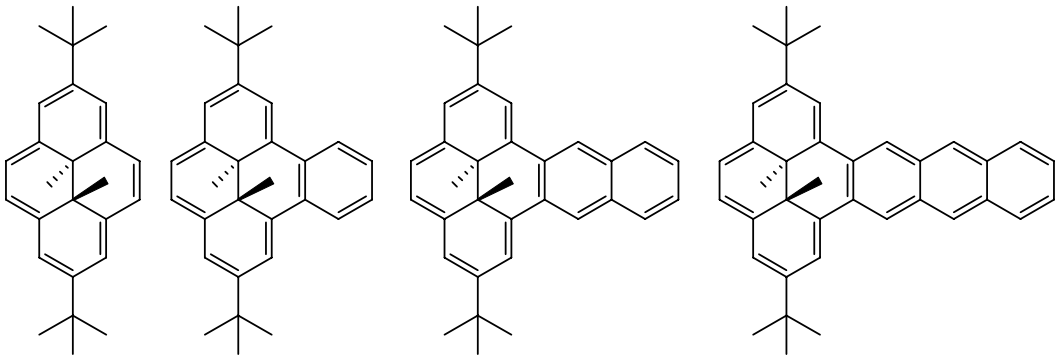

35 **36** **37** **38**

1.2 Objectives

Mitchell's method[42, 43, 54] was used to estimate strong aromaticity successfully. We are interested to apply this method to antiaromatic and weakly aromatic molecules. Thus our goals are as follows:

- To synthesize antiaromatic ring fused dihydropyrenes such as cyclopentadienone fused dihydropyrene.
- To investigate the bond-fixing ability of the antiaromatic ring and measure the bond-fixing ability relative benzene.
- To synthesize fulvene fused dihydropyrenes and investigate aromaticity in these weakly diatropic systems.

1.3 Syntheses

1.3.1 Synthesis of 2,7-di-*t*-butyl-*trans*-10b,10c-dimethyl-10b,10c-dihydropyrene 35

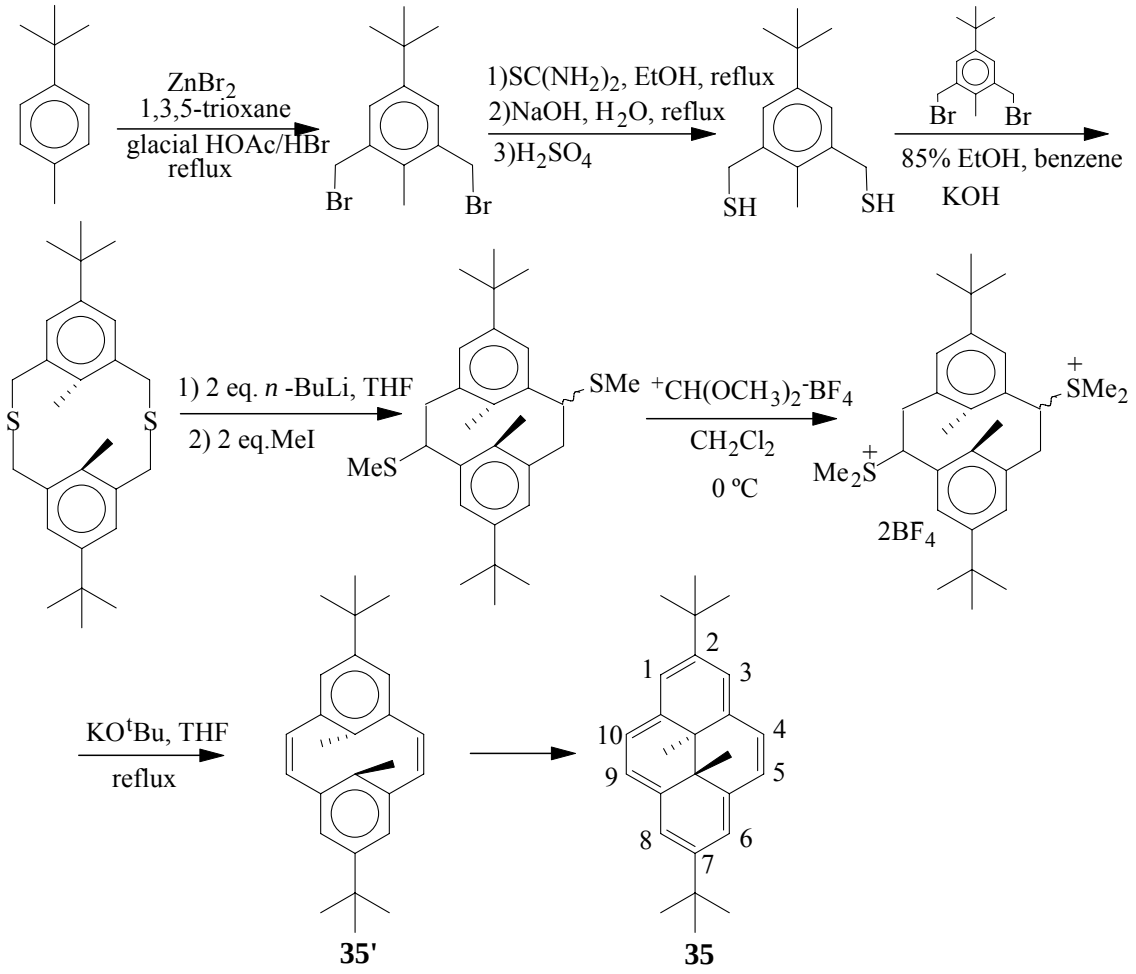

Scheme 1.6 Synthesis of DHP 35.[44]

The synthesis of our starting material, 2,7-di-*t*-butyl-*trans*-10b,10c-dimethyl-10b,10c-dihydropyrene **35**, was modified from that of Tahiro,[44] and is shown in **Scheme 1.6**. This method requires formation of a cyclic thioether typically by high dilution methods. In subsequent steps, the sulphur is first extruded to form the C-C bond, and then the sulphur bearing residue is eliminated to form the C=C. The overall yield is ~ 28%.

1.3.2 Syntheses of the cyclopentanone-fused dihydropyrene 43 and cyclopentadiene-fused dihydropyrene 45

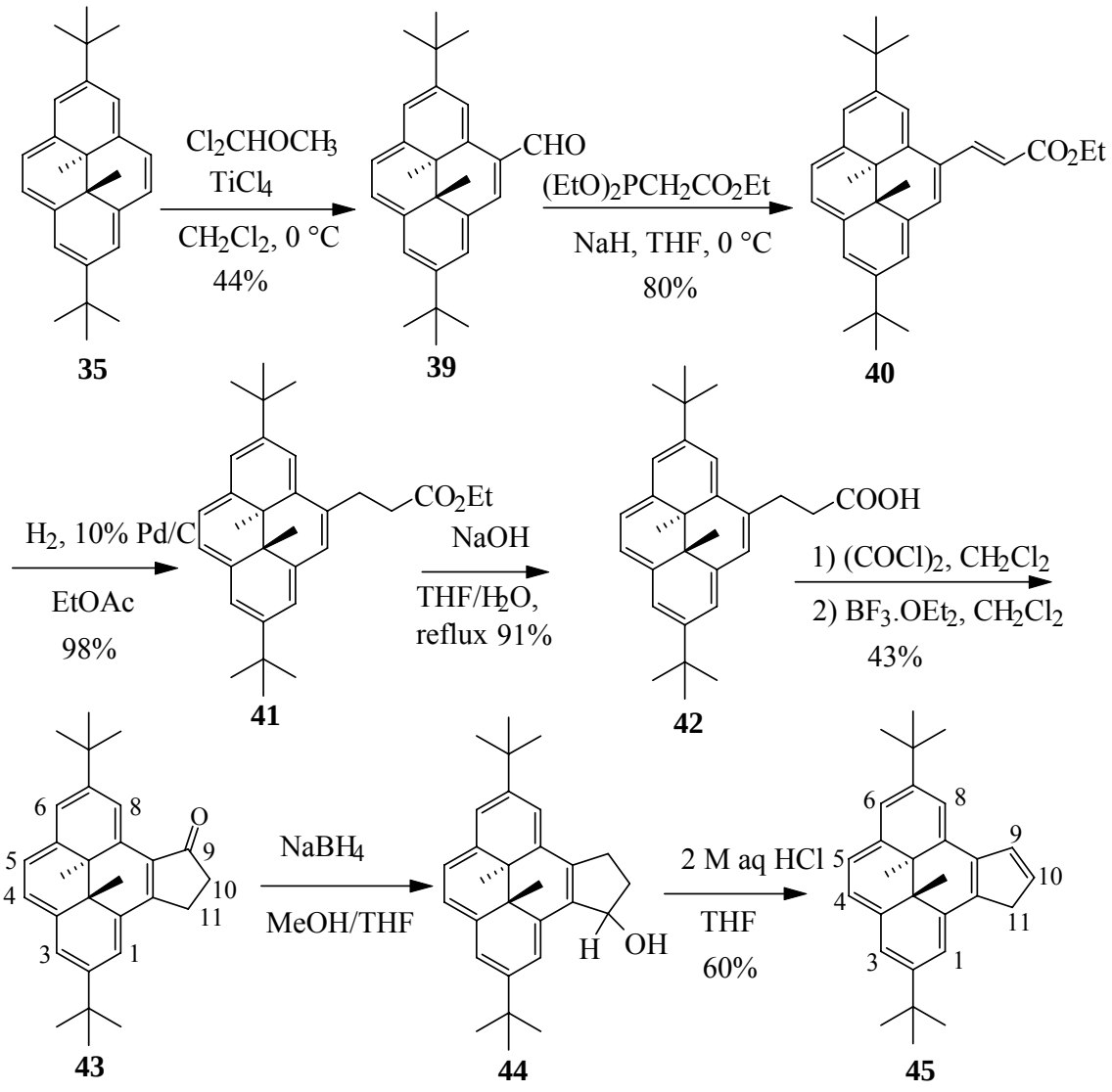

Scheme 1.7 Syntheses of cyclopentanone fused DHP 43 and CpDHP 45.

The synthesis of cyclopentanone-fused dihydropyrene **43** was reported by our group.[45] It is a five step synthesis from DHP **35** and the total yield is around 13% (**Scheme 1.7**). Cyclopentadiene-fused dihydropyrene (CpDHP) **45** can be obtained in two more synthetic steps from ketone **43** (**Scheme 1.7**).

1.3.3 Synthesis of cyclopentadienone-fused dihydropyrenes 46 and chloro derivative 47

1.3.3.1 Dehydrogenation of cyclopentanone-fused dihydropyrene

As mentioned above, the cyclopentanone-fused dihydropyrene **43** has been made by our group.[45] Therefore; in principle all that is required to synthesize **46** is to introduce the additional double bond into **43** (**Scheme 1.8**).

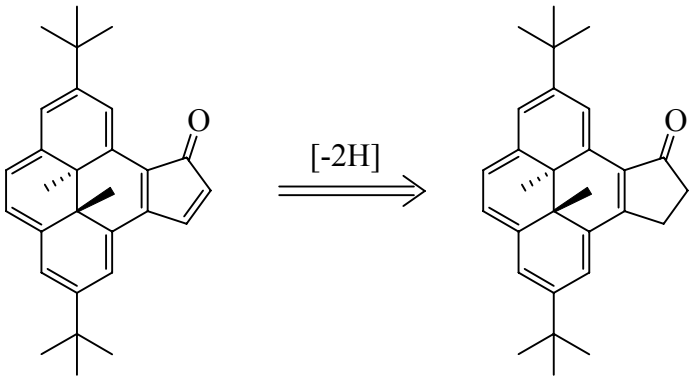

46 **43**

Scheme 1.8 Retrosynthetic strategy for 46.

There are several methods of making enones from the corresponding ketones, such as the well known 1-hydroxy-1,2-benziodoxal3(1H)-one-1-oxide (IBX).[46] But because dihydropyrenes are very reactive to electrophiles and oxidizing reagents, the choice of reagents needs to be selective to avoid the oxidation of that ring. The mild conditions used by Engman, in which $PhSeCl_3$ is used to introduce the $–SeCl_2Ph$ moiety to the α-position of the carbonyl group followed by elimination with mild base seems the first choice. Thus, reaction of **43** with $PhSeCl_3$ in ether at 0 °C for 1 h, followed by treatment with aqueous $NaHCO_3$ at 20 °C for 4 h, yielded at least six products, however, only 23% of the 5-chlorocyclopentadienone **47**, 26% of the 5-chlorocyclopentanone **48**, a trace of

cyclopentadienone **46** (was not obtained pure here but see below) and starting material **43** could be isolated by chromatography (**Scheme 1.9**).

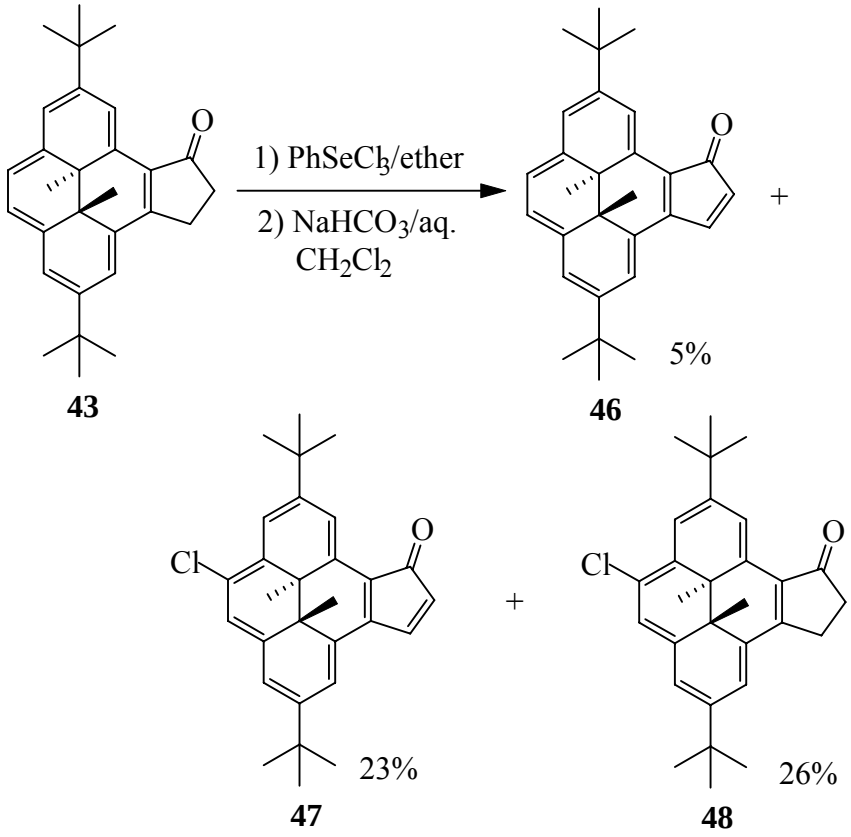

Scheme 1.9 Syntheses of 47 and 48.

The structure of **48** was indicated by electron ionization mass spectrometry (EI MS) at *m*/*z* 432 and 434 in a 3:1 ratio, indicating the presence of chlorine, and high-resolution mass spectrometry (HRMS) at 432.2227 (calcd for $C_{29}H_{33}ClO$ = 432.2220). Only five dihydropyrene ring protons could now be seen, indicating that this chlorine was on the dihydropyrene ring. Two-dimensional NMR proved that **48** was the 4-chloro isomer, and in fact it was the only isomer obtained. Fully assigned spectral data are given in the Experimental Section. The structure of **47** was again indicated by EI MS M and M + 2 signals in a 3:1 ratio at two mass units less than for **48**, with the HRMS at 430.2066

(calcd for $C_{29}H_{31}{}^{35}ClO$ = 430.2063). New alkene signals were found at δ 8.09 and 6.21, which were coupled with J = 5.8 Hz, corresponding to protons H-11 and H-10, respectively. They are just slightly different from **46** shown above. As well, one =CH DHP carbon was replaced by a =C-Cl carbon.

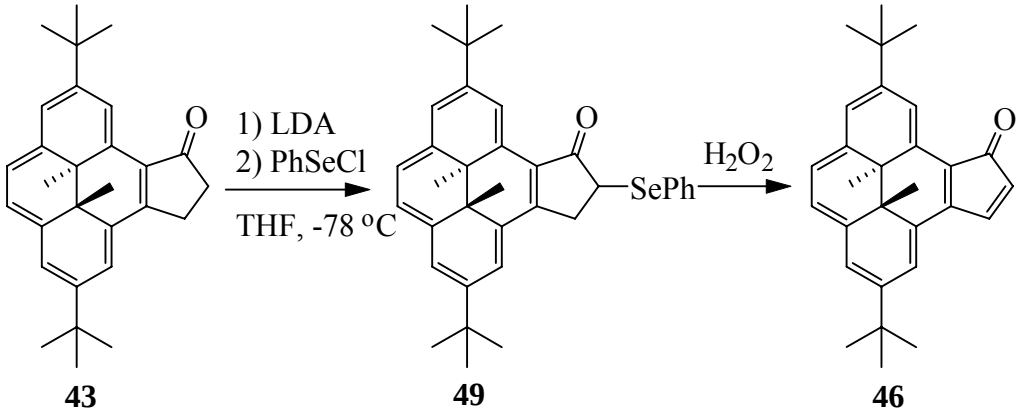

43 **49** **46**

Scheme 1.10 Synthesis of 46.

Because $PhSeCl_3$ is also a good chlorinating reagent,[48] side reactions took place on using Engman's procedure as shown above.[47] We thus tried an alternative route used by Sharpless et al.[49a] In this procedure, PhSeCl, instead of the chlorination reagent $PhSeCl_3$, is used to introduce the -SePh moiety to the α-position of the carbonyl group, which then can subsequently be oxidatively eliminated to the enone. However, direct use of PhSeCl in THF on **43** did not yield any useful product. We then tried Reich's procedure,[49b] in which the enolate is preformed with lithium diisopropylamide. The enolate is then reacted with PhSeCl in tetrahydrofuran (THF) and then with H_2O_2, which gave the desired product **46** in 28% yield (**Scheme 1.10**). The reason for the low yield might be because the enolate of **43** is not stable. In the literature, the time for generation of the enolate is 1 h. In our experiment, the time between the lithium diisopropylamide and PhSeCl addition was 5 min. A longer time resulted in a lower yield. Compound **46** is very

unstable when isolated. It decomposes on standing. However, after treating with molecular sieves, it can be stored in the solid state in the fridge for a couple of months. This is probably because traces of H_2O_2 remain which were removed by molecular sieves.

The overall structure of **46** was indicated by the electron ionization mass spectrometry (EI MS) with a molecular ion at *m/z* 396 (M^+), high resolution mass spectrometry (HRMS) at 396.2452 (Calculated for $C_{29}H_{32}O$: 396.2453) and by the change in the IR spectrum which now showed a conjugated ketone C=O stretch at 1661 cm^{-1} rather than 1681 cm^{-1} in **43**. In the ^{1}H-NMR spectrum, the internal methyl protons appeared at δ -1.91 and -1.87. New alkene signals were found at δ 8.07 and 6.18 with coupling constant of 5.7 Hz corresponding to H-10 and H-11. The coupling constant value is consistent with a *cis* alkene. The ^{13}C NMR spectrum showed loss of the two -CH_2- carbons of **43** but two new =CH carbons corresponding to C-10 and C-11. The ketone carbon was seen at δ197.34. The elemental analysis (C = 87.96% and H = 8.09%), (calculated: C = 87.83%, H = 8.13%), also confirms the structure.

1.3.3.2 Intramolecular *trans* Friedel-Crafts cyclization

The problems for the dehydrogenation procedures include low yields and a hard separation of product from by-products and starting material, because they all have very similar structures and polarities. Since the saturated ketone **43** was made by an intramolecular Friedel-Crafts cyclization route,[45] we thought it might work for **46** too. The *trans*-unsaturated ester **40** was an intermediate for making **43**, its hydrolysis to the unsaturated acid **50** should be easy. Even though cyclization of the *trans*-isomer of **50** would not be predicted to be unlikely, the DHP ring is very electron rich and so might help the *trans-cis* isomerization. So the intramolecular cyclization of **50** might be

possible. Thus the hydrolysis of unsaturated ester **40** to unsaturated acid **50** followed Fan's procedure (**Scheme 1.11**).[45] Around 20% of starting material stayed unchanged and was recovered. This hydrolysis seemed like an equilibrium reaction, since the yield didn't change much by extending the reaction time. The disappearance of the triplet (δ = 4.37) and quartet (δ = 1.41) of the ester group on the ^{1}H-NMR spectrum proved the success of the hydrolysis. The coupling constant of 15.5 Hz for the two alkene hydrogens (δ 6.90 and 9.31) indicated a *trans* isomer. As well, in the IR spectrum a strong and broad absorption at 3400-2400 cm^{-1} and a strong absorption at 1681 cm^{-1} confirmed the presence of an unsaturated carboxylic acid. The mass spectrum (EI) with a molecular ion at *m/z* 414 (M^+), further confirmed the structure of **50**.

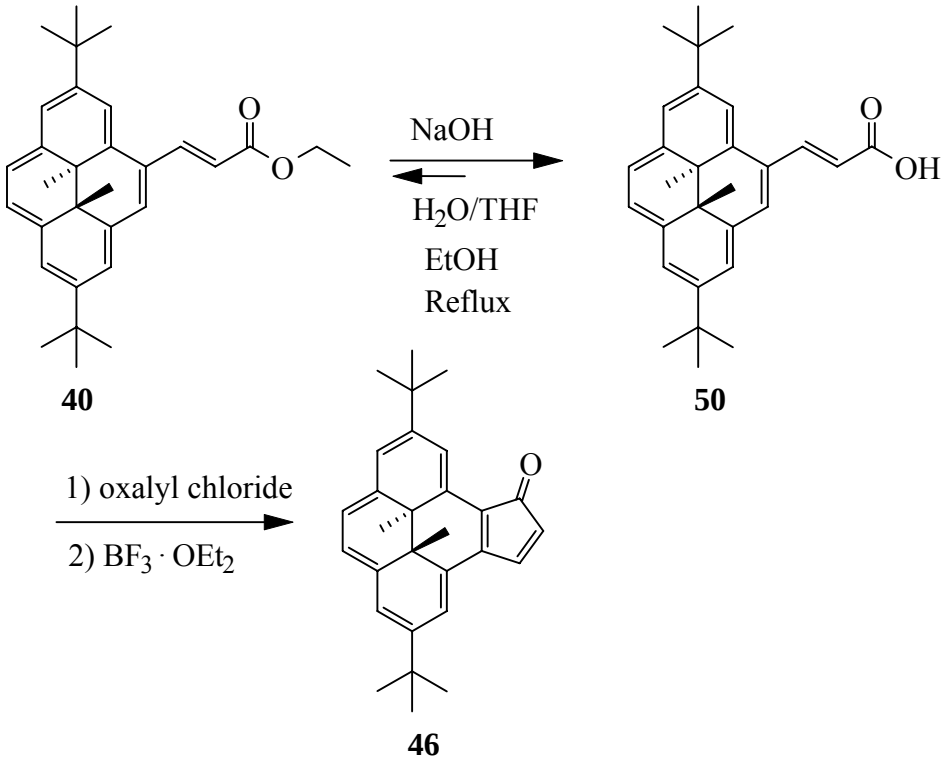

Scheme 1.11 Intramolecular *trans* Friedel-Crafts cyclization.

The Friedel-Crafts cyclization also followed Fan's procedure for the saturated acid.[45] Namely, the acid **50** was first converted to acid chloride with excess oxalyl chloride, which was then directly cyclized with BF_3 etherate (**Scheme 1.11**). This yielded 80% of **46** as a green crystalline solid.

It was a surprise to us that the intramolecular Friedel-Crafts cyclization went smoothly, although we hoped it would. A possible mechanism for that was shown in **Scheme 1.12**. The intermediate II is stabilized by the very electron rich dihydropyrene ring, which could either go to the *cis*-intermediate III or go back to the *trans*-intermediate I. From the *cis*-intermediate III, the cyclization could proceed.

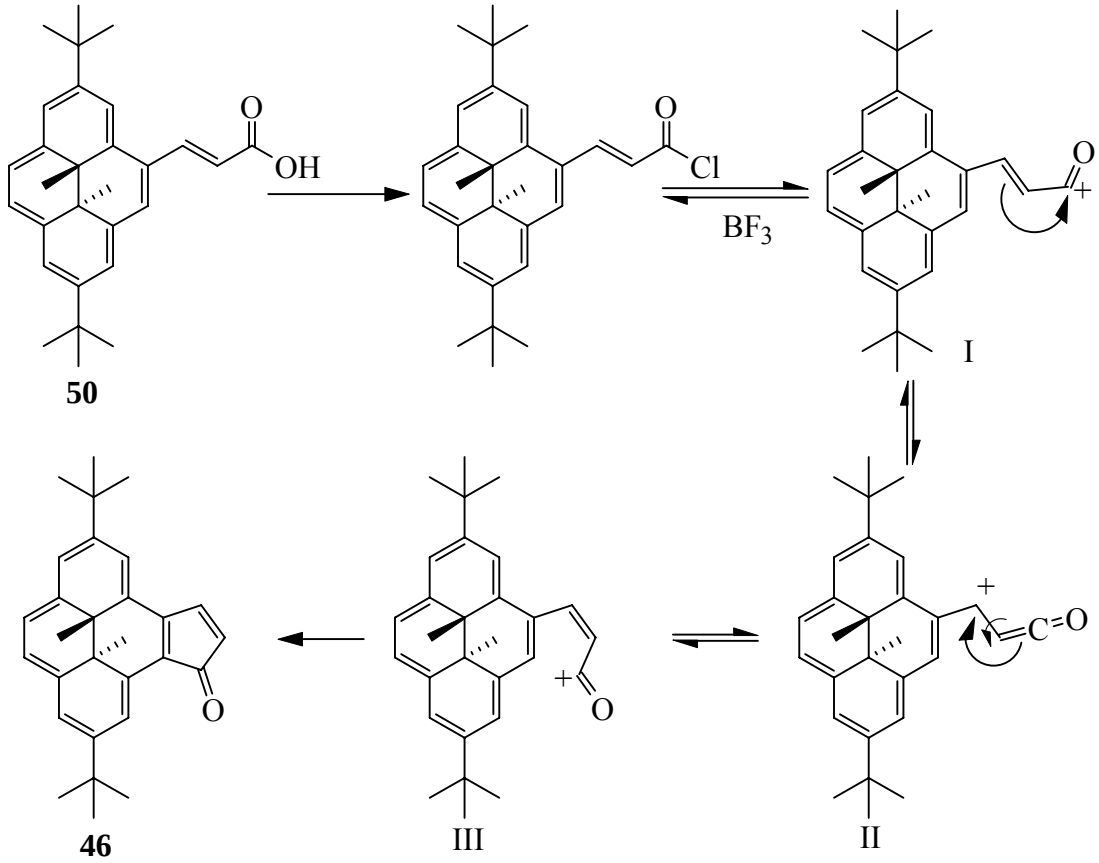

Scheme 1.12 The mechanism of intramolecular Friedel-Crafts cyclization.

We proposed the mechanism above in which the *trans* alkene can undergo the intramolecular Friedel-Crafts cyclization reaction because of the electron richness of the DHP ring. If that is true, then the similar cyclization reactions would happen for the electron rich benzene derivatives, such as cinnamic acid derivatives which have electron donating groups. Thus, we tried to synthesize indenones from 3-methoxycinnamic acid **51** and 4-methoxycinnamic acid **52**. The NMR of the crude product showed that some indenones **53** was produced using $SnCl_4$ as catalyst (**Scheme 1.13**) following the way to make **46** but failed to obtained pure **53** because of the lack of stability. This confirmed our proposed mechanism above (**Scheme 1.12**).

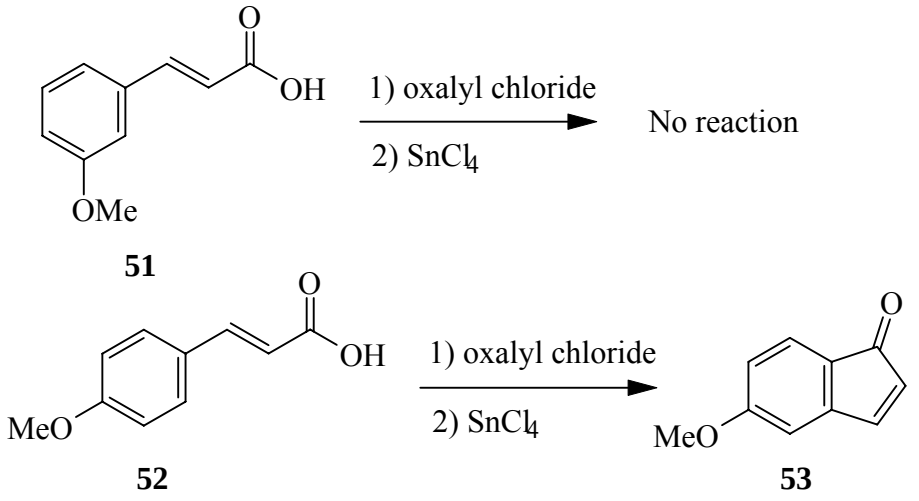

Scheme 1.13 Syntheses of indenones by cyclization.

1.3.4 Fulvane and fulvene fused DHP systems

1.3.4.1 Fulvane fused DHP 54

The Wittig reaction is generally a good olefination reaction. Thus, cyclopentanone-fused dihydropyrene **43** reacted smoothly with $(Ph)_3P{=}CH_2$ to give 70% yield of fulvane-fused dihydropyrene **54**, in which $(Ph)_3P{=}CH_2$ is prepared *in situ* from *n*BuLi and

methyltriphenylphosphonium bromide in THF (**Scheme 1.14**). The structure of **54** was confirmed by its proton NMR spectrum. The two protons on C-12 are different. The chemical shift of the proton (H_a) pointing toward the DHP ring (δ 6.46) was ca. 0.77 ppm downfield from that of the other proton (H_b) pointing away from the DHP ring (δ 5.69). This was because H_a is in the deshielding zone of the DHP ring current, while H_b is not. Both of them are split by each other and the two H-10 protons. H_a is also through space coupled to H-1 as shown in the 2D NOESY NMR spectrum. However, because all of these coupling constants are small and similar, the peaks overlap and both Ha and Hb just appear as a triplet. The two H-10 protons are coupled to both Ha, Hb and the two H-9 protons and appear as a multiplet from δ 3.18 to 3.06. The two H-9 protons have different chemical shifts. They are split by each other and the two H-10 protons and appear as two multiplets from δ 3.69 to 3.64 and from δ 3.59 to 3.53 respectively. H-1 appeared at δ 9.39, as usual shifted downfield from other DHP protons, because of the anisotropic effect of the double bond. The ^{13}C NMR DEPT spectrum also clearly showed the new $=CH_2$ carbon peak at 106.5 ppm. The overall structure of **54** was also confirmed by mass spectroscopy shown in the Experimental section.

Compound **54** is not stable. It easily rearranges to form **55** (**Scheme 1.14**) and also easily decomposes. After the rearrangement, the chemical shifts in C_6D_6 of the internal methyl protons changed from δ -3.27 and -3.29 for **54** to -3.43 and -3.44 for **55**. The methyl group on the five member ring appeared as a doublet at δ 2.88 in the ^1H-NMR spectrum. We always obtained the mixture of **54** and **55** or decomposition occurred. We could not separate **54** and **55**. The NMR data was obtained from the mixture of **54** and **55**, as they are easily distinguished from each other.

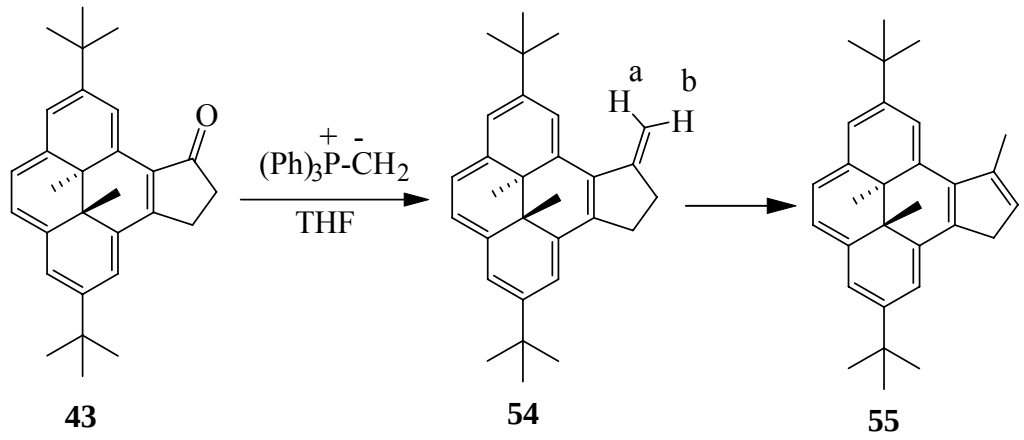

43 **54** **55**

Scheme 1.14 Synthesis of fulvane fused DHP 54 and its rearrangement.

1.3.4.2 Methylfulvene fused dihydropyrene 56

The cyclopentadienone fused dihydropyrene **46** was made and the bond localization in the DHP ring showed that the cyclopentadienone displayed antiaromatic character because of the strong electronegativity of the exo-oxygen (See **Section 1.1.4**). I was interested to see if when the oxygen atom was changed to a carbon atom, i.e. a change from a cyclopentadienone fused DHP to a fulvene fused DHP, the antiaromatic character of the five member ring would be lost and whether the DHP probe could still measure it.

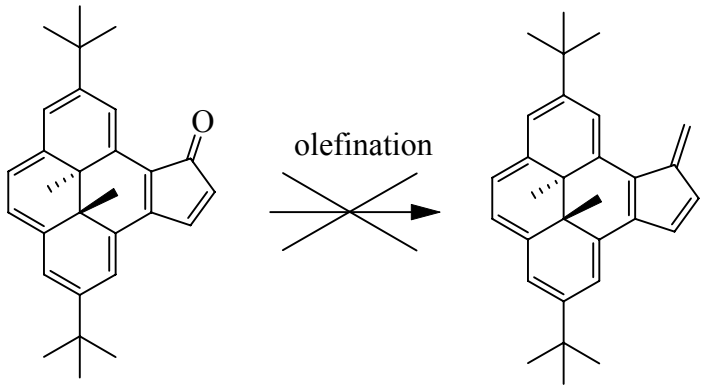

46 **59**

Scheme 1.15 Olefination of 46

Since the fulvane-fused DHP **54** can be easily made using the Wittig reaction, I thought the olefination reaction might work for fulvene-fused dihydropyrene **59** too. However, all attempts to make **59** by an olefination reaction failed. We tried the Wittig reaction, the Tebbe olefination reaction,[50] and Peterson olefination,[51] but all failed (**Scheme 1.15**).

Disappointed by the failure of the olefination reactions, I next tried condensation reactions to make fulvene-fused DHPs. I found that methylfulvene fused DHP **56** and phenylfulvene fused DHP **58** can be prepared from cyclopentadiene-fused dihydropyrene (CpDHP) **45** by either Ottoson's,[52] Shimizu's[53a] or Alper's[53b] procedure. Amongst these Ottoson's method gave the best results. Thus using Ottoson's procedure for preparing **56**, CpDHP **45** was reacted with excess $LiCH_2SiMe_3$ in toluene overnight at room temperature in the glovebox to produce a red suspension, which was then dried in vacuum. The pure LCpDHP **57** was obtained by washing the red residue with hexanes to remove the excess base (excess base would cause self-condensation of the acetaldehyde). The isolated pure LCpDHP **57** was removed from the glovebox in a Kontes flask and reacted with acetaldehyde in THF to yield methyl fulvene **56** in 68% as a dark brown solid. In the ^1H NMR spectrum of **56**, the internal methyl protons showed chemical shifts in C_6D_6 at δ -3.10 and -3.13 (they appeared at δ -3.52 and -3.55 in $CDCl_3$). Proton H-12 was split by the terminal methyl protons (H-13) and appeared as a quartet at 7.40 ppm, about 1.6 ppm downfield from normal alkene protons, which indicated that it sits very close to the DHP ring and strongly felt the ring current of the DHP. This was also confirmed by a strong through space coupling between H-12 and H-1 on the 2-D NOESY NMR spectrum. The methyl group avoids steric interaction with the DHP ring. These

methyl protons (H-13) appeared as a doublet at 2.14 ppm, which is normal. Proton H-8 appeared at δ 9.22 which is slightly downfield because of the deshielding by the C=C. Fully assigned data is given in the Experimental Section. It shows a strong NOESY with H-8. The mass spectrum (EI) also supported the structure of **56** by a correct molecular ion at *m/z* 408 (M^+) and a HRMS of 408.2814 (calculated for $C_{31}H_{36}$ = 408.2817).

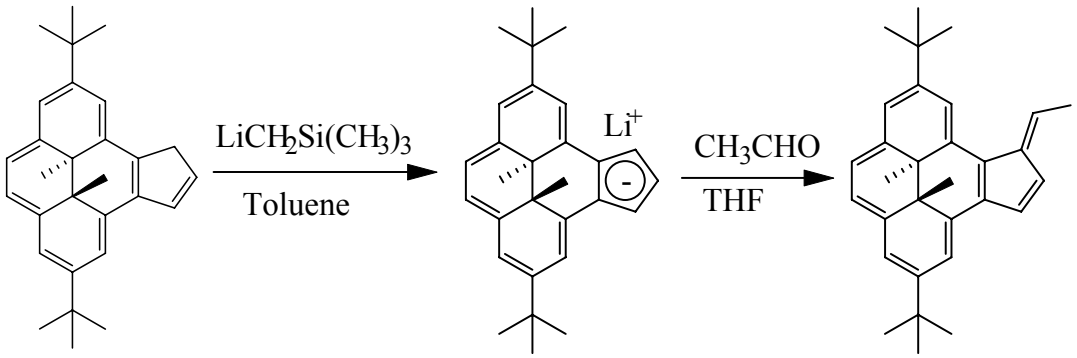

Scheme 1.16 Synthesis of methylfulvene fused DHP 56.

1.3.4.3 Phenylfulvene fused dihydropyrene 58

Phenylfulvene fused DHP **58** can also be made from cyclopentadiene-fused dihydropyrene (CpDHP) **45** by the one pot reaction following Ottoson's procedure.[52] The red suspension of anion **57** was made by reaction of CpDHP **45** with excess $LiCH_2SiMe_3$ in toluene overnight at room temperature and was used directly to react with benzaldehyde to yield the dark brown solid phenylfulvene fused DHP **58** in around 80% yield (**Scheme 1.17**). Phenylfulvene fused DHP **58** is not very stable. It decomposes in a couple of weeks in the solid state in the solid state in the fridge (-30 °C). The structure of **58** was confirmed by its analyses. In ^{1}H NMR spectra, the internal methyl protons of **58** appeared at δ -3.29 and -3.32 in $CDCl_3$, which is slightly upfield compared to those of **56**. Proton H-12 showed a singlet at 8.07 ppm. It is more than 2 ppm downfield from normal alkene

protons, somewhat greater than that of **56**. This is probably because of the anisotropic effect of the additional benzene ring. The chemical shifts of the protons on the phenyl ring were at δ 7.70, 7.48 and 7.34, respectively, which is in the normal range of benzene protons. Fully assigned NMR data are given in the Experimental Section. The mass spectrum (EI) also confirmed the structure of **58** by giving a correct molecular ion at *m/z* 470 (M^+), with the HRMS of 470.2982 (calculated for $C_{36}H_{38}$ is 470.2974).

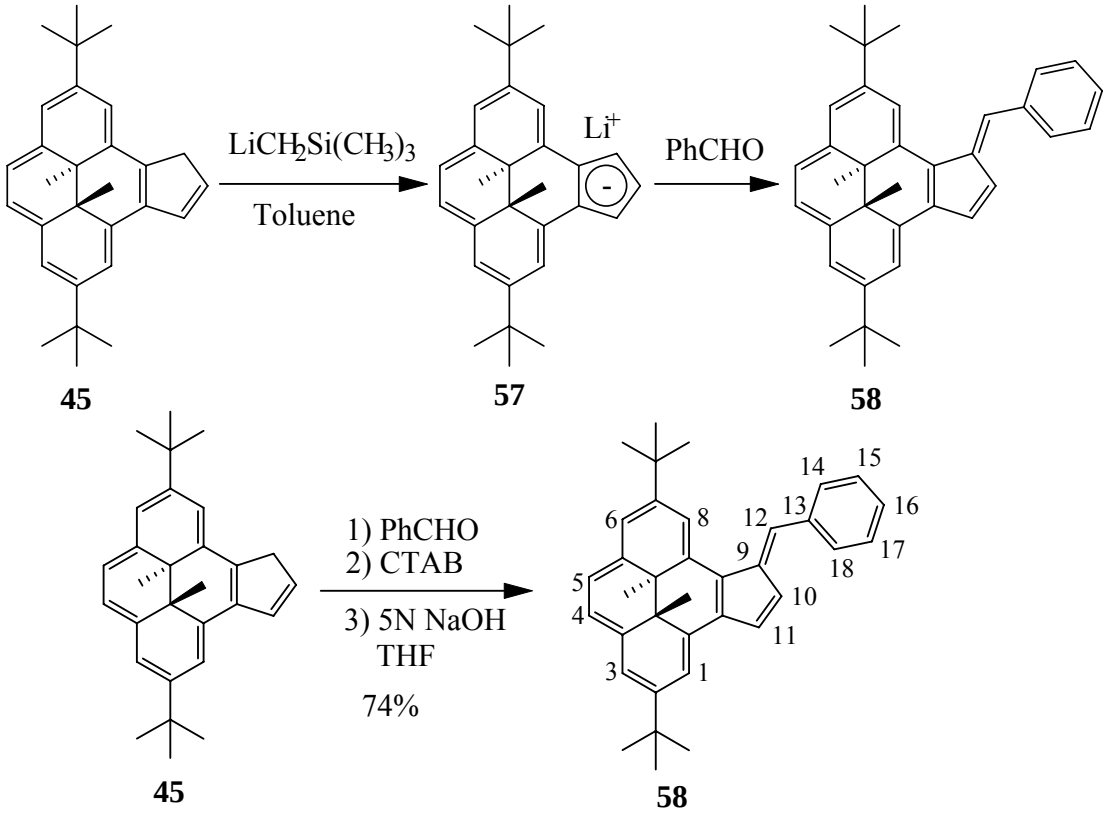

CTAB = cetyltrimethyl-ammonium bromide

Scheme 1.17 Synthesis of phenylfulvene fused DHP 58.

Compound **58** could also be made using Shimizu's,[53a] or Alper's[53b] procedure: reaction of CpDHP **45** in THF with benzaldehyde in NaOH aqueous solution in the

presence of phase-transfer catalyst cetyltrimethyl-ammonium bromide (CTAB) at 20 °C yielded 74 % of **58** as a dark brown solid.

We also tried to make the methylfulvene fused DHP **56** using Shimizu's[53a] and Alper's[53b] procedures. However, because of the basic conditions used, acetaldehyde underwent self-condensation and these self-condensed products, which are longer chain aldehydes, could also react with CpDHP to produce other fulvenes, causing lower yield (30%) and separation diffficulties from desired product **56**.

1.3.4.4 Attempts to synthesize the fulvene fused dihydropyrene 59

Inspired by the success of making **56** and **58** using Shimizu's[53a] and Alper's[53b] procedure, we launched the attempt to synthesize the parent fulvene-fused dihydropyrene **59.** Thus, reaction of CpDHP **45** in THF with formaldehyde in NaOH aqueous solution in the presence of the phase-transfer catalyst cetyltrimethyl-ammonium bromide (CTAB) at 20 °C yielded 37% of the alcohol **60** as a green solid, rather than **59**. The structure of **60** was confirmed by NMR spectroscopy. In the ^{1}H-NMR spectrum, both protons H-10 and H-11 were split by each other and by H-9 and appeared as doublets at δ 7.87 and 6.82 respectively, which are similar to the corresponding chemical shifts in CpDHP **45** (δ 7.90 and 6.63 respectively). H-9, on the other hand, was split by not only H-10 and H-11, but also by two H-12 protons, so appeared as a multiplet at δ 4.65 to 4.62. The two H-12 protons are different, with chemical shifts at δ 4.27 to 4.24 and 3.78 to 3.75 respectively. The chemical shift difference between these two diasterotopic protons is about 0.5 ppm, which is quite large. The IR spectrum further confirmed the structure of **60**. It showed the alcohol absorption at 3436 cm^{-1}. The mass spectra (LSI) also gave the correct molecular ion at *m/z* 412.2 (M^{+}).

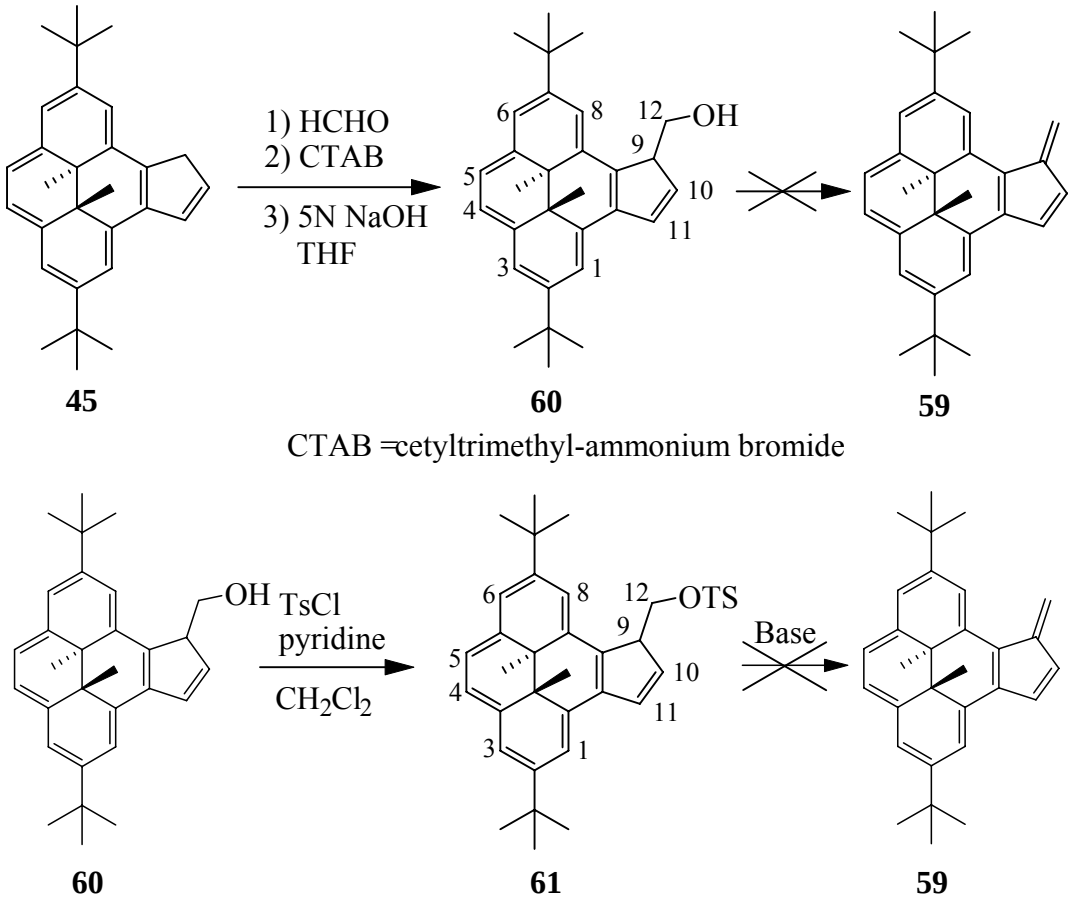

CTAB =cetyltrimethyl-ammonium bromide

Scheme 1.18 Attempts to synthesize fulvene fused DHP 59.

Because the elimination reaction of **60** to form **59** did not go under the reaction conditions, we thought that the tosyl group might be a better leaving group. Thus alcohol **60** was treated with excess tosyl chloride and pyridine in dry dichloromethane at room temperature to yield the tosylated compound **61** as a mixture of two isomers in a 1 to 1 ratio. In the ^{1}H-NMR spectrum of **61**, the chemical shifts for all the DHP and five-membered ring protons are similar to those of the corresponding alcohol **60**. The four protons on tosyl group appeared at 6.94 (2H) and 6.66(2H). Compound **61** was then used directly without purification in the elimination reaction. Unfortunately, the base catalyzed elimination reaction of **61** failed to yield **59**, but instead gave decomposed products.

1.3.4.5 Attempts to synthesize dimethyl and diphenylfulvene fused dihydropyrenes

The condensation reactions of CpDHP **45** with acetone and benzophenone both failed to yield any **62** and **63** respectively.

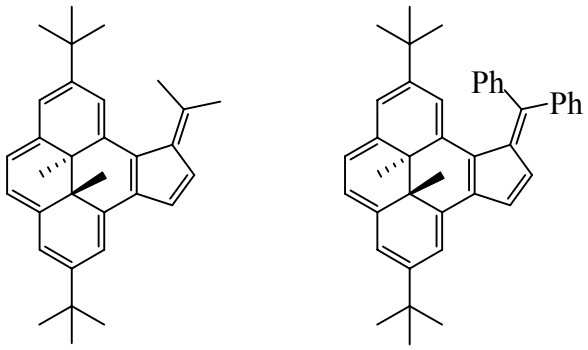

62 **63**

1.4 Results and discussion

1.4.1 Estimating antiaromaticity in cyclopentadienone-fused dihydropyrenes

1.4.1.1 Introduction

As we have mentioned previously, the Mitchell method[42, 43, 54] of estimating relative aromaticity is effective and good results are obtained with either the [a]-fused dihydropyrenes **30-34** or the [e]-fused dihydropyrenes **36-38**. Till now just the annelated aromatic (4*n* + 2)-π systems have reported. The question is then whether this can be extended to estimate antiaromaticity. In principle, the Mitchell method should also work when Ar is a 4*n*-π species. So far, the only example to investigate the ring current effect by a paratropic ring was reported by Scott et al.[55] In that work it was first shown unambiguously that fusion of a 4*n*-π system to a (4*n* + 2)-π system results in a reduction in the ring current in each. Thus the bridge protons of **65** are 1.6 ppm less deshielded than

those of **64** because of the reduction in the paratropic ring current of the 12π ring of **65** on benzannelation.

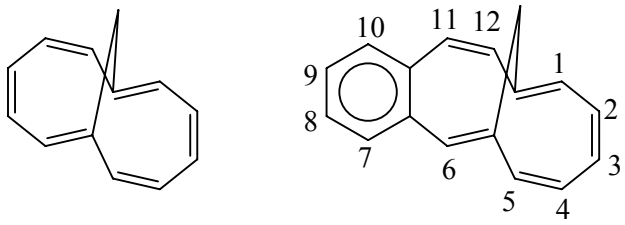

64 **65**

Likewise, the outside olefinic signals of the [12]-ring (H-1,2,3,4) of **65** (δ 5.6-6.2) are less shielded than those in **64** (δ 5.1-5.8). As well, the benzene ring diatropicity is reduced; its protons appear shielded at δ 6.78-7.14, with the two protons H-7,10 being most shielded. Scott estimates that benzannelation of **64**, reduced its paratropic ring current by about 40-50%. Estimating the magnitude of the change in ring current caused by the [12] π-ring on the benzene ring is more difficult. To quantify these results so that a comparison of the relative bond-localizing abilities of benzene and the 4*n*-π system (which we will loosely translate to aromaticity and antiaromaticity) may be made, then a common probe must be used. Dihydropyrene is in our view the best such probe, and so we synthesized **46**, where the fused aromatic ring equals cyclopentadienone. As we discussed above, the cyclopentadienone has the 4*n*-π resonance contributor shown in **23b** because the exo oxygen is electronegative. Thus compound **46** has the 4n-π resonance contributor shown in **46c** (**Scheme 1.19**). Compound **46** was compared to the analogous benzannelated system **36**.

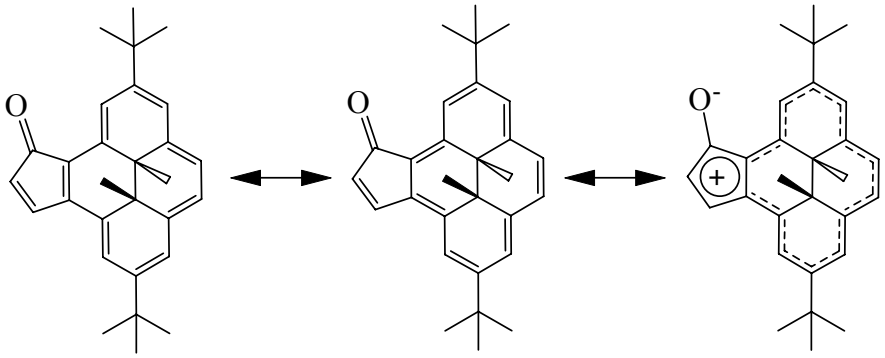

46a **46b** **46c**

Scheme 1.19 Resonance structures of 46.

1.4.1.2 Relative antiaromaticity

The relevant data for comparison are collected in **Table 1.2**. For dihydropyrenes, we have found that ^{1}H data give more reliable analyses than ^{13}C data, which however, should show the same general trends. Immediately evident from **Table 1.2** is that the chlorine atoms in both **47** and **48** (compare to **46** and **43**, respectively) have minimal effect on the internal methyl protons, consistent with our previous statements about substituents,[40, 42, 43, 54, 56] while introduction of the conjugating double bond into the five-membered ring has a huge effect. The magnitude of the ring currents flowing in the dihydropyrene rings can be taken as proportional to the chemical shift difference between the internal methyl protons for the annulene selected and a nonconjugated model, for example, **27**, where the internal methyl protons appear at δ +0.97[56a] (the *tert*-butyl groups are not expected to affect this shift significantly). However, because the cyclopentanone-fused annulenes **48** and **43** do not have *exactly* the same chemical shift as the parent **35**, then **47** must be compared to **48**, and **46** to **43**, rather than everything to **35**.

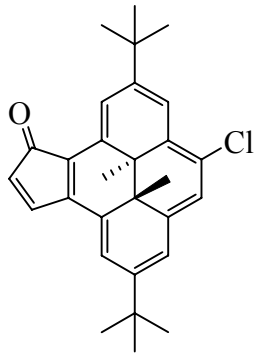

47

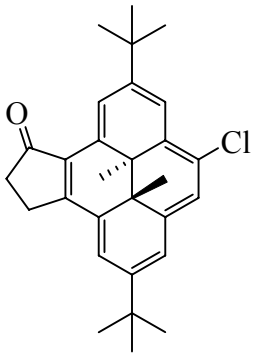

48

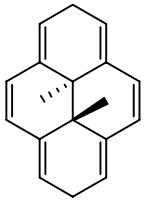

27

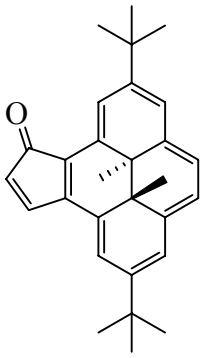

46

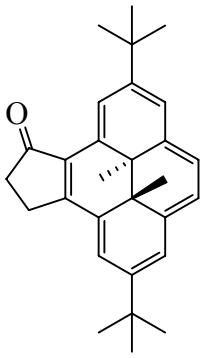

43

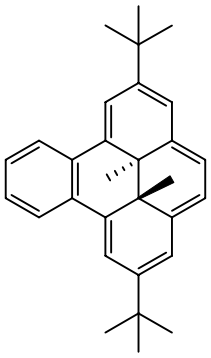

36

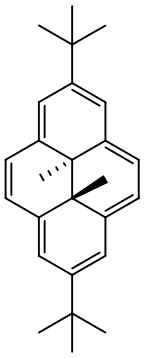

35

The effects of the cyclopentadienones in **47** and **46** on the ring currents of the cyclopentanone-fused dihydropyrenes **48** and **43** can then be calculated, for example, for the internal methyl protons of **47** as Δδ (**47 - 48**)/ Δδ (**27 - 48**) = 1.655/4.47 = 37%, and for **46** as Δδ (**46 - 43**)/ Δδ (**27 - 43**) = 1.835/4.70 = 39%. Likewise in **36**, benzene reduces the ring current in **35** by Δδ (**36- 35**)/ Δδ (**27 - 35**) = 2.48/5.03 = 49%. Thus cyclopentadienone has about 80% (=38/49) of the ability (effect) of benzene on reducing the ring current of dihydropyrene and, on the basis of our previous studies, [40, 42, 43, 54, 56] thus approximately 80% of the bond delocalization energy ("resonance energy") of benzene. While carbon shifts and external proton shifts in charged species[57] do not give such reliable indicators, it can be seen from **Table 1.2** that the trend is in the same

direction: the carbons of both **47** and **36** are less shielded than those of **48** and **35**. As well, the external protons H-4/5 of both **46** and **36** are less deshielded than those of **43** and **35**.

Table 1.2 NMR data (in $CDCl_3$) for comparison of ring currents

		47	**48**	**46**	**43**	**36**	**35**
^1H	δ (H-Me)	-1.86	-3.50	-1.91	-3.74	-1.58	-4.06
		-1.83	-3.50	-1.87	-3.71	-1.58	-4.06
	Δδ	1.64		1.83		2.48	
		1.67		1.84			
^{13}C	δ (C-Me)	21.03	15.57	21.54	15.40	17.3	14.3
		20.40	15.35	20.39	14.77		
	Δδ	5.46		6.04		3.0	
		5.05		5.62			
δ(H-4/5)				7.65	8.30	7.13	8.46
Δδ				0.65		1.33	
$J_{4,5}$ (Hz)				8.70	7.26	6.9[a]	7.3[a]

[a] Determined from nonconjugated nonsymmetric derivatives.

1.4.1.3 The paratropic ring current of cyclopentadienone

Fortunately Günther and co-workers[39,58] have unambiguously shown that when two (4*n* + 2)-π systems are fused (**A**, **Scheme 1.20**), the C2-C3 bond is shorter (the bond order is greater) than the C1-C2 bond (the total bond localization is as shown, with the ring junction being formally double, for resonance structure **46a**, **Scheme 1.19**), while when a 4*n*-π system is fused to a (4*n* + 2)- π system (**B**, **Scheme 1.20**), the reverse is true (note the ring junction is formally single, resonance structure **46b**, **Scheme 1.19**). This

has the effect that the C4-C5 bonds (arrowed) are also different (**Scheme 1.20**). In **A** (equivalent to the benz-fused system **36**) C4-C5 should be longer (lower bond order), and thus the coupling constant (**Table 1.2**) should be less than the parent **35**, which it is (6.9 versus 7.3 Hz), while in **B** (equivalent to the cyclopentadienone fused system **46**) C4-C5 should be shorter (the bond order greater), and thus the coupling constant should be larger than in parent **43** or **35**), which it is (8.7 vs 7.26 Hz). In my view, this leaves little doubt that the cyclopentadienone ring in **46** (and **47**) is behaving as an antiaromatic system. Günther and co-workers[39,58] have shown that their alterance parameter, *Q*, which equals the ratio of the bond orders of the benzene 9-10 and the 10-11 bonds, is <1.04 for antiaromatic systems, between 1.02 and 1.10 for nonaromatic systems, and >1.10 for aromatic systems. Unfortunately in **36** and **46** there is only one ^{3}J coupling in the probe (14π) ring, and so *Q* cannot be determined. However, in benzocycloheptatrienyl anion, a benzo-8π system, *Q* = 0.889 = antiaromatic according to his classification. In this case, the ^{3}J values involved were 7.84 and 7.10 Hz. The coupling constants in our cases, 8.7 and 6.9 Hz, are clearly different enough that little doubt remains that the aromaticity of the two π-systems of the cyclopentadienone and benzene annelating rings is quite different! The crystal structure data were clearly in agreement with the coupling constant data (See the crystal structure description below for more detail). A referee suggested that resonance structure **46b** could also be viewed as a [17]annulenone, which would have the same coupling constant consequences and IR data as described. That is true, but *if* the periphery conjugation was indeed the principal pathway, that is, really a [17]annulenone, then the total system is a 4*n*-π antiaromatic, and as such the internal methyl protons should be deshielded from those in the acyclic model **27**, that is, they should be at δ > 1.

We have shown this to be the case for other dihydropyrenes that are in total 4*n*-π species.[31,59] We therefore believe that **46** is best represented by **46c**, a fused cyclopentadienone-dihydropyrene system. Again, evidence from the crystal structure supports this (see below).

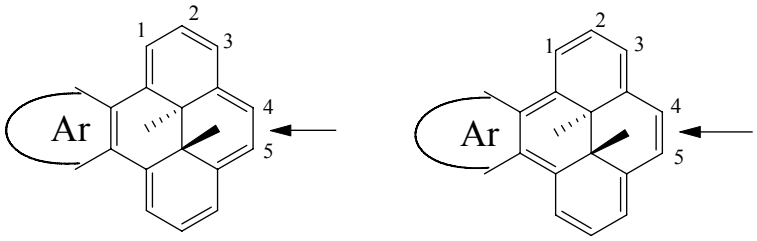

(4n+2)π-fusion, A **(4n)π-fusion, B**

Scheme 1.20 The bond alternation of (4*n* + 2)-π and (4*n*)-π fused DHP.

1.4.1.4 Computational studies

Nucleus independent chemical shifts (NICS), developed by Schleyer and co-workers,[60] are a powerful computational method to predict aromaticity and antiaromaticity. Schleyer et al. showed that aromatic systems have negative NICS values (e.g., -11.5 for benzene) while antiaromatic systems have positive NICS values (e.g., +28.8 for cyclobutadiene) and nonaromatics have values near zero (e.g., -2.1 for cyclohexane).[60a] It has more recently been demonstrated that NICS calculations are effective when applied on dihydropyrene systems.[54b] In this case the simple arithmetic average of NICS values ($NICS_{Av}$) calculated at the centers of the four six-membered rings (points 1-4, **Figure 1.3**) of the DHP nuclei gave the most reliable ordering of aromaticities of the DHP nucleus.[54b] Thus, we undertook a computational study of **43** and **46** here, to see what results were predicted for our system.

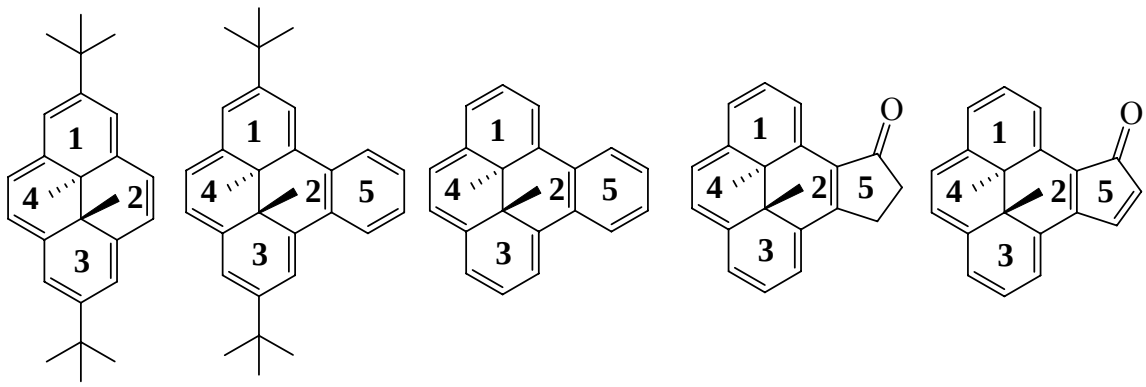

35 **36** **66** **67** **68**

Figure 1.3 Numbering scheme and location of the NICS points for DHPs nuclei. NICS points are shown in bold type.

Table 1.3 NICS values for compounds 35,[54b] 36,[54b] 43 and 46.

NICS	**43**[a]	**46**[b]	**35**[54b]	**36**[54b]
1	-13.62	-9.59	-18.91	-4.40
2	-13.57	-10.39	-17.66	-5.47
3	-13.77	-9.53	-18.91	-4.47
4	-14.01	-10.33	-17.66	-4.29
Av of 1-4	-13.74	-9.96	-18.29	-4.64
5	+3.82	+8.37	NA	-10.78

[a] the data was calculated from **67**. [b] the data was calculated from **68**.

All calculations were carried out by Dr. R. V. Williams (Univ. of Idaho) using a 6-31G* basis set, and the geometries for all of the compounds in this study were optimized using density functional theory (DFT with the B3LYP functional) as implemented in Jaguar 4.0.[61] Analytical energy second derivatives were calculated at the optimized

structures to confirm that these are minima. NICS values were calculated at the points shown using the Hartree-Fock (HF) GIAO method on the B3LYP/6-31G* geometry (GIAO-HF/6-31G*//B3LYP/6-31G*) with the Gaussian 94 suite of programs,[62] which is the same method as previous studies.[60, 54b] (NICS values are basis set dependent. Thus the same method must be used for comparison.) The NICS values were calculated at the centers of the five and six member rings, which are shown in **Figure 1.3**. The simple arithemetic average of the NICS values at points 1-4 were used as representative of the aromaticity of each DHPs, The larger negative NICS value indicating greater aromaticity. It has been shown that *t*-butyl substituents have a small effect on the NICS values, where the calculated NICS values for the 2, 7-di-^{t}Bu substituted DHPs, **35** and **36**, are similar to those of the corresponding 2, 7-dihydrogen DHPs, **11** and **66**, which lack the di-^{t}Bu.[54b] The differences between them are negligible.[54b] Thus, to simplify the calculations, we used the 2, 7-dihydrogen analogs of **67** and **68** instead of **43** and **46**.

Table 1.3 gives the calculated results for **43**, **46**, **35** and **36**. As can be seen, parent **35** has the most negative average NICS value, -18.29, and showed greatest aromaticity in the DHP ring. After fusion of the benzene ring, the average value dropped to the smallest negative value, -4.64, in these systems, indicating that benzene has the greatest aromaticity amongst these compounds. The aromaticity in the DHP ring was also dramatically reduced after cyclopentadienone fusion. The NICS average value for **46** dropped significantly to -9.96. Fusion of cyclopentanone also has some effect to the ring current of DHP. The average value is -13.74 for **43**. However, if **43** and **46** are compared, the average NICS value of **43** dropped from -13.74 to -9.96 for **46**, which clearly shows that the aromaticity of the DHP nucleus is reduced from **43** to **46**. This indicated that

there is a significant effect on introduction of the additional double bond into the five membered ring.

On the other hand, at point 5, the NICS value for the benzene ring in **36** was -10.78, indicating that benzene is still strongly aromatic. The NICS value for the cyclopentanone ring in **43** is + 3.82, which is small and near zero, indicating its non-aromatic character. However, the NICS value for **46** at point 5 was +8.37, which clearly shows its antiaromatic character. In conclusion, all the calculated results strongly support the antiaromatic character of cyclopentadienone.

1.4.1.5 The crystal structure of 43

The molecular structure of **43** was determined by X-ray crystallography. The molecular structure of **43** is shown in **Figure 1.4**. The bridge carbons C18-C21 were disordered above and below the molecular plane with refined occupancies of 80:20 %. The ketone was also disordered with a 91:9% refined occupancy. Only one contributor is shown here. The crystallographic data are summarized in **Table 1.4**. Selected bond lengths and bond angles for **43** are shown in **Table 1.5**.

As expected, the molecule is planar. The 17 carbon atoms for the DHP and five-member ring form almost a perfect plane with a maximum deviation of only 0.06 Å for C(6). The O atom lies in the plane too, only 0.02 Å (O(1A)) and 0.09 Å (O(1B)) out of it. The non-bonding distance between O(1A) and H(17A) is 2.44 Å (2.37 Å in a second molecule), smaller than the sum (2.72 Å) of the Van der Waals radius of hydrogen and oxygen, indicating there is an interaction between them. The two bridge carbons, C(18A) and C(20A), are +0.36 Å and -0.40 Å out of the plane respectively. The two internal

methyl carbons, on the other hand, are +1.91 Å and -1.94 Å above and below the plane respectively and are 3.95 Å from each other.

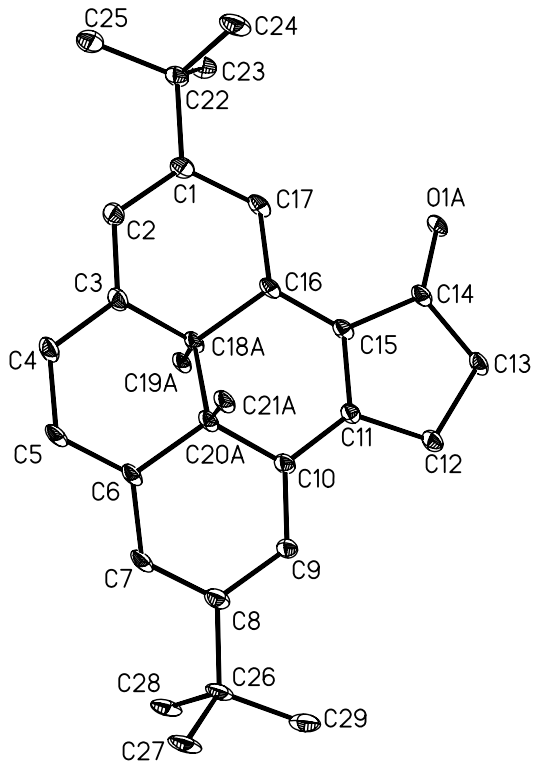

Figure 1.4 An ORTEP3 drawing[63] of complex 43 (30% probability thermal ellipsoids. Hydrogen atoms have been removed for clarity.)

The presence of the two *t*-butyl groups does not disturb the planarity of the DHP periphery significantly. The dihedral angle between the least square planes that include the *t*-butyl carbons [defined by C(22), C(1), C(2), C(17); C(7), C(8), C(9), C(26)] and the 17 carbon atom plane are only 2.7º and 5.5º. The *t*-butyl groups adopt a conformation in which one carbon atom of the methyl groups almost eclipses an adjacent aromatic C-C bond with torsion angles for C(25)-C(22)-C(1)-C(2) and C(29)-C(26)-C(8)-C(9) of 2.9º

and 5.6º. These values are all similar to the values found for other DHP compounds.[41, 54b, 64]

Table 1.4 Summary of crystallographic data of 43 and 46.

	43	**46**
Formula	$C_{29}H_{34}O$	$C_{29}H_{32}O$
Fw	398.56	396.55
Temperature (K)	86(2)	89(2)
Crystal system	Triclinic	Monoclinic
space group	P-1	P2(1)/c
a (Å)	9.685(4)	15.109(3)
b (Å)	10.666(4)	6.1735(12)
c (Å)	12.406(5)	24.395(5)
α (deg)	112.859(7)	90
β (deg)	91.953(8)	91.535(4)
γ (deg)	103.258(8)	90
V ($Å^3$)	1138.6(8)	2274.6(8)
Z	2	4
ρ (calcd) (Mg/m^3)	1.162	1.158
abs coeff (mm^{-1})	0.068	0.068
F (000)	432	856
Crystal size (mm^3)	0.26 x 0.11 x 0.04	0.21 x 0.19 x 0.18
θ range for data collection (deg)	1.80 to 25.25	1.35 to 25.25
reflections collected	12286	67823
independent reflections	4125	5990
	[R(int) = 0.0783]	[R(int) = 0.0000]
completeness to θ	25.25°, 99.8%	25.25°, 100%
data/restraints/params	4125/1/280	5990/1/288
goodness of fit on F^2	0.999	1.097
final R indices [$I>2\sigma(I)$][a]	R1 = 0.0668	R1 = 0.0685
	wR2 = 0.1474	wR2 = 0.1519
R indices (all data)[a]	R1 = 0.1308	R1 = 0.0954
	wR2 = 0.1758	wR2 = 0.1622

$R_1 = \Sigma||F_o| - |F_c||/\Sigma|F_o|$; $wR_2 = \{\Sigma[\, w(F_o^2 - F_c^2)^2]/\, \Sigma\, [w(F_o^2)^2]\}^{1/2}$

Table 1.5 Selected bond lengths [Å] and angles [°] for 43.[a]

C(1)-C(2)	1.389(4)	C(1)-C(17)	1.422(4)
C(2)-C(3)	1.400(4)	C(3)-C(4)	1.404(4)
C(4)-C(5)	1.393(4)	C(5)-C(6)	1.376(4)
C(6)-C(7)	1.407(4)	C(7)-C(8)	1.388(4)
C(8)-C(9)	1.421(4)	C(9)-C(10)	1.395(4)
C(10)-C(11)	1.411(4)	C(11)-C(15)	1.403(4)
C(11)-C(12)	1.503(4)	C(12)-O(1B)	1.195(11)
C(12)-C(13)	1.537(4)	C(13)-C(14)	1.513(4)
C(14)-O(1A)	1.226(3)	C(14)-C(15)	1.492(4)
C(15)-C(16)	1.404(4)	C(16)-C(17)	1.378(4)
C(2)-C(1)-C(17)	119.4(2)	C(1)-C(2)-C(3)	122.6(3)
C(2)-C(3)-C(4)	124.1(3)	C(5)-C(4)-C(3)	121.8(3)
C(6)-C(5)-C(4)	122.4(3)	C(5)-C(6)-C(7)	124.3(2)
C(8)-C(7)-C(6)	123.9(3)	C(7)-C(8)-C(9)	118.5(3)
C(10)-C(9)-C(8)	122.7(3)	C(9)-C(10)-C(11)	124.3(3)
C(15)-C(11)-C(10)	121.5(3)	C(15)-C(11)-C(12)	112.4(2)
C(10)-C(11)-C(12)	126.1(2)	O(1B)-C(12)-C(11)	128.9(10)
O(1B)-C(12)-C(13)	126.7(10)	C(11)-C(12)-C(13)	104.4(2)
C(14)-C(13)-C(12)	106.8(2)	O(1A)-C(14)-C(15)	127.1(3)
O(1A)-C(14)-C(13)	125.1(2)	C(15)-C(14)-C(13)	107.8(2)
C(11)-C(15)-C(16)	123.7(2)	C(11)-C(15)-C(14)	108.5(2)
C(16)-C(15)-C(14)	127.7(2)	C(17)-C(16)-C(15)	126.3(2)
C(16)-C(17)-C(1)	122.8(2)		

[a] X-ray numbering

The bond lengths of 1.537(4) and 1.513(4) Å for C(12)-C(13) and C(13)-C(14) clearly showed that it is a cyclopentanone fused DHP. Study of the bond lengths in the [14]-DHP ring showed that the alternation of the bond lengths is quite small. The average alternation ($\Delta\Sigma$)[65] of **43** is 0.018 Å. More interestingly, the bond C(3)-C(4) did not follow the alternation trend and appeared quite long (1.404(4) Å). At the same time the bond

C(4)-C(5) appeared quite short (1.393(4) Å), even shorter than C3-C4. This is the first time this has been observed and there is no obvious reason for it. Probably it arises from the substitution effect of the carbonyl group. Unfortunately, X-ray structures of other carbonyl substituted DHP have not been obtained. However, our experiments suggest that the C4 is more electron rich than C5 (note: the crystal numbering, not NMR numbering was used here) because during the reaction of **43** and $PhSeCl_3$, only one isomer, the 4-chloro-substituted derivatives **47** and **48** were obtained; no 5-chloro-substituted product was detected.

1.4.1.6 The crystal structure of 46

The structure of **46** was determined by single crystal X-ray diffraction analysis. An ORTEP 3 diagram of **46** is show in **Figure 1.5**. As with **43**, the internal methyls and the C=O group are disordered. The crystal data is given in **Table 1.4** and **Table 1.6** lists selected bond lengths.

The overall structure of **46** is very similar to that of **43** in terms of the planar ring systems, the positions of the internal methyls and the *t*-butyl groups. The oxygen atom and the 17 carbon atoms for the DHP and the five member rings are all in a plane. The maximum deviation is 0.08 Å from C(15). The bond lengths of 1.345(3) Å and 1.477(3) Å for C(11)-C(10) and C(10)-C(9) indicated the presence of the additional double bond, compared to those of **43**. Also it is clearly shown that the bond alternation is large. The average bond alternation $(\Delta\Sigma)$[65] around the [14]annulene ring of **46** is 0.062 Å, much greater than that of **43** ($\Delta\Sigma$= 0.018 Å), but somewhat smaller than that of **36** ($\Delta\Sigma$= 0.0804 Å). This suggests that introduction of the conjugating double-bond in the five membered ring causes a large bond fixing ability. Compared to benzene, cyclopentadienone has

about 77% (=ΔΣ(**46**)/ΔΣ(**36**) = 0.062/0.0804) of the ability of benzene on reducing the ring current of DHP. This agrees well with our chemical shift results and the calculated results discussed previously.

Table 1.6 Selected bond lengths [Å] and angles [°] for 46.[a]

C(5)-C(6)	1.372(3)	C(5)-C(25)	1.440(3)
C(6)-C(7)	1.419(3)	C(7)-C(8)	1.372(3)
C(8)-C(12)	1.439(3)	C(8)-C(9)	1.493(3)
C(9)-O(1A)	1.225(3)	C(9)-C(10)	1.477(3)
C(10)-C(11)	1.345(3)	C(11)-O(1B)	1.180(5)
C(11)-C(12)	1.472(3)	C(12)-C(13)	1.373(3)
C(13)-C(14)	1.413(3)	C(14)-C(15)	1.370(3)
C(15)-C(20)	1.439(3)	C(20)-C(21)	1.357(3)
C(21)-C(22)	1.426(3)	C(22)-C(23)	1.366(3)
C(23)-C(24)	1.430(3)	C(24)-C(25)	1.359(3)
C(6)-C(5)-C(25)	119.49(18)	C(5)-C(6)-C(7)	121.95(18)
C(8)-C(7)-C(6)	125.62(18)	C(7)-C(8)-C(12)	122.88(18)
C(7)-C(8)-C(9)	129.96(18)	C(12)-C(8)-C(9)	107.11(17)
O(1A)-C(9)-C(10)	126.2(2)	O(1A)-C(9)-C(8)	128.3(2)
C(10)-C(9)-C(8)	105.46(17)	C(11)-C(10)-C(9)	110.07(18)
O(1B)-C(11)-C(10)	124.3(8)	O(1B)-C(11)-C(12)	125.5(8)
C(10)-C(11)-C(12)	110.18(18)	C(13)-C(12)-C(8)	122.80(17)
C(13)-C(12)-C(11)	130.02(18)	C(8)-C(12)-C(11)	107.18(17)
C(12)-C(13)-C(14)	125.87(18)	C(15)-C(14)-C(13)	122.69(18)
C(14)-C(15)-C(20)	118.78(18)	C(21)-C(20)-C(15)	123.52(19)
C(20)-C(21)-C(22)	123.99(19)	C(23)-C(22)-C(21)	122.35(19)
C(22)-C(23)-C(24)	121.97(18)	C(25)-C(24)-C(23)	123.97(18)
C(24)-C(25)-C(5)	123.09(18)		

[a] X-ray numbering

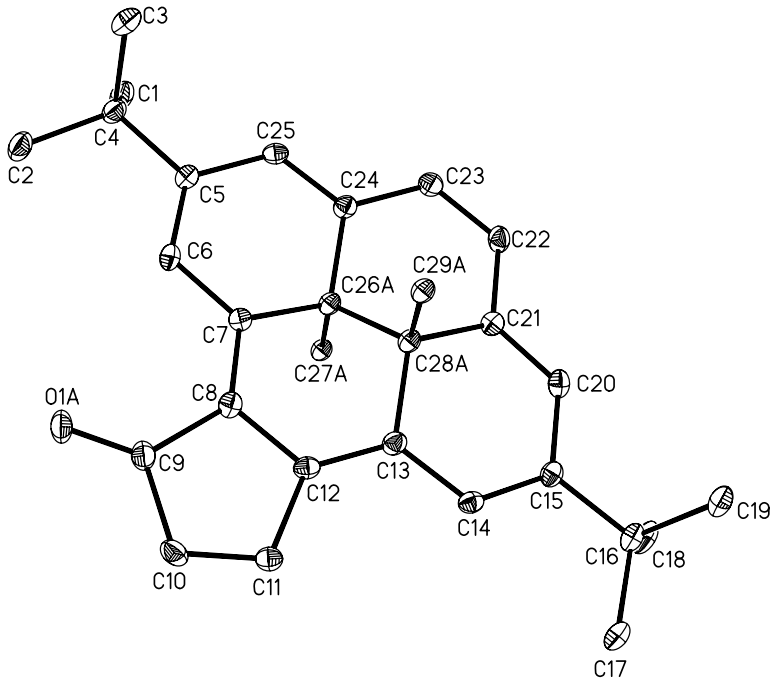

Figure 1.5 An ORTEP3 drawing[63] of complex 46 (30% probability thermal ellipsoids. Hydrogen atoms have been removed for clarity.)

The more interesting thing about the structure of **46** is the different bond alternating pattern around the [14]-DHP ring compared to those of other aromatic system fused DHP compounds.[54a, 54b] Actually, the bond alternation pattern around the periphery in **46** is in the opposite way to that of benzoDHP **36** (**Table 1.7**).[54b] This suggests that cyclopentadienone is an antiaromatic system. Otherwise, it would show the same alternation pattern as benzoDHP **36** does. This is actually consistent with the prediction of Günther and co-workers.[39,58] They showed that when two $(4n + 2)\pi$ systems are fused (**A**) (**Scheme 1.20**), the C2-C3 bond is shorter than the C1-C2 bond, while when a $4n\ \pi$ system is fused to a $(4n + 2)\ \pi$ system (**B**), the reverse is true. This has the effect that the C4-C5 bonds (arrowed) are also different. In **A** (equivalent to benzoDHP) C4-C5 should

be longer; while in **B** (equivalent to the cyclopentadienone fused system **46**) C4-C5 should be shorter. Clearly, the crystal structure agrees with this prediction and coupling constant data. The bond length of C4-C5 (note: the carbon labels follow **Figure 1.6**) in **36** was 1.426(3) Å,[54b] which is longer than that of **35** (1.389(3) Å.[54b]). In contrast, the bond length of C4-C5 (note: the carbon labels follow **Figure 1.6**) in **46** was 1.366(3) Å which is shorter than that of **35**. This combined with the ^{1}H-NMR analysis confirmed that the cyclopentadienone ring in **46** is behaving as an antiaromatic system.

Table 1.7 Periphery bond length for 36, 43 and 46.[a]

Bond	**36** (Å)	**43** (Å)	**46** (Å)
C1-C2	1.359(3)	1.389(4)	1.440(3)
C2-C3	1.429(3)	1.400(4)	1.359(3)
C3-C4	1.367(3)	1.404(4)	1.430(3)
C4-C5	1.429(3)	1.393(4)	1.366(3)
C5-C6	1.351(3)	1.376(4)	1.426(3)
C6-C7	1.431(3)	1.407(4)	1.357(3)
C7-C8	1.354(3)	1.388(4)	1.439(3)
C8-C9	1.440(3)	1.421(4)	1.370(3)
C9-C10	1.362(3)	1.395(4)	1.413(3)
C10-C11	1.463(3)	1.411(4)	1.373(3)
C11-C12	1.426(3)	1.403(4)	1.439(3)
C12-C13	1.450(3)	1.404(4)	1.372(3)
C13-C14	1.364(3)	1.378(4)	1.419(3)
C14-C1	1.437(3)	1.422(4)	1.372(3)

[a] numbering followed **Figure 1.6**

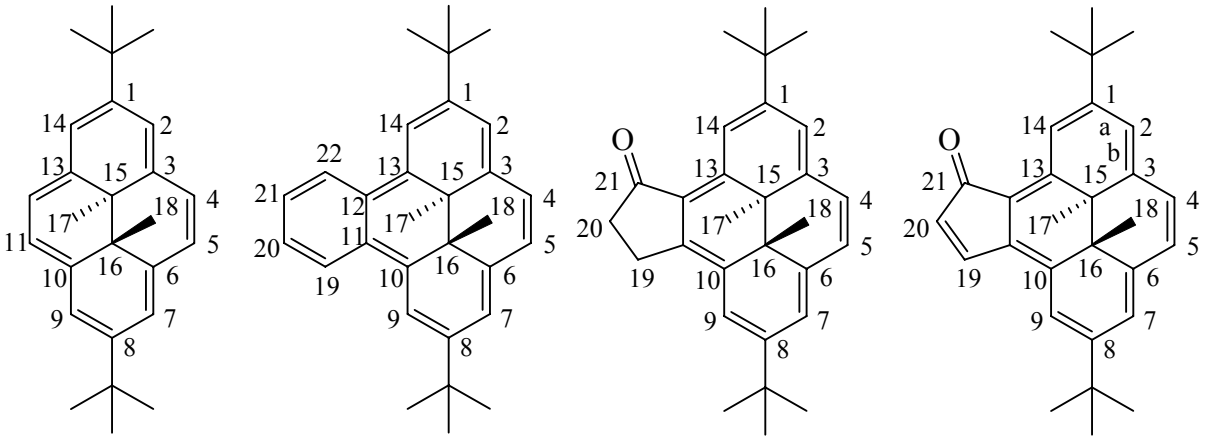

Figure 1.6 Carbon numbering for bond length comparison.

1.4.2 Investigation of the weak aromaticity of fulvenes

1.4.2.1 Introduction

As show above, the Mitchell method is effective for measuring both aromaticity and antiaromaticity. In general, if the principle is correct, the DHP probe should work for any system, including the weak aromatic fulvene systems. The question now is: How sensitive is the DHP probe? Is it sensitive enough to estimate the weak aromaticity of fulvenes?

Haley's group and our own jointly synthesized dehydrobenzoannulenne (DBA)-dihydropyrene and dehydroannulene (DA)-dihydropyrene hybrids (e.g. **69** and **70**) to estimate the aromatic characters of DBAs and DAs by the Mitchell method.[54c] Unfortunately, even though calculations showed the existence of weak diatropic ring currents in these molecules, the DHP probe failed to measure it, because the ^{1}H NMR chemical shifts of the internal methyls in these molecules only showed < 0.2 ppm difference from the parent DHP, which is of the same magnitude as the through space anisotropy effects. The reason that the DHP probe failed to measure the aromaticity of

DBA and DA might be the strong anisotropy effect of triple bonds which masks any aromaticity effects. Fulvenes, as discussed in the Introduction Section, on the other hand, do not have triple bonds, but show weak aromatic character. So it should be interesting to synthesize fulvene fused DHP and to see whether the DHP probe can determine the aromaticity or not.

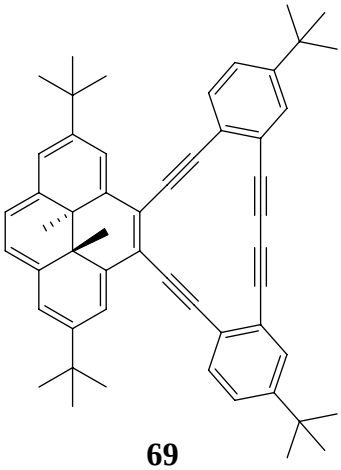

69

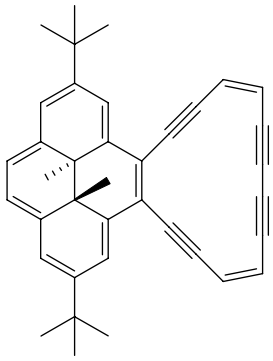

70

1.4.2.2 The weak aromaticity of fulvenes

The proton NMR study of **56** (**Table 1.8**) showed a downfield shift of the DHP internal methyl chemical shift (δ -3.54 ppm in $CDCl_3$) when compared to that of parent **35**, (δ -4.06 ppm). The difference of 0.5 ppm is distinctly larger than the through space anisotropic (<0.1 ppm) and substitution (<0.3 ppm) effects. A more valid comparison between **56** and **71** revealed that the internal methyl chemical shift of **71** (δ -3.88) is upfield more than 0.3 ppm (0.4 ppm in C_6D_6) comparing to that of **56**! This difference must be attributed to the bond-fixing ability of methylfulvene. In other words, the fusion of methylfulvene to DHP reduced the ring current of DHP and suggests the existence of weak aromaticity in the methylfulvene.

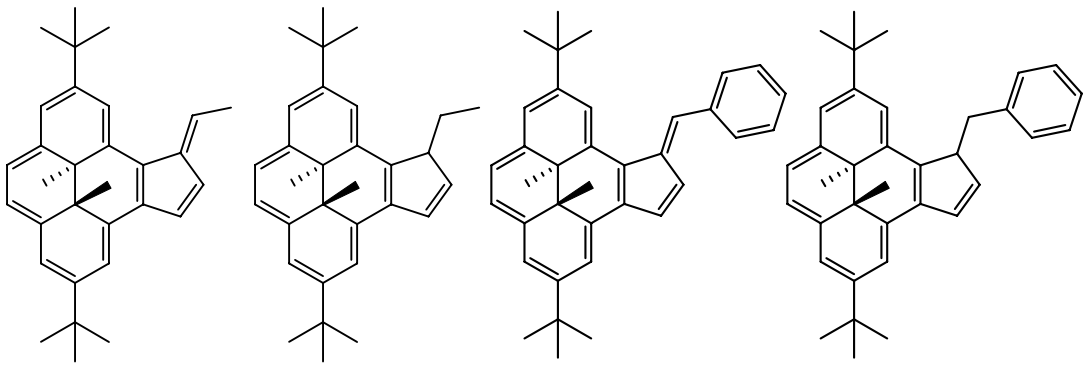

56 **71** **58** **72**

It has been shown that introducing an electron donating substituents on the exocyclic methylene of pentafulvene enhanced its conjugation and aromaticity.[23] Thus, to increase the aromaticity of the fulvene systems, phenylfulvene fused DHP **58** was synthesized. Its ^{1}H NMR spectrum showed that the DHP internal methyl protons resonance at δ -3.30 (in $CDCl_3$), which is 0.62 ppm downfield from that of **72** (δ -3.92 in $CDCl_3$) (**Table 1.8**). Compared to the 0.4 ppm difference between **56** and **71**, this 0.62 ppm difference clearly showed a larger reduction of the ring current and larger aromaticity of the phenylfulvene system.

Also if we compare **58** with **56**, the internal methyl chemical shift was downfield shifted by 0.24 ppm from **56** (δ -3.54) to **58** (δ -3.30), which means by changing the methyl substituent to phenyl, the DHP ring current was reduced more, indicating the increase of aromaticity with a better electron donating substituent on the exocyclic methylene of the pentafulvene.

In order to get more evidence for my suggestion, I also tried to put two electron donating groups on the exo methylene derivatives, such as compounds **62** and **63**, in which the pentafulvene should have stronger aromaticity. Unfortunately, all attempts failed. This is probably due to steric hindrance.

Table 1.8 Chemical shifts (ppm) of internal methyl protons in the annelated DHPs

compound	56	71	58	72	35	36
δ(H-Me)[a] ($CDCl_3$)	-3.54	-3.88[b]	-3.30	-3.92	-4.06	-1.58
δ(H-Me)[a] (C_6D_6)	-3.12	-3.51	-2.92	-3.55	-3.67	-1.22
$J_{4,5}$ (Hz)	8.1		8.1		7.3	6.9

[a] average value; [b] estimated, the internal methyl δ value difference in $CDCl_3$ and C_6D_6 is around 0.35 ppm.

In addition to using the internal methyl protons as the probe, the DHP arene protons can also be used to estimate the aromaticity of a fused ring system. The chemical shifts of H3/6 and H4/5 for **56**, **71** and **58**, **72** are given in **Table 1.9**. The chemical shifts for H3/6 and H4/5 in **56** are upfield shifted by ca. 0.15 ppm from those of **71**, indicating that the ring current of DHP is stronger in **71** than in **56**. In another word, this implied that the fused methylfulvene in **56** has greater aromaticity than the fused ethylcyclopentadiene in **71**. Since ethylcyclopentadiene is non-aromatic, methylfulvene must be just weakly aromatic.

Table 1.9 Chemical shifts (ppm) of selected arene protons in the annelated DHPs

compound	56	71	58	72	35	36
δ(H-4/5) ($CDCl_3$)	8.26/8.24	/	8.23/8.20	/	8.46	7.13
δ(H-4/5) (C_6D_6)	8.32/8.29	8.47/8.45	8.26/8.23	8.49-8.45		
δ(H-3/6) ($CDCl_3$)	8.35/8.33	/	8.29	/		7.35
δ(H-3/6) (C_6D_6)	8.45/8.44	8.61/8.60	8.39	8.62[a]		

[a] the average value.

The same phenomenon has also been observed between **58** and **72**. The chemical shifts for H3/6 and H4/5 in **58** are upfield shifted by ca. 0.22 ppm from those of **72**. This further supported the conclusion that the fulvene systems are weakly aromatic.

Comparison of fulvene fused dihydropyrenes **56** and **58** with the cyclopentadienone fused dihydropyrenes **46** and **47** showed that the internal methyl protons resonate at much higher field for **56** (δ -3.54) and **58** (δ -3.30) than those of **46** (δ -1.89) and **47** (δ -1.85). As the major difference between these compounds was the changing of an exocyclic C=O group to a C=C, we would think this huge difference in chemical shifts resulted from this change. The reason for the much larger reduction of the DHP ring current for **46** and **47** thus could only be explained by the existence of the antiaromaticity of the cyclopentadienone systems.

1.4.2.3 Computational studies

NICS values were calculated using the same method described above. Again, for simplification, **73** and **74** were used instead of their 2,7-di-*t*-Bu derivatives **54** and **59**. The calculation data is shown in **Table 1.10**. As can be seen, at the four six member rings of DHP (points 1-4, **Figure 1.7**), the average NICS value dropped from -17.62 for **54** to -16.43 for **59**, which is small but distinct and clearly showed that the aromaticity of DHP nucleus was reduced. In other words, the fusion of fulvene to DHP reduced its ring current more than the fusion of fulvane. At point 5, the NICS value for **54** was + 2.70, which is near zero. This suggested that fulvane was nonaromatic. In contrast, the NICS value for **59** at point 5 was -7.48, indicating that the fulvene showed some aromatic character. These results are consistent with the ^{1}H-NMR analysis.

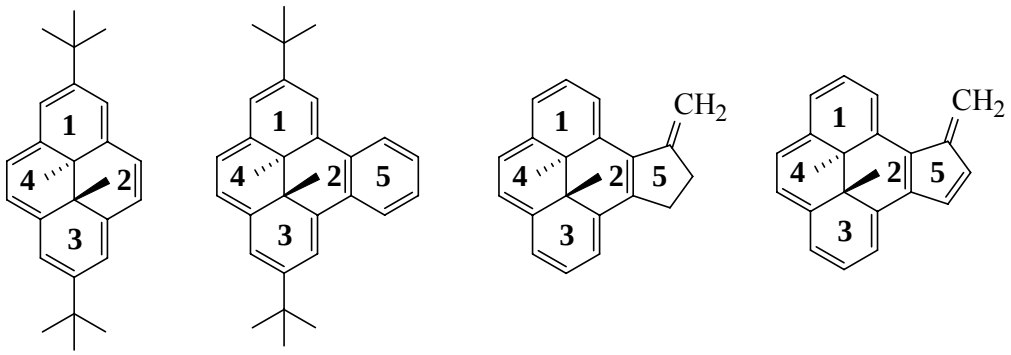

Figure 1.7 Numbering scheme and location of the NICS points for DHPs nuclei. NICS points are shown in bold type.

Table 1.10 NICS values for compounds 35,[54b] 36,[54b] 54 and 59.

NICS	fulvane **54**[a]	fulvene **59**[b]	**35**[54b]	**36**[54b]
1	-17.84	-16.75	-18.91	-4.40
2	-17.46	-16.22	-17.66	-5.47
3	-17.96	-16.55	-18.91	-4.47
4	-17.22	-16.21	-17.66	-4.29
Av of 1-4	-17.62	-16.43	-18.29	-4.64
5	+2.70	-7.48	NA	-10.78

[a] the data was calculated for **73**. [b] the data was calculated for **74**.

Chemical shifts of **56** and **58** were calculated for a further comparison of theory with experiment. The absolute shieldings for **56** and **58** were calculated using four methods-GIAO-HF/6-31G*//B3LYP/6-31G*, GIAO-B3LYP/6-31G*//B3LYP/6-31G*, CSGT-HF/6-31G*//B3LYP/6-31G*, and CSGT-B3LYP/6-31G*//B3LYP/6-31G*-employing Gaussian 94.[62] Predicted ^{13}C and ^{1}H chemical shifts were determined directly using **Eq.**

1.5 and also from Forsyth's procedure (**Eq. 1.6**) to scale the GIAO-B3LYP/6-31G*//B3LYP/6-31G* ^{13}C absolute shieldings to yield predicted ^{13}C chemical shifts.[66]

$$\delta_{calc} = \sigma_{TMS} - \sigma \qquad \textbf{Eq. 1.5}$$

$$\delta_{calc} (^{13}C) = -1.084\sigma + 203.1 \qquad \textbf{Eq. 1.6}$$

where δ_{calc} = predicted chemical shift, σ_{TMS} = absolute shielding for TMS, and σ = absolute shielding of nucleus under consideration.

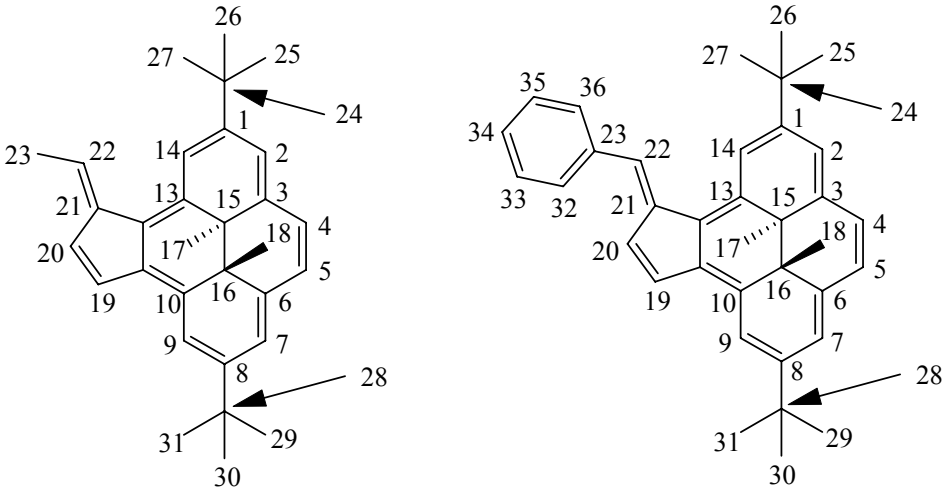

56 **58**

Figure 1.8 Numbering scheme for the NMR calculations of 56 and 58.

The calculated and experimental ^{1}H chemical shifts for compounds **56** and **58** are given in **Table 1.11** and ^{13}C data in **Table 1.12**. As the calculated results are for a single conformation of each compound, the predicted chemical shifts for the symmetry-related ^{1}H's and ^{13}C's made equivalent by rotation of the Me and/or ^{t}Bu groups are averaged.

From **Table 1.11** and **Table 1.12**, we can see that the calculated data, for both ^{1}H's and ^{13}C's, are in very good agreement with the experimental data. For compound **56**, both the calculated ^{1}H and ^{13}C chemical shifts matched the experimental data very well. The differences between calculated and experimental data for protons are smaller than 0.5

ppm (except internal methyl protons) and those for ^{13}C are smaller than 3 ppm. For compound **58**, the calculated ^{13}C chemical shifts give good agreement with the experimental results, generally within ±3 ppm. For ^{1}H, they are relatively worse but still within ±0.7 ppm (except internal methyl protons). This suggested that the calculations are reliable.

Table 1.11 Calculated and experimental ^{1}H chemical shifts for 56 and 58.

	56				**58**			
	δ_{calc}	Order*	δ_{exp}	Order*	δ_{calc}	Order*	δ_{exp}	Order*
H2	8.88	6	8.435	4	8.84	6	8.29	3/4
H4	8.94	5	8.29	6	8.91	5	8.20	6
H5	9.09	3	8.315	5	9.05	3	8.23	5
H7	8.97	4	8.45	3	8.92	4	8.29	3/4
H9	9.13	2	8.77	2	9.09	2	8.49	2
H14	9.42	1	9.22	1	9.41	1	8.96	1
H17	-4.56	13	-3.10	13	-4.29	17	-3.32	18
H18	-4.78	14	-3.13	14	-4.56	18	-3.29	17
H19	7.98	7	7.86	7	8.09	9	7.82	8
H20	7.29	9	7.17	9	7.60	13	7.30	14
H22	7.48	8	7.4	8	8.19	7	8.07	7
H23	2.28	10	2.139	10	/	/	/	/
H25-27	1.82	11	1.619	11	1.81	15	1.66	15
H29-31	1.78	12	1.618	12	1.72	16	1.64	16
H32					8.14	8	7.70	9
H33					7.73	11	7.48	11/12
H34					7.55	14	7.34	13
H35					7.69	12	7.48	11/12
H36					7.73	10	7.69	10

* Relative chemical shift order.

Table 1.12 Calculated and experimental ^{13}C chemical shifts for 56 and 58.

	56				**58**			
	δcalc	order	δexp	order	δcalc	order	δexp	order
C1	149.90	1	147.47	1	151.29	1	148.17	1
C2	123.63	16	121.3	16	123.85	22	120.98	22
C3	139.91	5	139.33	4	140.88	5	139.33	4
C4	125.55	14	125.05	13	125.94	20	124.03	20
C5	126.52	13	124.41	14	126.89	19	124.88	19
C6	136.43	6	137.62	6	137.05	8	137.42	6
C7	125.42	15	122.42	15	125.59	21	122.13	21
C8	146.95	3	145.61	3	147.61	2	145.89	2
C9	118.76	17	117.61	17	118.76	23	116.82	23
C10	130.66	11	129.84	9	131.29	11	129.55	13
C11	142.77	4	138.22	5	141.49	4	136.14	7
C12	131.86	9	128.29	11	132.92	12	127.52	17
C13	135.56	7	132.28	7	137.20	7	132.52	8
C14	117.39	18	116.93	18	118.49	24	116.2	24
C15	33.02	21	33.64	21/22	33.68	27	33.62	27
C16	32.26	23	33.64	22/21	33.15	28	32.12	28
C17	15.85	26	17.19	25	17.05	31	17.14	31
C18	14.07	27	16.71	27	15.031	32	16.81	32
C19	132.02	8	130.44	8	134.75	9	132.08	9
C20	129.92	12	128.69	10	131.83	13	129.7	12
C21	148.47	2	146.03	2	147.57	3	144.52	3
C22	131.33	10	127.61	12	133.50	10	129.26	14
C23	16.97	25	16.9	26	140.81	6	138.89	5
C24	39.67	19	36.55	19	39.71	25	36.45	25
C25-27	32.31	22	32.37	23	32.20	30	32	29
C28	39.18	20	36.35	20	39.38	26	36.16	26
C29-31	32.20	24	32.26	24	32.35	29	31.95	30
C32					130.79	15	130.4	10, 11
C33					129.54	17	128.78	15, 16
C34					127.90	18	127.43	18
C35					129.54	16	128.78	16, 15
C36					133.07	12	130.4	11, 10

1.5 Conclusions

The cyclopentadienone fused dihydropyrenes **46** and **47** were synthesized. The internal methyl resonances, the coupling constants, NICS calculations and X-ray results confirmed that the cyclopentadienone displays antiaromatic character resulting in bond localization in the annulene ring consistent with a $4n$-π fused system. The ring current of the dihydropyrene fragment is reduced by fusion of the antiaromatic system by about 80% of that caused by benzene.

The syntheses of methylfulvene fused dihydropyrene **56** and phenylfulvene fused dihydropyrene **58** have been accomplished. The ^{1}H-NMR analyses demonstrated that the fulvenes had weak diatropic ring currents and caused bond localizations in the DHP rings, in which phenyl fulvene has larger effect than that of methyl fulvene. The calculated NMR data agreed well with the experimental data. The NICS calculations also confirmed the existence of weak aromaticity of fulvene rings and the decreasing of the ring currents of DHP rings by fusing of the fulvene rings.

Chapter Two

Photoswitches based on bis-dihydropyrene

2.1 Introduction

2.1.1 Photochromism

"Photochromism is the reversible transformation of a chemical species **A** into a different species **B** having a different absorption spectra induced in one or both directions by absorption of electromagnetic radiation". [67] That is, the thermodynamically stable form **A** can be changed to form **B** by the irradiation of light of frequency ν_1, and the form **B** will change back to form **A** by the irradiation of light of frequency ν_2 (**Scheme 2.1**). Some photochromic compounds also thermally change back from form **B** to form **A**, and this is called T-type photochromism. Those that do not thermally return are termed P-type. Usually, the photochromic molecule has a colorless or pale yellow form **A** and a colored form **B**, and this is called positive photochromism. In contrast, the photochromism is termed negative or inverse if the form **B** is colored and more stable and the form **A** is colorless and thermally unstable.

$$A \underset{h\nu_2/\text{Thermal}}{\overset{h\nu_1}{\rightleftharpoons}} B$$

Scheme 2.1 The two states of a photochromic compound and their conversion.

Potential applications of photochromic compounds are optoelectric devices such as optical memories, switches, sensors and light filters and displays.[68] In order to be useful for practical application, photochromic compounds need to meet the following requirements:[69]

(1) Thermal stability of both isomers;

(2) Low fatigue (can be cycled many times without significant loss of performance);

(3) High sensitivity and rapid response;

(4) Nondestructive readout capability.

Among these requirements, the most important are thermal stability of both isomers and fatigue resistance. Thermal stability is farthest from meeting the requirements necessary for practical use. Much work needs to be done to make thermally irreversible systems. As well, sometimes side reactions such as rearrangement occur during the desired photoisomerization which destroy the material. Thus even though photoisomerization in principle is a nondestructive reaction, in practice fatigue resistance is difficult to obtain.

2.1.2 Types of organic photochromes

There are many organic photochromic systems. The most extensively studied ones are 1) the azobenzenes;[70] 2) the spiropyrans;[71] 3) the fulgides (and fulgimides) [72] and 4) the diarylethenes,[69,73] including stilbenes.[74] The spirooxazines,[71a] anils and others attract much less attention.

Some members of the dithienylethenes (types of diarylethenes)[71a] and fulgides,[72c] have achieved thermal stablility for both isomers (P-type), and are the closest to meeting the requirement of optical memories.

All photochromes may be easily classified according to their photoisomerization reactions: 1) *Cis-trans* isomerization; 2) Electrocyclization; 3) Intramolecular hydrogen transfer and intramolecular group transfer reactions; 4) Cycloadditions; 5) Heterolytic bond cleavages; 6) Homolytic bond cleavages.

(1) C*is-trans* (E, Z) isomerizations: Stilbene **75** and azobenzene **76** are typical examples. **(Scheme 2.2)**. Another example is Feringa's chiroptical switch **77** (**Scheme 2.3**).[75]

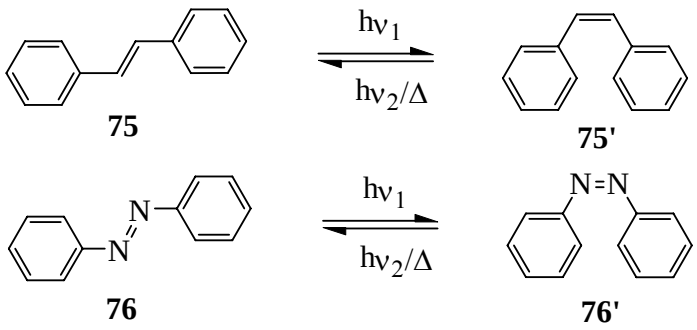

Scheme 2.2 The *cis-trans* isomerization for stilbene and azo-benzene.

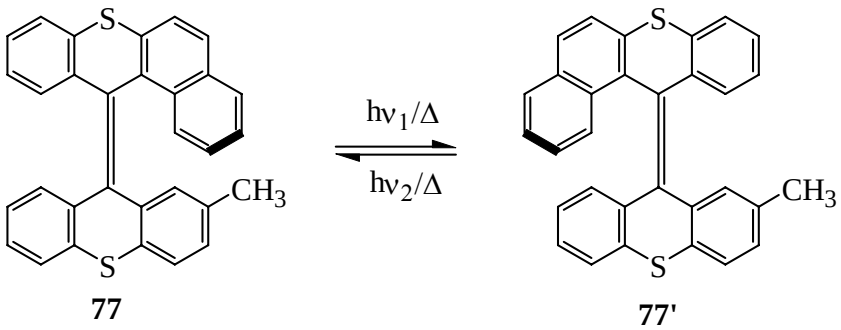

Scheme 2.3 Feringa's photochromes.

(2) Pericyclic reactions; Diarylethenes (e.g. **78**), fulgides (e.g. **79**) (and fulgimides), spiropyrans and spirooxazines (**Scheme 2.4**) all belong to the pericyclic reaction class. *Cis*-stilbene, besides *cis-trans* photoisomerization, also undergoes a photocyclization to produce dihydrophenanthrene, which undergoes dehydrogenation to give phenanthrene under oxidative conditions such as in presence of oxygen or iodine (**Scheme 2.5**).[76]

(3) Intramolecular hydrogen transfer and intramolecular group transfer; Intramolecular hydrogen transfer can be found in anils (e.g. **82**) and related compounds;[77] and an example of an intramolecular group transfer in a polycyclic quinone (periaryloxyparaquinones)[77b] is shown in **Scheme 2.6**.

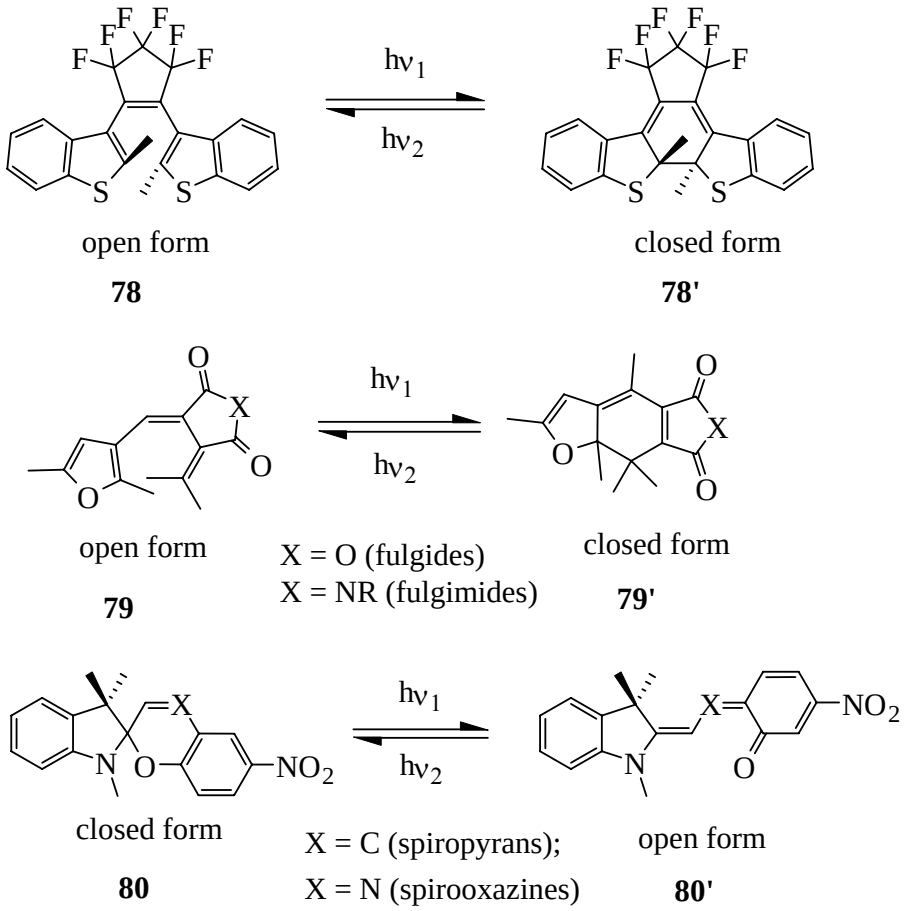

Scheme 2.4 Pericyclic reaction types of photochromic compounds.

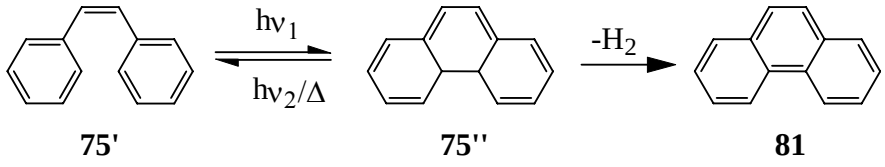

Scheme 2.5 Photocyclization of stilbene.

An example of a cycloaddition is the photochemical dimerization of anthracene, **84**, which undergoes a (4 + 4) cycloaddition to **84'**.[78a] Triarylmethanes (e.g. **85**) and related systems undergo heterolytic bond cleavage processes,[77b] and octaphenyl-1, 1′- bipyrrolyl, **86**, is an example of a homolytic bond cleavage. [78b]

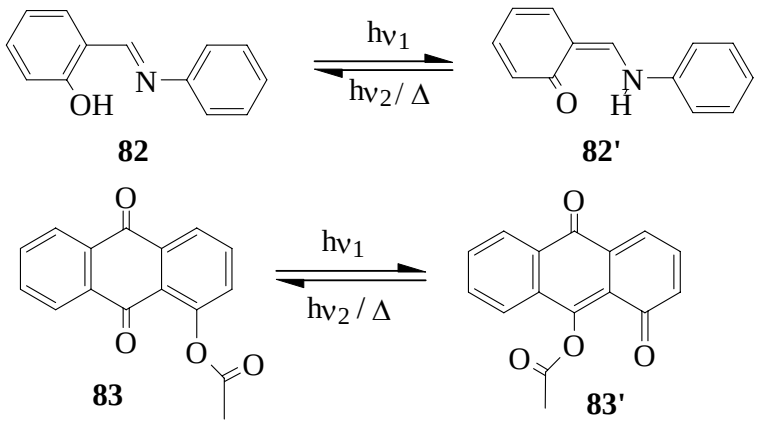

Scheme 2.6 Examples of intramolecular hydrogen and group transfer.

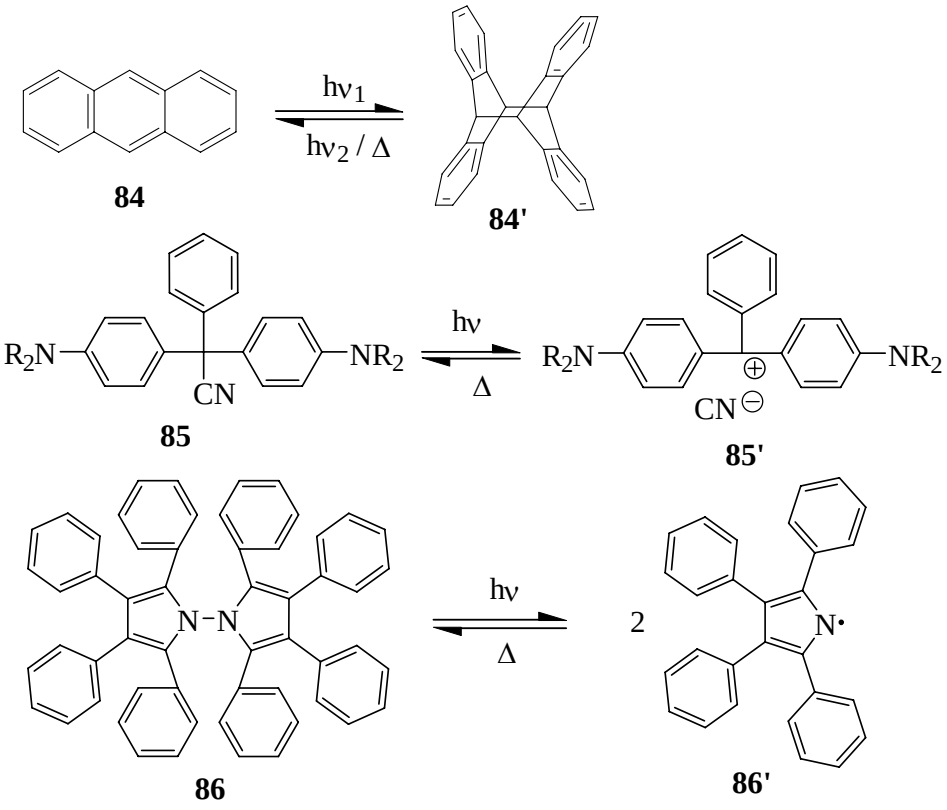

Scheme 2.7 Examples of cycloaddition and bond cleavage photochromes.

2.1.3 Dimethyldihydropyrenes (DHPs)

Dimethyldihydropyrene (DHP), **11**, is a photochromic molecule and it belongs to the pericyclic reaction type of photochrome. It is a negative photochromic system, which

means that the colored DHP form **11** is the thermally stable isomer (by about 3 kcal/mol) and the colorless metacyclophanediene (CPD) **11'** form is thermally less stable. Thus irradiation of DHP **11** with visible light converts it to colorless **11′**, which will return back to **11** on irradiation with UV light, or on heating (**Scheme 2.8**).

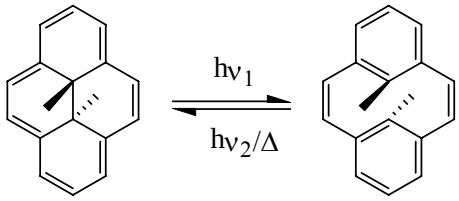

11
closed (DHP)
colored

11'
open (CPD)
colorless

Scheme 2.8 Isomerization between 11 and 11'.

The parent DHP **11** is not a good photochrome. The opening of **11** to **11′** is slow. The quantum yield ϕ was reported to be about 0.02 at 466 nm.[79] But a more recent report gives 0.006.[80] The thermal return of **11′** to **11** has a rate constant (k) of 0.001 min^{-1} at 30 °C, which means at this temperature its half life is about 12 hours.

Much work has been done trying to improve the photoswitching properties of the DHP system. The goal of higher quantum yields and higher thermal stabilities has been pursued by simple substitution, fusion of aromatic systems and changing of internal groups.

The substituent effect was extensively studied by Blatmann in 1970.[79] It was found that electron withdrawing groups at the 2 position, such as nitro and formyl, compounds **87** and **88** respectively, dramatically increased the photo opening quantum yield to 0.3-0.4, however, they also sped up the thermal return reaction.[79,81] The half life for the thermal return of **11'** to **11** is around 11.6 hours at 30 °C, while that of **88'** to **88** is only

13 minutes. The substituents appear to affect the activation barrier between the dihydropyrenes (DHPs) and metacyclophanedienes (CPD) substantially, although the enthalpy between the DHP isomer and CPD isomer does not change very much with such substituents.[79]

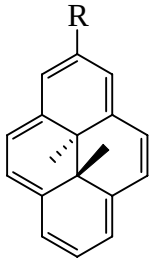

R = H, **11**
R = NO_2, **87**
R = CHO, **88**
R = COC_6H_5, **89**

Electron donating substituents have the opposite effect to that of electron withdrawing substituents, but the effect is much smaller. The quantum yield of opening for the 2, 7-di-butyl substituted derivative of DHP, **35**, is $\phi = 0.0015$,[80] which is about four times less than that of the parent **11**. The thermal return rate constant of **35′** to **35** is k = 0.0008 min^{-1} at 30 °C,[79, 82] which is a little bit slower than that of **11** (0.0010 min^{-1} at 30 °C).

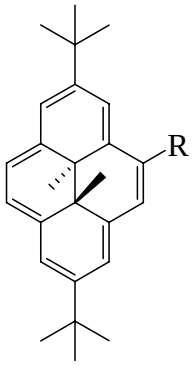

R = H, **35**
R = NO_2, **90**
R = COC_6H_5, **91**
R = $COCH_3$, **92**
R = COC_2H_5, **93**

For compound **35**, substitution occurs at the 4-position. Electron withdrawing groups at the 4-position decreased the thermal return rate of CPD to DHP. For example, for

compounds **90** to **93**, the rate constants were 0.0018, 0.0028, 0.0016, 0.0012 min^{-1} at 40°C, respectively, while for the parent **35** the rate constant was 0.0031 min^{-1}.[79,82]

Changing the size of the internal alkyl group had little effect on the quantum yield, but the thermal return rate increased with increasing size of the internal groups.[79,82] For example; the thermal return rate constants of **94′**, **95′** and **96′** were 0.0044, 0.0047 and 0.012 min^{-1} at 40°C. Moreover, those compounds are thermally much less stable, due to internal group migration.

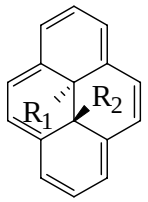

$R_1 = CH_3$, $R_2 = C_2H_5$, **94**

$R_1 = CH_3$, $R_2 = CH_2Br$, **95**

$R_1 = R_2 = C_2H_5$, **96**

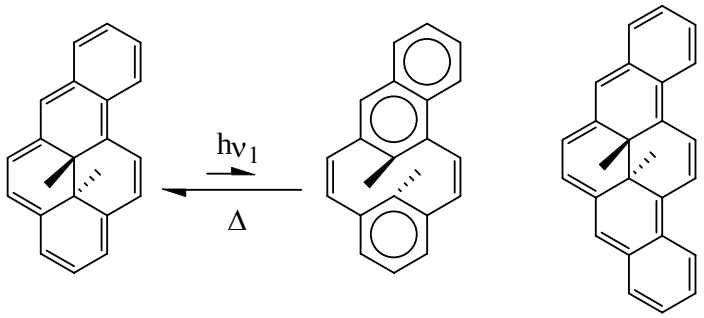

30 **30'** **97**

Scheme 2.9 Examples of [a]-annelated dihydropyrenes.

The effects of annelation of an aromatic ring have also been studied, where [a]-annelation and [e]-annelation have very different results. Fusion of an aromatic ring in the [a] position largely increased the thermal return rate. Visible light irradiation of [a]-benzannelated dihydropyrene **30** at room temperature gave no build up of the CPD form **30′** because the thermal return reaction of **30′** to **30** is extremely rapid (**Scheme 2.9**).[83] The [a]-dibenzo derivative **97** also does not photo bleach significantly. Indeed, all of the

[a] fused benzannulenes which have be made give no substantial amount of the CPD isomer[83,84,85] on irradiation.

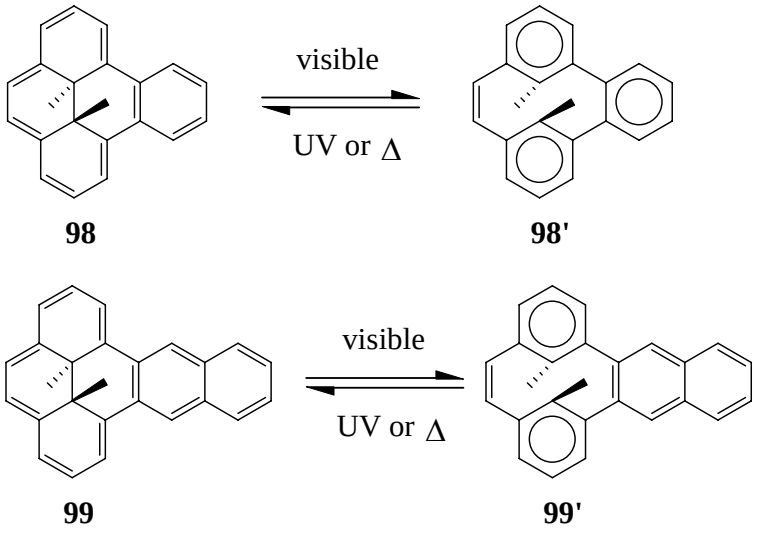

Scheme 2.10 Examples of [e]-annelated dihydropyrenes.

Fusion at the [e] position of DHPs gives very different results. Benzoannelation of the dihydropyrene at the [e] position has a dramatic effect on the equilibrium (**Scheme 2.10**). It increases the quantum yield of opening and slows down the thermal return rate (closing), which is very different from the [a]-annelated DHPs. The [e]-benzo analogue **98** is readily and quantitatively converted to **98′** by irradiation with visible light at room temperature. Irradiation with UV light then quantitatively converts **98′** back to **98**. The thermal return rate is around 0.00078 min^{-1} at 30 °C, which is much slower than that of the parent **11′** to **11 (**0.001 min^{-1}) under the same conditions. The naphtha[e] isomer **99′** thermally returns to DHP **99** even more slowly.[83,84] This is important for photoswitches because thermal stability is desirable for practical application.[69]

Photochromic studies were also conducted on the 2,7-di-*tert*-butyl series of **36** to **38**:[86] The thermal return rate of **36′** to **36** is 0.0020 min^{-1} at 46°C, which is three times

slower than that of **35′ to 35**. Quantum yield studies[80,87] on the 2,7-di-*t*-butyl substituted analogue **36,** showed that the ring opening quantum yield (Φ = 0.042) increased about 30 times compared to the non-annelated system **35** (Φ = 0.0015). However, fusion of naphtho- or anthro- groups increases the thermal return rate; in the case of compound **99**, without the t-butyl groups, the thermal return is slower. The compounds **37′** and **38′**, which are the CPD isomers of compounds **37** and **38**, had thermal return rates of 0.0101 and 0.0344 min^{-1} at 46°C, respectively.

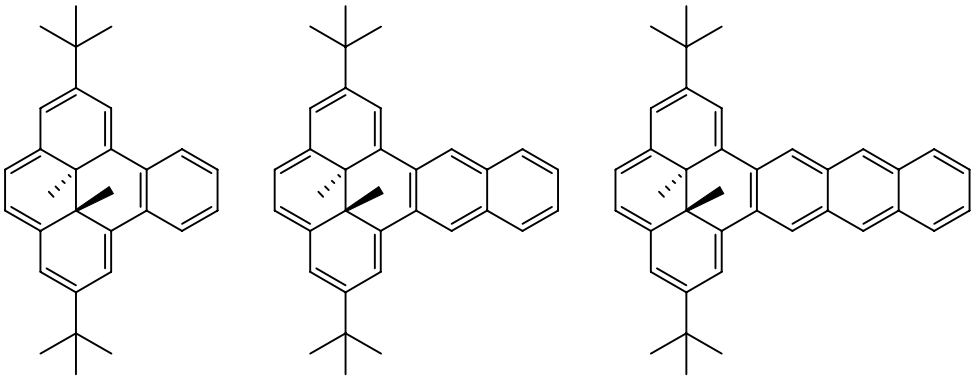

36 **37** **38**

Bis [e,l]-benzo annelated dihydropyrene **100**/**100′** is very interesting.[88] The colorless cyclophane isomer **100** is now the thermally stable isomer. Green [e,l]-dibenzodihydropyrene **100′** was obtained by irradiation with 300nm light at -90 °C. The thermal return of **100′** is quite fast, 0.256 min^{-1} at -10 °C. The activation energy of the thermal reaction at low temperature was estimated to be 20 kcal mol^{-1}. The reason that the thermally stable state of **100** is the open CPD form **100'** is because compound **100'** has the large resonance stabilization energy of the four benzene rings.[88]

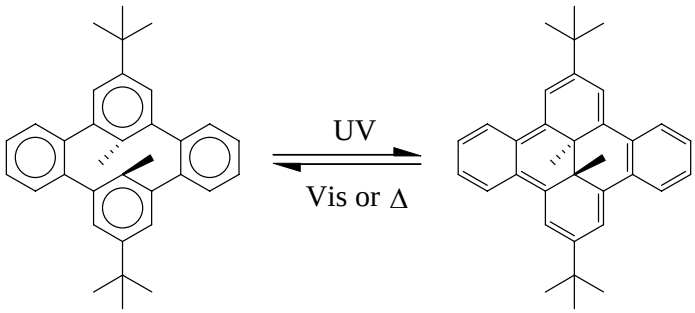

100' **100**

It is worth mentioning that the furan annelated analogue **101'** has the slowest thermal return rate constant so far, 0.000183 min^{-1} at 46 °C.[86, 89] Unfortunately compound **101** is not very stable. It is air sensitive and decomposes under UV light.

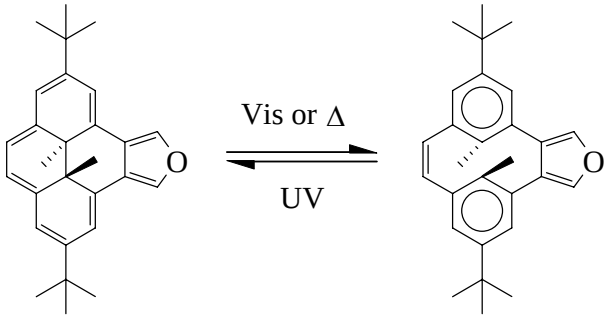

101 **101'**

2.1.4 Multiple photoswitches

Multiple photoswitches which link two or more photochromic units together are interesting because they might have applications in high-density digital data storage devices. For example, four states might exist if two photochromes are linked. There are the closed-closed(C-C), closed-open(C-O), open-closed (O-C) and open-open (O-O) states. (Only three states exist if the two photochromes are identical because the closed-open(C-O) state equals the open-closed (O-C) state.) It is also interesting to investigate the effect of linkers between the photochromes to get better stepwise multiple photoswitches.

2.1.4.1 Multiple photoswitches based on dimethyldihydropyrenes (DHPs)

Our group has studied multiple photoswitches for more than ten years. Ward[90] fused two DHP units together in the compound **102**.

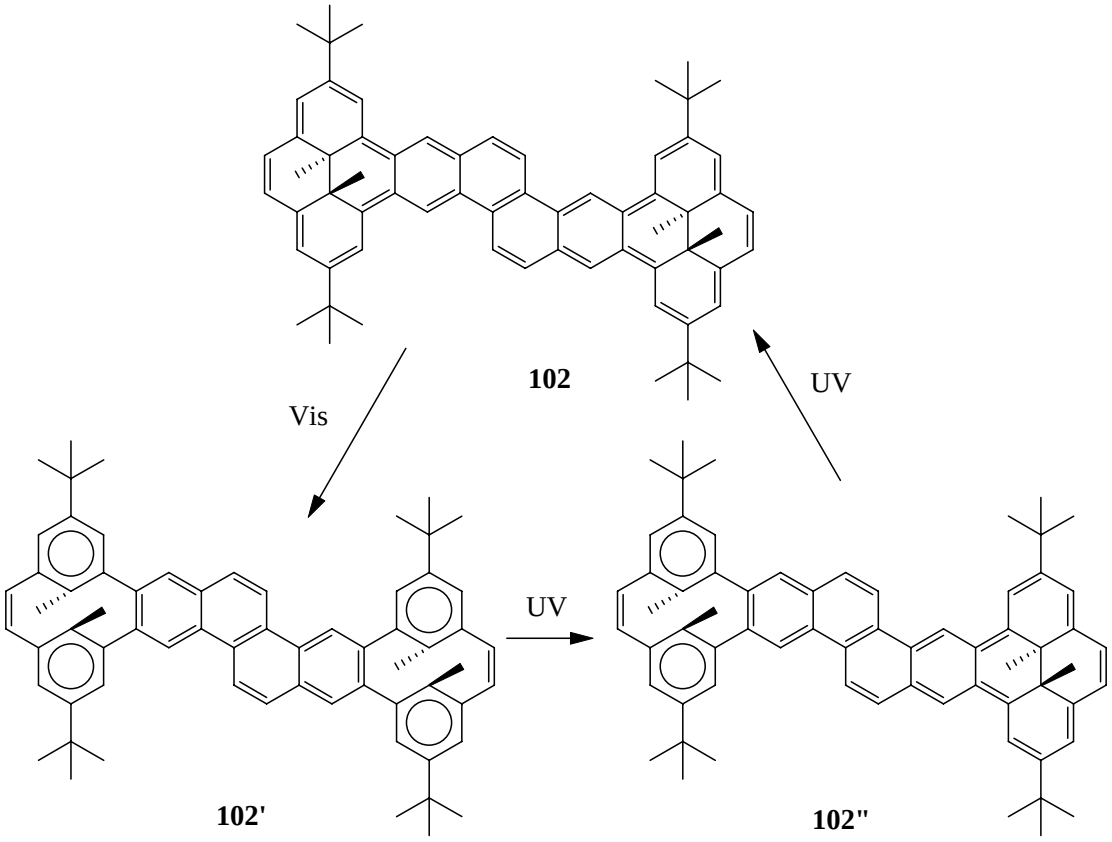

Irradiation of **102** with > 500 nm light converted it to the bis-open form **102′** quickly. When the latter was irradiated with UV light, the mono closed **102″** formed first before complete return to the bis closed **102**. This was proven by both ^{1}H NMR spectroscopy and UV-vis spectroscopy. The overall thermal return rate from bis open **102′** to bis closed **102** at 46°C was determined by NMR to be 0.0057 min^{-1} with an activation energy of 24.3 kcal mol^{-1}.

The fused tris-DHP system **103** was synthesized by Wang.[85, 91] The stable state is **103**, whose middle DHP unit is open and whose two end DHP units are closed.

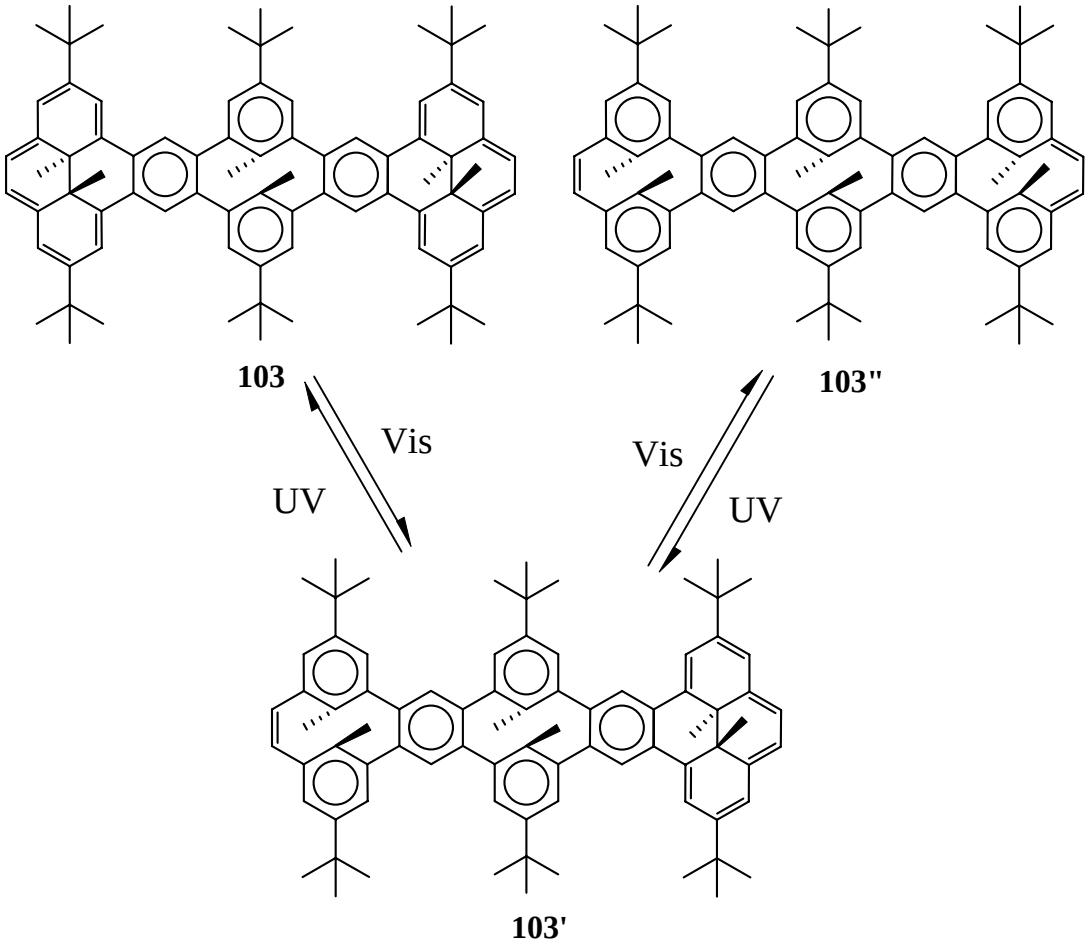

When compound **103** was irradiated at 550 nm, it was opened to **103′** and further opened to **103″**. This was confirmed by NMR and UV-vis spectroscopy. New internal methyl peaks appeared when the opening process was monitored by NMR spectroscopy, which indicated that one DHP opened ahead of the other. The solubility of the completely open state, **103″**, is limited and it precipitated as a white solid during the irradiation.

A true three way photoswitch, compound **104** was made by Ward.[85, 86] The thermally stable state is the open-closed form **104**. This is reasonable because the left DHP has two fused benzene rings, which is similar to **100**, with the open form as a thermally stable state. The right unit, on the other hand, has only one fused benzene ring, similar to **36**,

and it has the closed form as the thermally stable state. Irradiation of **104** with >598 nm light, opened the right DHP unit and gave the colorless **104′**, which on irradiation with UV light returned to **104**. Open form **104′** also changes back to **104** thermally, but slowly. The bis closed system **104″** was obtained using a 355 nm laser flash, and it thermally returned to **104** very rapidly. The thermal return rate constant (0.00224 min^{-1} at 46°C) and activation energy (E_{act} = 24.1 kcal $mol^{-}1$) of **104′** to **104** was found to be very close to that of **36′ to 36**. Compound **104** is very stable. There is no detectable decomposition even after flashing **104** with UV light more than 100 times.

If we compare compound **104** with compounds **102** and **103**, the two DHP units of **104** can be distinguished from each other. That is most likely the reason why **104** is a true three way photoswitch.

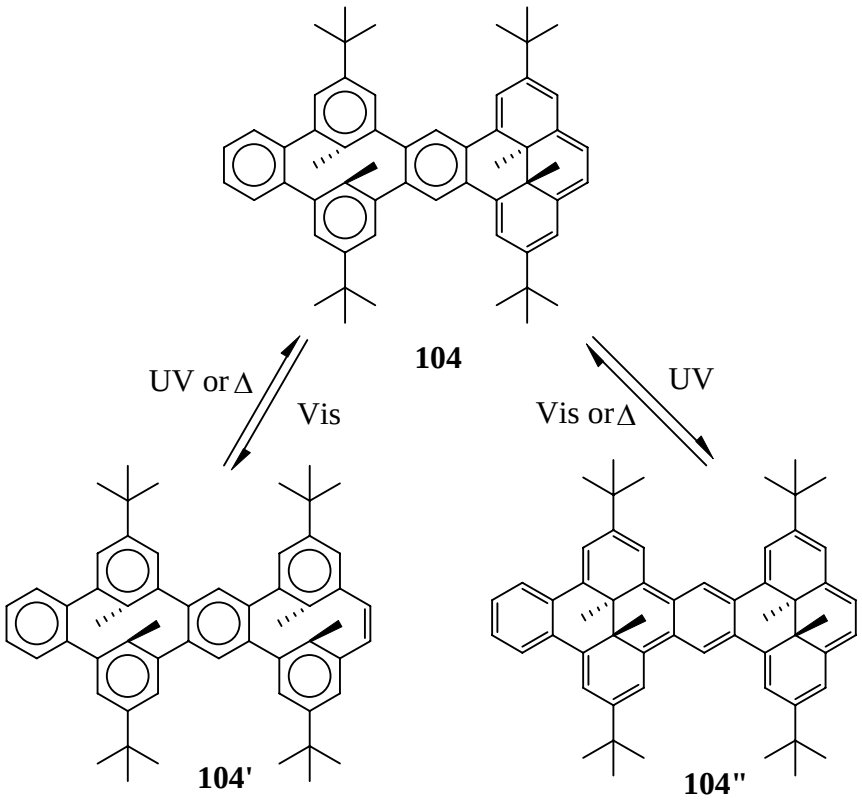

Different from the fused multiple DHP systems, Bandyopadhyay[92] synthesized the multiple photoswitch **105,** in which two DHP units were linked by a diethynyl spacer. The UV-vis spectroscopy showed that during the irradiation with UV light, **105'** (open-open state) was converted to the closed-open intermediate **105"** first and then to the closed-closed state. No NMR evidence of the closed-open state was found however.

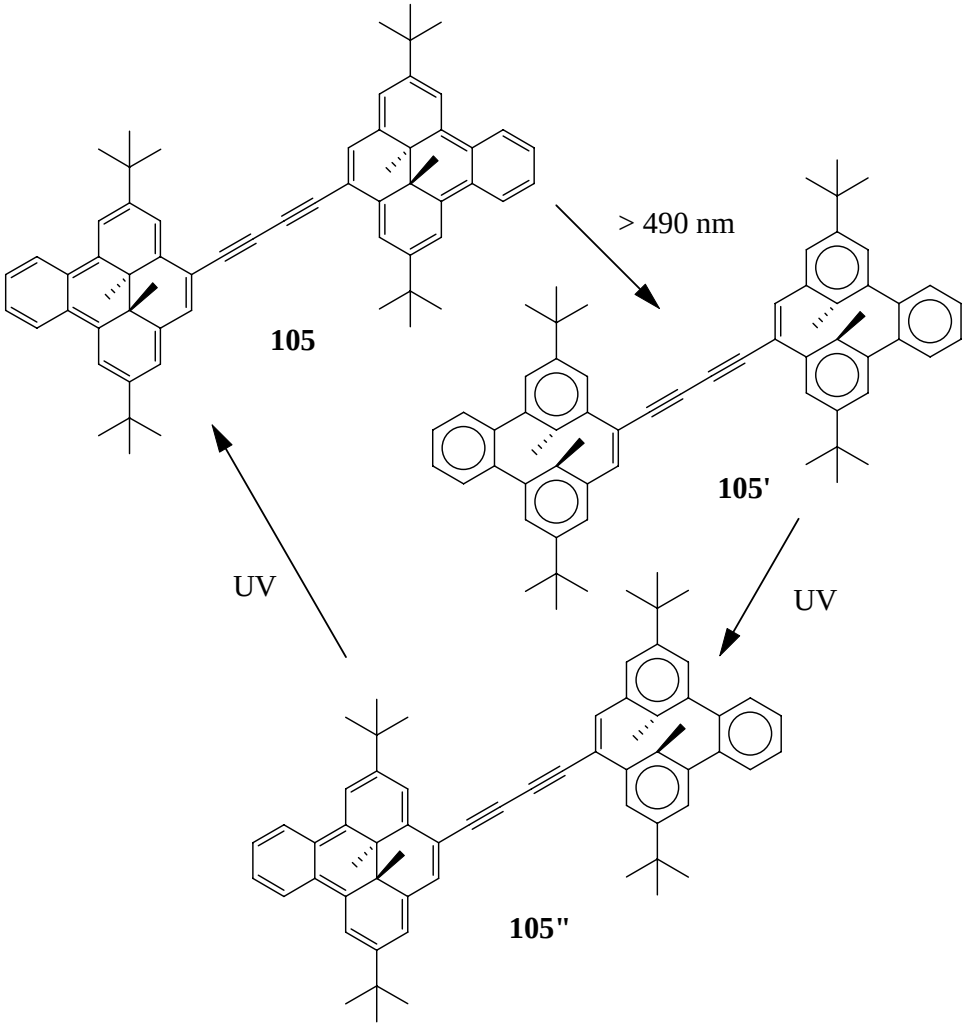

Bandyopadhyay also made the phenyl linked system **106** and the ethenyl linked system **107**.[92b] However, for compound **106**, there is no closed-open intermediate found in the visible light opening and UV closing process. Compound **107** could not be opened at all.

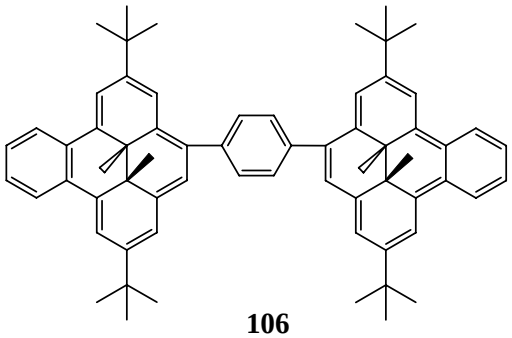

106

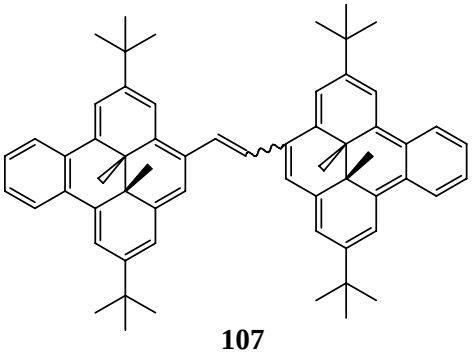

107

2.1.4.2 Other multiple systems

Branda[93] linked two dithienylethene photochromes together directly. It was found that only one of them underwent a photo-induced cyclization reaction, while that of the other was shut down. Irie and Branda reported the synthesis of dithienylene dimers connected by ethynylene,[94a] diyne[94b] spacers or connected directly.[94c] In all of these cases, only one of the dithienylenes can be converted to the close-ring form upon UV irradiation, which is similar to that found by Branda. The only example in dithienylene systems in which the two photochromes can be converted to closed-ring forms is the dithienylene dimer linked by a phenyl group, **108**.[95] The NMR spectrum showed that one photochrome closed first, then the second one was closed after further UV irradiation. The two closed-ring isomers **108** and **108'** directly returned to the two open-ring isomer **108** by irradiation with visible light (> 500nm).

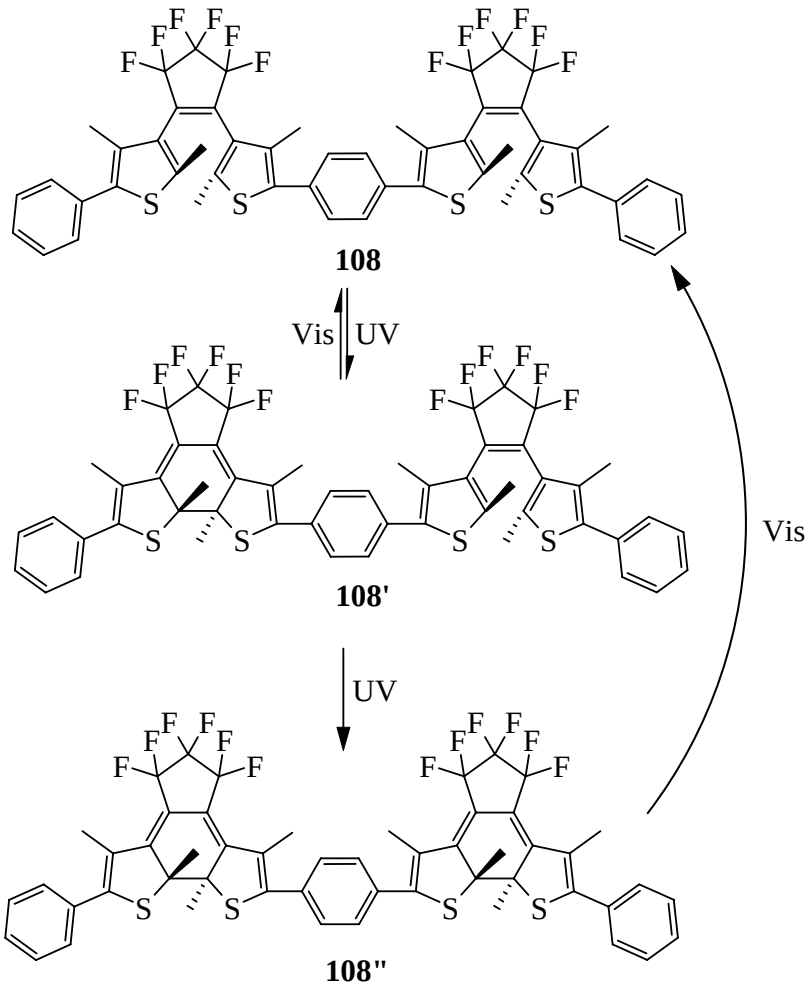

2.2 Objectives

Besides being a good aromatic probe, dimethyldihydropyrene is also a promising photochromic system where many studies have tried to improve the photo properties. The multi-state photoswitches based on it are also interesting. However most of the known multi-state photoswitches for the DHP system have fused or conjugated systems. No multiple photoswitches linked by cross-conjugated spacer and non-conjugated spacer have been reported for dihydropyrene systems. My research goals were thus as follows:

1. To synthesize multi-state systems linked cross-conjugated spacer and non-conjugated spacer.

2. To investigate how different linkers affect the photoisomerization.
3. To synthesize a system where the DHP units are different such that one side might open-close preferentially to the other.

2.3 Synthesis

2.3.1 Dihydropyrene starting materials: Synthesis of benzoDHP 36 and bromo-benzoDHP 111

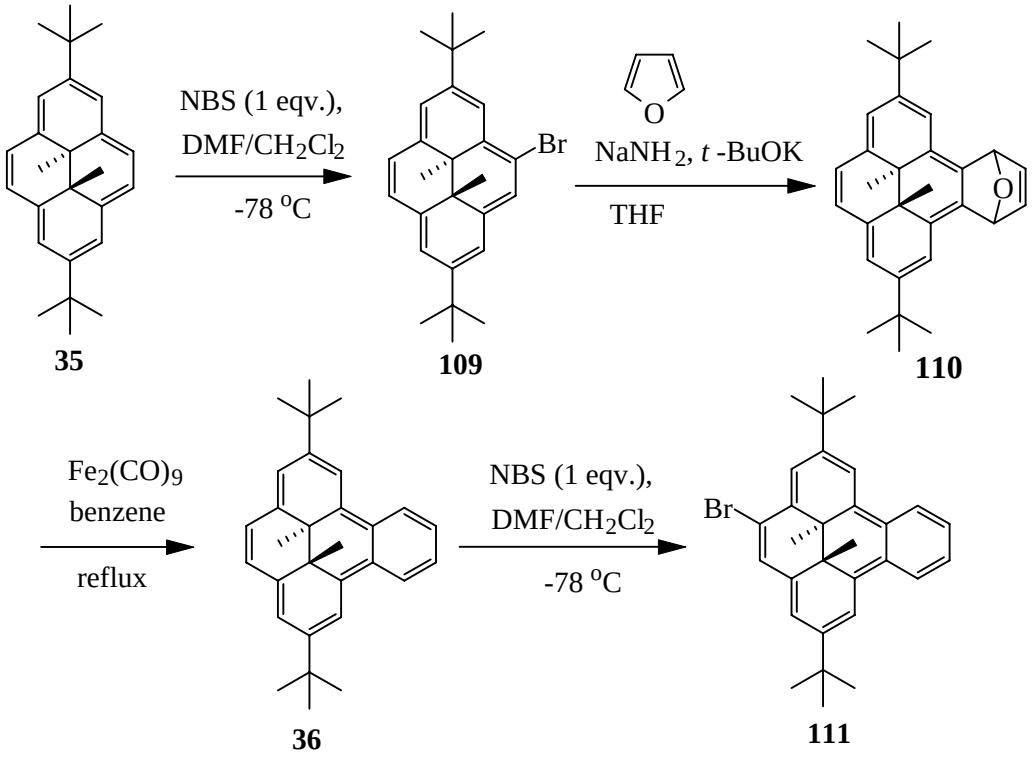

Scheme 2.11 Syntheses of benzo[e]eDHP 36 and monobromo derivative 111.

Because the [e]-annelated benzoDHP **36** shows the best photoswitching properties so far of the DHP systems, most of our compounds are thus based on it. Its synthesis and the synthesis of the bromide derivative **111**, both made by Ward,[43] are thus shown in **Scheme 2.11**.

2.3.2 Synthesis of 112 by formylation of 35

Boekelheide[96] formylated parent DHP **11** in 1967 using α,α-dichloromethyl methyl ether, using the Lewis acid titanium (IV) chloride. Miyazawa[97] and Fan[45] reported the use of this method to give **39** from **35**. Wang[91] also tried to formylate BDHP **36** using this method but obtained mono- and dichloro- substituted products instead of the 4-formyl-BDHP. However when I tried this reaction, the ipso-de-*t*-butylated product **112** was also obtained in 2% yield. This was not reported in the work above. When this reaction was studied carefully, besides the formylated product **39** and **112**, we believe that the chlorinated by-products **113**, **114** and **115** (**Scheme 2.12**) are formed. These products are consistent with Wang's result.[91] Compound **112**, in which the aldehyde group replaced one *tert*-butyl group of DHP **35**, was isolated as a purplish red solid in 2% yield.

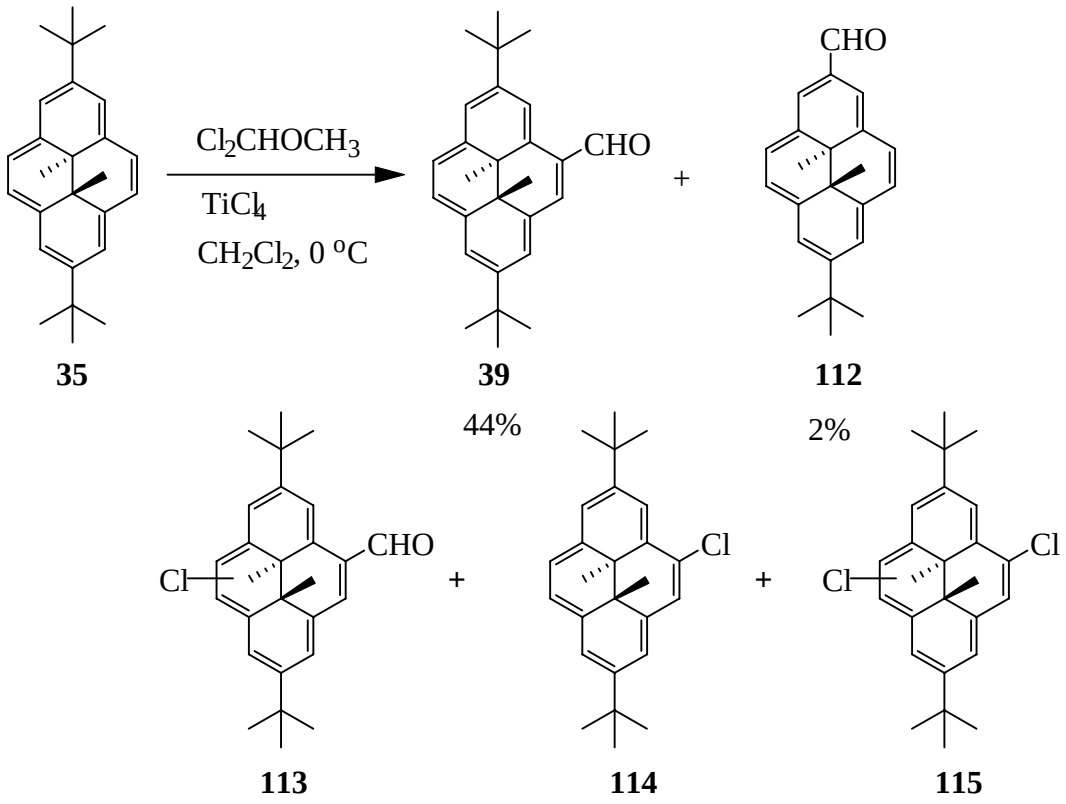

Scheme 2.12 The formylation reaction of 35.

The structure of **112** was proven by NMR spectroscopy. Only one *tert*-butyl group was seen in the ^{1}H NMR spectrum at δ 1.68. The formyl proton appeared at δ 10.53 and in the ^{13}C NMR spectrum the formyl carbon appeared at δ 193.64. The internal methyl protons have resonances at δ –3.82 and –3.84. These data plus the coupling of the formyl proton with C1 and C3 (in the HSQC and HMBC spectrum) proved the presence of the formyl group at the 2-position. The structure of **112** was also supported by mass spectroscopy with a molecular ion at *m/z* 316 (M^{+}) and high resolution mass at 316.1823 (calculated for $C_{23}H_{24}O$: 316.1827). The IR spectrum showed the C=O stretch at 1675 cm^{-1}.

2.3.3 Linked DHP systems with a carbonyl as spacer

Note: For all bis-systems in this chapter, we use the symbols (C-C), (C-O), (O-C) and (O-O) to mean (closed-closed), (closed-open), (open-closed) and (open-open) respectively. (C-O) means the left side unit is closed and the right side unit open and (O-C) means the left side unit open and the right side unit is closed.

2.3.3.1 Syntheses of the carbonyl linked homo-switches 117 and 119

As mentioned above, we were interested in the cross-conjugated linked systems other than the annelated or conjugated systems. The plan was to convert bromides **109** and **111** via their lithio derivatives into the alcohols **116** and **110** and then to oxidize to **117** and **119**. We thus first tried the reaction of DHP-Li with methyl formate (**Scheme 2.13**). DHP-Li was generated in situ from Br-DHP **109** and *n*-BuLi at -78 °C and was then warmed to room temperature. Methyl formate was then added and the reaction was

stirred at room temperature for an hour. After workup the bis-dihydropyrenyl methanol **116** was obtained in 82% yield as green crystals.

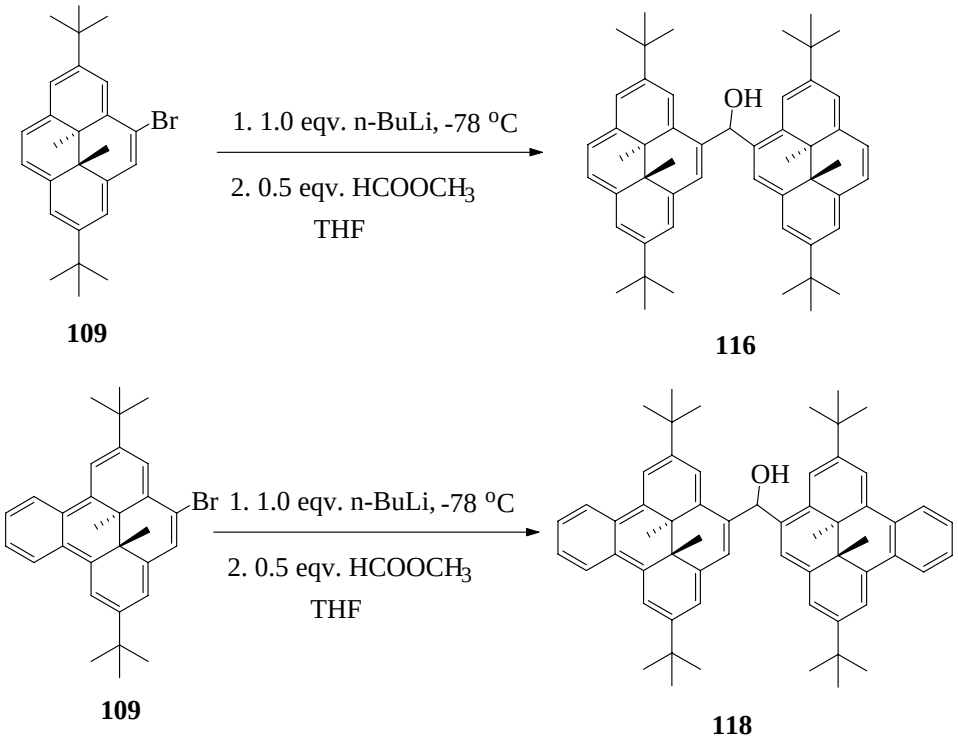

Scheme 2.13 Syntheses of 116 and 118.

The structure of **116** was confirmed by NMR, IR and mass spectroscopy. In theory, four isomers, shown in **Scheme 2.14**, should exist for **116**. Two internal methyl signals and two *t*-butyl signals should be seen for **116A** and **116B**. Isomer **116C** should show four internal methyl signals and four *t*-butyl signals. Isomer **116D** also show four internal methyl and four tert-butyl singals but they should overlap with those of **116C**. In the ^{1}H NMR spectrum, the *tert*-butyl protons appeared as 8 peaks from δ 1.56 to 1.54 and the internal methyl protons appeared from δ -3.46 to -3.69 as 8 peaks, too. This is consistent with all isomers of structure of **116** being present. The C<u>H</u>OH protons appeared far downfield at δ 8.82 to 8.78, because of the deshielding effect of two DHP ring currents.

The CHOH carbon appeared in the ^{13}C spectrum as three peaks at δ 72.46, 71.97 and 71.12 as expected. In the IR spectrum, the strong and broad absorption at ~3500 cm^{-1} confirmed the presence of an OH group. The mass spectrum (EI) showed a correct molecular ion at *m/z* 717 (M^+) and high resolution mass at 716.4969 (calcd for $C_{53}H_{64}O$: 716.4957).

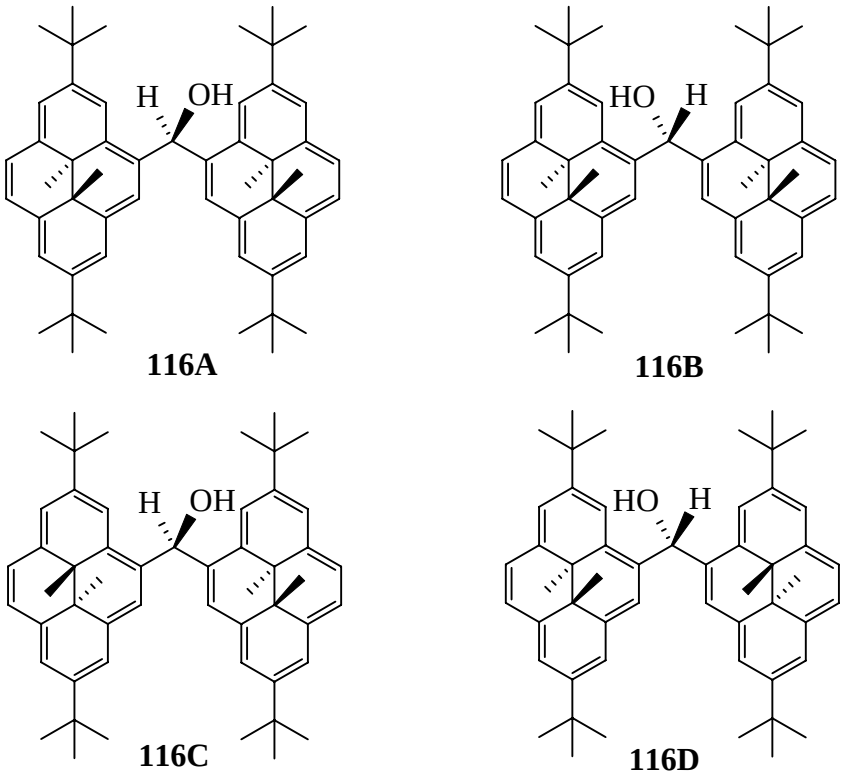

116A **116B** **116C** **116D**

Scheme 2.14 Four isomers of 116.

The oxidation of **116** needs care, because the dihydropyrene is very electron rich and very reactive to electrophiles or oxidizing reagents. Oxidation with pyridium chlorochromate (PCC) leads to decomposition while the Oppenauer reaction failed. Finally oxidation with pyridinium dichromate (PDC) succeeded and gave the desired DHP-CO-DHP **117** in 78% yield as brown crystals (**Scheme 2.15**). However, even

though **118** could be prepared in 47% yield from **111**, all attempts to oxidize **118** to **119** led to decomposition (**Scheme 2.15**).

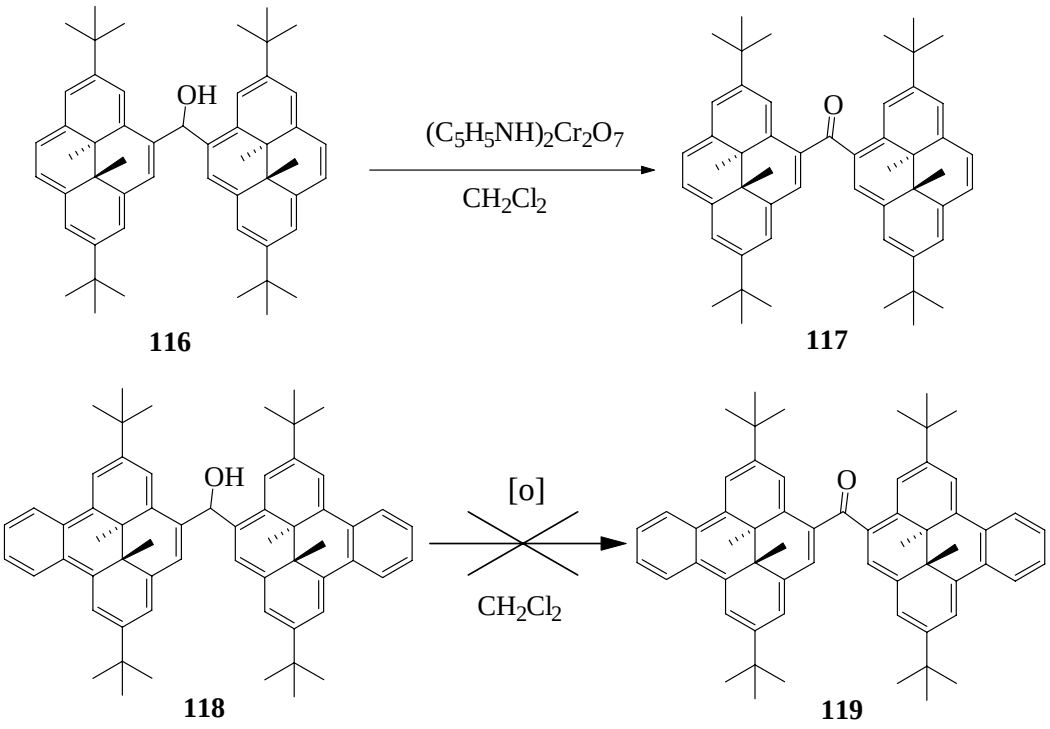

Scheme 2.15 The oxidation of alcohols 116 and 118.

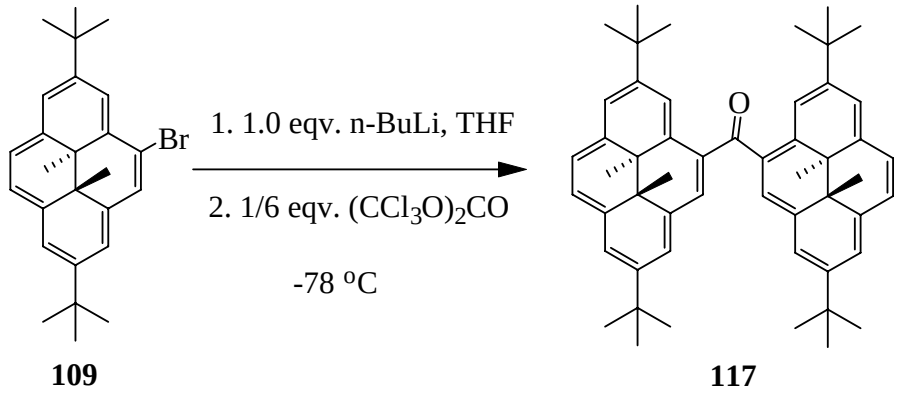

Scheme 2.16 Synthesis of 117 using triphosgene.

We thus tried to avoid this oxidation step for the homo derivative **119**, by reaction of the lithio derivative with the equivalent of $COCl_2$ (phosgene). Thus DHP-Li was made in

situ at -78 °C and was reacted with triphosgene. The reaction was successful, but the yield was low (15%) and some impurities are formed which are not easy to remove by chromatography or by recrystallization. We thus next tried dimethyl carbonate. The reaction of DHP-Li with dimethyl carbonate was carried out at 20 °C for 1h and then warmed to 50 °C for another hour. After workup, the desired product **117** was obtained in 82% yield as brown crystals (**Scheme 2.16**).

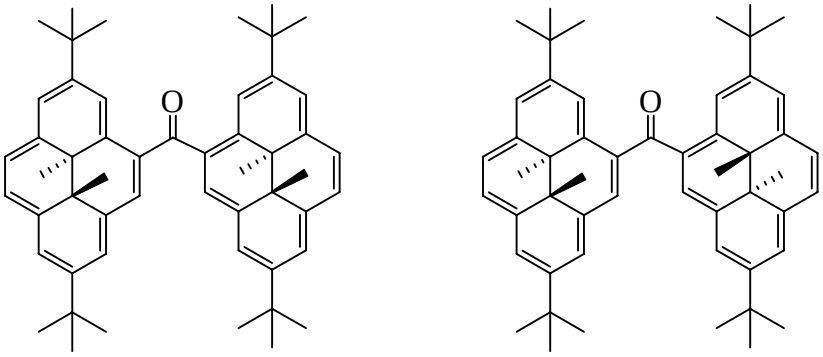

117A **117B**

Scheme 2.17 Two isomers of 117.

Characterization of **117** was accomplished by NMR, IR, MS and elemental analysis. Compound **117** has two isomers as shown in **Scheme 2.17**. In theory they should have four different internal methyl groups and four *t*-butyl groups. In the ^{1}H NMR spectrum, three signals were seen for the internal methyl protons at δ -3.28, -3.33 and -3.35, where the integration for the signal at δ -3.28 is twice that of the other two, indicating the overlap of two signals. The *tert*-butyl groups showed four peaks at δ 1.62, 1.61 1.39 and 1.38 as expected. Proton H-3 had a chemical shift of δ 10.29 and δ 10.27 for the two isomers respectively, downfield shifted compared to other DHP protons due to the anisotropic effect of the carbonyl group, which has been seen in other carbonyl

substituted DHP compounds. In the ^{13}C NMR spectrum, the peaks at δ 202.30 and 201.97 clearly showed the presence of a carbonyl group. In the IR spectrum, the strong absorption at 1673 cm^{-1} further confirmed the presence of a carbonyl group. The mass spectroscopy also supported the structure of **117** by giving a correct molecular ion (M^+) at *m/z* 715 and a high-resolution mass at 714.4869 (calcd for $C_{53}H_{62}O$, 714.4801).

Compound **119** was made by reacting of BDHP-Li with dimethyl carbonate using the same procedure as that of **117**. The desired product **119**, a mixture of two isomers, was obtained in 78% yield as red crystals after chromatography.

The structure of **119** was confirmed by NMR, IR and Mass spectroscopy. The ^1H NMR spectrum showed four internal methyl signals at δ -1.278, -1.284, -1.333, -1.352 and three *tert*-butyl signals at δ 1.48, 1.46, 1.44 respectively for the two isomers. The two *t*-butyl groups farthest from the carbonyl group have the same chemical shift δ 1.44. The carbonyl carbon appeared at δ 200.79 and 200.73 for the two isomers. The IR spectrum also confirmed the presence of a C=O group with a strong absorption at 1642 cm^{-1}. The EI MS gave a correct molecular ion at m/z 815 for $C_{61}H_{66}O$ and the HRMS gave the exact mass as 814.5104 (calculated 814.5114), all consistent with the structure of **119**.

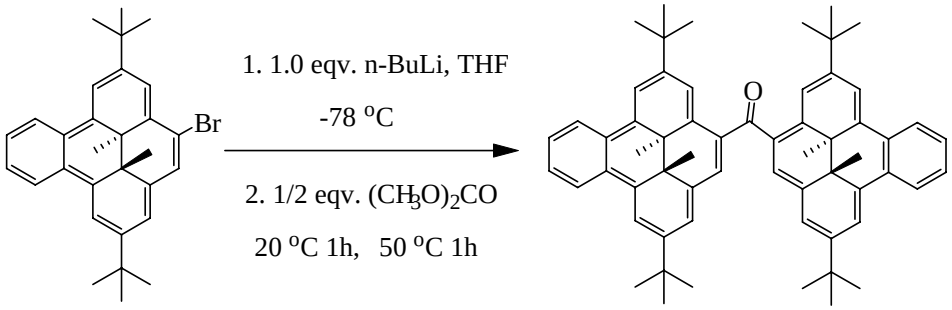

118 **119**

Scheme 2.18 Synthesis of 119.

2.3.3.2 Synthesis of hetero-switch 122

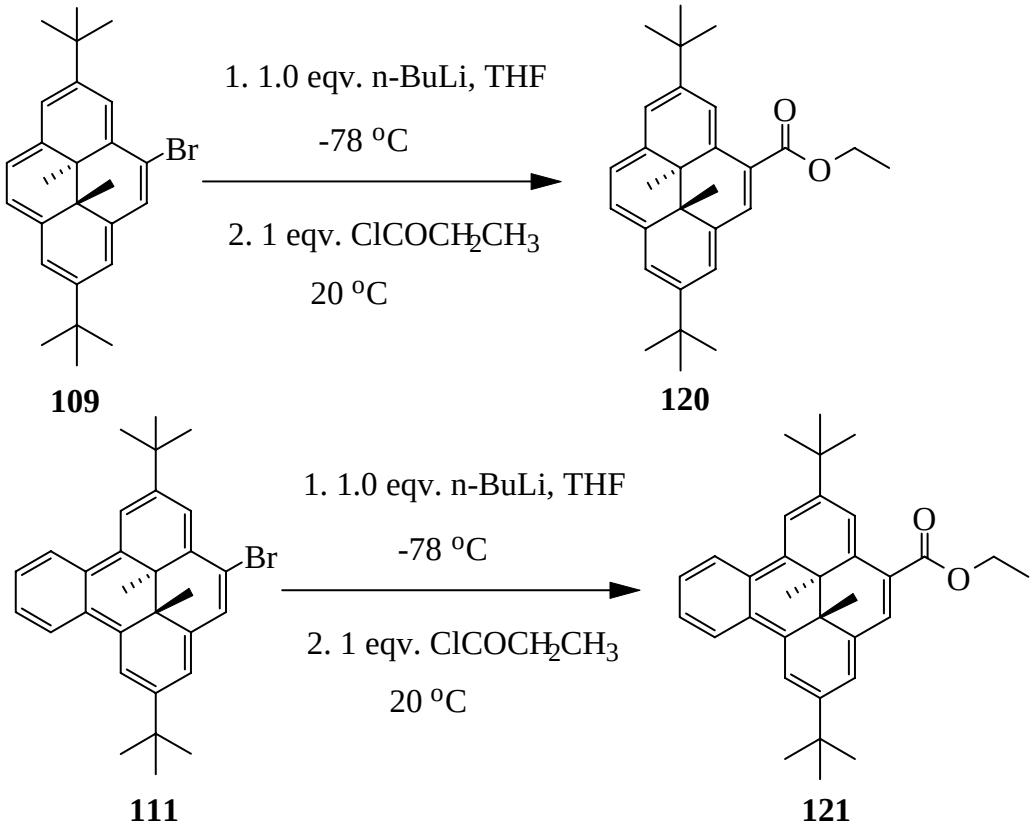

Scheme 2.19 Syntheses of 120 and 121.

The synthesis of hetero-switch **122** could be attempted by two routes shown in **Scheme 2.20**. One is the coupling between BDHP-Li and DHP-COOEt **120** and the other is the coupling of DHP-Li and BDHP-COOEt **121**. The intermediates **120** and **121** are made from the coupling of DHP-Li and BDHP-Li with ethyl chloroformate. Thus DHP-Li (or BDHP-Li) was made in situ at –78 °C and then quenched with ethyl chloroformate to give DHP-COOEt **120** (or BDHP-COOEt **121)** in 87% (or 80%) yield as a green (or dark purple) solid (**Scheme 2.19**). The overall structures of **120** and **121** were confirmed by NMR, MS, IR spectroscopy and elemental analysis. In the ^{1}H NMR spectra, the CH_3

protons of the ethyl groups appeared at δ 1.61 for **120** and δ 1.49 for **121.** The two CH_2 protons are diastereotropic with chemical shifts at δ 4.63 and 4.64 for **120** and δ 4.46 and 4.45 for **121**. The coupling constants between them are 10.8 Hz (**120**) and 10.7 Hz (**121**) respectively. The DHP internal methyl protons appeared at δ -3.93 and -3.94 for **120** and δ -1.42 and -1.47 for **121**; and the tert-butyl protons were found at δ 1.71 and 1.67 for **120** and δ 1.53 and 1.48 for **121**.

The ^{13}C spectra showed all the expected carbon resonances. The carbonyl carbon atoms of the ester groups appeared at δ 169.09 (**120**) and δ 168.04 (**121**). The ^{13}C NMR DEPT spectra also showed the CH_2 groups of the ethyl groups at δ 61.04 (**120**) and δ 60.77 (**121**). The IR spectra supported the structures by showing strong absorptions at 1698 cm^{-1} (**120**) and 1702 cm^{-1} (**121**) for the ester C=O stretches. The mass spectra (EI) also supported the structures by giving correct molecular ions at *m/z* 416 and *m/z* 466 and for **121**. The high resolution mass gave the correct result at 416.2711 (calcd for $C_{29}H_{36}O_2$ 416.2715) for **120** and 466.2865 (calcd for $C_{33}H_{38}O_2$: 466.2872) for **121**. The elemental analysis (C, 83.75%; H, 8.72%) for **120** (Calcd for $C_{29}H_{36}O_2$: C, 83.61%; H, 8.71%) also comfired the structure.

The synthesis of hetero bis-switch **122** was carried out by reacting BDHP-Li (or DHP-Li) and **120** (or **121**) at 20 °C for 1h and then warming to 50 °C for another hour (**Scheme 2.20**). After chromatography, the desired product **122** was isolated as reddish brown crystals in 80% yield.

The structure of **122** was confirmed by NMR, IR, MS and HRMS. In the proton NMR spectrum, eight internal methyl signals and eight *tert*-butyl signals were seen. Four of the methyl signals appeared at δ -1.175, -1.183, -1.240 and -1.264 and four *tert*-butyl signals

appeared at δ 1.420, 1.414, 1.412 and 1.409 corresponding to the BDHP side. The DHP side internal methyl protons and *tert*-butyl protons were found at δ -3.755, 3.757, -3.78, -3.80, and δ 1.69, 1.68, 1.62, 1.61 respectively. In the ^{13}C NMR spectrum, the C=O carbon atoms appeared at 202.07 and 201.79 for the different isomers. In the IR spectrum, the absorption for the C=O stretch was found at 1644 cm^{-1}(highly conjugated ketone). The mass spectrum supported the structure by giving the correct molecular ion at *m/z* 764 [M^+] and high resolution mass for **122** at 764.4985 (calcd for $C_{57}H_{64}O$ 764.4957).

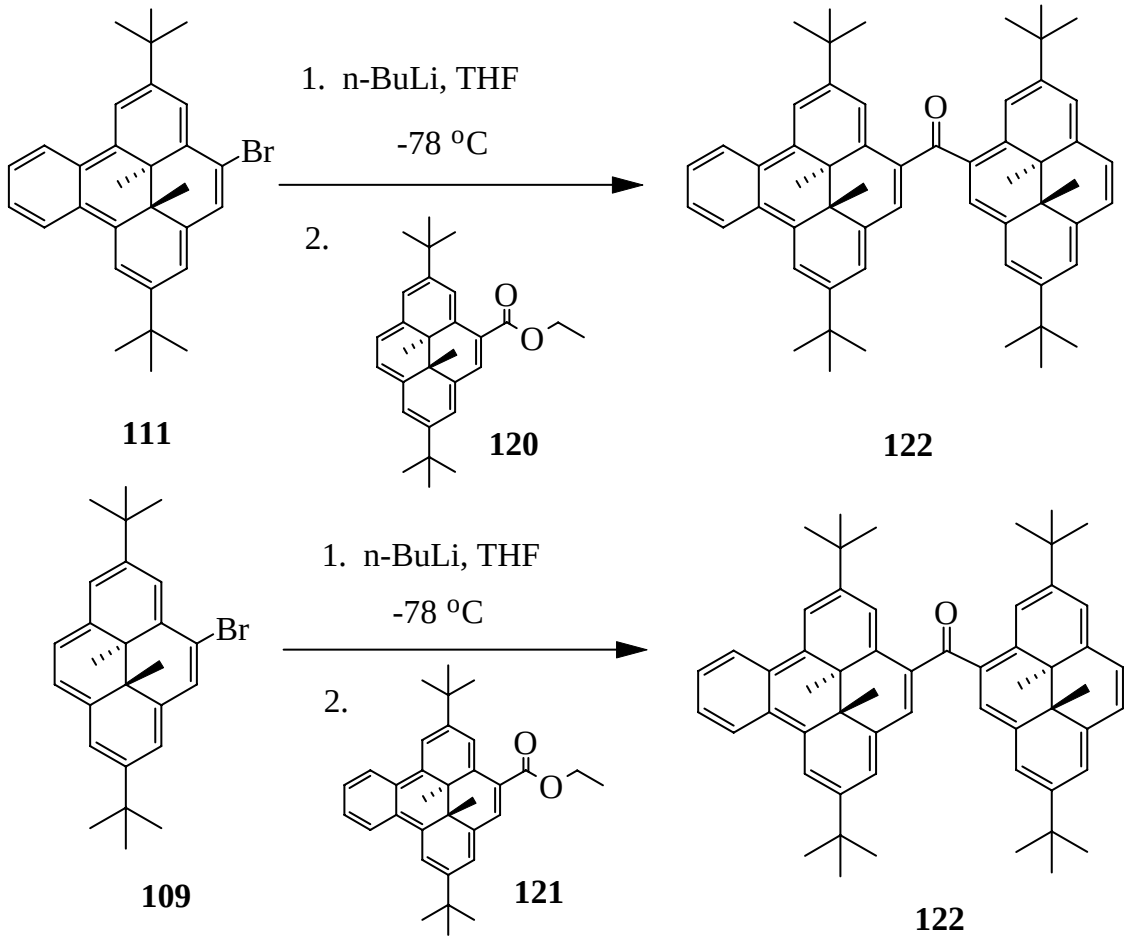

Scheme 2.20 Synthesis of 119.

2.3.4 Linked DHP systems with a methylene group as spacer

2.3.4.1 Synthesis of the methylene linked homo-switch 123

Compound **123** was synthesized by the reduction of alcohol **116**. We tried several methods but the procedure[98] in which $NaBH_4$ and the Lewis acid $BF_3{\cdot}OEt_2$ were used gave the best result (86% yield). A large excess of $NaBH_4$ and $BF_3{\cdot}OEt_2$ were required for completion of the reaction. Gribble's method,[99] in which protic acid, CF_3COOH, instead of Lewis acid was used, did not work. The reaction led to decomposition. On the other hand, Olah's procedure,[100] the hydrogen transfer reaction from cyclohexene using $Pd/C/AlCl_3$ as catalyst, also gave a good result. Thus, **116** and $Pd/C/AlCl_3$ refluxing in cyclohexene for 36 hours gave 80% yield of **123** (**Scheme 2.21**). Hydrogenolysis using $Pd/C/H_2$[101] was not successful even after refluxing for 24 hours in ethanol.

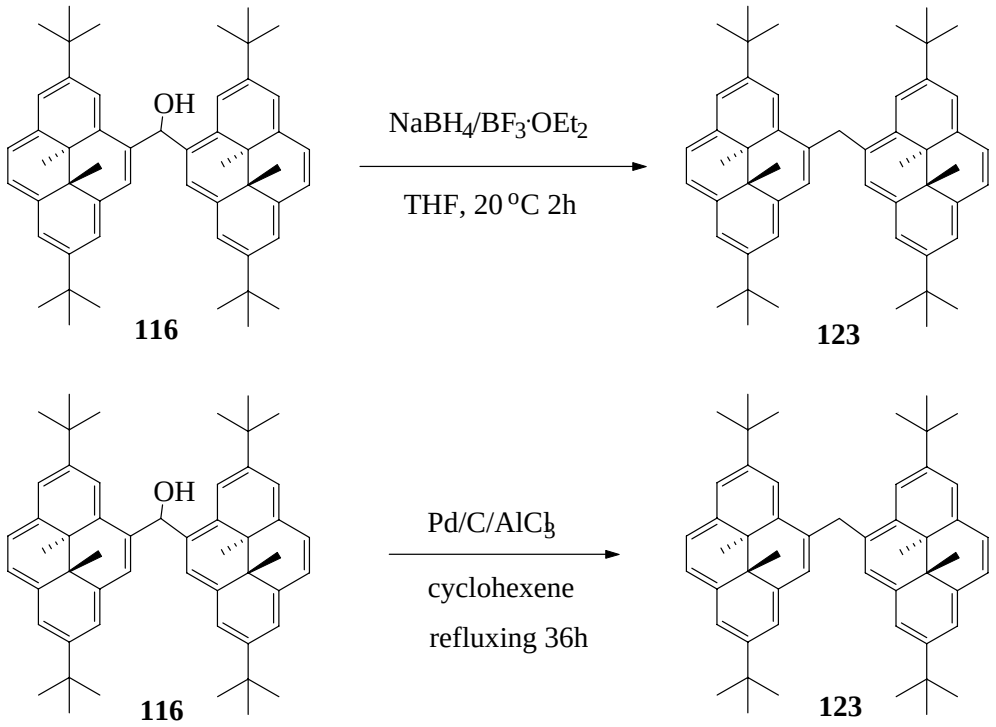

Scheme 2.21 The reduction of alcohol 116.

In the ^{1}H NMR spectrum of **123**, the methylene protons appeared at δ 5.96 for isomer **123A** and δ 6.01 and 5.91 for isomer **123B** (**Scheme 2.22**). In **123A**, the two CH_2 protons are equivalent and appear as one signal, but in **123B**, they are diastereotropic and appear at two different chemical shifts. The coupling constant between them is 15.5 Hz, which is reasonable for a germinal coupling. In the ^{13}C NMR spectrum, the methylene carbon signal appeared at δ 38.70 and 38.50 for the two isomers. The chemical shifts for the methylene protons and the methylene carbons are all deshielded compared to those of the normal methylene groups, because they are in the deshielding zone of the two DHP ring currents. In the IR spectrum, the absence of absorptions at ~3500 cm^{-1} indicated the disappearance of the OH group. The mass spectrum (EI) also supported the structure by showing a correct molecular ion at *m/z* 701 (M^+) for **123** and the high resolution mass gave the correct result at 700.5004 for **123** (Calcd for $C_{53}H_{64}$ 700.5001).

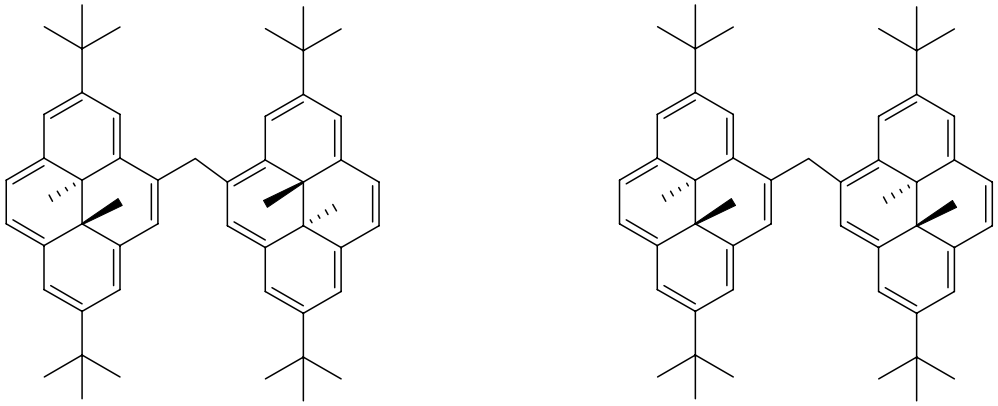

123A **123B**

Scheme 2.22 Two isomers of 123.

2.3.4.2 Synthesis of the methylene linked homo-switch 124

Compound **124** was synthesized in a similar way as **123**, except that the starting material used was ketone **119.** Thus reduction of **119** with $NaBH_4$ and $BF_3{\cdot}OEt_2$ in THF gave out 74% yield of **124** as dark red crystals (**Scheme 2.23**).

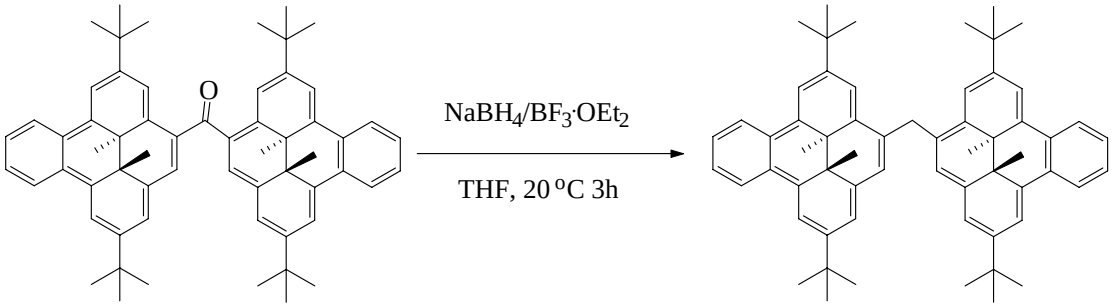

119 **124**

Scheme 2.23 Synthesis of 124.

Similar to **123**, **124** is a mixture of two isomers (**Scheme 2.24**) in a ratio of about 1:1. However, an impurity travels very close to desired product on column and so just the front part of the band was collected by column chromatography in order to get pure product. This sample showed a 2:1 ratio of isomers in the NMR spectrum. In the ^1H NMR spectrum, the methylene protons appeared at δ 4.83 for isomer **124A** and δ 5.00 and 4.64 for isomer **124B** respectively. The coupling constant between the two different CH_2 protons in **124B** is 15.3 Hz. In the ^{13}C NMR spectrum, the C=O carbon signals at δ 200.79 and 200.73 in **119** were replaced by new methylene carbon signals at δ 36.26 and 36.24, indicating that the reduction of a C=O group to a CH_2 group had taken place. The chemical shifts for the methylene protons and the methylene carbon atoms are less deshielded than those of **123** consistent with the reduced the ring currents caused by benzannelation of the DHP rings. In the IR spectrum, the C=O stretch at 1642 cm^{-1} in **119**

was absent. The mass spectrum (EI) also supported the structure by showing a correct molecular ion at *m/z* 801 (M^+) for **124** with a high resolution mass at 800.5317, (calcd for $C_{61}H_{68}$: 800.5321).

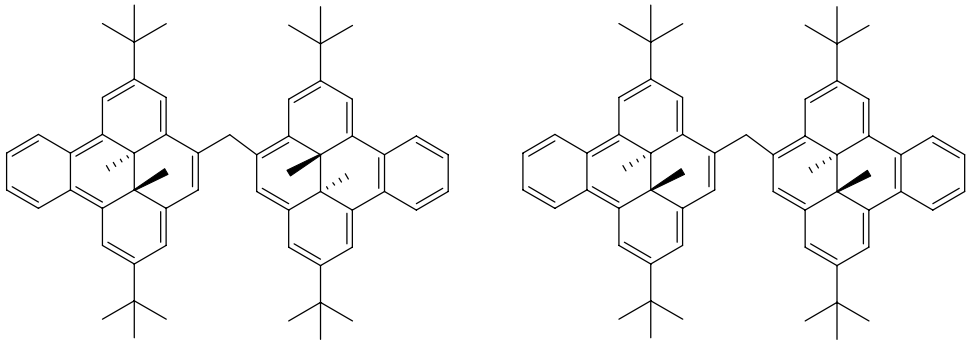

124A **124B**

Scheme 2.24 Two isomers of **124**.

2.3.5 Linked DHP system with an enthynyl as spacer 130

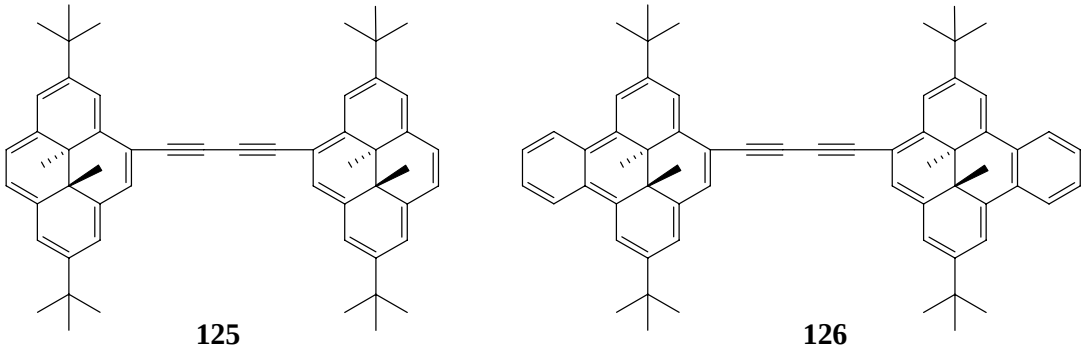

125 **126**

A former group member Bandyopadyhay[92b] made the diethynyl linked dihydropyrene **125** and the diethynyl linked benzodihydropyrene **126** by Eglington coupling. However, when he tried to make a cross coupled compound such as **130** by Sonogashira coupling, only homo-coupled product was isolated because of the sluggish activity of DHP-I **129**. We have found that compound **130** can be made by the two step Sonogashira coupling reactions shown in **Scheme 2.25**. The side reaction - homo-coupling - was suppressed by

the addition of KI and gave about 60% of the desired cross coupling product **130**. The homo-coupled byproduct **126** was also isolated in ~30% yield along with the desired **130**.

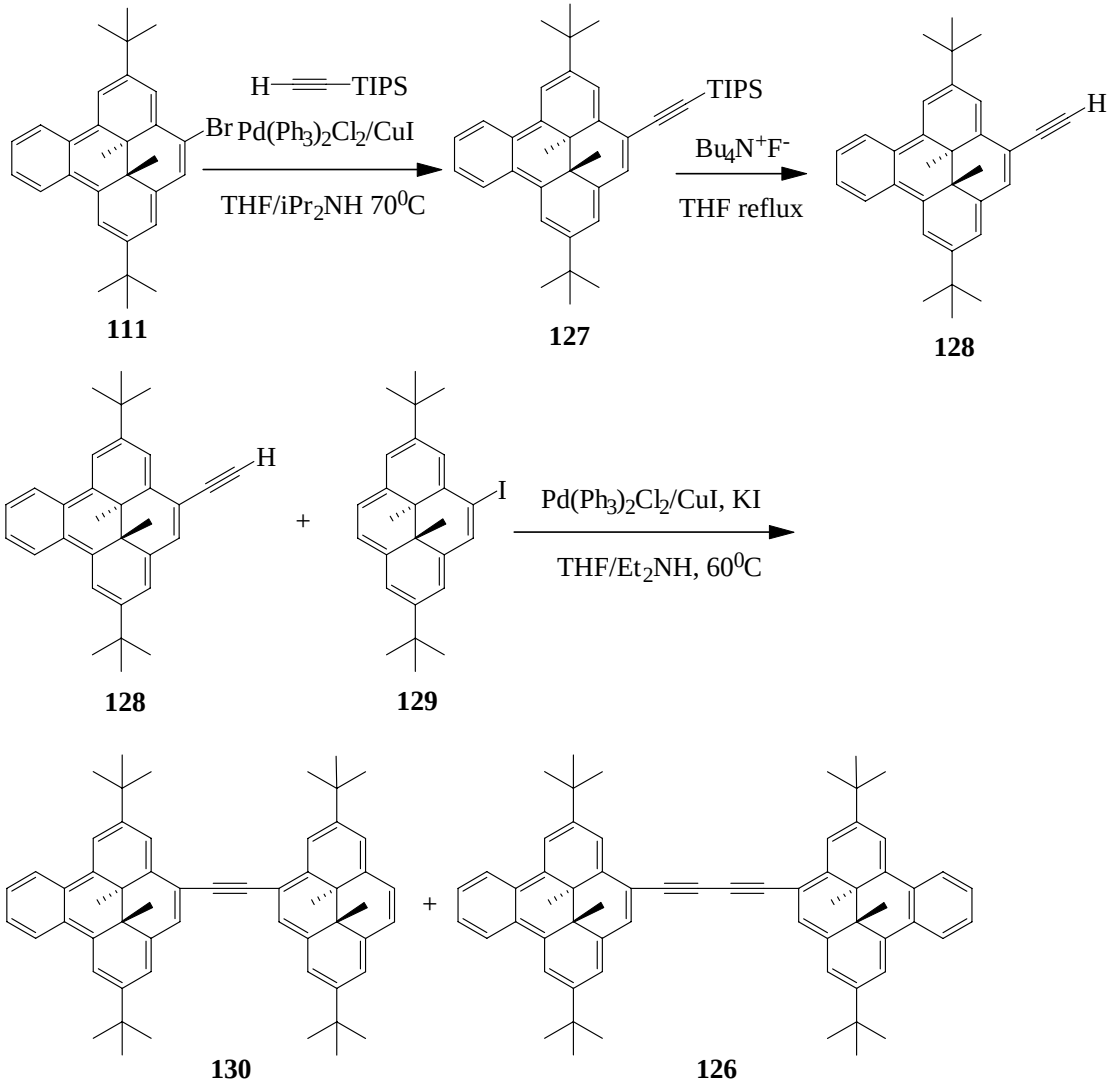

Scheme 2.25 Syntheses of 130.

The structure of **130** was confirmed by NMR, IR, MS spectroscopy and elemental analysis. In the ^{1}H NMR spectrum of **130**, the DHP side showed two internal methyl signals at δ -3.77 and -3.78 and two *tert*-butyl signals at δ 1.78 and 1.70. The BDHP side showed four peaks for internal methyl protons at δ -1.285, -1.291, -1.303 and -1.309 and

two signals for *tert*-butyl protons at δ 1.64 and 1.53. The two ethynyl carbon atoms appeared at δ 96.24 and 95.77 in the ^{13}C NMR spectrum, downfield shifted comparing to a normal ethynyl carbon because of the deshielding by the aromatic DHP rings. In the IR spectrum, the weak absorption at 2178 cm^{-1} indicated the presence of the C≡C triple bond. The mass spectrum (LSI-MS) also supported the structure by giving the correct molecular ion at *m/z* 760.4 [M^+]. The elemental analysis was satisfactory.

2.4 Results and discussion

2.4.1 Photochromism of 2-formyl-7-*tert*-butyl dihydropyrene 112

As discussed in the introduction, substituents affect the photochromic properties of dihydropyrenes. Substitution of electron withdrawing groups increases the opening quantum yields but speeds up the thermal return reactions. On the other hand, electron donating substituents decrease the opening quantum yields but slow down the thermal return slightly.[79,80,81] Electron withdrawing groups at the 2 or 7 position have the largest effect. They increased the photo opening quantum yield but speeded up the thermal return reaction dramatically.[79,81] We thought that it would be interesting to study the photochromic properties of 2-formyl-7-*tert*-butyl dihydropyrene **112** since it has both an electron withdrawing and a weak donating group at the 2 and 7 positions respectively.

Compound **112** has a purplish red color. The visible light opening process of **112** occurred rapidly in solution (**Scheme 2.23**). When a deaerated solution of **112** was irradiated with >490 nm visible light (white light from a 500 W household tungsten bulb with 490 nm cut-off filter), the purplish red solution gradually bleached. The UV-vis spectrum was recorded at successive intervals and the series of spectra are shown in

Figure 2.1. As irradiation continued, the visible region bands at 347, 402, 515 and 596 nm, which are the principle absorptions characteristic of the DHP form, decreased and disappeared and new bands at 229 and 279 nm appeared in the UV region, characteristic for the CPD form **112'**.

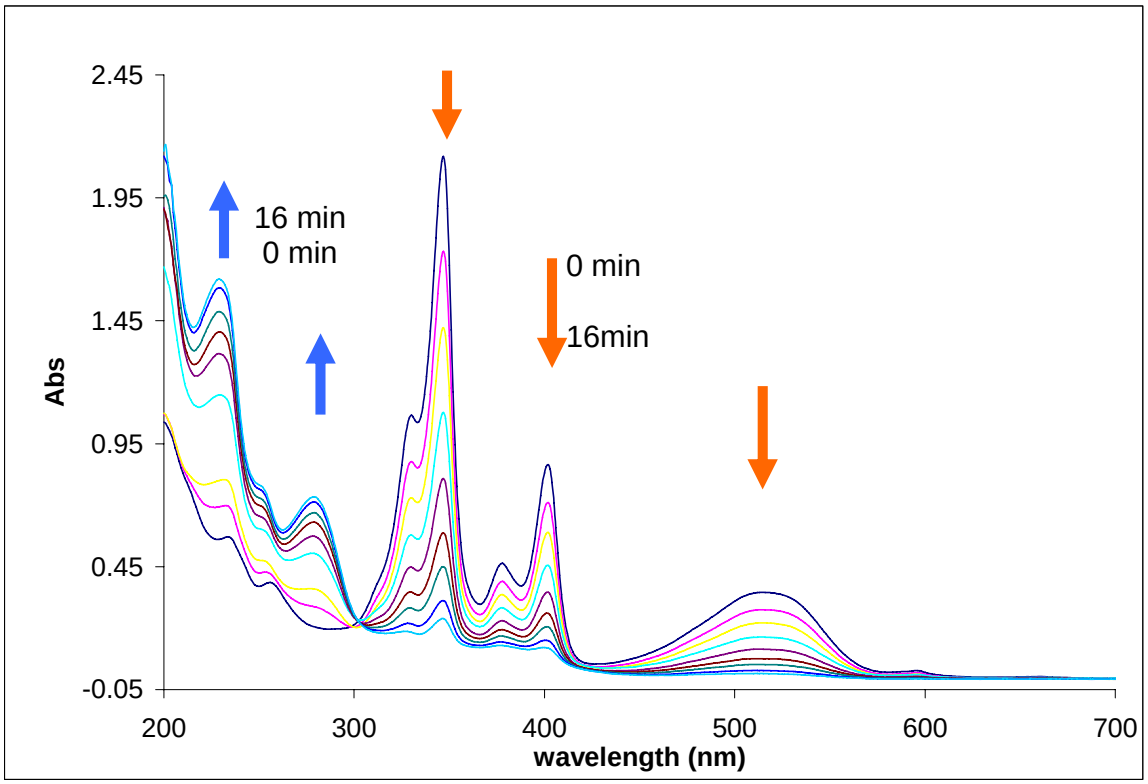

Figure 2.1 The sequential UV-vis spectra of photo opening of 112.

Proton NMR spectroscopy also showed the conversion from **112** to **112'**. For the purposes of NMR study, a deaerated $CDCl_3$ solution of 5-10 mg of **112**, chilled with ice water, was irradiated with > 490 nm visible light in an NMR tube. The conversion was completed in ca. 20 minutes. The NMR spectrum of the closed form **112** and of the open form **112'** is shown in **Figure 2.2**. The chemical shifts for the internal methyl protons moved from δ -3.82 and -3.84 in **112** to δ 1.56 and 1.48 in **112'**, as they are no longer in the center of the large annulene ring.

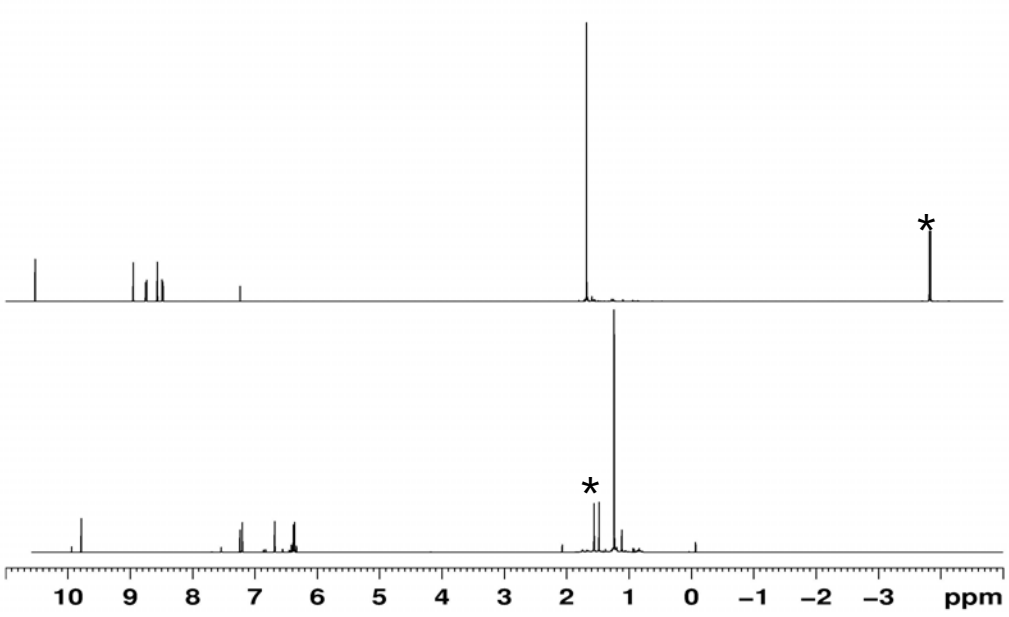

Figure 2.2 ^{1}H NMR spectra of 112(C) (top) and 112'(O) (bottom).

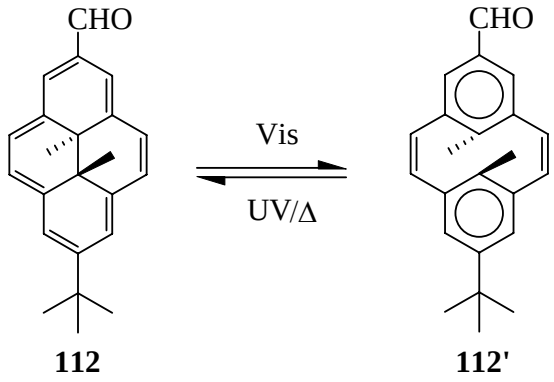

Scheme 2.26 Isomerization between 112 and 112'.

We have not measured quantum yields for our compounds, but instead use the relative opening rate compared to benzoDHP **36**.[64, 91] For comparison purposes, equimolar solutions of the samples e.g. **112** and **36** in cyclohexane were irradiated parallel to each other with the same lamp at the same time. UV-vis spectra were recorded at intervals, so that the relative rates of opening could be determined (see **Section 2.4.3** for experimental and data analysis details). The photo opening of **112** to **112'** is thus

about 4 times slower than benzoDHP **36** to **36'** (**Figure A.1** in Appendices). This agreed with a former report,[80] in which the quantum yield of 2-acetyl DHP **131** is Φ = 0.012 and that of **36** is Φ = 0.042, about 3.5 times as large as that of **131**.

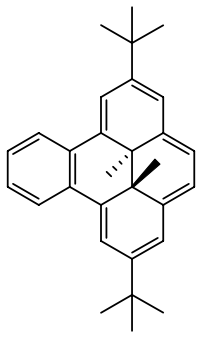

Φ = 0.042

36

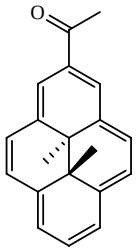

Φ = 0.012

131

The UV closing reaction, e.g. **35′** to **35**, is fast for most of the systems studied[63] (see **Section 2.4.3** for experiment and data analysis details). Compound **112′** is no exception. When equimolar solutions of **36′** and **112′** in cyclohexane were irradiated side by side with a pencil mercury lamp (254 nm), **112′** actually closed at about 1.8 times faster than that of the benzo-derivative **36′** (**Figure A. 2** in Appendices).

Substitution of a formyl group at the 2-position substantially speeds up the thermal return reaction: at 30 °C, $\tau_{1/2}$ = 12 h for parent **11'**, while for formyl **88'** $\tau_{1/2}$ = 13 min. On the other hand, substitution of *t*-butyl groups at the 2 and 7 positions slows down the thermal return reaction slightly, comparing $\tau_{1/2}$ of 14 h for **35'** to 12 h for parent **11'** at 30 °C. The thermal return reaction of **112'** was studied by UV-vis spectroscopy. The plots are given in Appendices **Figure A.3**. It was found that the half life of **112'** was 17 min at 30 °C, slightly longer than that of **88'**, but substantially faster than that of **35'** (**Table 2.1**), indicating the combination of the effects of the formyl group and the *t*-butyl

group. This is expected and consistent with substitution effects that have been found before.[79,80,81]

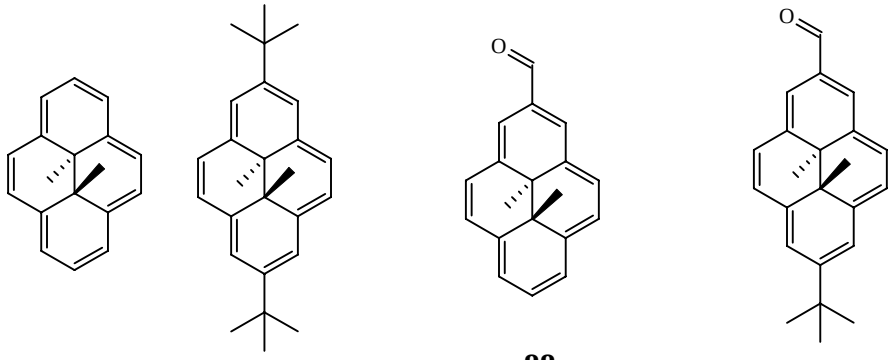

11 **35** **88** **112**

Table 2.1 The thermal decay rate constants and half-lives at 30 °C

CPD form isomers	k (min^{-1})	$\tau_{1/2}$
11'[79]	0.0010	12 h
35'[79, 82]	0.0008	14 h
88'	0.053	13 min
112'[a]	0.042	17 min

* Errors: Former students who carried out replicate runs found ± 4% errors in rate constant k.[91, 92]

When compound **112** was irradiated with visible light without prior deoxygenation, epidioxy-bridged compound **132** formed instead of **112'** (**Scheme 2.27**). This compound is not stable and reforms **112** very fast at room temperature. The structure of **132** was determined by NMR spectroscopy at -30 °C. The methyl on C-16, which is connected to a benzene ring, appears in the ^{1}H NMR spectrum at δ 1.99 while the carbon appeared at δ 24.08 in the ^{13}C spectrum. On the other hand, for the methyl on C-8, the protons appeared at δ 0.06 and the carbon was at δ 13.52. C-5 and C-8, which are connected with

the epidioxy bridge, appeared at δ 83.61 and 83.47. The *tert*-butyl group's protons appeared at δ 1.02. The formyl proton appeared at δ 9.66 and the formyl carbon appeared at δ 190.81.

The formation of **132** is not too surprising. Such reactions have been observed occasionally before for DHP systems. It was reported that irradiation of **11** or **35** with visible light under oxygen resulted in the formation of small amounts of the corresponding epidioxy-bridged compounds **133** and **134** (**Scheme 2.27**).[102] Actually, it is known that singlet oxygen can add to aromatic compounds through a (4 + 2) photo cycloaddition. For example, compound **135** undergoes photocycloaddition with O_2 to give compound **135'** (**Scheme 2.28**).[60]

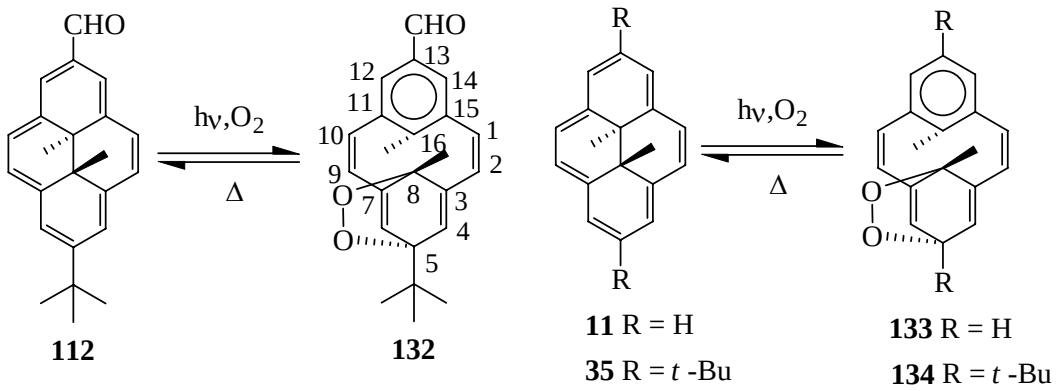

Scheme 2.27 Oxygen adducts of dihydropyrenes

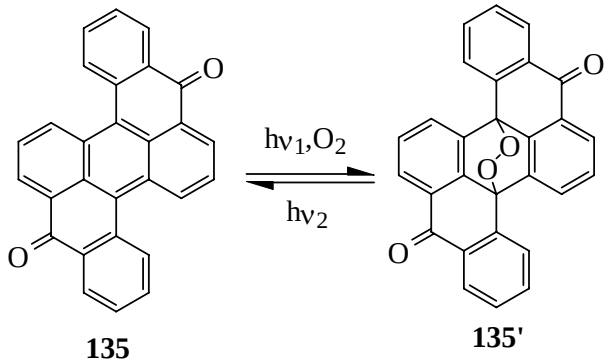

Scheme 2.28 Example of the addition of singlet oxygen to an aromatic compound.

2.4.2 Multiple photoswitching properties of bis-DHP systems

As mentioned previously, Ward[85,86,90] studied the photochromic properties of the fused bis-DHP photoswitches **102** and **104**. They were connected by means of a planar conjugated arene spacer and showed three way photoswitching properties. Wang[85,91] synthesized a fused tris-DHP system **103**, which also showed three way photoswitching properties. This result is not surprising. Since the middle DHP unit stayed open all the time, this molecule was actually a bis-DHP system in which two DHP units were connected by double non-planar conjugated spacers. Bandyopadhyay[92] investigated several bis-DHP systems linked by non-planar conjugated spacers, in which the diethynyl linked bis-DHP system **105** showed three way photoswitching properties; the phenyl linked system **106**, on the other hand, only showed two states; and the ethenyl linked system **107** shut down the photoswitching property completely.[92] Thus we knew that spacers have played important roles in terms of the multiple photoswitching properties of bis-DHP systems. Therefore we were interested to see what other spacers such as cross conjugated spacers and even non-conjugated spacers would do to the multiple photoswitching properties of bis-DHP systems.

The multiple photoswitching properties of compounds investigated in this thesis were studied by UV-vis and ^{1}H NMR spectroscopy. For the UV-vis study, a deaerated solution of the compound in cyclohexane, sealed in a quartz UV cell, chilled by ice water, was irradiated with visible light using a 490 nm cut-off filter unless otherwise stated. A 500W tungsten lamp served as the visible light source. UV-vis spectra were taken at various time intervals. For the ^{1}H NMR study, 5-10 mg of the sample was dissolved in an appropriate NMR solvent. The solution was bubbled with argon for 30 min and sealed.

The sample was then irradiated with visible light and ^{1}H-NMR spectra were recorded at various time intervals. For the photo closings, the solutions of the samples were first irradiated by visible light to the corresponding open CPD forms. Their reversion to the DHP form by UV light (a 254 nm mercury pen light) was thus monitored by UV-vis or ^{1}H-NMR spectroscopy at various time intervals.

2.4.2.1 Bis-DHP systems linked by a carbonyl group

2.4.2.1.1 Homo bis-switch 117

Previous studies showed that substitution of carbonyl group enhanced the quantum yields of DHP systems. For example the quantum yield of acetyl-DHP **92** is Φ = 0.0038,[80] about 2.5 times larger than that of the parent **35**. Thus we synthesized DHP-CO-DHP **117**, in which two DHP units were linked by a carbonyl group, to see how the carbonyl group would affect the photoswitching properties of a bis-DHP system.

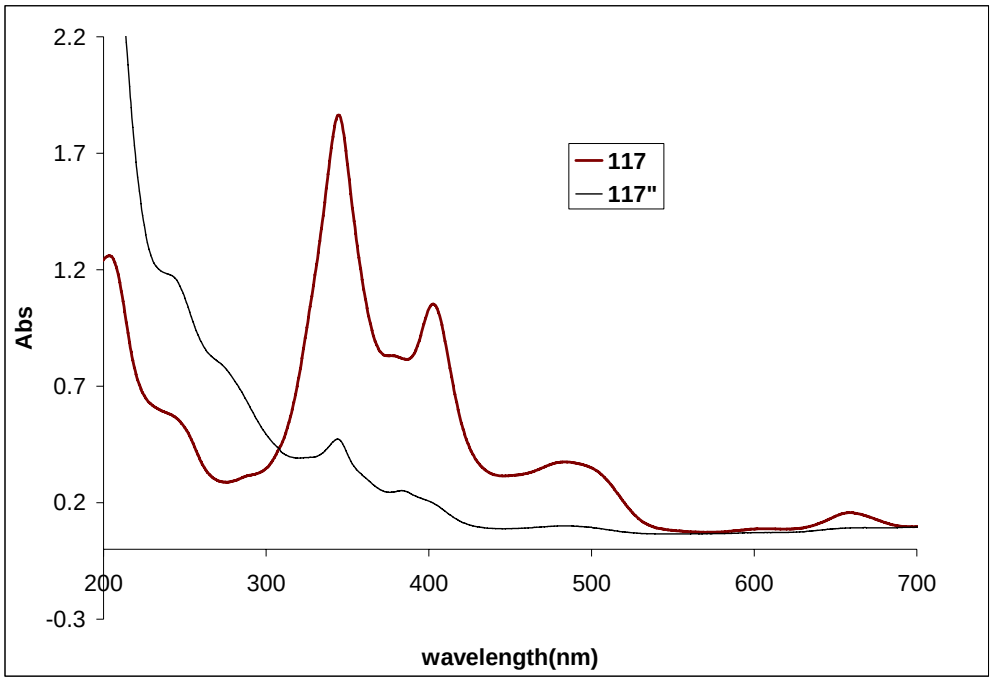

Figure 2.3 UV-vis spectra of 117(C-C) and 117”(O-O).

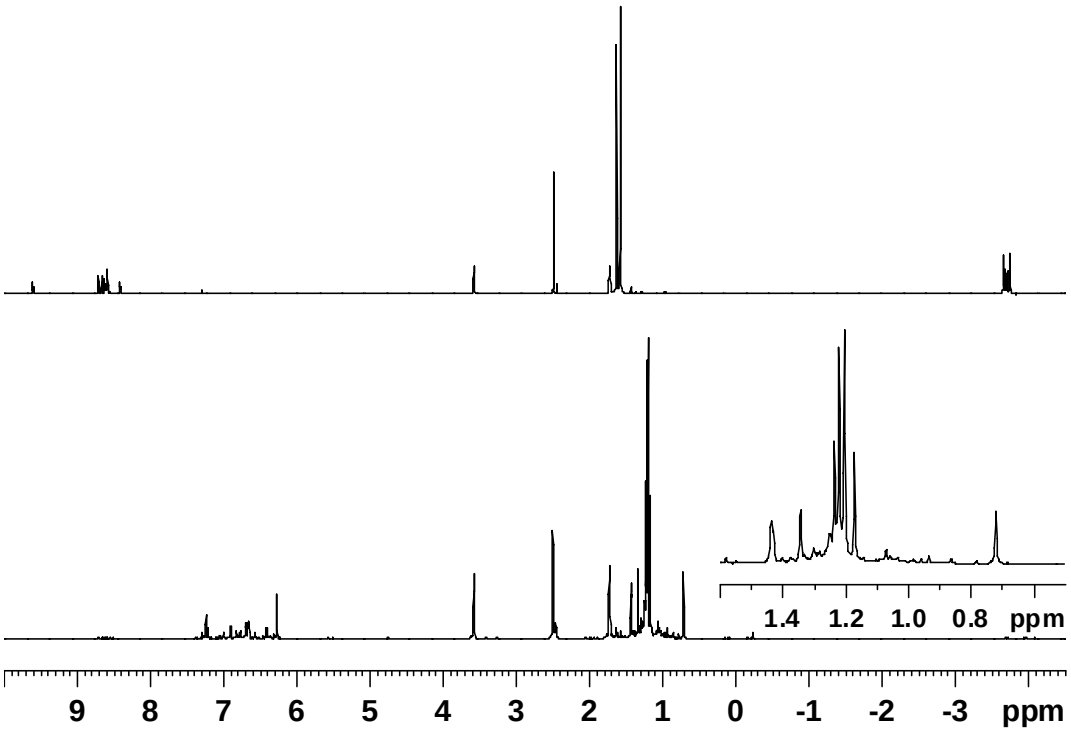

Figure 2.4 Proton NMR spectra of 117(C-C) (top) and 117”(O-O) (bottom).

Compound **117** has a brown color. It showed four visible region bands at 344.9, 405, 485 and 660 nm and their absorption coefficients were 86200, 49800, 15900 and 3540 $M^{-1}cm^{-1}$ respectively. Irradiation with visible light converted it to the completely open form **117’’**. After convertion to **117”**, all the absorptions in the visible region, the principle absorption characteristics of DHP form, almost disappeared and absorption in the UV region, which are the principle absorptions of CPD form, increased to a maximum, which is shown in **Figure 2.3**.

The conversion of **117** to **117”** was also investigated by proton NMR spectroscopy. The NMR spectra of **117** and **117”** are shown in **Figure 2.4**. The internal methyl signals between δ -3.6 and -3.9 for **117** move to δ 1.44, 1.43, 1.35, 1.25 and 0.72 in **117’’**, because they are no longer in the center of the large annulene ring. The aryl protons move upfield, not subject to the strong DHP ring current.

Detailed study of the photo opening and closing by proton NMR spectroscopy revealed that **117** underwent a stepwise photo opening and closing process. In other words, it showed multi-state photoswitching properties. The sequential partial opening proton NMR spectra are shown in **Figure 2.5** (left). As we can see, when the sample is irradiated, the original internal methyl peaks at δ -3.66, -3.68, -3.71 and -3.74 decrease and new internal methyl peaks at δ -3.92, -3.96, -4.08 and -4.16 rise. These new internal methyl peaks indicate the formation of a new species **117'**. As irradiation was continued, the original internal methyl signals continue to decrease, while the new internal methyl peaks increase at first, and then stay constant, which means that the formation rate and the conversion rate to the completely open form **117''** reach the same value. After that, with the decreased amount of the starting form **117** present, the formation rate of **117'** slows down, but the conversion rate stays the same, so the internal methyl peaks from both species start to decrease together until all have gone, which indicates the complete conversion of **117** to **117"**. The UV closing process of the fully opened isomer **117"** was studied the same way as the opening process of **117**. The sequential NMR spectra are shown in **Figure 2.5** (right). On UV irradiation, eight internal methyl peaks appeared at δ -3.66, -3.68, -3.71, -3.74, -3.92, -3.96, -4.08 and -4.16, indicating that **117** and **117'** appeared. As time increased, the peaks at δ -3.66, -3.68, -3.71 and -3.74 (corresponding to **117**) continued to increase, while the peaks at δ -3.92, -3.96, -4.08 and -4.16 (corresponding **117'**) stayed constant at first and then decreased and disappeared, which suggested that **117'** was converting to **117** until all was gone. The exact ratios of three states, C-C, O-C, O-O, in photo opening and closing processes can not be obtained because of the overlapping of the peaks, but sketches are shown in **Figure 2.6** (p109)

which give a rough idea of the concentration changes for the three states. These sketches are based on the approximate sizes of the internal methyl peaks of the closed side(s).

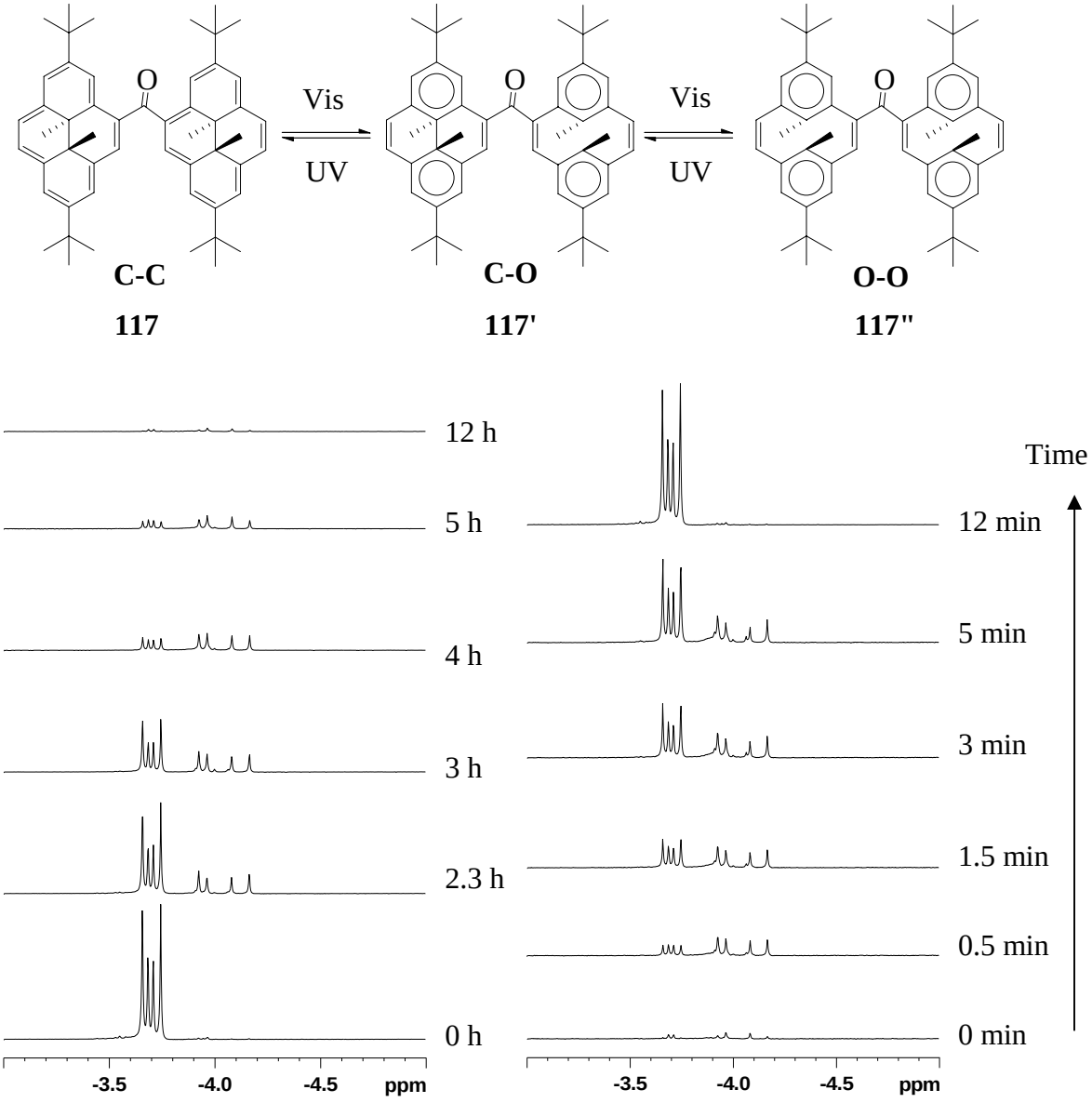

Figure 2.5 Sequential partial NMR spectra for the visible light opening (left) of 117 with wavelength > 490 nm light and UV closing (right) of 117" with 254 nm light.

The above NMR evidence strongly suggested that the closed-open intermediate **117'** was involved in both the photo opening and photo closing processes. This is similar to Wang's fused tris-DHP system **103**, in which both of the photo opening and photo

closing processes went through the closed-open intermediate **103'**. But it is different from the fused bis-DHP system **102** and the diethynyl linked bis-DHP system **105**. In those systems, the closed-open intermediate can only be observed in the photo closing process, but not in the photo opening process. For **105**, the existence of the closed-open intermediate **105'** was only indicated by two isosbestic points in the UV-vis spectra. No evidence could be found by proton NMR spectroscopy.

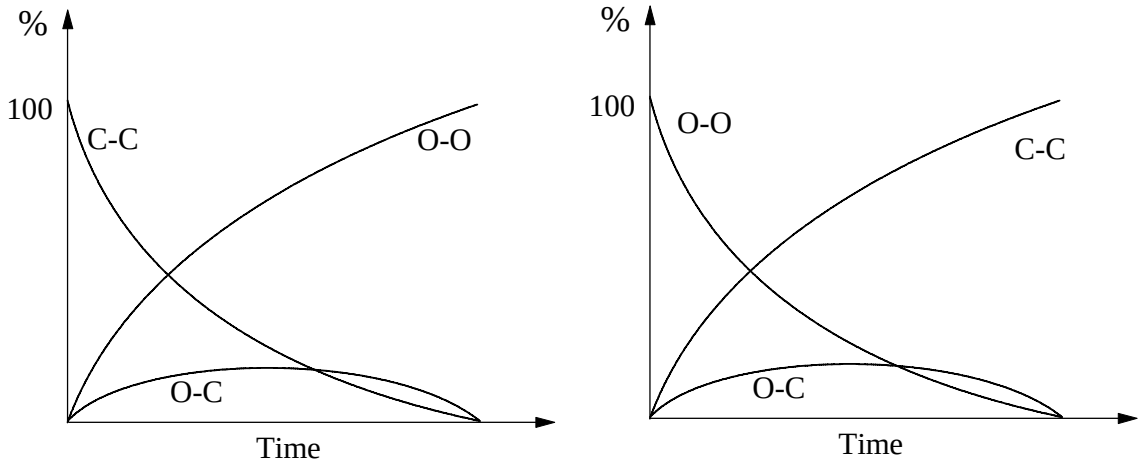

Figure 2.6 Sketches of C-C, O-C and O-O isomer concentration changes in the photo opening and closing processes

2.4.2.1.2 Homo bis-switch 119

Irradiation of a degassed solution of bis-benzoDHP **119** with visible light caused rapid isomerization to **119".** **Figure 2.7** shows the closed and fully opened spectra of **119** and **119"**. Compound **119** showed four visible bands at 325, 339, 407 and 514 nm with absorption coefficients of 30200, 31500, 51100 and 10900 $M^{-1}cm^{-1}$ respectively. There is some red shifting from its parent DHP analog **117**, as the result of the elongated conjugation. After **119** was converted to **119"**, all the visible bands attributing to the DHP form disappeared and new absorptions in the UV region, the principle absorption of the CPD form, increased to a maximum.

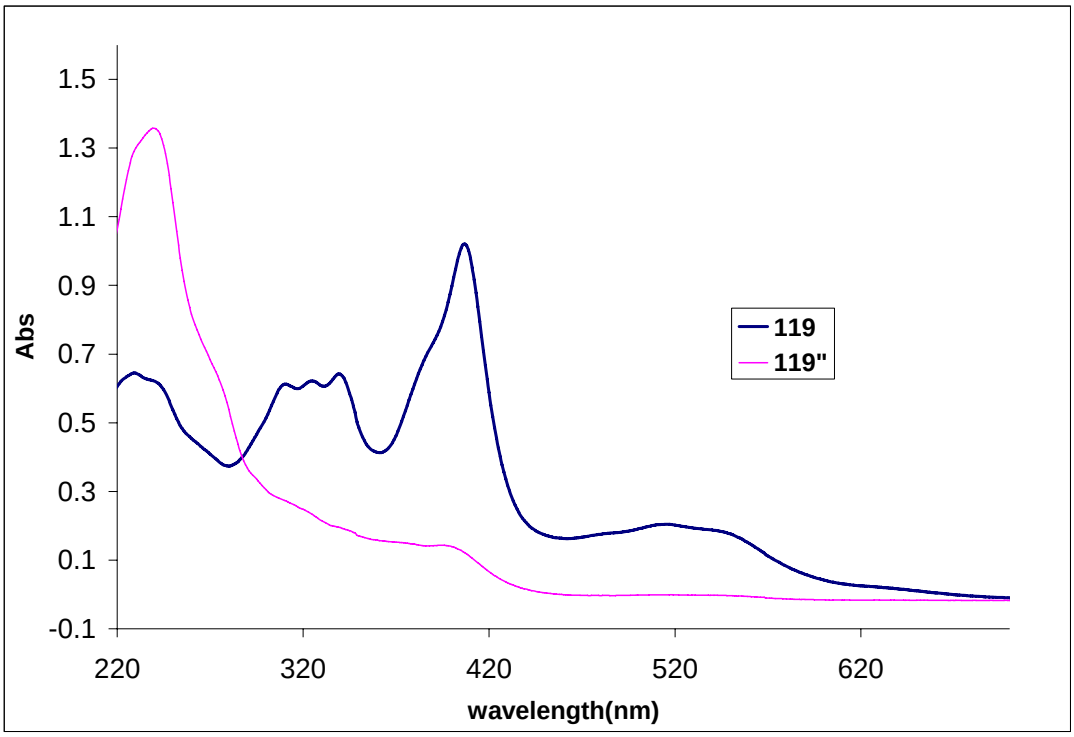

Figure 2.7 UV-vis spectra of 119(C-C) and 119”(O-O).

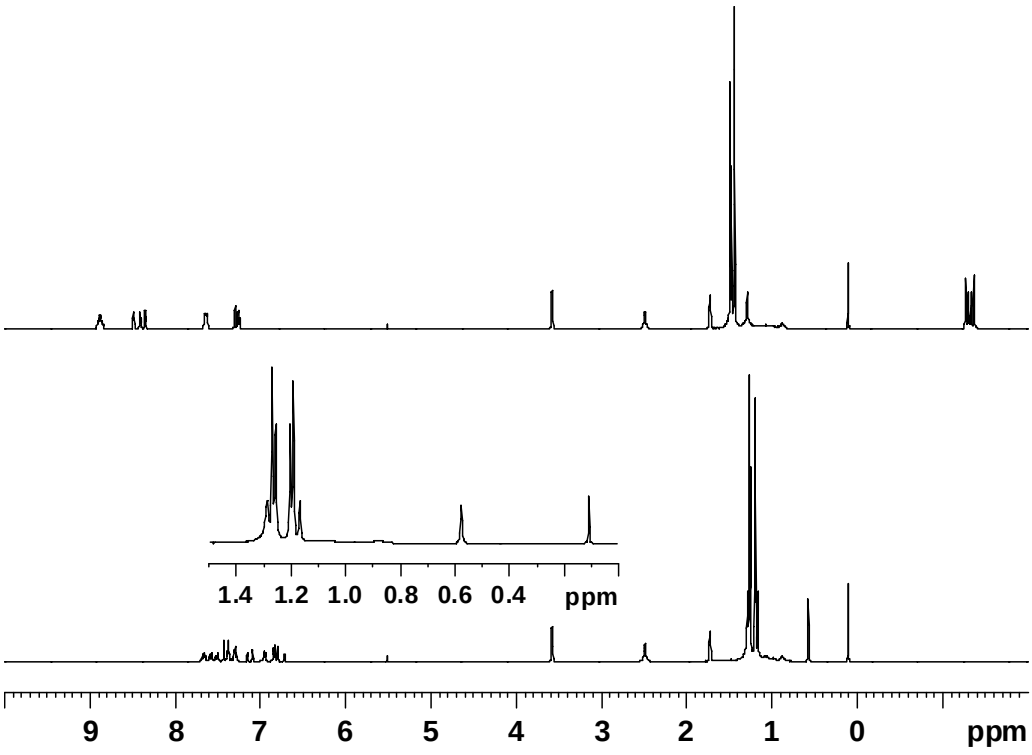

Figure 2.8 Proton NMR spectra of 119(C-C) (top) and 119”(O-O)(bottom).

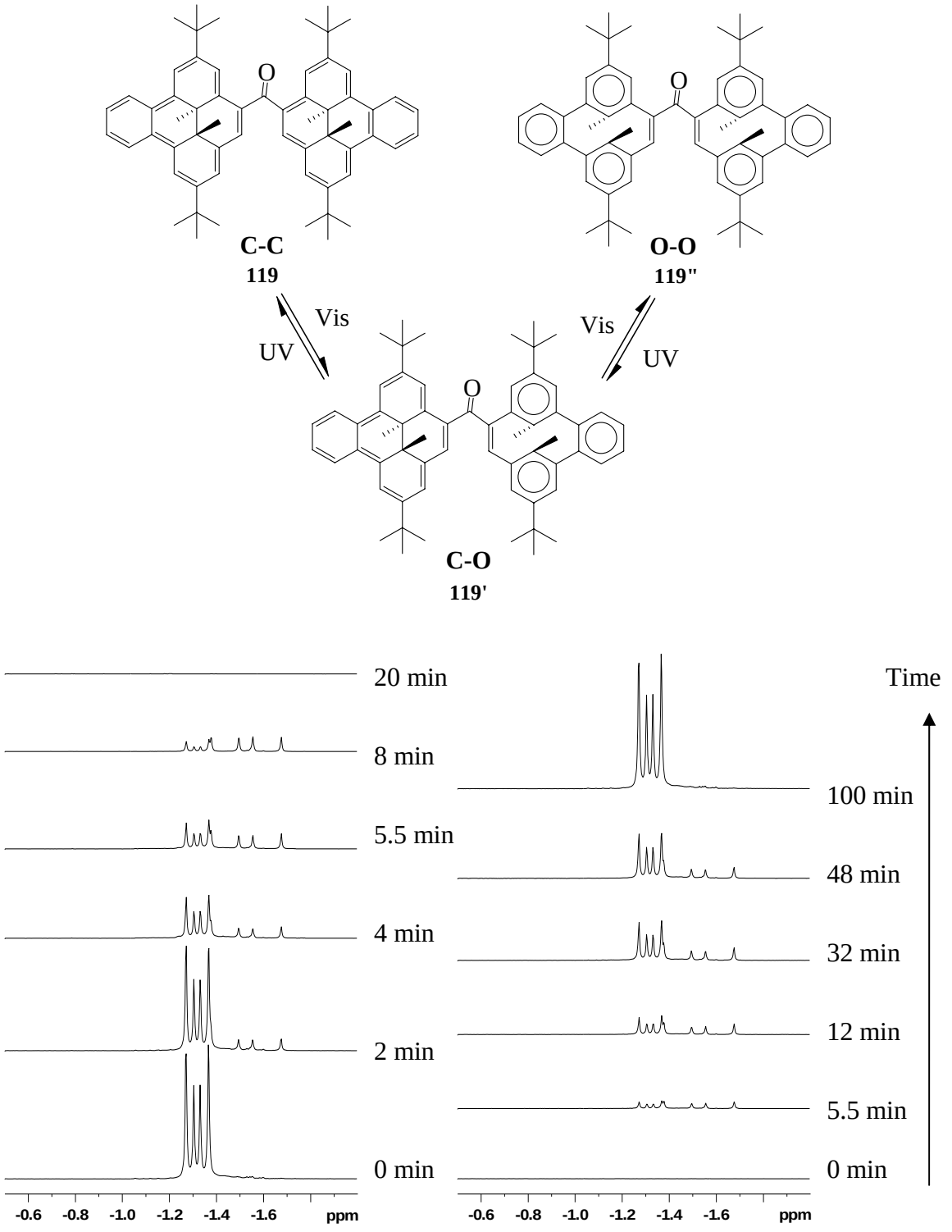

Figure 2.9 Sequential partial NMR spectra for the visible light opening (left) of 119 with wavelength > 490 nm light and UV closing (right) of 119" with 254 nm light.

The conversion of **119** to **119”** was also followed by proton NMR spectroscopy. The NMR spectra of **119** and **119”** are shown in **Figure 2.8**. As we can see, after irradiation the internal methyl signals for **119** at δ -1.27, -1.30, -1.33 and –1.37 disappeared and new signals rose at δ 1.27, 1.17, 0.58 and 0.11 for **119’’** consistent with the formation of the open-open form **119’’**.

The sequential partial ^{1}H-NMR spectra for the photo opening and photo closing are shown in **Figure 2.9**. Similar to **117**, both the photo opening and photo closing processes of **119** involved the closed-open intermediate **119’**. This was shown by the appearance of new internal methyl signals at δ 1.26, 1.17 and 0.58 on irradiation. While the original internal methyl signals for **119** or **119’’** keep decreasing all the time upon irradiation, the new internal methyl signals for the intermediate **119’** increased first, then stayed constant, and then decreased to zero. This indicated that on irradiation, **119’** formed. As it formed, it also started to convert to **119’’** (opening process) or **119** (closing process) upon irradiation. At a certain stage, the formation and the conversion reached the same rate and the concentration of **119’** then stayed constant. After that, because of the consumption of the starting material **119** or **119’’**, the formation rate started to decrease but the conversion rate stayed the same, then the concentration started to drop. When all the starting material **119** or **119’** has converted, the formation rate decreased to zero and **119’** continued converting to **119’’** or **119** until all gone. Then the whole process was complete. The sketches were given in **Figure 2.6** (p109) for the roughly idea of concentration changes of there isomers, C-C, O-C, O-O, in photo opening and closing processes.

2.4.2.1.3 Hetero bis-switch 122

So far most of bis-DHP photoswithes are homo-switches, in which the two photochromic units are the same but connected through a spacer. It is not difficult to see that the absorption of both sides would be the same or similar. Thus, it's hard to achieve a real multiple photoswitch. On the other hand, hetero-switches, in which the two photochromic units with different absorptions are connected together, should have more chance to show multiple photoswitching properties. So we synthesized hetero-switch **122** and studied its multiple photoswitching properties.

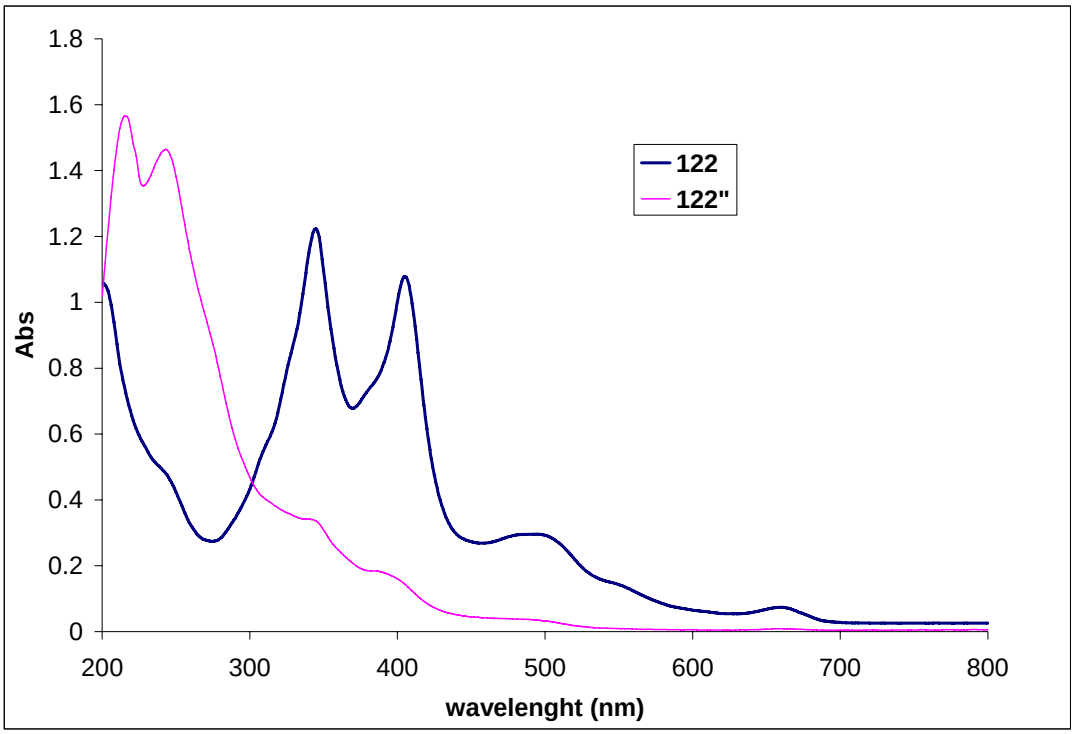

Figure 2.10 UV-vis spectra of 122(C-C) and 122"(O-O).

The UV-vis spectra and NMR spectra of **122** (C-C) and **122"** (O-O) are shown in **Figure 2.10** and **Figure 2.11** respectively. As we can see, in **Figure 2.10**, all the absorptions in the visible region, the characteristic absorptions of the DHP form, disappeared in the spectrum of **122''**, instead new absorptions in the UV region appeared,

which is characteristic for the CPD form. In the proton NMR spectra, the internal methyl proton signals at δ -1.17, -1.20, -1.24 and -1.28 (from BDHP side) and at δ -3.75, -3.78, -3.79 and -3.82, (from DHP side) for **122** disappeared and new signals at δ 1.51 to 0.52 appeared for these methyl groups in **122"**, which are consistent with their structures.

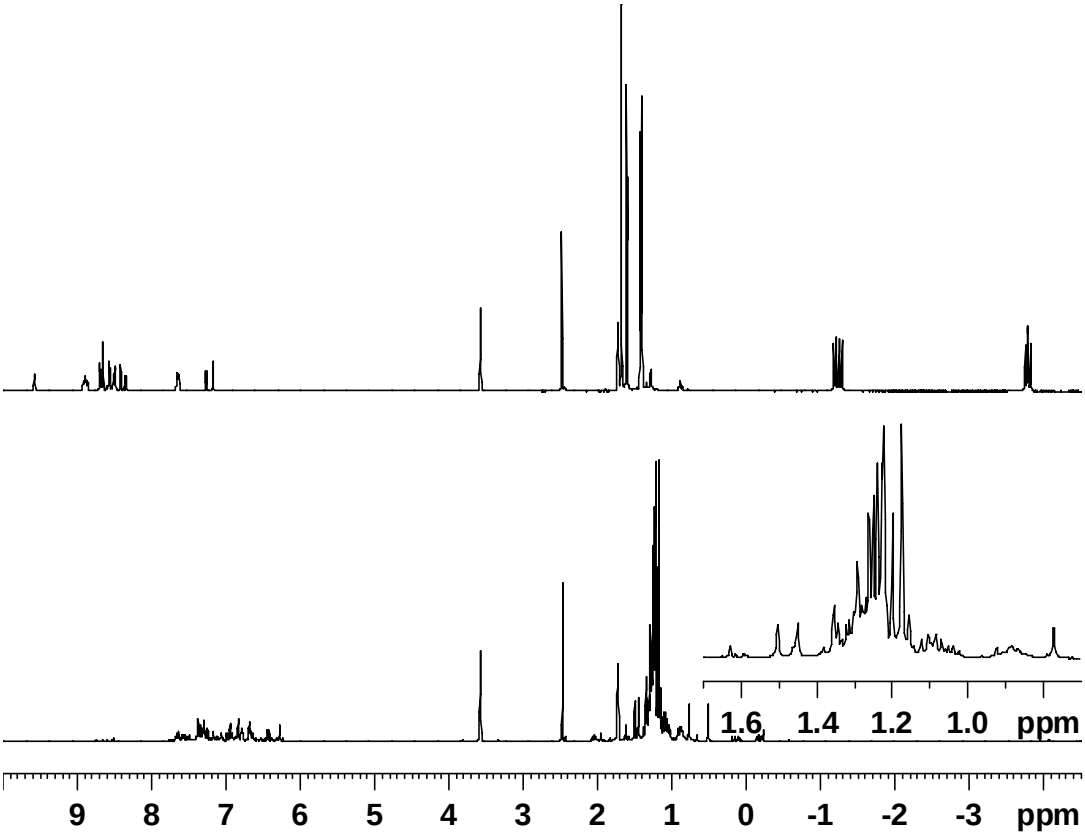

Figure 2.11 Proton NMR spectra of 122(C-C) (top) and 122"(O-O)(bottom).

In **122**, the two DHP units are different and have different absorption patterns. Thus it might be possible to selectively irradiate just one end instead of two and manually control the photo opening or closing steps. **Figure 2.12** shows the absorption spectra of **117**, **119** and **122**. The second highest wavelength band for compound **117** appeared at 485 nm and tailed to ~ 540 nm. Compound **119** was red shifted on comparison to **117.** Its highest wavelength band appeared at 514 nm and tailed to ~ 600 nm. Thus we believe that the

shoulder at around 550 nm (from 540 nm to 600 nm) for **122** can be attributed to BDHP side (**Figure 2.12**). Actually, a digital combined spectrum of **117** and **119** is similar to the UV-vis spectrum of **122** (**Figure 2.13**). Thus, it's possible to irradiate just the BDHP side of **122** if we use the light source of 550 nm to 600 nm.

Thus, a degassed NMR sample of **122** was irradiated with 550 nm to 600 nm visible light (from a 500W tungsten lamp fitted with a 550 nm to 600 nm window filter). The NMR spectrum was recorded at successive intervals. **Figure 2.14** shows the sequential NMR spectra for the opening process. As we can see, when the sample was irradiated, the original internal methyl peaks at δ -1.17, -1.20, -1.24, -1.28 (from BDHP side) and -3.75, -3.78, -3.79, -3.82 (from DHP side) decreased; and new peaks arose at δ -3.91, -3.95, -4.07 and -4.13, indicating formation of a new DHP form, that could only be **122'**. As time went by, the original internal methyl peaks continued to decrease and the new internal methyl peaks continued to increase. At the end, the original internal methyl peaks decreased to zero and the new internal methyl peaks grew to a maximum, suggesting that all of **122** has converted to **122'**. At this point we switched the window filter to a 490 nm cut-off filter and continued irradiation. Then the peaks at δ -3.91, -3.95, -4.07 and -4.13 started to decrease while two new AB patterns (from two isomers) of peaks started to grow in at δ 6.46, 6.41 and 6.30, 6.27. These are the H-9',10' in the cyclophanediene form of the DHP side in **122"** (**Scheme 2.29**) and are upfield compared to the AB pattern of H-9',10' (corresponding to H9',10' in the CPD form of **122"**) at δ 8.59 and 8.56 in **122** (where the DHP side is closed). Finally, all of the upfield internal methyl signals disappeared and the AB pattern peaks at δ 6.46, 6.41 and 6.30, 6.27 grew to a maximum, indicated that **122'** has fully opened to the open-open isomer **122"**.

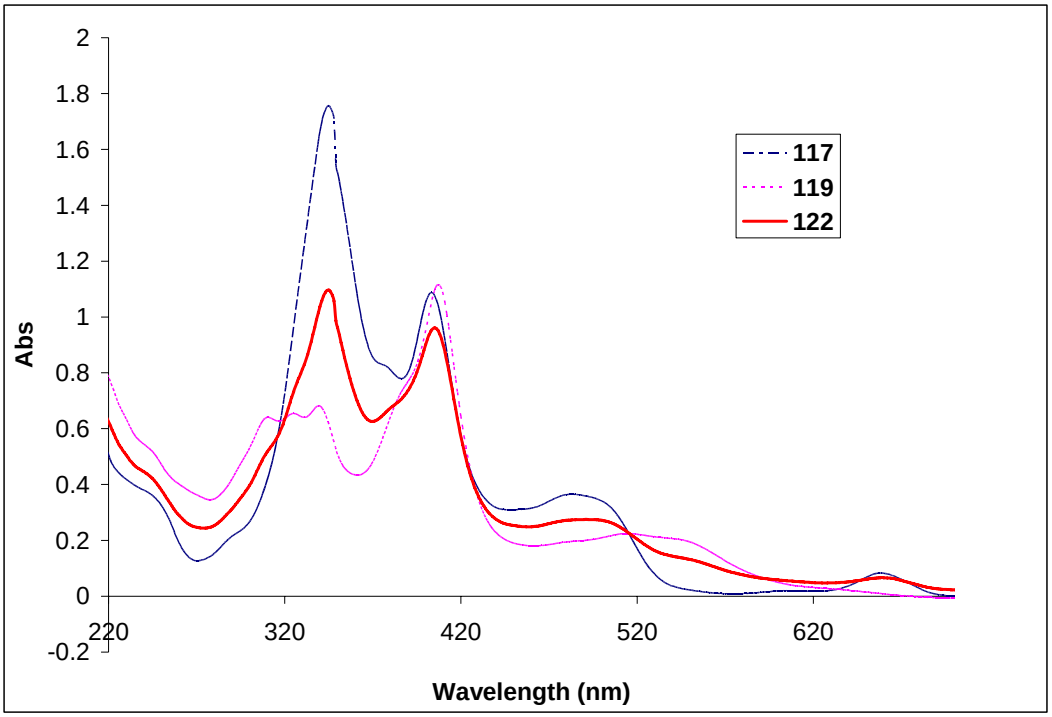

Figure 2.12 Comparison of UV-vis spectra of 117, 119 and 122.

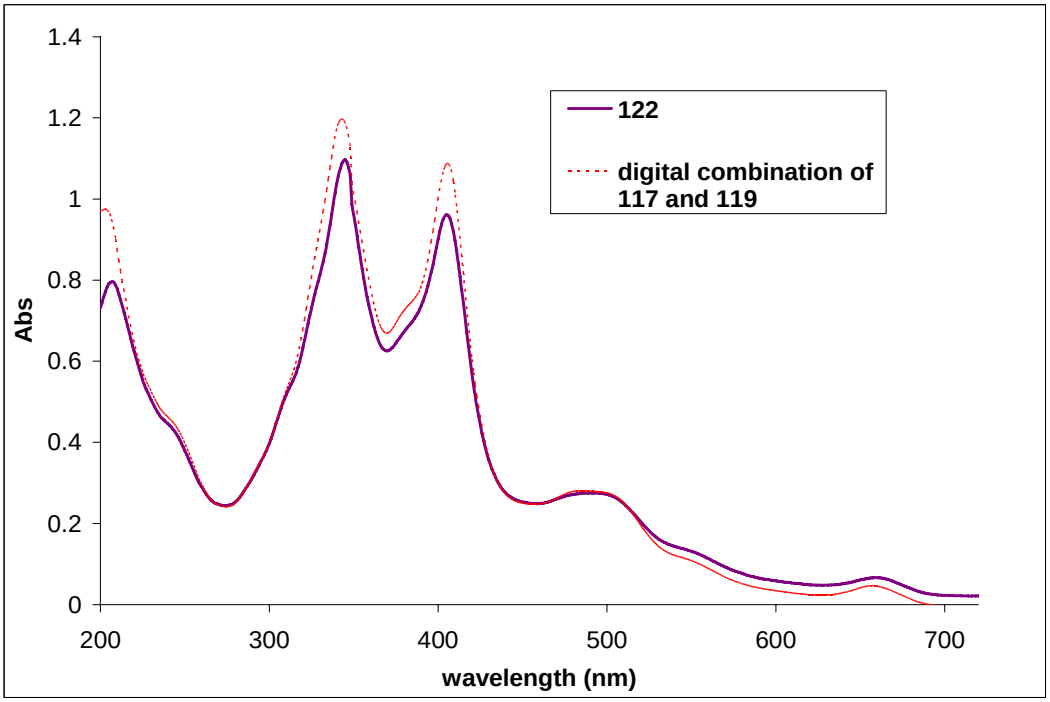

Figure 2.13 Comparison of UV-vis spectrum of 122 and the combination spectrum of 117 and 119.

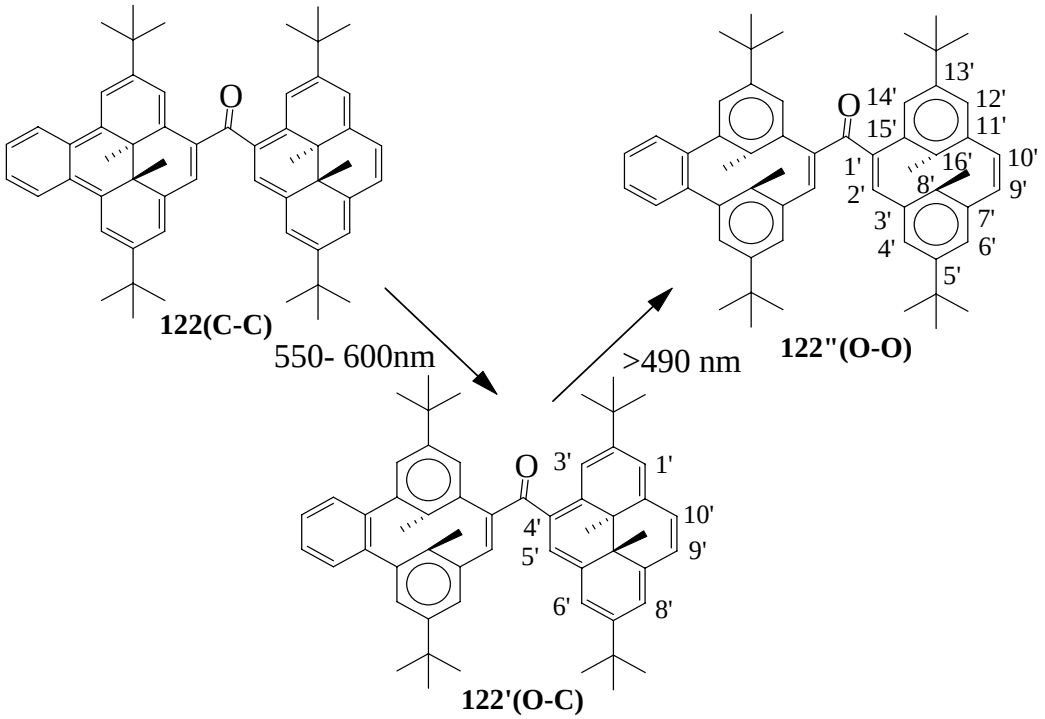

Scheme 2.29 The stepwise opening of 122.

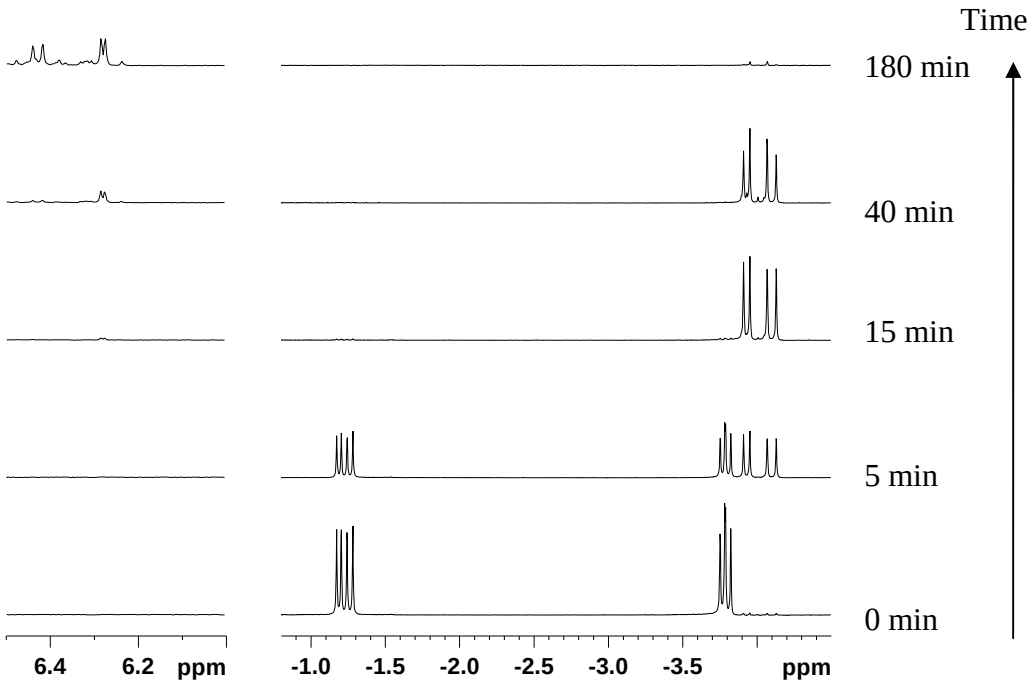

Figure 2.14 Sequential partial NMR spectra for the visible light opening of 122 first with 550-600 nm light and then with > 490 nm light.

As seen above, the BDHP side of **122** can be selectively opened almost without affecting the DHP side. Thus, we have a true three way photoswitch during the photo opening process.

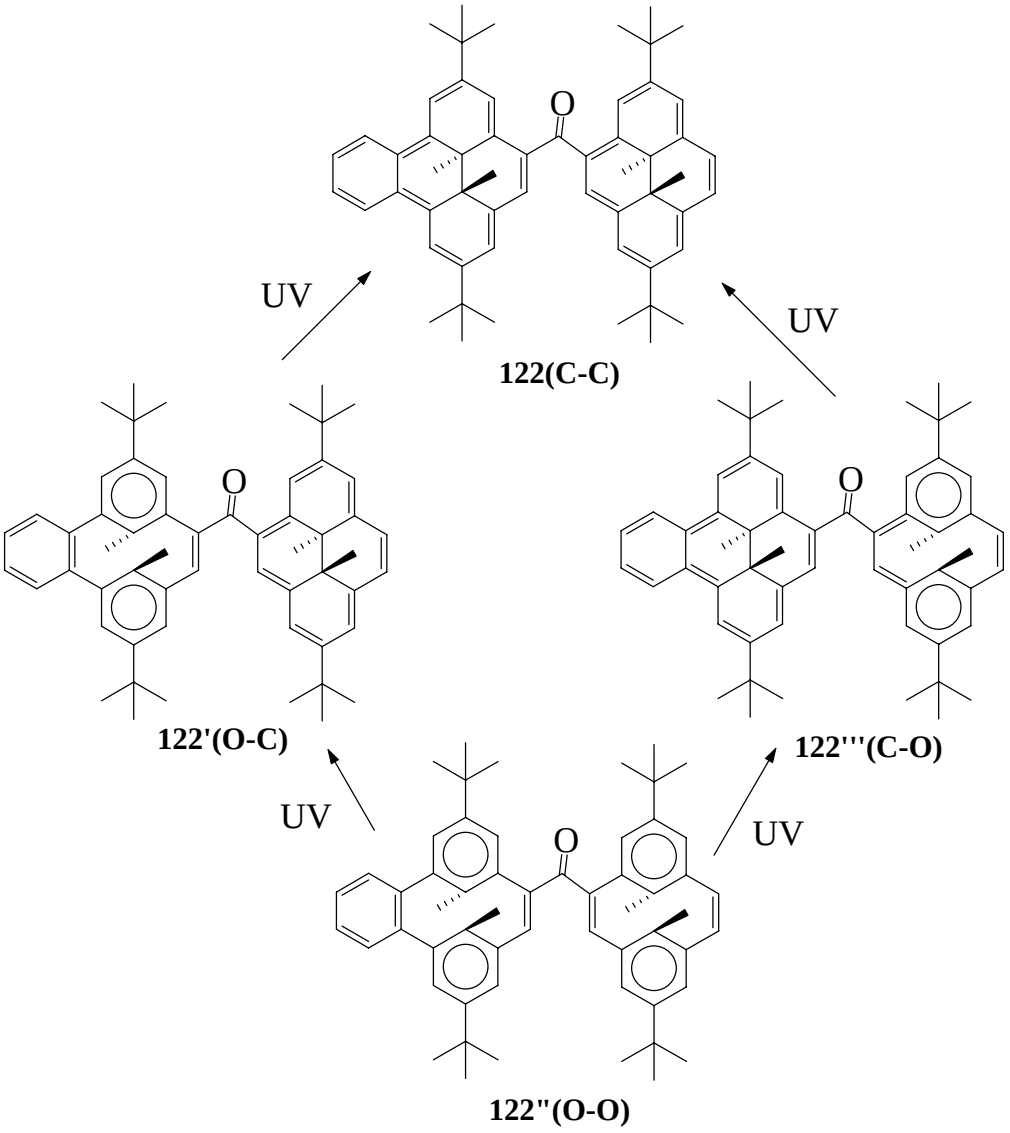

Scheme 2.30 The stepwise closing of 122”

The sequential NMR spectra of the UV closing processes of **122** are shown in **Figure 2.15**. Four groups of internal methyl protons were found after irradiation, in which the signals with chemical shifts at δ -1.17, -1.20, -1.24, -1.28 and δ -3.75, -3.78, -3.79, -3.82

belong to the closed-closed isomer **122**; the signals with chemical shifts at δ -3.91, -3.95, -4.07 and -4.13 belong to the closed DHP side of the open-closed isomer **122'**. The chemical shifts at δ -1.37 to -1.71 are new. They can only be from the other closed-open intermediate **122'''**, in which the BDHP side is closed but the DHP side is open. As irradiation continued, all the peaks increased at first. Then the peaks at δ -3.91, -3.95, -4.07 and -4.13 and at δ -1.37 to -1.71 decreased to zero and the peaks at δ -1.17, -1.20, -1.24, -1.28; and -3.75, -3.78, -3.79, -3.82 increased to maximum, suggesting that the open-open form **122''** has all closed back to the closed-closed form **122.**

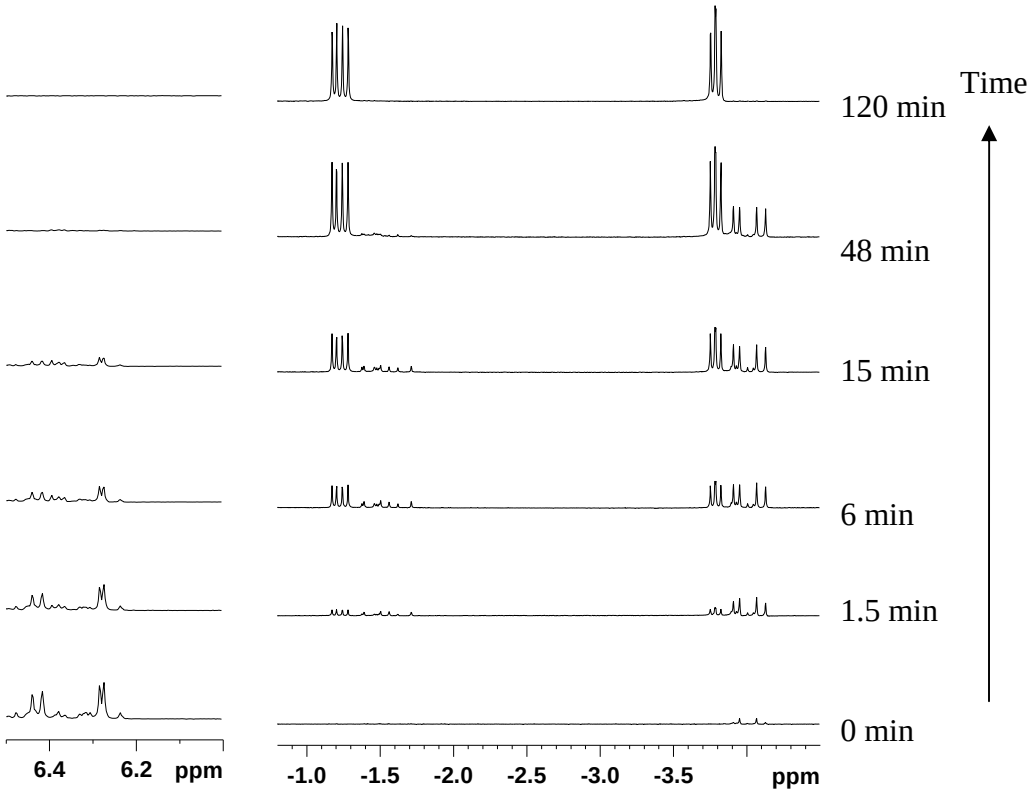

Figure 2.15 Sequential partial NMR spectra for the UV (254 nm) closing of 122".

Thus, the ^{1}H NMR studies have showed us that we can selectively open the BDHP side of **122** without affecting the DHP side during the photo opening process. So the pure

open-closed isomer **122'** can be obtained. This is so far the best result at this moment, in comparison to other bis-DHP systems in which only a mixture of closed-closed, open-closed (or closed-open) and open-open isomers can be obtained. Furthermore, the open-closed isomer **122'** is stable and can be further converted to the fully open-open isomer **122''** by using different wavelength light. So a true three way photoswitch has been achieved during the photo opening process. This is the first example where we can manually control the multiple photoswitching properties.

The UV closing of **122''** went through two intermediates **122'** and **122'''**. It also went from the open-open **122''** to the closed-closed **122** directly, just as **117''** and **119''** did. This is the first time we can see all the four states of the bis-DHP systems. However we could not selectively obtain **122'** or **122'"** in the UV closing process.

2.4.2.2 Bis-DHP systems linked by non-conjugated spacers

The bis-DHP photoswitches we had studied above are connected by a cross-conjugated spacer. We thought that systems linked by non-conjugated spacers might have interesting properties too. Thus we have synthesized the compounds DHP-C(OH)-DHP **116**, DHP-CH_2-DHP **123** and BDHP-CH_2-BDHP **124** and have studied their multiple photoswitching properties.

2.4.2.2.1 DHP-C(OH)-DHP 116 and DHP-CH_2-DHP 123

As we know, the parent DHP **35** is not a good photoswitch. Its quantum yield for visible light opening is low and its thermal return is fast.[79, 82] So it was not surprising for us to see that the bis-DHP systems **116** and **123** did not undergo photoswitching under our conditions (the sample was put in ice-water bath, irradiated with light of wavelength > 490 nm or >590 nm).

2.4.2.2.2 BDHP-CH_2-BDHP 124

When the degassed NMR solution or UV-vis solution of **124** was irradiated with > 490 nm visible light, compound **124** was easily converted to open-open isomer **124”**. The UV-vis spectra and NMR spectra of **124** and **124”** are shown in **Figure 2.16** and **Figure 2.17** respectively.

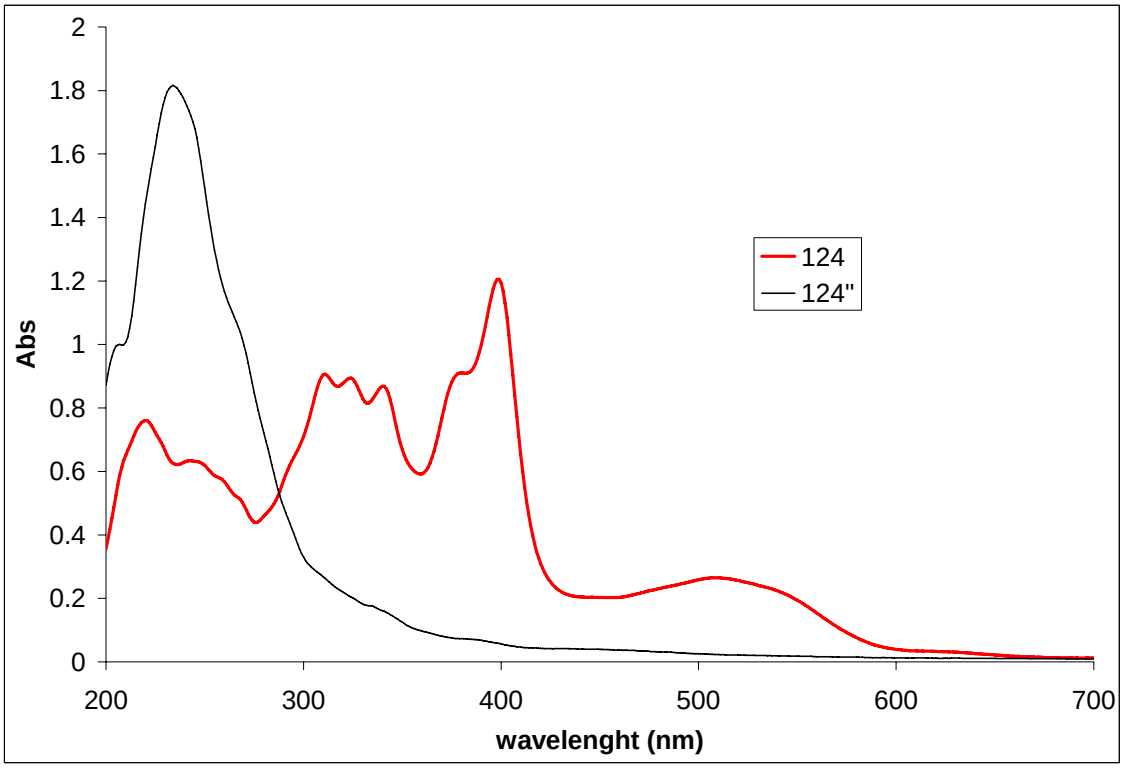

Figure 2.16 UV-vis spectra of 124 (C-C) and 124”(O-O).

As we can see from **Figure 2.16**, all the absorptions in the visible region, characteristic for the DHP form, disappeared and new absorptions in the UV region, the principle region for the CPD form, increased to a maximum. In the proton NMR spectra (**Figure 2.17**), the internal methyl protons at δ -1.54, -1.55, -1.57 and -1.62 for **124** moved to δ 1.33 and 1.29 for **124’’** since they are no longer in the center of the large annulene rings.

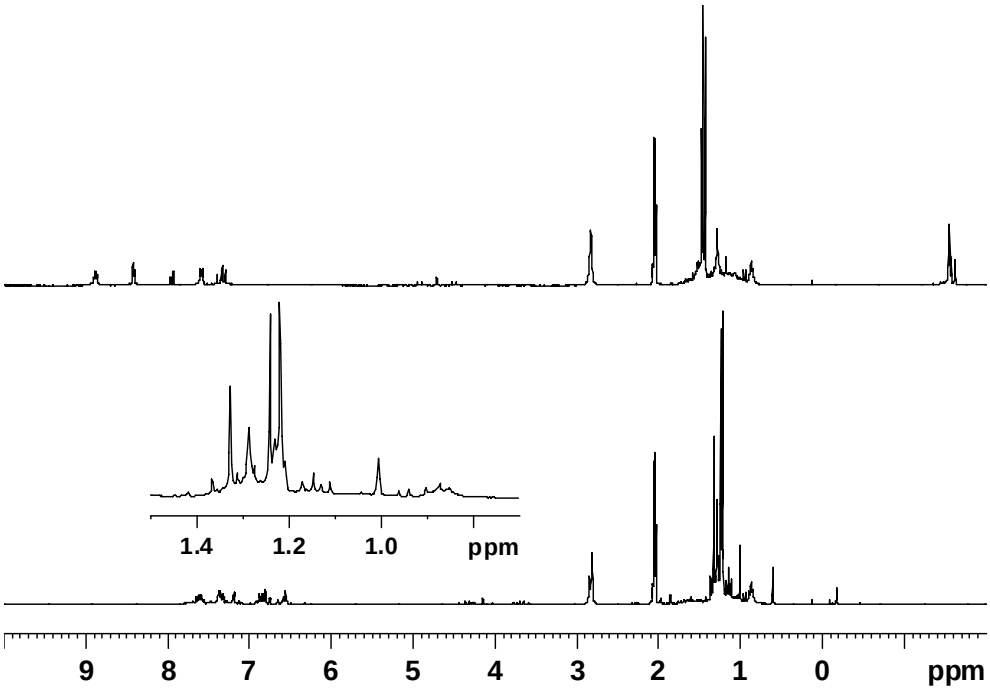

Figure 2.17 Proton NMR spectra of 124(C-C) (top) and 124"(O-O) (bottom).

The sequential NMR spectra of visible opening and UV closing processes of **124** were shown in **Figure 2.18**. As we can see, when **124** is irradiated with visible light, the original internal methyl peaks at δ -1.12, -1.16 and -1.18 decreased, and new internal methyl peaks at δ -1.24, -1.27, -1.33 and -1.55 arose, indicating the formation of a new species, **124'**. As irradiation continued, the original internal methyl signals continued to decrease, while the new internal methyl peaks increased at first, then stayed constant, which means the formation and conversion rate of **124'** has reached the same value. After that, as the consumption of the starting **124**, the formation rate of **124'** started to slow down, but the conversion rate stayed the same, so the internal methyl peaks for **124'** started to decrease too until all had gone, which indicated the complete conversion of **124** to **124"**.

When the fully opened isomer **124”** was irradiated with UV light, eight internal methyl peaks appeared at δ -1.54, -1.55, -1.57, -1.62 and δ -1.60, -1.62, -1.63, -1.66, indicating the formation of the closed-closed isomer **124** and closed-open isomer **124’** at the same time. As irradiation continued, the peaks at δ -1.60, -1.62, -1.63 and -1.66 increased first, then stayed constant and finally decreased to zero while the peaks at δ-1.54, -1.55, -1.57, -1.62 increased during all the process. The sketches were given in **Figure 2.6** (p109) for giving the roughly idea of concentration changes of there isomers, C-C, O-C, O-O, in photo opening and closing processes.

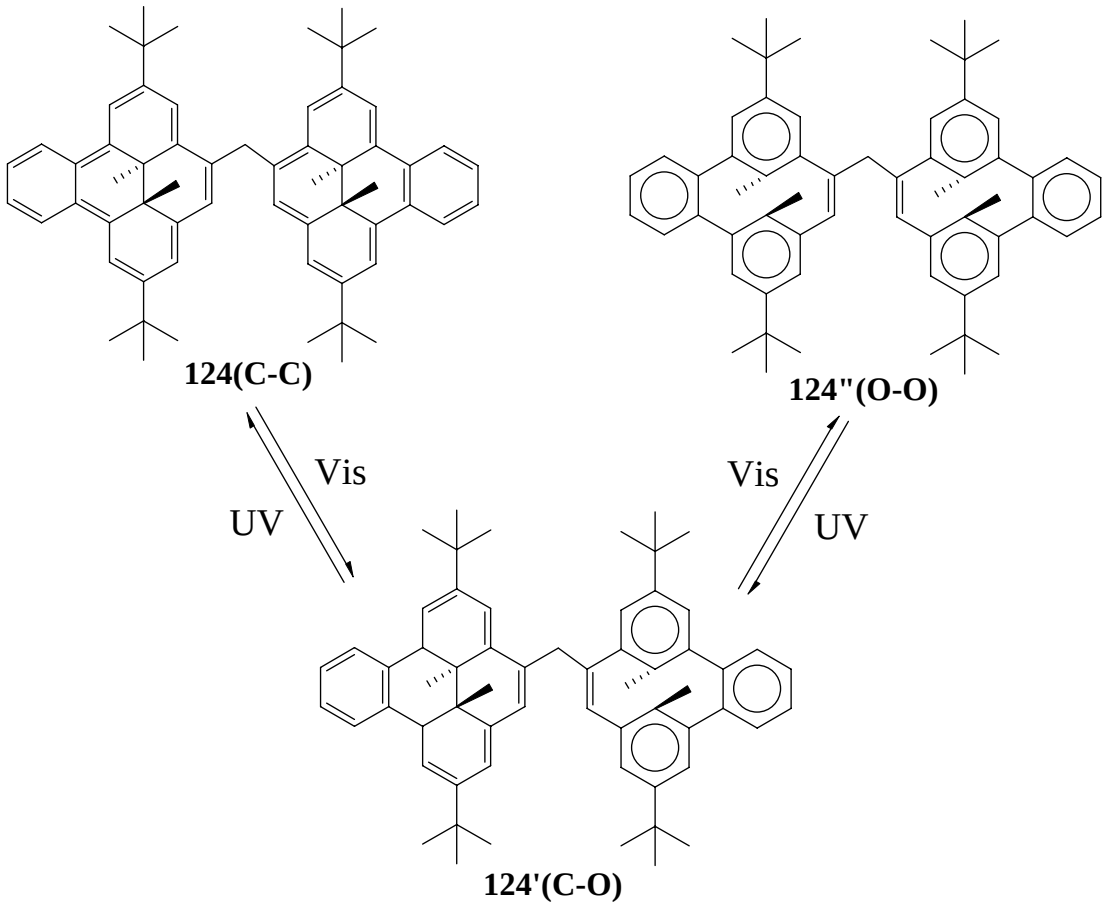

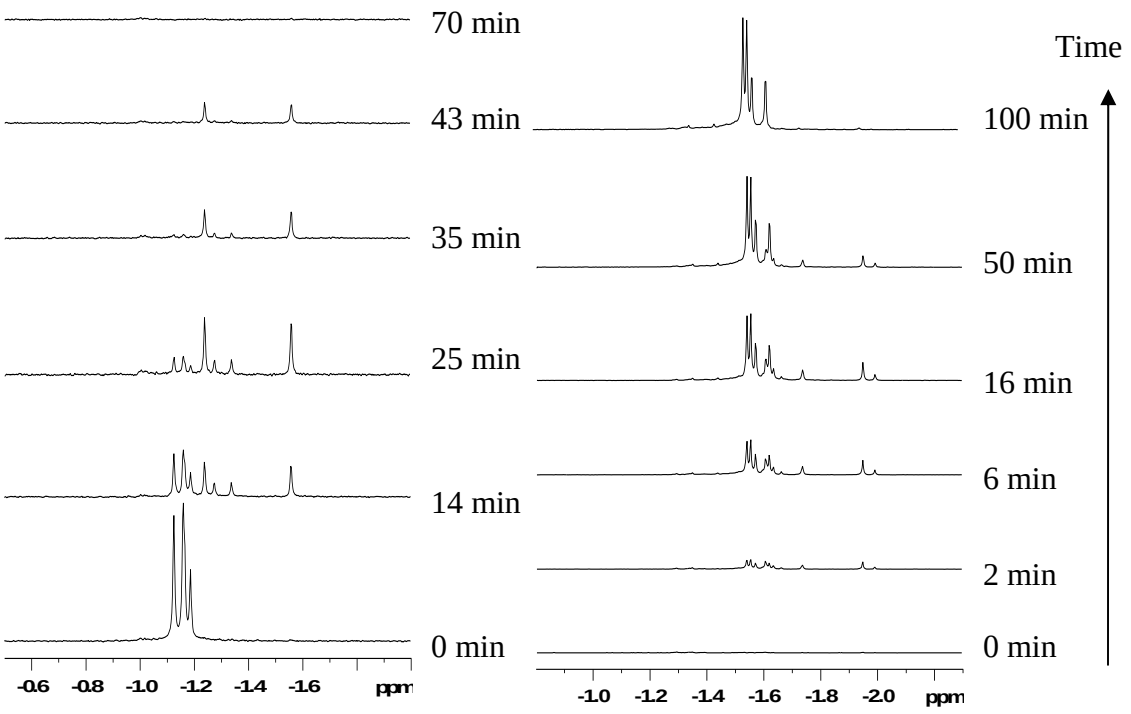

Figure 2.18 Sequential partial NMR spectra for the visible light opening (left) with wavelength > 490 nm light and with UV closing (right) of 124" with 254 nm light.

The above NMR evidence strongly suggested that compound **124** did show multiple photoswitching properties, in which both the photo opening and photoclosing processes involved the closed-open intermediate **124'**, just like the carbonyl connected systems **117** (DHP-CO-DHP) and **119 (**BDHP-CO-BDHP).

For **105**, no intermediate could be detected by ^{1}H NMR in the photo opening and closing processes but it showed an intermediate in UV closing process based on the observation of two isosbestic points when the UV closing was followed by UV-vis spectroscopy. In the cases of **117**, **119** and **124**, in which the two photochromes were connected by cross-conjugated spacers (**117** and **119**) and a non-conjugated spacer (**124**), C-O species in both photo opening and photo closing could be detected.

2.4.2.3 Ethynyl spacer linked bis-DHP system 130

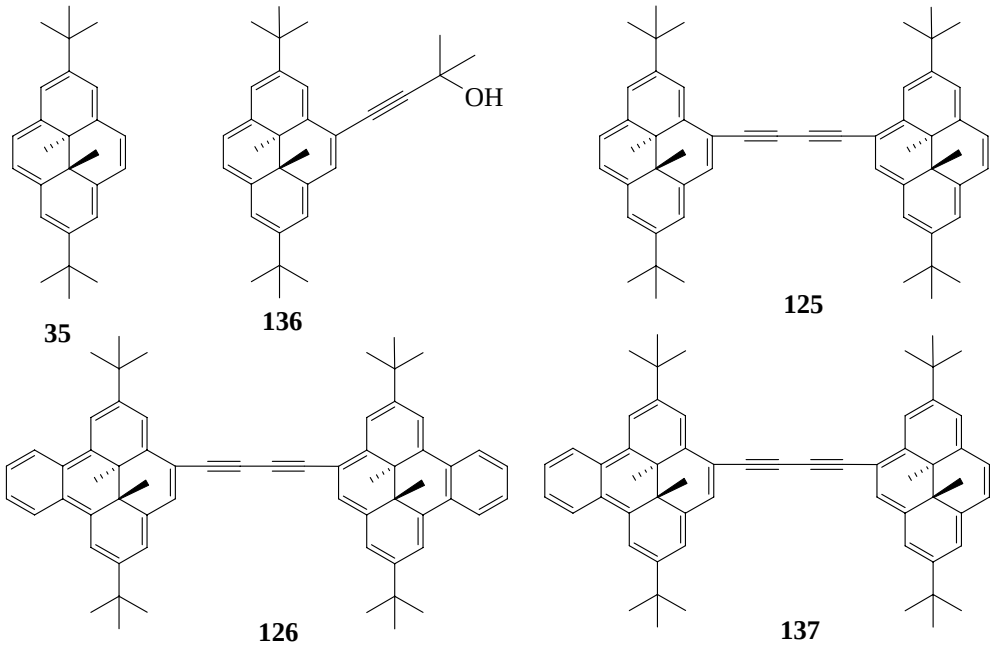

The parent DHP **35** is a poor photoswitch and the ethylnyl substituted DHPs, such as **136**, are even poorer photoswitches than the parent (Φ (**35**) = 1.5 x 10^{-3}, Φ (**136**) = 5.6 x 10^{-4}).[87] The diethynyl linked bis-benzoDHP **126**[92] is a photoswitchable molecule but **125**[87] does not undergo photoswitching at all. For diethynyl spaced hetero-switch **137**, only the BenzoDHP side could be opened.[92b]

Compound **130** is difficult to be open even for the BenzoDHP side. We were only able to fully open the BDHP side once for one NMR sample shown in **Figure 2.19**. We were not able to repeat this even though we tried several times. We could open the BDHP side slightly for a UV-vis sample. The DHP side always stayed closed under our conditions. The NMR spectra of the closed-closed isomer **130** and the closed-open isomer **130'** are shown in **Figure 2.19**. As can be seen, the internal methyl signals for the BenzoDHP side of **130** at δ -0.92 and -0.96 disappeared and new signals appeared at δ 0.38 and 2.27 for **130'**, while the internal methyl signals for the DHP side only shifted

from at -3.36 and -3.38 in **130** to at δ -3.47 and -3.48 in **130'** and the total intensity remained unchanged.

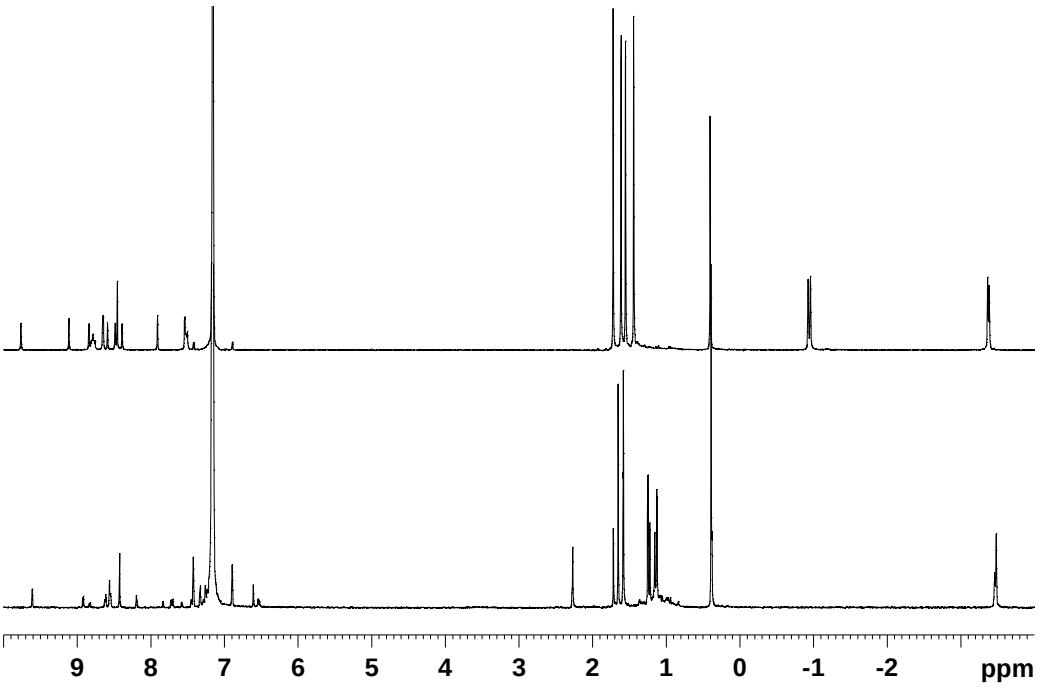

Figure 2.19 Proton NMR spectra of 130(C-C) (top) and 130'(O-C) (bottom).

2.4.3 Study of the relative photo opening and closing rates

Quantum yields are very important properties for photochromic molecules because it is important for photochromic materials to have a short photo response time. For our DHP system, the quantum yield for visible light opening reaction is low. For example, the opening quantum yield for parent DHP **35** to **35'** is just Φ = 0.0015 and that for **11** to **11'** is 0.006.[80] The opening quantum yield increases dramatically by annelation of benzene, that is, the quantum yield for the visible light opening of benzo[e]DHP **36** to **36'** is Φ = 0.042,[87] which is 28 times larger than that of **35**. Quantum yields have only been measured for a few of our compounds, and instead relative rates of opening and closing

are used for comparison. As BenzoDHP **36** is the best photoswitch in the DHP systems so far, it is used as a reference compound to compare the photo opening and photo closing rates of the photoswitchable molecules in this thesis.

Photo openings were followed by means of a UV-vis spectrometer. The solution of benzoDHP **36** and the compound to be compared were prepared in equal molarity in quartz UV cells using cyclohexane as solvent (unless otherwise stated). The prepared solutions were bubbled with argon for 30 min and the UV cells were sealed. Then two cells, one containing the reference **36** and the other one containing the compound, were placed side by side and irradiated with visible light with wavelength > 490 nm. An electrical fan was used to cool the samples. UV-vis spectra were taken at various time intervals. For the photo closings, a similar procedure was used as the photo opening processes. The fully opened **36'** solution and equimolar fully opened sample solutions in cyclohexane were placed side by side and irradiated by a pencil mercury lamp and monitored by their UV-vis spectra.

The relative rate constants (assuming constant and excess light flux, pseudo first order kinetics) for photo openings were obtained by using the following equation: $-\ln(x) = kt + A$, where x is the mole fraction of the closed form at each time = closed/(closed + open), and A is a constant. The plot of -ln(x) vs *t* (s) was linear and yielded the relative rate constants. The relative rate constants for the UV closing processes were obtained in the same way. All the rate comparison plots are given in the Appendices. The ratios of the rate constants of photo opening and photo closing between the standard **36** and the samples obtained listed in **Table 2.2**.

As can be seen from **Table 2.2**, the opening speed of DHP-CO-DHP **117** is about 5 times slower than benzoDHP **36**, while the BDHP-CO-BDHP **119** opens 8.7 times faster than **36**. This is reasonable because the electron withdrawing groups speed up the photo opening processes. The opening speed of BDHP-CH_2-BDHP **124** is about the same as that of **36**. This is understandable because compound **124** is connected by an electron donating methylene group that should not have much effect on the photo opening process.

Table 2.2 Relative pseudo 1st order photo opening rate constants (vis-open) of some DHP systems compared to benzoDHP 36 at room temperature and relative photo closing rate constants (UV-close) of their photoisomers compared to benzoDHP 36'.

compound	vis-open	compound	UV-close
36 to 36'	1.0	**36' to 36**	1.0
117 to 117'	0.20	**117" to 117**	0.23
119 to 119'	8.7	**119" to 119**	0.59
124 to 124'	1.2	**124" to 124**	0.84

Although the quantum yields of UV closing reactions are much higher than those of opening reactions for most of the DHP systems studied,[86] there are however small differences between them. For our bis-systems, the bis-BDHP switches **119"** and **124"** photo close at about 0.84 and 0.59 times as fast as **36'** respectively. For the bis-DHP system **117"**, the photo closing rate is about 4.4 time slower than **36'**.

2.4.4 Thermal return reactions

For photochromic compounds, the thermal stability of both isomers is very important in terms of practical applications. Our DHPs are T-type systems which means that the

less stable CPD form (open form) spontaneously returns to the thermodynamically more stable DHP form (closed form). Thus, study of the thermal return reactions and efforts to increase the thermal stability are important for DHP systems. The studies of the thermal return reactions of our compound are presented here.

The thermal return reactions follow first order kinetics and were studied by UV-vis spectroscopy or/and NMR spectroscopy.[72] For the UV-vis method, closed form in cyclohexane was first photo opened and then was placed in a thermostat inside the spectrometer. The UV-vis absorptions were then monitored. The thermal return rates were determined at various temperatures. The logarithmic plot of the growth in absorbance at the chosen band at each temperature (T), against time gave the first order rate constant, *k*, of the thermal reversal reaction. For the NMR method, the opened NMR samples were monitored by NMR at various temperatures. The molar fraction of the closed form was obtained by comparison with a standard or by choosing a corresponding peak in the open and closed forms. The logarithmic plot of the molar fractions of the closed form against time at each temperature (T) gave the first order rate constant, *k*.

After obtained the rate constant data, Arrhenius and Eyring plots were used to determine the activation energy and other thermodynamic data.[103] The activation energy can be obtained from **Eq. 2.1**; and enthalpies ΔH^* and entropies ΔS^* can be obtained from **Eq. 2.2**. Also the half-life can be obtained from **Eq.2.3**.

$$-\ln(k) = E_{act}/RT - \ln(A) \qquad \textbf{Eq. 2.1}$$

$$-\ln(k/T) = (1/T)(\Delta H^*/R) + (-\Delta S^*/R) + \ln(\mathbf{k_b}/h) \qquad \textbf{Eq. 2.2}$$

$$\tau_{1/2} = (\ln 2)/k \qquad \textbf{Eq. 2.3}$$

For **117''**, **119''** and **124''**, the thermal return reactions went through the closed-open intermediates to form the closed-closed isomers. Thus in order to apply this method, we need to assume that the rate constants of the two consecutive reactions, k_1 and k_2, are the same and the UV-vis absorptions (at least the major peak we chose for monitoring) are also same for closed-closed and closed-open isomers. Actually, because all three switches are homo-switches, the rate constants of the two consecutive reactions, k_1 and k_2, should be very similar since each step contains the closing of the same CPD unit (DHP for **117**" and benzoDHP for **119''** and **124''**). We found that the shift of the visible absorptions for the closed-open intermediates of the homo bis-DHP switches is less than 2 nm in cyclohexane from those of the closed-closed forms, which is consistent with the former studies.[91]

Scheme 2.31 General thermal closing process for bis-switches.

Table 2.3 Rate constants and half-lives at 46 °C.

CPD form isomers	k (x10^{-3} min^{-1})	$\tau_{1/2}$ (h)
35'[86]	6.10	1.88
36'[86]	2.00	5.75
117"	3.14	3.67
119"	1.02	11.4
122' (BDHP side)	0.879	13.1
122" (DHP side)	1.94	5.96
124"	2.29	5.05

* Errors: Former students who carried out replicate runs found ± 4% errors in rate constant k.[91, 92]

In fact, our results fitted a first order reaction very well and suggested that k_1 and k_2 are similar. All the rate plots, Arrhenius plots and Eyring plots are given in the

Appendices. The rate constants and the half-life at 46 °C were shown in **Table 2.3**. The activation energies E_{act}, enthalpies ΔH^* and entropies ΔS^* are presented in **Table 2.4**.

Table 2.4. Thermal return data derived from kinetic results.

CPD form isomers	E_{act} (kcal mol^{-1})	ΔH^* (kcal mol^{-1})	ΔS^* (cal K^{-1} mol^{-1})
35'[86]	21.8	23.3	4
36'[86]	24.5	23.9	4
112"	20.3	19.7	0
117"	22.0	21.4	-3
119"	26.7	26.0	9
122' (BDHP side)	25.4	24.7	5
122" DHP side	22.2	21.5	-3
124"	22.8	22.2	-1

*UV-vis was used except for **122'** and **122"** (NMR).

** Errors: Former students found that the errors are 0.6 or 0.7 kcal/mol (sd%<3%) for E_{act} and ΔH^*.[91, 92]

From **Table 2.3** and **2.4**, we can see that the half-life of **117"** at 46 °C is 3.67 h, which is shorter than that of **36'**, but longer than that of **35'** (1.88h). Also **119"** had much slower thermal return rates than **36'**. The half-life increased from 5.75h for **36'** to 11.37 h for **119"**. The activation energy E_{act} of **119"** is 26.7 kcal mol^{-1}, increased by more than 2 kcal mol^{-1} from that of **36'**. This agrees with the previous examples where the presence of an electron withdrawing groups at 4-position decreases the thermal return reaction. Compound **124"** has a slightly shorter half-life (5.05 h) than that of **36'** (5.75h). The activation energy E_{act} of **124"** is 22.8 kcal mol^{-1}, slightly smaller than that of **36'** (24.5 kcal mol^{-1}). This is also different from the single DHP systems in which the substitution of electron donating groups slow down the photo opening quantum yields as well as the thermal return reactions. The faster thermal return of **124''** along with the slowing down of the thermal return reactions of **117''** and **119''** strongly suggested the bis-DHP

systems work the opposite way on the substitution of both electron donating groups and electron withdrawing groups as the single DHP systems do. Actually it's a very good sign that the carbonyl linker has increased the photo opening rates but slowed down the thermal return reaction substantially in the bis-DHP systems.

The thermal return reactions of hetero-switch BDHP-CO-DHP **122** were studied by ^{1}H-NMR spectroscopy as well. The degassed NMR sample was irradiated to open the benzoDHP side. Then the half-open sample **122'** was monitored using ^{1}H NMR by a temperature controlling NMR spectrometer. The logarithmic plot of molar fraction of open form on the BenzoDHP side against time at each temperature (T) gave the first order rate constant, k_1, of the thermal reversal reaction of **122'** (**Scheme 2.32**). For the thermal return rates of DHP side, the degassed NMR sample was opened completely to open-open isomer **122"**. Then a similar procedure was used to that of **122'**, but just the change of the methyl peaks on the DHP side was monitored this time and the rate constants of k_2 were obtained at various temperature (**Scheme 2.32**). The rate constants, Arrhenius and Eyring plots are given in the **Appendices**. The rate constants and the half-life at 46 °C are shown in **Table 2.3**. The activation energy E_{act}, enthalpy ΔH^{*} and entropy ΔS^{*} are presented in **Table 2.4**. We can see that the thermal return rate of the benzoDHP side of **122'** is much slower than that of the parent benzoDHP **36'**. Its half-life has increased from 5.75 h for **36'** to 13.1 h, slightly longer than that of the homo-switch **119"** (11.4 h). Also the thermal return of the DHP side of **122''** showed a much slower rate and longer half life ($\tau_{1/2}$ = 5.96 h) than those of the parent DHP **35'** ($\tau_{1/2}$ = 1.88h) and slightly longer than those of the homo-switch **117''** (τ = 3.67 h). This

suggested that the carbonyl linked hetero-switch (**122**) actually slowed down the thermal return reactions more than the corresponding homo-switches.

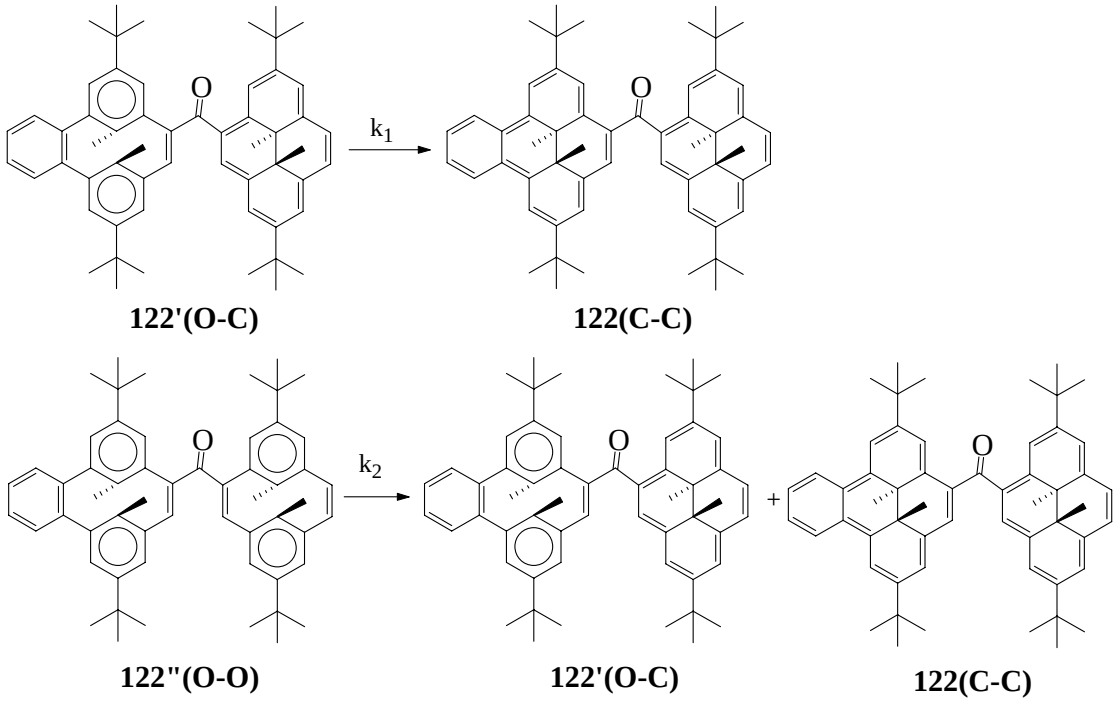

Scheme 2.32 The thermal return rate constants k_1 and k_2.

2.5 Conclusions

A number of bis-DHP systems, **117**, **119**, **122, 124** and **130**, have been synthesized. Studies of their multiple photoswitching properties showed that all of these systems except **130** showed multi-states during the photo opening and photo closing processes. In the homo systems **117**, **119** and **124**, both the photo opening and closing processes involved the closed-open intermediates. However differentiation for the homo systems **117**, **119** and **124** between the closed-closed isomers and closed-open isomers is not significant. Selective control of one end over the other for the photo opening and closing processes is not possible. On the other hand, the hetero-system **122** showed fully differentiated photo opening processes for the two ends and a pure closed-open isomer **122'** has been achieved. Also **122** was the first example which showed four states in the UV closing process.

Study of the relative photo opening and closing rates showed that the carbonyl linker has increased the relative photo opening rates. Thus BDHP-CO-BDHP **119** opens 8.7 times faster than **36**. The methylene linker also increased the photo opening rate, but only slightly. The BDHP-CH_2-BDHP **124** photo opens about 1.2 times as fast as that of **36**. The photo closing processes are fast, similar to former studies. The photo closing of **117"**, **119"** and **124"** is slower than the photo closing of **36'**, especially for **117"**, where the photo closing rate is about 3.6 times slower than that of **36'**.

The studies of the thermal return reactions of these systems showed that the carbonyl linker substantially slowed down the thermal return reactions of the DHP units. The half life at 46 °C for the DHP units has increased from 1.88 h in the parent DHP **35** to 3.67 h in **117** and to 5.96 h in **122**. For the BDHP units, the half life at 46 °C has

increased from 5.75 h for the parent benzoDHP **36** to 11.37 h for **119** and to 13.14 h for **122**. The methylene linker, on the other hand, increased the thermal return reaction rates slightly. Compound **124** showed half life as 5.05 h at 46 °C, which is quite similar with that of the parent benzoDHP **36** (5.75 h at 46 °C).

In the hetero-system, BDHP-C≡C-DHP **130**, only the BDHP side underwent photoisomerization under our conditions. The DHP side remained closed.

The single DHP system, 2-formyl-7-*t*-butyl DHP **112** with the combination of electron donating and electron withdrawing groups showed properties consistent with the electron withdrawing group dominating the substituent effects.

Chapter Three

Iron complexes based on dihydropyrene

3.1 Introduction

3.1.1 Metal complexes of dihydropyrenes

As we mentioned before, the parent dihydropyrene **11** and di-*tert*-butyl-dihydropyrene **35** are photochromic molecules. But they have two drawbacks. First, the quantum yield of visible light opening is very low; Φ_{open} are 0.006 and 0.0015, respectively.[80] Second, the thermal return rates for both are very fast, $\tau_{1/2}$ at 30 °C are 11.6 h and 14.4 h, respectively.[79]

There are several strategies to improve the photochromic properties of dihydropyrenes. We discussed three of them in the introduction to **Chapter 2**. They are modification by substitution, annelation and by changing the internal groups. The [e]-annelated compound, benzo[e]dihydropyrene **36** shows the best photoswitching properties so far. We are also interested in metal modified dihydropyrenes since the metal could not only modify the photochromic properties, but introduce interesting electrochemical behavior as well.

Photochromic studies on metal complexed DHP systems were first investigated by Brkic.[104] Irradiation of the deep purple solution of complex **138** by visible light gave very pale violet cyclophanediene complex **138'**. The opening speed of complex **138** was about 3 times slower than that of benzo[e]dihydropyrene **36**. It closed back to complex **138**

very quickly when complex **138'** was irradiated with UV light. There is no noticeable difference in photoclosing rates between **138'** and **36'**. The thermal closing of complex **138'** was 2.6 times faster than that of uncomplexed **36'**. The thermal return half life of complex **138'** at 46 °C was 2.2 h and the activation energy was 23.0 kcal/mol. Thus, the complexation decreased the relative thermal stability of the open form. Interestingly, the molecule is also electrochromic. Electrochemical reduction of the open form **138'** converted it to the closed form **138**.

Brkic[104] also made the tricarbonylchromium complex **139**, which was not photochromic at all. The chemical shifts of the internal methyl protons are at δ -0.83 and -1.22,[54a] downfield relative to those in **36** at δ -1.58, which indicates that the relative bond fixing ability (loosely aromaticity) of complexed benzene is ~25% greater than benzene itself in this complex.

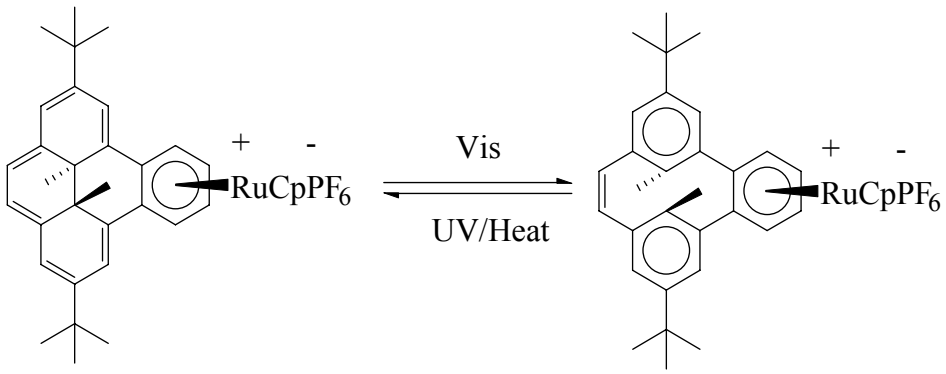

138 **138'**

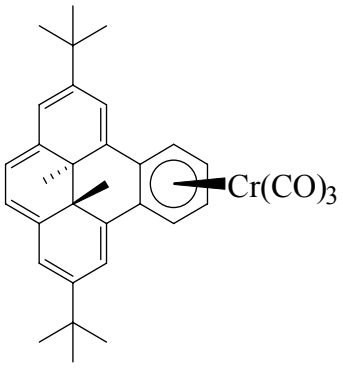

139

The most extensively studied metal complexes are the complexes based on cyclopentadienyl dihydropyrene **45**.[64] Both the rhenium(I) complex **140** and the ruthenium(II) complex **141** are photochromic, but the iron complex **142** and the ytterbium complex **143** are not.[105] Whereas anion **57** only partially opens with visible light, the Re(I) and Ru(II) complexes **140** and **141** fully open. The relative opening and closing rates of both are quite similar to those of anion **57**, but the thermal return reactions are slowed down by complexation. The activation energies for **140'** and **141'** are 23.6 kcal/mol and 24.9 kcal/mol, respectively, increased from that of **57'** (21.1 kcal/mol). The half-life at 46 °C improved from 2.2 h for the anion **57'** to 10.4 h for **141'** and 11.8 h for **140'**, which are 4.7 and 5.7 times slower than that of anion **57'**, respectively.

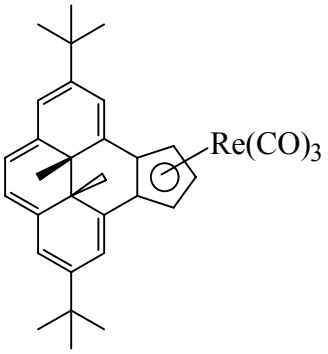

140

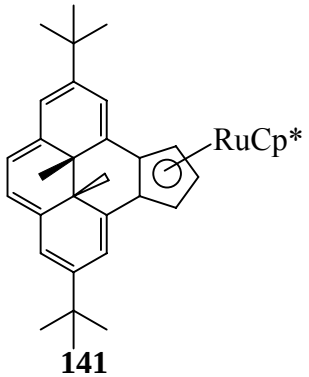

141

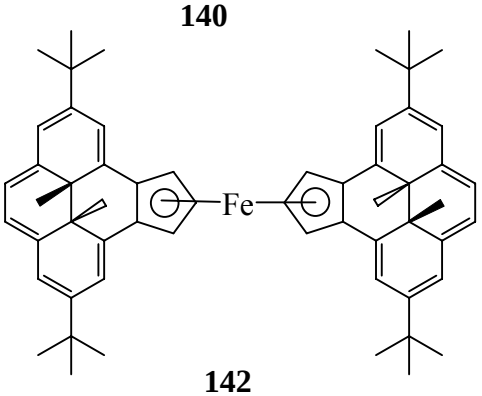

142

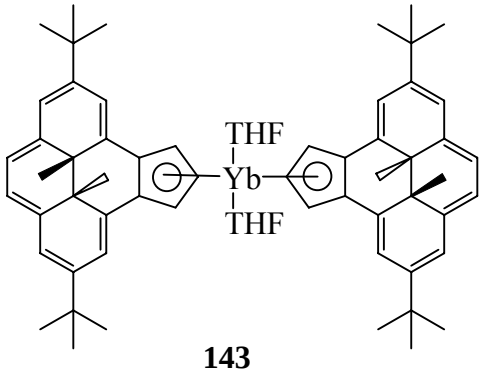

143

3.1.2 Annulene iron carbonyl complexes

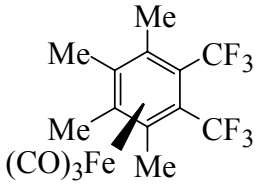

144

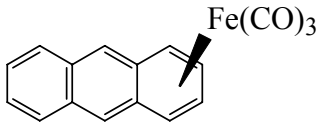

145

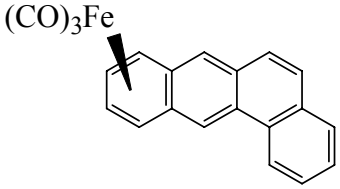

146

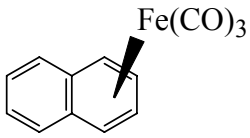

147

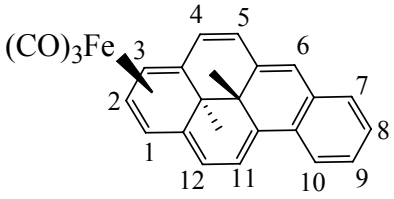

148

Benzene itself has a low tendency to form diene-type iron tricarbonyl complexes, and only one example, complex **144**, is known, which was synthesized[106] by the reaction of the tetramethylcyclobutadiene iron tricarbonyl complex and $CF_3C{\equiv}CCF_3$. Its structure was determined by X-ray crystallography in 1977.[106] Extended conjugation appears to make complexation of benzene with iron tricarbonyl groups easier. Addition of a substituent vinyl group provides a more reactive center for initial complexation, such that a stable intermediate, (vinyl)$Fe(CO)_4$, is formed prior to the (diene)$Fe(CO)_3$. In some fused polycyclic benzenoids, the bonds are relatively localized making complexation easier because the resonance energy lost on coordination is relatively small. Thus the stable iron tricarbonyl complexes **145** and **146,** on a terminal ring of anthracene[107] and benzanthracene[108] are isolable. The formation of (naphthalene)$Fe(CO)_3$, **147**, was first reported by Harper,[109] based on an infrared analysis. However, Manuel[107] later cast doubt on its identity. More recently, our group reported the formation of **148**, in which one

$Fe(CO)_3$ group is coordinated on the annulene ring of the benzo[14]annulene,[59b] which is thus a higher homologue of naphthalene. However, thus far no crystal structures of any of these iron tricarbonyl complexes have been reported.

3.2 Objectives

Benzo[e]dihydropyrene **36** has the best photoswitching properties. Metal modified **36** may show interesting photochromic properties, but so far just two BDHP complexes, **138** and **139**, were obtained. My research goals were thus as follows:

- To synthesize a metal modified dihydropyrene with a metal other than Cr or Ru, e.g. Fe.
- To investigate the photochromic and aromatic properties of any such complexes.

3.3 Synthesis

Although it has been reported by our group[59b] that **148** can be synthesized by direct reaction of the benzo[a]DHP with $Fe_2(CO)_9$ in refluxing benzene, no reaction was found between benzo[e]DHP **36** and $Fe_2(CO)_9$, $Fe(CO)_5$ or $Fe_3(CO)_{12}$ under similar conditions.

Fortunately, we have studied extensively the photochromic benzannulene **36**.[85] This is usually prepared by deoxygenation of the adduct **149** (prepared in a Diels-Alder reaction of furan and the aryne **150**[43]) with $Fe_2(CO)_9$. Often however, iron containing by-products are formed. A more careful study of this deoxygenation reaction resulted in the isolation of three iron complexes **151**, **152** and **153**.

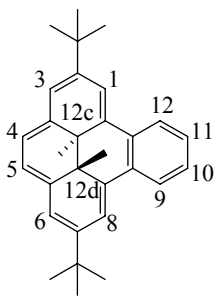

36

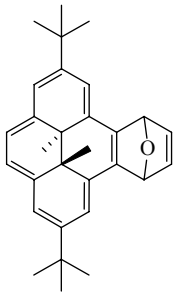

149

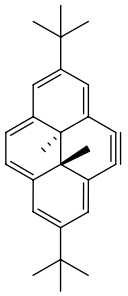

150

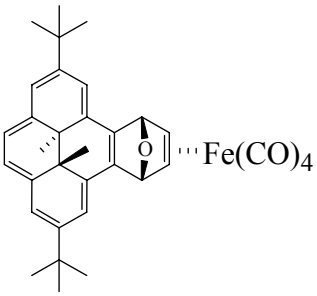

151

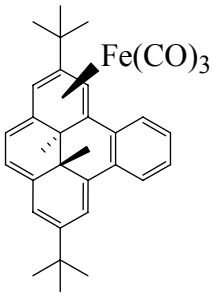

152

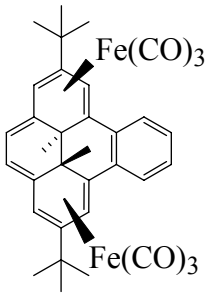

153

Reaction of adduct **149** with $Fe_2(CO)_9$ at room temperature yielded mostly complex **151** (60%) along with some **36** (20%). On the other hand, reaction in refluxing benzene gave mostly **36** (70%), some mono-iron complex **152** (10%), bis-iron complex **153** (12%) and a very small amount of tetracarbonyl complex **151** (1.5%). This suggested that coordination to the DHP ring proceeds more easily at high temperature.

The structures of **151, 152** and **153** were determined from their ^{1}H and ^{13}C NMR, mass and IR spectra. As well, X-ray structures were obtained for **152** and **153**. In their IR spectra, the carbonyl stretches were all strong. For **151**, they appear at 2082, 2021, 1991 and 1968 cm^{-1} consistent with those for the analogous epoxynaphthalene derivative[110a] at 2085, 2020, 2010 and 1985 cm^{-1}. The carbonyl stretches are at 2032, 1977 and 1954 cm^{-1} for **152** and at 2032, 2025 and 1956 cm^{-1} for **153**, which are at lower frequency than those[110b,c,d] for butadiene irontricarbonyl at 2054, 1988 and 1978 $cm.^{-1}$

This is consistent with substantial donation of electron density from the 14π-ring into the iron tricarbonyl fragment.

The ^{1}H NMR spectrum of **151** shows the DHP peripheral proton resonances in the typical DHP region (δ 8.31-8.22). The internal methyl protons appear at δ -3.01 and -3.17, which are again typical for a DHP and so both sets of protons indicate the presence of a strong ring current in the 14-ring. This suggests that the site of complexation is not directly on the DHP ring. The coordination position of the iron tetracarbonyl was indicated by the shielded chemical shifts of the bridging ethene protons H-10 and H-11 at δ 3.29 and 3.04, relative to their shifts of δ 7.12 in **149**. The bridgehead ether hydrogens, H-9 and H-12, are both singlets at δ 5.97 and 5.92 respectively. Since protons H-10 and H-11 are doublets (J = 5.1 Hz), while H-9 and H-12 are singlets, the fused six-member ring is most likely bent along the C-9…C-12 axis, such that the H-9 – C-9 – C-10 – H-10 dihedral angle is about 90°. Then the coupling between H-9 and H-10, (and likewise between H-12 and H-11) would be very small. The ^{13}C NMR spectrum showed all the expected carbon signals with the carbonyl carbon at δ 211.8 and the coordinated C-10 and C-11 carbons at δ 59.6 and 59.5, shielded due to complexation. The bridgehead ether carbon atoms (C-9 and C-12) appear at δ 81.43 and 81.38. Finally the structure of **151** was further confirmed by $^{3}J_{H,C}$ couplings between H-12 and C-9 and also H-9 and C-12 in their ^{1}H-^{13}C HMQC spectra, which would not be possible in the absence of the ether bridge. The LSI and the high resolution mass spectra confirmed the structure of **151** to be a tetracarbonyl.

The chemical shifts for the internal methyl protons of **152** appeared at δ 2.01 and 2.47, which are similar to those found in **148**, the analogous [a]-fused benzoDHP

tricarbonyl iron complex (δ 2.00 and 1.71).[59b] Such chemical shift values indicate that the coordination of the $Fe(CO)_3$ moiety is on the DHP ring, and not on the benzenoid ring, in which case a value close to that of **11** (δ -4.2) would have been expected. The position of complexation in **152** is evident from the shielded chemical shift of H-3 (δ 3.67), the proton at the end of the complexed diene unit. The ^{13}C NMR spectrum of **152** clearly shows the carbonyl carbon signals at δ 212.3 and the four upfield carbon signals (δ 64.1-108.5) of the complexed diene unit. The structure of **152** was finally confirmed by a single crystal X-ray structure determination (discussed below).

The tetracarbonyl **151** is not thermally stable, and at room temperature slowly loses iron and forms benzo[e]DHP **36**. At elevated temperatures it converts more quickly to **36** and also forms some complex **152** in a ratio of 2.3 to 1. For example, in refluxing benzene for 2 hours, over 90% of **151** has been converted to **36** and **152**. The half life of **151** in refluxing benzene is about 30 minutes. This explains the high yield of **151** at room temperature, and the lower yield at elevated temperature, when it decomposes to **36** and **152**. It also explains the higher yield of **36** at higher temperature. However, no di-iron complex **153** was detected in this process. Since no reaction was found between **152** and $Fe_2(CO)_9$ in refluxing benzene, we conclude that **153** must have formed directly from the reaction of **149** and $Fe_2(CO)_9$.

Thermal study of **152** and **153** found that **152** slowly loses the $Fe(CO)_3$ moiety to form **36** at elevated temperatures. For example, refluxing in benzene for 2 hours converts several percent of **152** to **36**. Similarly, **153** first loses one $Fe(CO)_3$ to form **152**, which then continues to lose another $Fe(CO)_3$ to form **36**, but at a much slower rate.

Also as we mention at the beginning of this part, the iron-BDHP complexes can not be obtained by using benzo[e]DHP **36** as starting material, which suggests that complexes **152** and **153** are formed before or during the deoxygenation process, and not after it.

All of the above results support a mechanism for the reaction of **149** and $Fe_2(CO)_9$ that goes via one or more intermediate states, which can directly decompose to the deoxygenated product **36** or react with $Fe_2(CO)_9$ to form the iron complexes.

3.4 Results and discussion

3.4.1 Ring current effects and structures

The fact that the chemical shifts of the internal methyl protons of **152** are close to those of **148** and that both are more deshielded than those of the nonaromatic model **27** (δ 0.97) is interesting. In **148**, we attributed[59b] these deshielded internal methyl protons to a weakly paratropic ring current due to the back donation of two electrons by iron to the 14π system to form an antiaromatic 16π system. This conclusion was supported by the fact that the chemical shifts of *all* the protons in the fused benzene ring (δ 6.77-7.24 in $CDCl_3$) were shielded when compared to those in benzene itself (δ 7.36 in $CDCl_3$). As well, the coupling constants ($J_{7,8}$ = 7.5 Hz, $J_{8,9}$ = 7.4 Hz, $J_{9,10}$ = 7.6 Hz) of the fused benzene ring were almost equal, which indicates that any ring current in the large ring is small. It is not quite so obvious whether **152** is behaving similarly. First, two of the protons on the fused benzene ring, H-9 and H-12 at δ 7.42 and 7.19 in C_6D_6, are deshielded somewhat compared to benzene itself (δ 7.15 in C_6D_6). This may be in part due to steric deshielding of the bay protons. The other two protons, H-10,11, are shielded

at δ 6.91 and 6.97. Second, the coupling constants in the fused benzene ring of **152** appear to alternate more, with $J_{9,10}$ = 8.0 Hz, $J_{10,11}$ = 7.0 Hz, and $J_{11,12}$ = 8.1 Hz, though again these can be affected by steric compression. One would expect the geometries of **152** and **148** to be somewhat different, because the complexed end of the dihydropyrene in **152** is obviously more crowded than that in **148**. Unfortunately, no crystal structure of the [a]complex **148** is available, but we have performed DFT (B3LYP/6-31G*) calculations[111] on both it and **152** and **153** (since we have X-ray structures of the latter two, which will enable us to assess the goodness of the calculations). In all three cases, the calculations suggest that most of the dihydropyrene framework is relatively flat, with the plane of the carbon atoms of the complexed diene part (e.g. C-1,2,3,3a in structure **148**) bent out of the plane formed by the central atoms (e.g. C-3a,4,5,5a,10b,11,12,12a in structure **148**) of the DHP ring. For compound **148**, this angle between the planes is 28.9.° From a p-orbital overlap point of view, the worst misalignment is between atoms 3, 3a and 4 (~24°), which is not exceptionally bad in terms of ring current effects.[112] The ^{1}H NMR data then suggest that the π electrons in the DHP ring of **148** are still delocalized and show a weak paratropic ring current. In the [e]-complex **152**, the angle between the corresponding planes (above) to **148** is almost the same, 29.3° by DFT calculation, and 30.7° from the X-ray structure (see below). Repeating the calculation for **148** with a *t*-butyl substituent at the 2-position, does not significantly (<0.5°) change this situation. Comparison of the calculated and experimental structures for **152** gives excellent agreement (see **Table 3.2** below), as they do for **36** and **11** (see below), and so it seems reasonable that both **148** and **152** are behaving similarly and both show a small paratropic ring current, explaining why the chemical shifts for the internal methyl protons

for both compounds are more deshielded than those of the nonaromatic **27**. However, anisotropy effects must also play a role, since the internal methyl protons which are *cis* to the $Fe(CO)_3$ group are very close to one of the CO groups, while the *trans* internal methyl protons are close to the complexed diene. Both groups have deshielding regions, which must impact the observed chemical shifts. We have observed previously that for **43**, H-1 is about 1 ppm further downfield than H-8.[45] The observed variation in the chemical shifts of the internal methyl groups in **148** and **152**, may then reflect these anisotropies, rather than a substantial difference in ring current.

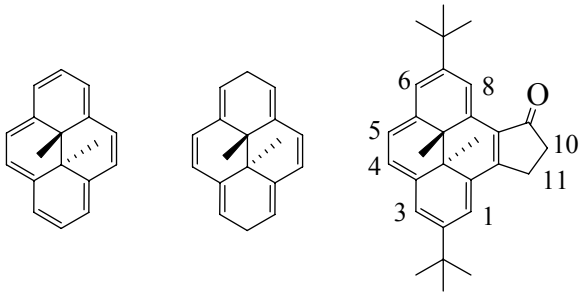

11 **27** **43**

For complex **153**, similar to **152**, the downfield chemical shifts for the internal methyl protons suggest only a small ring current, and imply the loss of aromaticity of the macro-ring on the coordination of the two $Fe(CO)_3$ groups. In this case, the chemical shift difference between the two internal methyl groups is quite large ($\Delta\delta = 1.47$) compared to that for **152** ($\Delta\delta = 0.46$). This suggests that the two internal methyl groups have rather different environments, and implies that the two $Fe(CO)_3$ groups are coordinated on the same side of the DHP ring. This was actually confirmed by a single crystal X-ray structure, which is discussed below. Similar to complex **152**, the downfield chemical shifts of protons H-3 (δ 3.78) and H-6 (δ 3.89) reveal the position of the complexation.

3.4.2 The crystal structure of 152

The crystal structure of **152** is shown in **Figure 3.1**. The crystallographic data are summarized in **Table 3.1**, selected bond lengths are given in **Table 3.2**. Selected bond angles are in **Table 3.3**. Clearly, coordination has occurred on one side of the DHP ring such that the $Fe(CO)_3$ group is furthest away from an internal methyl group, i.e. on the same side as C(26) in **Figure 3.1**, rather than on the side of C(24). The main feature of **152** is the bending of the DHP ring. The angle between the planes defined by the four carbon atoms of the complexed diene (C(7)-C(6)-C(5)-C(22), **Figure 3.1**) and the central carbon atoms of the DHP (C(22) to C(18), C(14)-C(13) and C(8)-(C7), **Figure 3.1**) is 30.7°, which is smaller than, but similar to those of compounds related to (1,3-cyclohexadiene)$Fe(CO)_3$ (36.3-39.9°)[113] and also smaller than those of other η^4-arene complexes (37.4-47.9°),[114] but as mentioned above, agrees very well with a DFT (B3LYP/6-31G*)[111] calculated value of 29.3°.

The butadiene iron tricarbonyl portion of the molecule, shows typical characteristics of all (butadiene)$Fe(CO)_3$ complexes. For example, the four carbon atoms of the diene unit are planar. The iron atom is closer to the inner carbon atoms (C(5), C(6)) than the outer ones (C(7), C(22)), and the inner C(5)-C(6) bond is shorter than the outer C(5)-C(22), C(6)-C(7) bonds. The three CO groups are not equivalent, with one CO group lying over the "open" side of the *cis*-C-C-C-C chain, while the other two lie over the outer C-C bonds. The arrangement of the ligands can thus be described as square pyramidal with the C(33)-O(3) group forming the quasifourfold axis and the other two CO groups and the mid-points of the outer C(5)-C(22) and C(6)-C(7) bonds forming the

basal square. This is a typical stereochemistry for this type of compound. The bite angle of 61.1° for the complexed diene is normal.

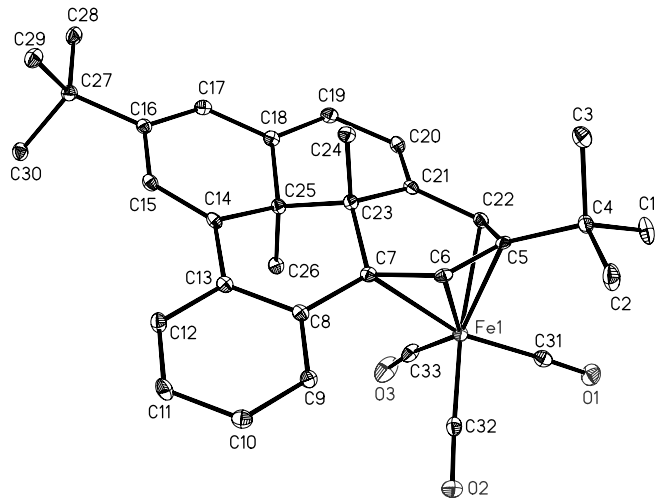

Figure 3.1 An ORTEP3 drawing[63] of complex 152 (30% probability thermal ellipsoids). Hydrogen atoms have been removed for clarity.

However, because of the presence of the t-butyl and internal methyl groups, the molecule is crowded at the complexed end of the DHP framework. The shortest contacts are found between C(31)…H(1C), C(33)…H(26A) and C(33)…H(26B) with distances of 2.578 Å, 2.613 Å and 2.696 Å respectively, which are all shorter than the sum of Van der Waals radii of hydrogen and carbon atoms (2.9 Å). To avoid space conflicts with the t-butyl protons, the Fe(1)-C(31)-O(1) (175.5º(2)) is bent away from linearity and C(1) and C(2) of the t-butyl group are pushed away from the metal center with the C(1)-C(4)-C(5) and C(2)-C(4)-C(5) angles being 112.0(2) and 113.7(2) respectively, away from ideal tetrahedral geometry. The quaternary t-butyl carbon (C(4)), however, is only 0.235 Å away from the complexed diene plane, and does not deviate much from coplanarity

with the diene plane. Similarly the interactions between the C(33)-O(3) group and the *cis*-internal methyl protons (H(26A) and H(26B)) push C(33) toward C(31) and result in a tilt of the internal methyl carbon (C(25)) away from the iron center with the C(23)-C(25)-C(26) angle being 114.8(2)º. Thus the C(33)-Fe(1)-C(31) angle is only 91.5(1)º, significantly smaller than the values (95-103º)[113] found in other (butadiene)$Fe(CO)_3$ complexes, and the Fe(1)-C(33)-O(3) angle is only 172.6(2)º, significantly different from 180º. To relieve the strain in the molecule, the iron atom is also situated further (1.71 Å) from the diene plane than in other butadiene $Fe(CO)_3$ complexes (1.55-1.64 Å).[115, 116] This in turn causes longer bond lengths between the iron and the outer carbon atoms. The average of 2.26 Å for Fe(1)-C(7) and Fe(1)-C(22) distances falls well outside of the normal range of 2.10-2.16 Å for (butadiene)$Fe(CO)_3$ complexes.[113] However the bond lengths between the iron and the inner carbon atoms (2.064(2) and 2.057(2) Å) are normal. The average Fe-carbonyl distance of 1.798 Å is comparable with the many reported values (1.75-1.80 Å).[117] Three of four C-C-C angles in the complexed diene portion are significantly smaller than 120º, which is not common in (butadiene)$Fe(CO)_3$ complexes, but has been observed in η^4-naphthalene complexes before.[114b]

The uncomplexed part of the ligand does not deviate significantly from coplanarity. The largest deviations are found at C(15) (0.195 Å). However, more careful study found that the free *t*-butyl end of the DHP ring is slightly bent toward the metal center with a dihedral angle of 8.9º between planes defined by C(15) - C(17) and the central part of the ligand (C(7) - C(14) and C(18) - C(22)). The benzene ring retains planarity and is almost bond equal. The bond alternation around the DHP ring is discussed below.

Table 3.1 Summary of crystallographic data for 152 and 153.

	152	**153**
Formula	$C_{33}H_{34}FeO_3$	$C_{36}H_{34}Fe_2O_6$
Fw	534.45	674.33
cryst syst	Monoclinic	Orthorhombic
space group	P2(1)/n	Pbca
a (Å)	10.3156(7)	16.2931(7)
b (Å)	13.1485(9)	18.4265(8)
c (Å)	19.4451(13)	20.3460(9)
α (deg)	90	90
β (deg)	91.235(1)	90
γ (deg)	90	90
V ($Å^3$)	2636.8(3)	6108.4(5)
Z	4	8
ρ (calcd) (Mg/m^3)	1.346	1.467
abs coeff (mm^{-1})	0.605	0.997
F (000)	1128	2800
θ range for data collection (deg)	1.87 to 25.24	1.95 to 25.25
reflections collected	38554	93472
independent reflections	4778	5529
	[R(int) = 0.0289]	[R(int) = 0.0410]
completeness to θ	25.24°, 99.9%	25.25°, 100.0%
data/restraints/params	4778 / 0 / 342	5529 / 0 / 405
goodness of fit on F^2	1.099	1.067
final R indices [$I>2\sigma(I)$][a]	R1 = 0.0381	R1 = 0.0378
	wR2 = 0.0971	wR2 = 0.0916
R indices (all data)[a]	R1 = 0.0410	R1 = 0.0414
	wR2 = 0.0988	wR2 = 0.0940

$R_1 = \Sigma||F_o| - |F_c||/\Sigma|F_o|$; $wR_2 = \{\Sigma[\ w(F_o^2 - F_c^2)^2]/\ \Sigma\ [w(F_o^2)^2]\}^{1/2}$

Table 3.2 Selected experimental (exp) and calculated [DFT B3LYP/6-31G*][111] (calc) bond[a] lengths (Å) for complexes 36,[54b] 152 and 153.

bond[a]	**36 exp**	**calc**	**152 exp**	**calc**	**153 exp**	**calc**
C(5)-C(22)	1.354(4)	1.377	1.447(3)	1.445	1.440(3)	1.512
C(5)-C(6)	1.440(4)	1.442	1.405(3)	1.422	1.422(3)	1.349
C(6)-C(7)	1.362(3)	1.366	1.431(3)	1.431	1.427(3)	1.512
C(7)-C(8)	1.463(4)	1.459	1.484(3)	1.491	1.491(3)	1.498
C(8)-C(9)	1.413(4)	1.418	1.404(3)	1.408	1.400(3)	1.406
C(9)-C(10)	1.362(4)	1.380	1.381(3)	1.389	1.379(3)	1.390
C(10)-C(11)	1.397(4)	1.406	1.391(3)	1.397	1.389(3)	1.396
C(11)-C(12)	1.363(4)	1.380	1.380(3)	1.387	1.382(3)	1.391
C(12)-C(13)	1.411(4)	1.418	1.407(3)	1.409	1.398(3)	1.404
C(13)-C(14)	1.450(4)	1.459	1.480(3)	1.477	1.493(3)	1.500
C(14)-C(15)	1.364(3)	1.366	1.347(3)	1.355	1.420(3)	1.415
C(15)-C(16)	1.437(4)	1.442	1.469(3)	1.463	1.422(3)	1.432
C(16)-C(17)	1.359(4)	1.377	1.355(3)	1.365	1.448(3)	1.464
C(17)-C(18)	1.429(4)	1.420	1.439(3)	1.438	1.461(3)	1.455
C(18)-C(19)	1.367(4)	1.378	1.357(3)	1.366	1.349(3)	1.372
C(19)-C(20)	1.429(3)	1.423	1.449(3)	1.450	1.455(3)	1.447
C(20)-C(21)	1.351(4)	1.378	1.353(3)	1.358	1.351(3)	1.385
C(21)-C(22)	1.431(3)	1.420	1.450(3)	1.458	1.449(3)	1.425
C(8)-C(13)	1.426(3)	1.377	1.423(3)	1.430	1.426(3)	1.438
Average C-C (DHP)	1.4044	1.4101	1.4206	1.4249	1.4324	1.4431
Average C-C (Benz)	1.3953	1.4060	1.3977	1.4033	1.3957	1.4042
Ave dev C-C (DHP)	0.0385	0.0312	0.0409	0.0369	0.0300	0.0409
Ave dev C-C (Benz)	0.0219	0.0173	0.0137	0.0123	0.0123	0.0119
C(5)-Fe(1)			2.064(2)	2.080	2.065(2)	2.870
C(6)-Fe(1)			2.057(2)	2.066	2.059(2)	2.879
C(7)-Fe(1)			2.265(2)	2.266	2.282(2)	2.193
C(22)-Fe(1)			2.147(2)	2.147	2.171(2)	2.049
C(14)-Fe(2)					2.262(2)	2.318
C(15)-Fe(2)					2.068(2)	2.088
C(16)-Fe(2)					2.039(2)	2.023
C(17)-Fe(2)					2.167(2)	2.174

a. X-ray numbering

Table 3.3 Selected bond angles (deg) for complexes 152 and 153.

Angle	**152**	**153**
C(31)-Fe(1)-C(33)	91.48(9)	92.15(11)
C(31)-Fe(1)-C(32)	90.57(9)	89.31(10)
C(33)-Fe(1)-C(32)	96.80(10)	96.44(11)
C(34)-Fe(2)-C(35)		96.76(11)
C(36)-Fe(2)-C(34)		94.28(12)
C(36)-Fe(2)-C(35)		91.93(12)
O(1)-C(31)-Fe(1)	175.50(19)	176.9(2)
O(2)-C(32)-Fe(1)	177.09(18)	176.0(2)
O(3)-C(33)-Fe(1)	172.61(19)	171.1(2)
O(4)-C(34)-Fe(2)		174.8(2)
O(5)-C(35)-Fe(2)		176.4(2)
O(6)-C(36)-Fe(2)		177.3(3)
C(6)-C(7)-C(23)	114.27(16)	113.78(19)
C(5)-C(6)-C(7)	117.93(18)	118.0(2)
C(6)-C(5)-C(22)	114.73(17)	114.3(2)
C(5)-C(22)-C(21)	120.37(18)	121.4(2)
C(15)-C(14)-C(25)		120.66(19)
C(14)-C(15)-C(16)		119.4(2)
C(15)-C(16)-C(17)		112.8(2)
C(16)-C(17)-C(18)		117.7(2)
C(2)-C(4)-C(1)	108.56(18)	108.9(2)
C(2)-C(4)-C(5)	112.02(17)	112.4(2)
C(1)-C(4)-C(5)	113.71(17)	112.7(2)
C(2)-C(4)-C(3)	108.73(19)	108.7(2)
C(1)-C(4)-C(3)	108.58(18)	108.1(2)
C(5)-C(4)-C(3)	105.06(16)	105.85(19)
C(30)-C(27)-C(29)		107.9(2)
C(30)-C(27)-C(16)		111.7(2)
C(29)-C(27)-C(16)		112.4(2)
C(30)-C(27)-C(28)		109.4(2)
C(29)-C(27)-C(28)		108.9(2)
C(16)-C(27)-C(28)		106.5(2)
C(14)-C(25)-C(26)	106.02(16)	112.89(18)
C(18)-C(25)-C(26)	105.73(16)	107.24(18)
C(23)-C(25)-C(26)	114.81(16)	110.42(18)
C(21)-C(23)-C(24)		108.54(18)
C(7)-C(23)-C(24)		108.31(18)
C(25)-C(23)-C(24)		110.46(18)

3.4.3 The crystal structure of 153

The crystal structure of **153** is shown in **Figure 3.2**. The crystallographic data are summarized in **Table 3.1** and selected bond lengths are given in **Table 3.2** and bond

angles in **Table 3.3**. The two iron tricarbonyl groups are coordinated to the two butadiene units at the two *t*-butyl ends and on the same side. The DHP ring is thus bent at both ends and a boat structure is formed. The central part of the boat structure, a plane defined by C(7)-C(8), C(13)-C(14) and C(17)-C(22) is quite flat with maximum deviations found at C(20) (0.177 Å), C(18) (0.104 Å), and C(7) (0.090 Å), respectively. The dihedral angles between the two complexed diene planes and the central plane are 31.3° and 51.4° respectively. The larger angle is for the diene unit which has the $Fe(CO)_3$ group and the closer internal methyl group on the same side, (i.e. Fe2 and C26 in **Figure 3.2**) and is obviously caused by stronger intramolecular interactions. The dihedral angle between the two diene planes is 71.3°.

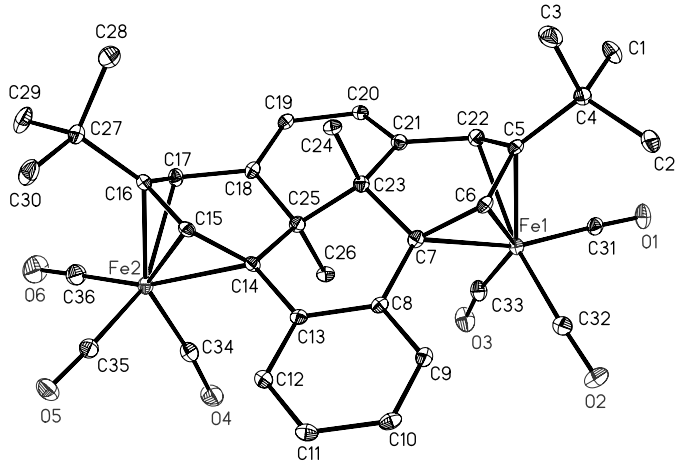

Figure 3.2 An ORTEP3 drawing[63] of complex 153 (30% probability thermal ellipsoids). Hydrogen atoms have been removed for clarity.

The two tricarbonyl iron butadiene portions of the molecule show similar structural features to those found in **152**, but show larger molecular distortions. The two iron atoms are 1.713 Å and 1.726 Å from the diene planes respectively, similar to that in **152**. The

average inner and outer C-C bond lengths are same for the two complexed diene units. The average inner bond lengths (1.422 Å) are longer and the average outer bond lengths (1.434 Å) are shorter than those of **152** (1.405 Å and 1.439 Å), suggesting stronger π-back donation from iron in **152**. Similar to **152**, the shortest intramolecular contacts are found between C(33)…H(26C) (2.453 Å) and C(34)…H(26A) (2.352 Å) on the internal methyl side and C(31)…H(1A) (2.717 Å), C(31)…H(2C) (2.780 Å) and C(36)…H(29C) (2.645 Å) on the *t*-butyl sides. These data display the congestion in the molecule. They also show that the accommodation of two $Fe(CO)_3$ groups on one side of the DHP ring results in a more crowded environment for the *cis*-internal methyl group compared to that of **152**. Also the Fe-C-O angles in **153** are all significantly smaller than 180º, rather than just some of them as in **152**. This implies a great deal of molecular strain in **153**. The C-Fe-C angles are all similar to those in **152**.

The structure of **153** was a surprise to us, as one might expect that coordination of the two tricarbonyl iron groups on opposite sides of the ligand would cause less strain in the molecule. In that way both of the $Fe(CO)_3$ groups could stay away from the *cis*-internal methyl group, unlike in **153**, where one $Fe(CO)_3$ has to be next to the *cis*-internal methyl. However, calculations of ΔH_f disagree, and a PM3 calculation[111] for **153** and the analogous *trans*-$Fe(CO)_3$ isomer suggest that the *cis*-isomer **153** is more stable by 110 kJ/mole! Of course, it may be that the kinetic approach of the second iron moiety is favored on the outside "of the saucer" shaped molecule. Interestingly, a similar structure has been observed before in the heptalene bis(tricarbonyliron) system, **154**.[118]

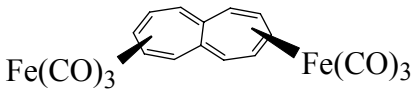

154

3.4.4 Bond localization effects

When two annulenes are fused along a common side, bond localization occurs in both rings and leads to alternating bond lengths and coupling constants. The actual bond localization effects depend on the aromaticity or antiaromaticity of each annulene. If one annelated annulene is aromatic and has a large resonance energy, it will cause a large bond fixation on the fused annulene. Antiaromatic annulenes cause the same effect, though the bond alternation pattern is different.[39]

The experimental and calculated bond lengths in the free ligand **36**[54b] and complexes **152** and **153** are given in **Table 3.2**. Note that Spartan[111] (DFT, B3LYP/6-31G*) tends to overestimate the average bond lengths 1.4044 (exp DHP), 1.4101 (calc DHP), 1.3953 (exp Benz), 1.4060 (calc Benz) for **36** and also in similar annulenes, and underestimate the average deviation of each bond from the average bond length 0.0385 (exp DHP), 0.0312 (calc DHP), 0.0219 (exp Benz), and 0.0173 (calc Benz) for **36**. Nevertheless, the correlations are quite good.[26a, 42, 54b] This average deviation can be used as a measure of the bond alternation around each ring, and in turn as a measure of the size of the ring current.[26a, 54b]

Both the DHP and the benzene ring in **36** show stronger bond alternation (ave dev = 0.0385 and 0.0219 respectively) than in the parent **11** (ave dev = 0.0027) or its 2,7-di-*t*-butyl derivative (ave dev = 0.0049) and the ring current in each ring is reduced by about 50%[26a, 42] from that of the parents, because both fused rings, DHP and benzene are strongly aromatic. However, in **152** the DHP ring displays greater alternation (ave dev = 0.0409) than in **36**, but the benzene ring (ave dev = 0.0137) shows less. This suggests now that the DHP ring in **152** is less aromatic than that in **36**. However, this DHP ring

must still retain considerable delocalization, since the non-cyclically conjugated model **27** has an ave dev = 0.0562. Our conclusion then, is that this delocalization is contributing to a small paratropic ring current, which would account for the chemical shifts of the internal methyl protons, relative to those in **36**, and the weak effect on the benzene ring, and the back donation of iron suggested from the X-ray structure above. The greater calculated ave dev in the benzene ring of **152** (0.0123) than in **148** (0.0092) is consistent with the observed coupling constants for these compounds. Overall, the average carbon-carbon bond length of the dihydropyrene ring increases from **36** to **152** to **153**, consistent with increasing electron withdrawal from the DHP π-system by the iron tricarbonyl groups. Interestingly though, the calculations for the bis-iron complex **153** do not agree so well with the X-ray structure. As can be seen from **Table 3.2**, the calculated structure has considerably more bond fixation in the DHP ring than is found in the crystal structure. This is especially apparent at the C7-C6-C5-C22 end of the molecule, where the iron tricarbonyl moiety, Fe1 in **Figure 3.2**, has slipped towards the methyl group (C26) such that the bonding appears to be ene-diyl, i.e. C5-C6 has more double bond character and C5-C22 and C6-C7 have more single bond character. The energy well may be rather shallow with a consequence that the crystal structure and calculated structures are not so different in energy. Certainly in solution, the bis-iron complex **153** does not appear to be more delocalized in the DHP ring than the mono-complex **152**, as the crystal structures suggest!

3.4.5 Photoswitching properties

Both the parent DHP **11** and the benzoDHP **36** are photochromic. Irradiation of a benzene solution of **36** with visible light from a 500W tungsten lamp, using a 490 nm cut

off filter quickly converts it to the cyclophane diene (CPD) **36'** (Scheme 1). We were interested in how the coordination of $Fe(CO)_3$ and $Fe(CO)_4$ groups would modify the photochromic properties of DHPs. However, under similar conditions, irradiation of a benzene solution of complexes **152** or **153,** yielded none of the CPD forms and very little or no decomposition. Irradiation of **151,** on the other hand, resulted in the formation of benzoDHP **36** along with some precipitate. None of the open form of **151** could be detected. It is interesting that no iron complexes of any DHP systems we have made have turned out to be photochromic,[119] while some other metal systems, including those containing Ru,[104] are. The reasons for this are not yet clear but differences in the ligand field state energies no doubt play an important role, where the first row transition metals appear to quench the photochemistry.

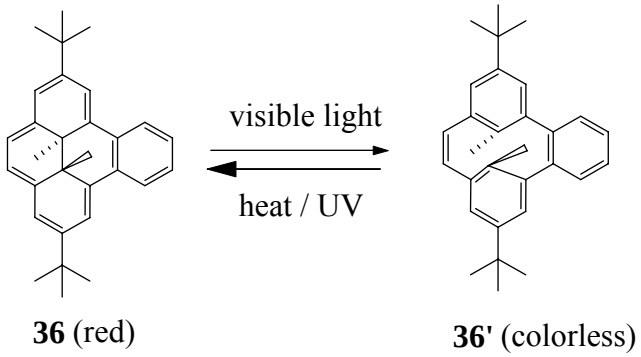

Scheme 3.1 Isomerization of 36 and 36'

3.5 Conclusions

Three iron dihydropyrene complexes have been synthesized and X-ray structures of two, **152** and **153**, have been obtained. In these two, coordination of the metal occurs on the DHP ring and causes a distortion of about 30° from planarity of the large ring. This ring then shows increased bond alternation and loss of aromaticity relative to the ring in

the ligand **36**. Some delocalization however remains, and possibly a paratropic ring current coupled with strong anisotropic effects cause the downfield shifts of the internal methyl protons in **152**. Crystal packing forces may override other considerations in the very crowded **153**, such that the chemical shifts are driven more by anisotropic effects than ring currents. Complexation suppresses the photochromic behavior of the dihydropyrenes.

Chapter Four

Experimental

4.1 General experimental conditions and instrumentation

Proton and Carbon-13 NMR spectra were recorded on a Bruker AVANCE 500 (500.1 MHz for ^{1}H, 125.7 MHz for ^{13}C), a Bruker AMX 360 (360 MHz for ^{1}H, 90.6 MHz for ^{13}C) or a Bruker AC 300 (300MHz for ^{1}H, 75.0 MHz for ^{13}C) spectrometer, using residual solvent peaks as calibration. Where peaks within the same sample are very close in chemical shift, a third decimal place is given. Solutions of oxygen sensitive compounds for NMR spectroscopy were prepared by dissolving the compound in a minimum amount of deareated solvent, then filtering it through alumina deactivated with 3% water, next rinsing the alumina with sufficient deareated solvent to make up the correct volume for the spectrometer, and finally by bubbling argon through the filtrate in the NMR tube for 5 to 10 minutes. The tubes were then carefully capped under argon, and the spectra obtained. The faster thermal returning photoisomerizable compounds were recorded at the stated low temperature.

For NMR assignment, H-1,2 means H-1 and H-2. H-1/2 means H-1 or H-2. The same is true for ^{13}C assignments. Where NMR assignments are made, these were on the basis of 2D COSY/NOESY experiments for ^{1}H and HSQC/HMBC experiments for ^{13}C

Infrared spectra were recorded on a Bruker IFS25 FT-IR spectrometer. All spectra were acquired at room temperature, as KBr discs, thin film or in solution and only the major peaks are reported. The thin film was made by spin coating the sample solution on a NaCl plate. For the solution phase, KBr cells equipped with PTFE spacers giving a pathlength of 0.1 mm were used. The solutions were introduced into the cell via a syringe. The open ends were then sealed with 5 mm white PTFE stoppers.

UV-Vis spectra were recorded on a Cary 5 UV-VIS-NIR spectrometer in the stated solvents. Units for ε_{max} are $Lmol^{-1}cm^{-1}$. Melting points were determined on a Reichert 7905 melting point apparatus intergrated to an Omega Engineering Model 199 Chromel-alumel thermocouple.

Mass spectra were recorded on a Finnigan 3300 gas chromatography-mass spectroscopy system using methane as a carrier gas for chemical ionization or electron impact (EI) at 70 eV. FAB or LSI mass spectra and exact mass measurements were taken on a Kratos Concept-H instrument using perfluorokerosene as the standard. Elemental analyses were performed by Canadian Microanalytical Services Ltd., Vancouver, B.C..

All evaporations were carried out under reduced pressure on a rotary evaporator, and all organic extracts were washed with water and dried over anhydrous $MgSO_4$, $NaSO_4$, or K_2CO_3 as appropriate. Silica gel (SiGel) refers to Merck silica gel, 60-200 mesh. Alumina refers to Aldrich aluminum oxide, activated, neutral, Brockmann I, standard grade, ~150 mesh. All alumina and deactivated silica gel were deactivated with 5% water (by weight).

General procedures for visible light opening and UV closing: Photoisomerization for thermal return kinetic studies were performed using broadband irradiation from a 500 W tungsten incandescent lamp at a distance of 50 cm from the sample unless otherwise mentioned, with an ice/water bath and pyrex filter. All DMDHP compounds studied were photoisomerized to CPD forms using a 490 nm cut off filter unless otherwise stated, placing the filter in the ice bath between lamp and sample. For UV closing, the solutions of the samples were first irradiated by visible light to the corresponding open CPD forms. Then they were irradiated by UV light (a 254 nm

mercury pen light). All samples for opening and closing were degassed by purging argon through the solution for about 30 minutes.

General procedures for the rate comparison: The solution of the reference, benzoDHP **36**, and the compound to be compared were prepared in equal molarity in quartz UV cells using cyclohexane as solvent (unless otherwise stated). The prepared solutions were bubbled with argon for 30 min and the UV cells were sealed. Then two cells, one containing the reference **36** and the other one containing the compound, were placed side by side and irradiated with visible light with wavelength > 490 nm. An electrical fan was used to cool the samples. UV-vis spectra were taken at various time intervals. For the photo closings, a similar procedure was used as the photoopening processes. The fully opened **36'** solution and equimolar fully opened sample solutions in cyclohexane were placed side by side and irradiated by a pencil mercury lamp and monitored by their UV-vis spectra (see **Section 2.4.3** for data analysis details).

Note: all the bis-dihydropyrene systems are a mixture of two or more isomers with almost equal amounts. Some ratios shown in NMR data are not equal because they were collected after chromatography in order to get pure samples.

4.2 Syntheses

2,7-Di-*tert*-butyl-5-chloro-*trans*-11c,11d-dimethyl-11c,11d-dihydro-9-oxo-9*H*-cyclopenta[*e*]pyrene 47 and 10,11-Dihydroderivative 48.

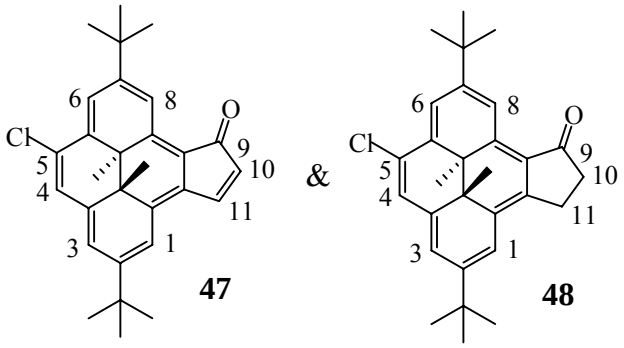

A solution of cyclopentanone fused dihydropyrene[45] **43** (100 mg, 0.25 mmol) in dry ether (5 mL) was added dropwise under argon to a stirred suspension of $PhSeCl_3$ (65.6 mg, 0.25 mmol) in dry ether (5 mL) at 0 °C. After the reaction mixture was stirred for 1 h at 0 °C, the solvent was removed under vacuum and replaced with dichloromethane (7 mL), followed by aqueous $NaHCO_3$ solution (84 mg, 1 mmol, in 5 mL water). Stirring was continued for 4 h, and then hexane (15 mL) was added. The dark green organic layer was separated, washed, dried (Na_2SO_4), and evaporated. The residue was then chromatographed on silica gel with hexane/ethyl acetate (10:1). Eluted first and second were small amounts (a few milligrams) of products, which were subsequently identified as 10-chloro derivatives of **43** and **46** by ^1H NMR spectroscopy. Eluted third was about 5 mg (5%) of product **46** (see below for characterization). Eluted fourth was product **47** (26 mg, 23%) as dark green crystals. Eluted fifth was ~4 mg (4%) of unchanged starting material **43**. Eluted sixth was the chlorocyclopentanone **48** (29 mg, 26%) as dark brownish-green crystals.

Compound **47**: mp ~210 °C (decomp); ^{1}H NMR (500 MHz, $CDCl_3$) δ 8.97 (d, *J* = 1.2 Hz, 1H, H-8), 8.12 (d, *J* = 1.2 Hz, 1H, H-6), 8.09 (d, *J* = 5.8 Hz, 1H, H-11), 7.81 (s, 1H, H-4), 7.75 (d, *J* = 1.2 Hz, 1H, H-1), 7.66 (br s, 1H, H-3), 6.21 (d, *J* = 5.8 Hz, 1H, H-10), 1.53 [s, 9H, 7-C(CH_3)$_3$], 1.48 [s, 9H, 2-C(CH_3)$_3$], -1.83 (s, 3H, 11c-CH_3), -1.86 (s, 3H, 11d-CH_3); ^{13}C NMR (125.7 MHz, $CDCl_3$) δ 197.13 (C-9), 154.53 (C-7), 149.36 (C-2), 145.00 (C-11), 142.11 (C-5a), 138.76 (C-11b/e), 137.33 (C-3a), 132.77 (C-11e/b), 132.37 (C-10), 132.09 (C-11a), 128.95 (C-5), 127.07 (C-4), 123.88 (C-3), 121.77 (C-11f), 121.40 (C-6), 117.15 (C-8), 115.47 (C-1), 38.33 (C-11d), 36.69 (2-C(CH_3)$_3$), 36.35 (C-11c), 35.98 (7-C(CH_3)$_3$), 31.00 & 30.92 (2,7-C(CH_3)$_3$), 21.03 (11d-CH_3), 20.40 (11c-CH_3); IR (KBr) ν 1667, 1607, 1556, 1260, 1173, 1134, 1070, 954, 892, 860, 820, 734, 668 cm^{-1}; UV-vis (cyclohexane) λ_{max} (ε_{max}) nm 235 (19 000), 316 (38 000), 399 (32 000), 475sh (11 000), 569 (1000), 625 (1300), 690 (1700); EI MS *m*/*z* 430 (M^+) and 432 (M + 2) 3:1 (Cl); HRMS calcd for $C_{29}H_{31}{}^{35}ClO$: 430.2063, found: 430.2066.

Compound **48**: mp 214-216 °C; ^{1}H NMR (500 MHz, $CDCl_3$) δ 9.81 (d, *J* = 1.0 Hz, 1H, H-8), 8.69 (d, *J* = 1.3 Hz, 1H, H-6), 8.67 (d, *J* = 1.3 Hz, 1H, H-1), 8.40 (s, 1H, H-3), 8.29 (s, 1H, H-4), 3.92 & 3.83 (~dt, $J_{11,11'}$ = 17.4 Hz, $J_{11,10}$ = 5.7 Hz, 2H total, H-11), 3.09 (~t, *J* = 5.7 Hz, 6.5 Hz, 2H, H-10), 1.68 (s, 9H, 7-C(CH_3)$_3$), 1.65 (s, 9H, 2-C(CH_3)$_3$), -3.50 (s, 6H, 11c,d- CH_3); ^{13}C NMR (125.7 MHz, $CDCl_3$) δ 208.92 (C-9), 151.60 (C-7), 150.52 (C-11a), 146.39 (C-2), 136.82 and 132.91 (C-3a/11e), 132.72 (C-5a), 131.81 (C-11b), 126.91 (C-11f), 125.55 (C-4), 124.63 (C-5), 123.59 (C-3), 121.57 (C-1), 119.98 (C-8), 117.90 (C-6), 37.63 (C-10), 37.00 (7-C(CH_3)$_3$), 36.25 (2-C(CH_3)$_3$), 33.66 (C-11d), 31.98 (2-C(CH_3)$_3$), 31.91 (7-C(CH_3)$_3$), 31.20 (C-11c), 24.79 (C-11), 15.57 and 15.35 (11c,d-CH_3); IR (KBr) ν 1694, 1464, 1362, 1303, 1253, 1132, 1088, 957, 947, 891, 668

cm^{-1}; UV-vis (cyclohexane) λ_{max} (ε_{max}) nm 238 (12,000), 288 (6,100), 345 (32,000), 363 (33,000), 378 (27,000), 402 (39,000), 509 (6,100), 606 (1,000), 678 (3,600); EI MS *m*/*z* 432 (M+) and 434 (M + 2) 3:1 (Cl); HRMS calcd for $C_{29}H_{33}$ ^{35}ClO: 432.2220, found: 432.2227.

trans-3-(2',7'-Di-_tert_-butyl-4'-_trans_-10b',10c'-dimethyl-10b',10c'-dihydropyrenyl) acrylic acid 50

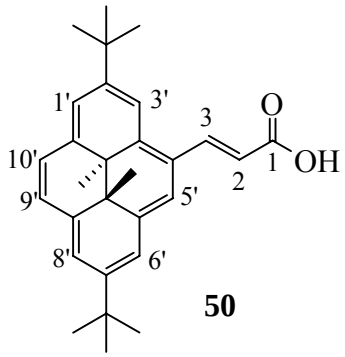

50

Ethyl 3-(2',7'di-*tert*-butyl-4'-*trans*-10b',10c'-dimethyl-10b',10c'-dihydropyrenyl) acrylate **40**[45] (640mg, 1.45 mmol) in THF (100 mL) was refluxed with 2 M NaOH (200 mL) for 18 h under argon. The solution was then cooled to room temperature, neutralized with 2 M HCl (200 mL) and extracted with CH_2Cl_2 (300 mL). The combined organic extracts were washed with water, dried and evaporated to give a green residue, which was chromatographed over deactivated silica gel using hexane/CH_2Cl_2 (1:1) as eluant. Eluted first was the starting ester **40** (132 mg, 21%). Eluted next with CH_2Cl_2 was the acid **50** as a brownish green solid (430 mg, 72%), mp 239-241°C. ^{1}H NMR δ 9.31 (d, *J* = 15.5 Hz, 1H, H-3), 8.94 (s, 1H, H-3'), 8.74 (s, 1H, H-5'), 8.52 (s, 1H, H-6'), 8.50 (s, 1H, H-1'), 8.48 (s, 1H, H-8'), 8.44 (AB, *J* = 7.95 Hz, 1H, H-9'), 8.40 (AB, *J* = 7.95 Hz, 1H, H-10'), 6.90 (d, *J* = 15.5 Hz, 1H, H-2) 1.72 (s, 9H, 2-C(CH_3)$_3$), 1.67 (s,

9H, 7-C(CH_3)$_3$), -3.738 and -3.744 (s, 3H each, 10b',10c'-CH_3); ^{13}C NMR δ 173.02(C-1), 148.41(C-2'), 146.85 (C-7'), 143.78(C-3), 139.49(C-10a'), 137.74(C-3a'), 137.38(C-8a'), 136.70(C-5a'), 125.23(C-9'), 124.47(C-4'), 124.18(C-10'), 122.82(C-8'), 122.19(C-6'), 121.85(C-1'), 119.97(C-5'), 116.08(C-3',C-2), 36.72(2'-C(CH_3)$_3$), 36.14(7'-C(CH_3)$_3$), 32.10 and 31.99 (2',7'-C(CH_3)$_3$), 31.86(C-10b'), 30.12(C-10c'), 15.66 and 15.57 (10b',10c'-CH_3); IR (KBr) ν ~ 3400-2400 (vbr), 1681, 1599, 1384, 1360, 1298, 1202, 971 885, 673 cm^{-1}; UV (methanol) λ_{max} (ε_{max}) nm 284 (9,900), 356 (35,700), 396 (40,200), 492 (8,700), 668 (1,800); EIMS *m/z* 414(M^+); HRMS calcd for $C_{29}H_{34}O_2$: 414.2559, found: 414.2556.

2,7-Di-*tert*-butyl-*trans*-11c,11d-dimethyl-11c,11d-dihydro-9-oxo-9H-cyclopenta[*e*] pyrene 46

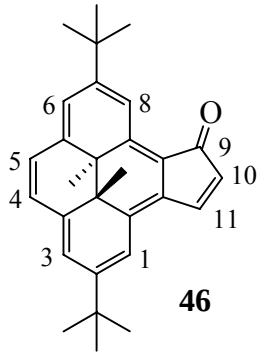

46

Method A: A solution of *i*-Pr_2NLi (0.13 mmol in 0.26 mL of hexane) was added at -78 °C to a stirred solution of cyclopentanone fused dihydropyrene **43** (50 mg, 0.125 mmol, vacuum-dried) in dry THF (20 mL) under argon. The red solution was stirred for 5 min and then PhSeCl (24.9 mg, 0.13 mmol) in dry THF (5 mL) was added dropwise. The cooling bath was removed and the solution was stirred for another 30 min. Water (1 mL) was then added, followed by 30% H_2O_2 (1 mL, 11.6 mmol), and then stirring was

continued for 1 h. The mixture was then extracted with hexane (15 mL), and the organic phase was washed, dried (Na_2SO_4), and evaporated. The dark green residue was chromatographed on silica gel with hexane/ether (4:1) as eluant. Eluted first was the product **46** (14 mg, 28%) as a green solid. Eluted next was unchanged cyclopentanone fused dihydropyrene **43** (22 mg, 44%).

Method B: Oxalyl chloride (0.8 mL, 9 mmol) was added to the acid **50** (350 mg, 0.84 mmol) in dry dichloromethane (100 mL) under argon. The resulting solution was stirred at room temperature for 6 h, after which the solvent was removed under vacuum and the green residue was evacuated for 1.5 h to get rid of the excess chlorinating reagent. The brown solid was then taken up in dry dichloromethane (200 mL) and $BF_3.OEt_2$ (0.3 mL, 2.4 mmol) was added to the mixture under argon. The solution was further stirred at room temperature for 12 h. Then ice water was added and the aquous layer was extracted with dichloromethane. The combined organic extracts were washed with water, dried and evaporated to give a reddish brown solid, which was chromatographed on deactivated silica gel with hexane / CH_2Cl_2 (1:1) to yield the cyclopentadienone[e]DHP **46** as a green solid (266 g, 80 %), mp ~210 °C (dec). ^{1}H NMR (500 MHz, $CDCl_3$) δ 8.91 (d, *J* = 1.3 Hz, 1H, H-8), 8.07 (d, *J* = 5.7 Hz, 1H, H-11), 7.74 (s, 1H, H-1), 7.68 (s but broad 1H, H-6), 7.671 (s, 1H , H-3), 7.665 (AB, *J* = 8.8 Hz, 1H, H-4), 7.63 (AB, *J* = 8.8 Hz, 1H, H-5), 6.18 (d, *J* = 5.7 Hz, 1H, H-10), 1.51 (s, 9H, 7-$C(CH_3)_3$), 1.49 (s, 9H, 2-$C(CH_3)_3$), -1.88 (s, 3H, 11d-CH_3), -1.92 (s, 3H, 11c-CH_3); ^{13}C NMR ($CDCl_3$, 125.7MHz) δ 197.34 (C-9), 154.86 (C-7), 148.9 (C-2), 144.85 (C-11), 142.95 (C-5a), 142.66 (C-11e), 139.95 (C-3a), 133.02 (C-11b), 132.07 (C-10), 131.73 (C-11a), 127.53 (C-4), 126.24 (C-5), 123.66 (C-3), 122.29 (C-6), 121.23 (C-11f), 116.17 (C-

8), 114.89 (C-1), 36.97 (C-11d), 36.52 (C-11c), 36.46 (7-$\underline{C}(CH_3)_3$), 35.95 (2-$\underline{C}(CH_3)_3$), 30.97 & 30.96 (2,7-C($\underline{C}H_3)_3$), 21.54 (11d-CH_3), 20.39 (11c-CH_3); IR (KBr) ν 1661, 1556, 1463, 1263, 1193, 886, 820, 737 cm^{-1}; UV (cyclohexane) λ_{max} (ε_{max}) nm 236 (10,000), 310 (45,100), 398 (31,400), 416 (28,100), 566 (1,000), 620 (1,200), 687 (1,400); EI MS *m/z* 396 (M^+); HRMS Calcd for $C_{29}H_{32}O$ 396.2453, found 396.2452; Anal. Calcd for $C_{29}H_{32}O$: C, 87.83; H, 8.13; Found: C, 87.96; H, 8.09.

2,7-Di-*tert*-butyl-*trans*-11c,11d-dimethyl-10,11,11c,11d-tetrahydro-9-methylenyl-cyclopenta[*e*]pyrene 54

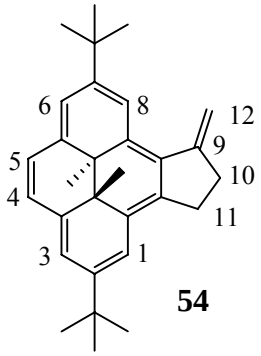

54

n-BuLi (200μL, 1.6 M solution in hexane, 0.32 mmol) was added to $(Ph)_3P$-CH_3Br (120 mg, 0.34 mmol) in dry THF (20 mL) under argon at –78 °C (dry ice-acetone bath). The color changed to yellow immediately. The dry ice-acetone bath was removed after 3 minutes and the solution was warmed to room temperature (20 ^oC) and left stirring for 5 minutes. Then a solution of cyclopentanone fused dihydropyrene **43** (80 mg, 0.20 mmol) in dry THF (10 mL) was added dropwise and the mixture was stirred at room temperature (20 °C) for another hour. Hexanes (30 mL) were then added and the solution was washed with water (4 x 50 mL). The organic layer was then dried over anhydrous Na_2SO_4 and evaporated to give a dark green solid, which was chromatographed over

silica gel with hexane to elute the fused dihydropyrene **54** (57 mg, 71 %) as a green crystalline solid, ^{1}H NMR (500 MHz, C_6D_6) δ 9.39 (s, 1H, H-1), 8.55 (d, *J* = 1.0 Hz, 1H, H-8), 8.49 (s, 1H, H-6), 8.48 (s, 1H, H-3), 8.30 (AB, *J* = 7.4 Hz, 1H, H-4), 8.28 (AB, *J* = 7.4 Hz, 1H, H-5), 6.46 (t, *J* = 2.2 Hz, 1H, one of H-12), 5.69 (t, *J* = 1.9 Hz, 1H, one of H-12), 3.69-3.64 and 3.59-3.53 (m, 1H each, H-11), 3.18-3.06 (m, 2H, H-10), 1.64 (s, 9H, 2-C(CH_3)$_3$), 1.62 (s, 9H, 7-C(CH_3)$_3$), -3.27 (s, 3H, 11c-CH_3), -3.29 (s, 3H, 11d-CH_3); ^{13}C NMR (C_6D_6, 125.7 MHz) δ 153.04 (C-9), 146.08 (C-7), 144.32 (C-2), 141.24 (C-11f), 138.09 (C-3a), 136.57 (C-5a), 132.27 (C-11a), 131.48 (C-11e), 131.20 (C-11b), 123.05 (C-5), 122.57 (C-4), 121.29 (C-6), 120.47 (C-3), 118.69 (C-8), 118.59 (C-1), 106.54 (C-12), 34.91 (C-10), 31.89 (C-11c), 31.57 and 31.53 (2,7-C($\underline{C}H_3$)$_3$), 30.84 (C-11d), 29.12 (C-11), 15.18 (11c,11d-CH_3); EI MS *m/z* 396 (M^+), 381 (M^+-CH_3), 366 (M^+-2CH_3), 325 (M^+-C(CH_3)$_3$-CH_3); HRMS Calcd for $C_{30}H_{36}$, 396.2817, found 396.2813. Compound **54** is not stable and rearranges to compound **55**. A pure sample could not be obtained, and so a mp and UV-vis spectrum are not reported.

9-Ethylidene-2,7-di-*tert*-butyl-*trans*-11c,11d-dimethyl-11c,11d-dihydrocyclopenta [*e*]pyrene 56

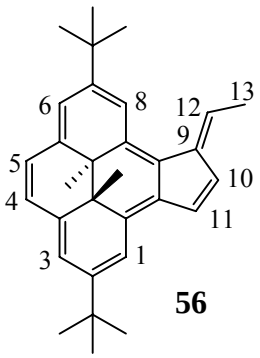

56

Method A: This method followed Ottosson's procedure.[52] The preparation of anion **57** was carried out in a glovebox.

The preparation of pure anion **57**: The cyclopentadienyl fused dihydropyrene (CpDHP) **45** (100 mg, 0.26 mmol) and $LiCH_2SiMe_3$ (26 mg, 0.28 mmol) in toluene (10 mL) were stirred overnight at 20 ºC in a glovebox. The color changed from green to red. The lithium cyclopentadienide fused dihydropyrene (LCpDHP) **57** formed. Then the reaction mixture was dried under vacuum. The pure LCpDHP **57** was obtained by washing the red residue with small mount of hexanes three times to remove the excess base.

The isolated pure LCpDHP **57** (50 mg, 0.13 mmol) was placed in a Kontes flask with a stir bar and then it was taken out from the glovebox. After the addition of solvent THF (10 mL), acetaldehyde (0.14 mmol, 1.4 mL of 1 M solution in dried THF, dried overnight over molecular sieve) was slowly added by syringe. The resulted mixture was stirred at 20 ºC for 30 min. Then the solvent was removed under vacuum and the dark brown solid was chromatographed on deactivated silica gel with hexane to yield the methylfulvene fused dihydropyrene **56** as a dark brown solid (36 mg, 68%).

Method B: This followed Shimizu's[53a] and Alper's[53b] procedures.

Cyclopentadienyl fused dihydropyrene (CpDHP) **45** (50 mg, 0.13 mmol), aqueous NaOH solution (5 M, 3 mL) and cetyltrimethylammonium bromide (CTAB) (2 mg, 4 mol%) were placed in a 50 mL two-necked flask containing THF (3 mL). The resulting mixture was stirred at room temperature (20 ºC) and a solution of acetaldehyde (0.4 mmol, 4 mL of 0.1 M solution in dried THF) was added dropwise over 30 min. After the addition finished, the reaction mixture was stirred at 20 °C for another 30 min. Water (5

mL) was then added and the reaction mixture was extracted with hexane (20 mLx3). The combined extracts were washed with water (50 mLx5), dried with anhydrous $MgSO_4$ and evaporated to give a dark brown solid, which was chromatographed on deactivated silica gel with hexane to yield the methylfulvene fused dihydropyrene **56** as a dark brown solid (16 mg, 30%), mp 124-125 °C; ^{1}H NMR (C_6D_6, 500MHz) δ 9.22 (s, 1H, H-8), 8.77 (d, J = 1.2 Hz, 1H, H-1), 8.45 (s, 1H, H-6), 8.44 (s, 1H, H-3), 8.32 (AB, J = 8.1 Hz, 1H, H-4), 8.29 (AB, J = 8.1 Hz, 1H, H-5), 8.07 (s, 1H, H-12), 7.86 (dd, $J_{11/10}$ = 5.75 Hz, J = 1.6 Hz, 1H, H-11), 7.40 (q, J = 7.4 Hz, 1H, H-12), 7.174 (dd, $J_{10/11}$ = 5.7 Hz, J = 0.7 Hz, 1H, H-10) (In THF-d8, these are not overlapped by benzene, and are doublet of doublets. At δ 7.21 $J_{10/11}$ = 5.7 Hz, J = 0.9 Hz) , 2.14 (d, J = 7.4 Hz , 3H, H-13), 1.619 (s, 9H, 7-C(C<u>H</u>$_3$)$_3$), 1.618 (s, 9H, 2-C(C<u>H</u>$_3$)$_3$), -3.10 (s, 3H, 11c-C<u>H</u>$_3$), -3.13 (s, 3H, 11d-C<u>H</u>$_3$); ^{13}C NMR (C_6D_6, 125.7MHz) δ 147.47 (C-7/2), 146.03 (C-9), 145.61 (C-2/7), 139.33 (C-5a), 138.22 (C-11a), 137.62 (C-3a), 132.28 (C-11e), 130.44 (C-11), 129.84 (C-11b), 128.69 (C-10), 128.29 (C-11f), 127.61 (C-9a), 125.05 (c-5), 124.41 (C-4), 122.42 (C-3), 121.30 (C-6), 117.61 (C-1), 116.92 (C-8), 36.55 and 36.35 (2,7-<u>C</u>(CH$_3$)$_3$), 33.64 (C-11d and C-11c), 32.31 and 32.26 (2,7-C(<u>C</u>H$_3$)$_3$), 17.19 (11c-<u>C</u>H$_3$), 16.90 (C-9b), 16.71 (11d-<u>C</u>H$_3$); EI MS m/z 408 (M^+), 393 (M^+-CH_3), 378 (M^+-2CH_3), 337 (MH^+-CH_3-C(CH$_3$)$_3$); HRMS calcd for $C_{31}H_{36}$ (M^+): 408.2817, found: 408.2814. Note: no IR and UV-Vis spectra are reported because of the lack of stability of the product.

9-Benzylidene-2,7-di-*tert*-butyl-*trans*-11c,11d-dimethyl-11c,11d-dihydrocyclopenta [*e*]pyrene 58

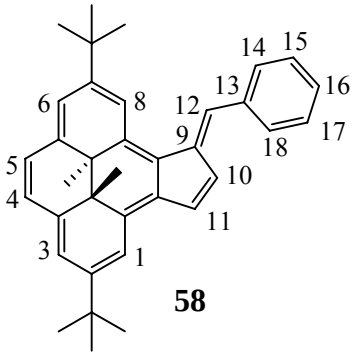

58

Method A: This method followed Ottosson's procedure.[52] The reaction was carried out in a glovebox.

The cyclopentadienyl fused dihydropyrene (CpDHP) **45** (50 mg, 0.13 mmol) and $LiCH_2SiMe_3$ (13 mg, 0.14 mmol) in toluene (10 mL) were stirred overnight at 20 ºC in a glovebox. The color changed from green to red. The lithium cyclopentadienide fused dihydropyrene (LCpDHP) **57** formed. Benzaldehyde (~40 mg, 0.38 mmol, dried by molecular sieve type 4A) was then added and the reaction mixture was stirred at room temperature (20 ºC) for 30 min. The solvent was then removed to give a reddish brown solid. This was chromatographed on deactivated silica gel with hexane to yield the phenylfulvene fused dihydropyrene **58** as a reddish brown solid (49 mg, 80%).

Method B: This procedure is followed Shimizu's[53a] and Alper's[53b] procedures. CpDHP **45** (50 mg, 0.13 mmol), benzaldehyde (~40 mg, 0.38 mmol, excess) and cetyltrimethylammonium bromide (CTAB) (2 mg, 4 mol%) were placed in a 50 mL two-necked flask containing THF (3 mL). Aqueous NaOH solution (5 M, 3 mL) was then added and the resulting mixture was stirred at room temperature (20 ºC) for 1.5 h under argon. Water (5 mL) was then added and the reaction mixture was extracted with hexane

(20 mLx3). The combined extracts were washed with water (50 mLx5), dried with anhydrous $MgSO_4$ and evaporated to give a reddish brown solid, which was chromatographed on deactivated silica gel with hexane to yield the phenylfulvene fused dihydropyrene **58** as a reddish brown solid (45 mg, 74 %), mp 132-133 °C; ^{1}H NMR (500 MHZ, $CDCl_3$) δ 8.96 (s, 1H, H-8), 8.49 (d, J = 1.1 Hz, 1H, H-1), 8.29 (s, 2H, H-3 and H-6), 8.23 (AB, J = 8.1 Hz, 1H, H-4), 8.20 (AB, J = 8.1 Hz, 1H, H-5), 8.07 (s, 1H, H-12), 7.82 (dd, $J_{11/10}$ = 5.7 Hz J = 1.6 Hz, 1H, H-11), 7.70 & 7.69 (m, 1H each , H-14/18), 7.48 (m, 2H, H-15/17), 7.34 (m, 1H, H-16), 7.30 (dd, $J_{10/11}$ = 5.7 Hz, J = 0.7 Hz, 1H, H-10), 1.66 (s, 9H, 7-C$(CH_3)_3$), 1.64 (s, 9H, 2-C$(CH_3)_3$), -3.29 (s, 3H, 11c-CH_3), -3.32 (s, 3H, 11d-CH_3); ^{13}C NMR($CDCl_3$, 125.7MHz) δ 148.17 (C-7), 145.89 (C-2), 144.52 (C-9), 139.33 (C-5a), 138.89 (C-13), 137.42 (C-3a), 136.14 (C-11a), 132.52 (C-11e), 132.08 (C-11), 130.40 (C-14 and C-18), 129.70 (C-10), 129.55 (C-11b), 129.26 (C-12), 128.78 (C-15 and C-17), 127.52 (C-11f), 127.43 (C-16), 124.88 (C-4), 124.03 (C-5), 122.13 (C-3), 120.98 (C-6), 116.82 (C-1), 116.20 (C-8), 36.45 (7-$\underline{C}(CH_3)_3$), 36.16 (2-$\underline{C}(CH_3)_3$), 33.62 (C-11d), 32.12 (C-11c), 32.00 (7-C($\underline{C}H_3)_3$), 31.95 (2-C($\underline{C}H_3)_3$), 17.14 and 16.81 (11c, 11d-CH_3); IR (KBr) ν 3039, 2962, 2923, 2865, 1596, 1459, 1388, 1361, 1261, 866, 701, 680 cm^{-1}; UV-vis (cyclohexane) λ_{max} (ε_{max}) nm 325 (32,400), 418 (41,300), 493 (10,200, shoulder), 590 (1,090), 651 (1,450), 733 (4,730); EI MS *m/z* 470 (M^+), 455 (M^+-CH_3), 454 (M^+-H-CH_3), 440 (M^+-2CH_3), 399 (MH^+-CH_3-C$(CH_3)_3$); HRMS Calcd for $C_{36}H_{38}$: 470.2974, found 470.2982.

9-Hydroxymethyl-2,7-di-*tert*-butyl-*trans*-11c,11d-dimethyl-11c,11d-dihydrocyclopenta[*e*]pyrene 60

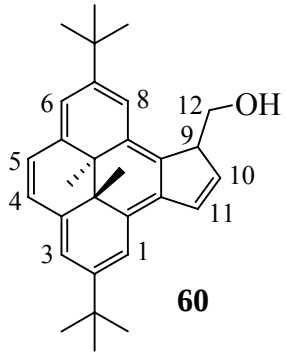

60

CpDHP **45** (50 mg, 0.13 mmol), formaldehyde (0.5 mL of 37% wt in water, 6.7 mmol, excess) and cetyltrimethylammonium bromide (CTAB) (2 mg, 4 mol%) were placed in a 50 mL two-necked flask containing THF (3 mL). Aqueous NaOH solution (5M, 3 mL) was then added. The resulted mixture was stirred at room temperature (20 ºC) for 1.5 h under argon. Water (5 mL) was then added and the reaction mixture was extracted with hexane (20 mLx3). The combined extracts were washed with water (50 mLx5), dried with anhydrous $MgSO_4$ and evaporated to give a green solid, which was chromatographed on alumina (3% water deactivated) with hexane : ethyl ether (2:1) to yield alcohol **60** as a green solid (20 mg, 37 %), mp 168-169 °C. ^{1}H NMR (500 MHZ, C_6D_6) δ 8.86 (d, J = 0.9 Hz , 1H, H-1), 8.83 (d, J = 0.9 Hz, 1H, H-8), 8.60 (s, 1H, H-3), 8.58 (s, 1H, H-6), 8.47 (AB, J = 5.3 Hz, 1H, H-4), 8.44 (AB, J = 5.3 Hz, 1H, H-5), 7.87 (dd, $J_{11/10}$ = 5.7 Hz, J = 1.5 Hz 1H, H-11), 6.82 (dd, $J_{10/11}$ = 5.7 Hz J = 2.0 Hz, 1H, H-10), 4.65-4.62 (m, 1H, H-9), 4.27-4.24 and 3.78-3.75 (m, 1H each, H-12), 1.67 and 1.66 (s, 9H each, 2,7-C(CH_3)$_3$), -3.52 and -3.57 (s, 3H each, 11c,11d-CH_3); ^{13}C NMR (C_6D_6, 125.7MHz) δ 145.97 and 145.15 (C-2, 7), 138.43 (C-11a), 137.83 (C-3a), 137.61 (C-10), 137.24 (C-5a), 136.57 (C-11f), 132.29 (C-11), 131.19 (C-11b), 129.43 (C-11e), 124.64

(C-4), 124.06 (C-5), 121.90 (C-3), 121.25 (C-6), 117.90 (C-1), 117.04 (C-8), 67.74 (C-12), 54.93 (C-9), 36.47 (2, 7-$\underline{C}(CH_3)_3$), 32.43 (2, 7-C($\underline{C}H_3)_3$), 31.97 and 31.50 (C-11c, 11d), 15.68 and 15.28 (11c, 11d-$\underline{C}H_3$); IR (thin film) ν 3436 (OH), 2955, 2923, 2857, 1651, 1460, 869 cm^{-1}; LSI MS *m/z* 412.2 (M^+), 397.2 (M^+-CH_3), 382.2 (M^+-$2CH_3$), 381.2 (MH^+-CH_3-OH), 341.1 ((MH^+-$C(CH_3)_3$-CH_3).

9-Tosyloxymethyl-2,7-di-*tert*-butyl-*trans*-11c,11d-dimethyl-11c,11d-dihydro-cyclopenta[*e*]pyrene 61

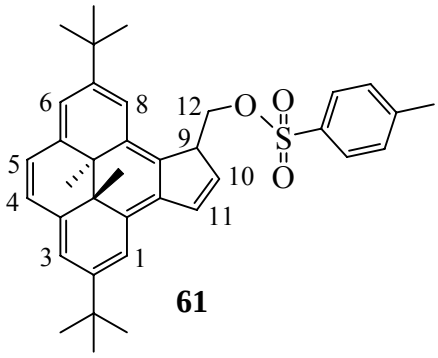

61

Alcohol **60** (35 mg, 0.073 mmol) and dried pyridine (0.5 mL) were placed in a 50 mL two-necked flask containing dry CH_2Cl_2 (10 mL). Then tosyl chloride (30 mg, 0.16 mmol) was added. The reaction mixture was stirred at room temperature (20 ºC) for 1.5 h under argon. Water (5 mL) was then added and the reaction mixture was extracted with hexane (20 mLx3). The combined extracts were washed with water (50 mLx5), dried with anhydrous $NaSO_4$ and evaporated to give a green solid, which was used directly in next step (elimination reaction). ^{1}H NMR (300 MHz, C_6D_6) δ 8.87 and 8.86 (s, 1H total), 8.60 and 8.58 (s, 1H total), 8.53 (AB, J = 7.9 Hz, 1H), 8.50 (AB, J = 7.9 Hz, 1H), 8.46 and 8.45 (s, 1H total), 8.28 and 8.26 (s, 1H total), 7.67 (s, 1H), 6.97-6.90 (2H), 6.68-6.64

(3H), 4.73 to 4.68 (m, 1H), 4.39 to 4.33 (m, 1H), 3.81 to 3.75 (m, 1H), 1.67 and 1.66 (s, 9H each, 2, 7-C(CH_3)$_3$), -3.53 and -3.57 (s, 3H each, 11c, 11d-CH_3).

7-*tert*-Butyl-2-formyl-*trans*-10b, 10c-dimethyl-10b, 10c-dihydropyrene, 112

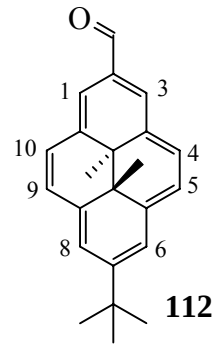

112

Tin tetrachloride (12.00 mL, 100.0 mmol) was added under nitrogen to a solution of DHP **35** (7.54g, 21.9 mmol) and α,α-dichloromethyl methyl ether (2.40 mL, 28.0 mmol) in dichloromethane (650 mL) at 0 °C. The resulting red-brown solution was then stirred at room temperature for 5 h, after which it was slowly added to ice-water (700 mL) and the resulting solution was extracted with dichloromethane (500 mL).The combined organic extracts were washed with water (3 x 600 mL), dried with anhydrous $MgSO_4$ and evaporated to yield a brown solid, which was chromatographed over silica gel. The unreacted DHP (3.2g, including 25% 4-chloro-DHP **114** and dichloro-DHP **115**) was eluted first with hexane. Further elution with hexane / dichloromethane (2: 1) gave the 4-formyl derivative **39**[45] and the chloro derivative **113** (4.2 g) as a brown powder. Eluted next was purplish red compound **112** (140 mg, 0.44 mmol 2%), mp 116-117°C; ^{1}H NMR ($CDCl_3$, 500MHz) δ 10.53 (s, 1H, CHO), 8.95 (s, 2H, H-1,3), 8.74 (d, J = 7.8 Hz, 2H, H-4,10), 8.56 (s, 2H, H-6,8), 8.48 (d, J = 7.8 Hz, 2H , H-5,9), 1.68 (s, 9H, 7-C(CH_3)$_3$), -3.82 (s, 3H, 10b-CH_3), -3.84 (s, 3H, 10c-CH_3); ^{13}C NMR ($CDCl_3$, 125.7 MHz)

δ 193.64 (CHO), 151.42 (C-7), 142.41 (C-5a,8a), 134.94 (C-3a,10a), 129.28 (C-4,10), 128.54 (C-2), 125.13 (C-1,3), 123.66 (C-5,9), 121.95 (C-6,8), 36.65 (7-$\underline{C}(CH_3)_3$), 31.94 (7-C($\underline{C}H_3)_3$), 31.46 (C-10b), 31.33 (C-10c), 16.45 (10c-CH_3), 14.72 (10b-CH_3); IR (Thin film on NaCl plate) 2961, 1675, 1552, 1134, 885 cm^{-1}; UV-vis (cyclohexane) λ_{max} (ε_{max}) nm 212 (14,500), 240 (11,600), 256 (9,880), 330 (35,600), 347 (73,300), 378 (15,400), 402 (29,000), 515 (1,180), 596 (889), 661 (264); EI MS *m*/*z* 316 (M^+), 301 (M^+-CH_3), 286 (M^+-$2CH_3$), 271 (M^+-$3CH_3$), 245 (MH^+-CH_3-$C(CH_3)_3$), 217 (MH_2^+-CHO-CH_3-$C(CH_3)_3$), 202 (MH_2^+-CHO-$2CH_3$-$C(CH_3)_3$); HRMS calcd for $C_{23}H_{24}O$ (M+): 316.1827, found: 316.1823.

The CPD form of 112

The opening of **112** followed the general procedures for photo opening and closing described above.

^{1}H NMR ($CDCl_3$, 360MHz) δ 9.79 (s, 1 H, CHO), 7.20 (s, 2H, H-1, 3), 6.68 (s, 2H, H-6, 8), 6.36 (AB, J = 11.3 Hz, 2H, H-4, 10), 6.40 (AB, J = 11.3 Hz, 2H, H-5, 9), 1.56 and 1.48 (s, 3H each, CH_3), 1.24 (s, 9H, $C(CH_3)_3$); ^{13}C NMR ($CDCl_3$, 90.6 MHz) δ 191.97, 154.47, 152.96, 138.25, 138.06, 133.42, 131.47, 122.78, 34.34, 31.37, 20.79, 19.54.

Oxygen adduct 132

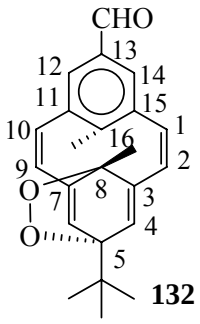

132

The non-degassed NMR sample of **112** was placed in an cold water bath and irradiated with a 500-W tungsten lamp with use of a 490-nm filter such that the sample was irradiated with visible light of >490 nm wavelength. The conversion to oxygen adduct **132** was complete after 40 minutes of irradiation. ^{1}H NMR (-20 °C, $CDCl_3$, 500MHz) δ 9.66 (s, 1H, 13-CHO), 7.20 (d, *J* = 11.2 Hz 2H, H-1,10), 6.27 (d, *J* = 0.8 Hz, 2H, H-4,6), 6.07 (dd, *J* = 11.2 Hz, 1.1 Hz, 2H, H-2,9), 1.99 (s, 3H, 16-CH_3), 1.02 (s, 9H, 5-$C(CH_3)_3$), 0.06 (s, 3H, 8-CH_3); ^{13}C NMR ($CDCl_3$, 125.7 MHz) δ 190.81 (CHO), 152.96 (C-3,7), 145.64 (C-16), 142.14 (C-11,15), 134.92 (C-13), 132.48 (C-4,6), 131.89 (C-2,9), 130.90 (C-1,10), 127.00 (C-12,14), 83.61 (C-5), 83.47 (C-8), 33.35 ($\underline{C}(CH_3)_3$), 25.41 ($C(\underline{C}H_3)_3$), 24.08 (5-CH_3), 13.52 (8-CH_3). The adduct **132** is very unstable and no other data was obtained.

Bis-4, 4′-(2,7-di-*tert*-butyl-10b, 10c-dimethyl-dihydropyrenyl) methanol 116

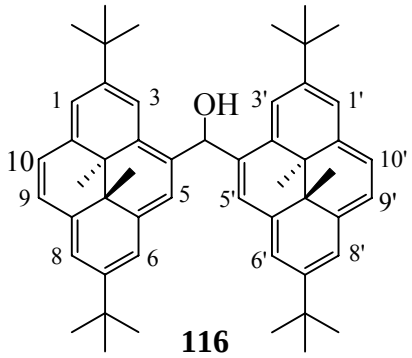

116

n-BuLi (0.48 mmol, 0.30 mL of 1.6M solution in hexane) was added to a solution of Bromo-DHP **109** (200 mg, 0.472 mmol) in THF (10 mL) at -78 ^{o}C under argon. The color of the solution changed from green to dark green instantaneously. The cooling bath was removed after 3 minutes; and the solution was stirred at room temperature for a further 5 minutes and then methyl formate (0.120 mL of 1.95 M solution in THF, 0.234

mmol) was added slowly by syringe. The resulting mixture was stirred at room temperature for an hour. Methanol (1 mL) was then added and stirring was continued for 10 minutes. Hexane (20 mL) was then added and the solution was washed repeatedly with cold water (10x 50 mL). The organic layer was then dried over anhydrous Na_2SO_4 and the solvent was removed to give a solid residue, which was chromatographed over deactivated alumina (5% water). After elution of the parent DHP **35** (19 mg) by hexanes, the desired product **116** was eluted by dichloromethane : hexanes (1:1) as a green crystalline solid (140 mg 83%), mp 166-167 °C; ^{1}H NMR (C_6D_6, 500MHz) δ 9.42-9.22 (4H, aromatic H), 8.82-8.78 (m, 1H, HCOH), 8.61-8.34 (m, 10H, aromatic H), 1.56-1.45 (8 peaks, 36H, -C(CH_3)$_3$), -3.46 to -3.69 (8 peaks, 12H, internal CH_3); ^{13}C NMR (C_6D_6, 125.7MHz) δ 146.37, 146.35, 146.32, 145.89, 145.79, 145.76, 145.61, 138.04, 137.95, 137.92, 137.90, 137.74, 137.72, 137.51, 137.49, 137.33, 137.32, 137.16, 137.09, 137.03, 136.44, 136.34, 133.24, 132.85, 132.71, 132.42, 124.03, 124.00, 123.97, 123.95, 123.85, 123.81, 123.76, 123.69, 123.60, 1233.41, 122.58, 122.52, 122.31, 121.76, 121.75, 121.68, 121.67, 121.60, 121.49, 117.79, 117.13, 117.09, 72.46 & 71.97 & 71.12(HCOH), 36.68, 36.65, 36.59, 36.27, 36.24, 36.21; 32.51, 32.49, 32.26, 32.24; 31.40, 31.36, 31.27, 31.24, 30.81, 30.78, 30.77, 30.73; 15.65, 15.49, 15.39, 15.35, 15.26, 15.17, 15.00, 14.69; IR (Thin film on NaCl plate) 3584, 3434, 3039, 2962, 2866, 1596, 1461, 1360, 1231, 887, 739, 674 cm^{-1}; UV-Vis (cyclohexane) λ_{max} (ε_{max}) nm 342 (11,200), 391 (5,500), 482 (1,700), 650 (210); EI MS *m*/*z* 717 (M^+), 701 (MH^+-OH), 685 (M^+-OH-CH_3), 597, 555; HRMS calcd for $C_{53}H_{64}O$: 716.4957, found: 716.4969.

Bis-4, 4′-(2,7-di-*tert*-butyl-*trans*-10b, 10c-dimethyl-dihydropyrenyl) ketone 117

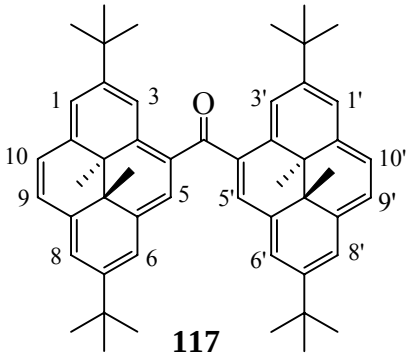

117

Method A: Alcohol **116** (50 mg, 0.07 mmol) was added to a suspension of pyridinium dichromate (PDC, 50 mg, 0.13 mmol) in dry CH_2Cl_2 (20 mL) at room temperature (20 °C) under argon. The mixture was allowed to stir for 3 h and then was filtered through the Celite, which was washed by CH_2Cl_2 until the filtrate stream was colorless. The filtrate was then evaporated and gave the solid product, which then was chromatographed over a deactived silica gel using hexanes/ CH_2Cl_2 (3:1) as eluant. The first brownish green band was collected and dried to yield the brown crystalline product (39 mg 78%).

Method B: Dry THF (100 mL) was added to vacuum dried bromo-DHP **109** (500 mg 1.45 mmol) using a syringe under the argon atmosphere. The resulting solution was cooled using a dry ice-acetone bath. A solution of *n*-BuLi (0.95 mL of 1.6M solution in hexane, 1.52 mmol) was added to the cold solution. The green color of the solution changed to dark green instantaneously. The dry ice-acetone bath was removed after 3 minutes, and then the solution was stirred at room temperature (20 ^{o}C) for 5 minutes. Dimethyl carbonate (0.76 mL of 0.95 M solution in dry THF, 0.722 mmol) was then added to the solution by syringe. Then the mixture was allowed to stir for one hour at room temperature (20 °C) and one hour at 50 °C. Methanol (1 mL) was then added and

stirred for 10 minutes to quench the reaction. Hexanes (200 mL) were added to the reaction mixture and the solution was washed repeatedly with cold water (3 x 50 mL). The organic layer was then dried over anhydrous Na_2SO_4 and the solvent was removed using a rotary evaporator to give the solid product. The solid was chromatographed using deactivated silica gel (5% water). Hexane eluted first DHP **35** (50 mg) and then the desired product **117** was eluted with dichloromethane : hexanes (1:2) to give the brown crystalline product **117** as a mixture of two isomers (420 mg, 82%), mp 208-209 °C; ^{1}H NMR (C_6D_6, 500 MHz) δ 10.29 and 10.27 (d, *J* = 1.2 Hz, 2H, H-3,3'), 8.99 and 8.98 (s, 2H, H-5,5') 8.73 and 8.72 (d, *J* = 1.6 Hz, 2H, H-1,1'), 8.593 and 8.590 (d, *J* = 1.6 Hz, 2H, H-8,8'), 8.52 (s, 4H, H9,9', H-10,10'), 8.323 and 8.315 (s, 2H, H-6,6') , 1.62 and 1.61 (s, 18H, 2,2'-C(CH_3)$_3$), 1.39 and 1.38 (s, 18H, 7,7'-C(CH_3)$_3$), -3.28 (12H, 10b,10b'-CH_3), -3.33 and -3.35 (12H, 10c,10c'-CH_3); ^{13}C NMR (C_6D_6, 125.7MHz) δ 202.30 and 201.97 (<u>C</u>O), 149.93 and 149.87 (C-2,2'), 146.44 (C-7,7'), 139.64 and 137.60 (C-10a,10a'), 137.41 and 137.40 (C-8a,8a'), 137.00 and 136.98 (C-3a,3a'), 135.30 and 135.28 (C-5a,5a'), 134.05 and 134.01 (C-4,4'), 126.46 and 126.43 (C-5,5'), 125.35 (C-9,9'), 124.44 (C-10,10'), 123.80 (C-6,6'), 123.34 (C-8/8'), 123.33 (C-1,1'), 123.30 (C-8'/8), 121.49 and 121.42 (C-3,3'), 36.97 (2,2'-<u>C</u>(CH_3)$_3$), 36.13 (7,7'-<u>C</u>(CH_3)$_3$), 32.32 (2,2'-C(<u>C</u>H_3)$_3$), 32.06 (7,7'-C(<u>C</u>H_3)$_3$), 31.83 and 31.79 (C-10b,10b'), 30.52 and 30.51 (C-10c,10c'), 15.74 (10b,10b'-CH_3), 15.54 (10c,10c'-CH_3); IR (Thin film on NaCl plat) 3038, 2962, 2866, 1673, 1593, 1460, 1344, 1192, 889, 667 cm^{-1}; UV-Vis (cyclohexane) λ_{max} (ε_{max}) nm 344.9 (86,200), 405 (49,800), 485 (15,900), 660 (3,540); EI MS *m*/*z* 715 (M^+), 700 (M^+-CH_3), 685 (M^+-2CH_3), 643 (M^+-C(CH_3)$_3$-CH_3); HRMS calcd for $C_{53}H_{62}O$: 714.4801, found: 714.4869.

The CPD forms (two isomers) for 117:

The opening of **117** followed the general procedures for photo opening and closing described above.

^{1}H NMR (THF-d8, 300MHz) δ 7.30-7.22 (m, 2H), 7.01-6.91 (m, 2H), 6.86-6.72 (m, 2H), 6.70-6.58 (m, 4H), 6.46-6.36 (m, 2H), 6.28 (s, 2H), 1.44 and 1.43 (3H total), 1.35 (3H), 1.25 (3H), 1.24 and 1.22 (18H), 1.21 and 1.17 (18H), 0.72 (3H); ^{13}C NMR (THF-d8, 75.0MHz) δ 151.47, 147.69, 142.49, 140.76, 138.94, 138.83, 138.71, 133.66, 133.22, 133.17, 125.67, 125.51, 124.91, 124.77, 124.10, 123.88, 123.81, 123.61, 34.77, 34.70, 31.63, 31.53, 20.19, 19.92, 19.69, 19.62.

Bis-4,4'-(2,7-bis-(tert-butyl)-12c,12d-dimethyl-12c,12d-benzo[e]dihydropyrenyl) methanol 118

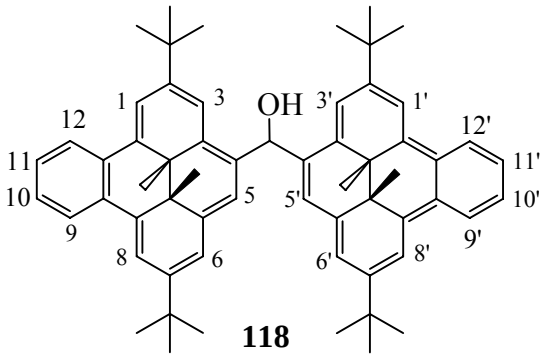

118

n-BuLi (0.3 mL 1.6 M solution in hexane, 0.48 mmol) was added to a solution of Bromo-BDHP **111** (200 mg, 0.422 mmol). The red color of the solution darkened instantaneously. The dry ice-acetone bath was removed after 3 minutes and then the solution was stired at room temperature (20 ^{o}C) for a further 5 minutes. The reaction mixture was recooled by dry ice-acetone and then methyl formate (0.108 mL 1.95 M solution in THF, 0.211 mmol) was added slowly by syringe. Then the mixture was

allowed to stir for one hour at room temperature (20 °C) and one hour at 50 °C. Methanol (1 mL) was then added and stirred for 10 minutes to quench. Hexane (20 mL) was then added to the reaction mixture and the solution was washed repeatedly with cold water (10x 50 mL). The organic layer was then dried over anhydrous Na_2SO_4 and the solvent was removed using a rotary evaporator to give the solid product. The solid was chromatographed using deactivated alumina (5% water). After elution of BDHP **36** (56 mg) by hexanes, the desired product was eluted with dichloromethane : hexanes (1:1) as a red crystalline solid (82 mg, 47.5%), mp 185-188 °C; ^{1}H NMR (CD_2Cl_2, 500 MHz) δ 8.81-8.71 (m, 4H), 8.36-8.23 (s, 4H), 7.97 and 7.95 (s, 1H total), 7.83 and 7.79 (s, 1H total), 7.68-7.56 (m, 6H), 7.45 and 7.44 (s, 1H total), 7.31 and 7.27 (s, 1H total), 1.50, 1.47, 1.44, 1.43 and 1.35 (s, 36H total $C(CH_3)_3$), -1.42, -1.470, -1.475, -1.56, -1.58, -1.59, -1.64 and -1.75 (s, 8 peaks, 12H total, CH_3);

Bis-4,4′-(2,7-di-tert-butyl-*trans*-12c,12d-dimethyl-12c,12d-benzo[e]dihydropyrenyl) ketone 119

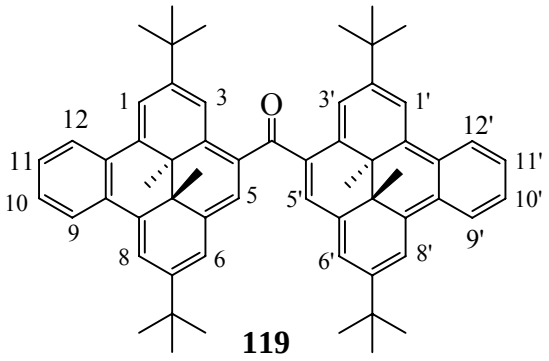

119

Bromo-BDHP **111** (200 mg, 0.422 mmol) was added to a two neck-flask with a stir bar and was dried under vacuum. THF (50 mL) was then added using a syringe under an argon atmosphere. The resulting solution was cooled using a dry ice-acetone bath. *n*-

BuLi (0.3 mL 1.6 M solution in hexane, 0.48 mmol) was then added. The red color of the solution darkened instantaneously. The dry ice-acetone bath was removed after 3 minutes, and the solution was stirred at room temperature (20 ^{o}C) for 5 minutes. The reaction mixture was then recooled by a dry ice-acetone bath, and dimethyl carbonate (0.22 mL of 0.95 M solution in dry THF, 0.209 mmol) was added to the solution by syringe. Then the mixture was allowed to stir for one hour at room temperature (20 °C) and one hour at 50 °C. The presence of the product was indicated by TLC. Methanol (1 mL) was added and stirred for 10 minutes to quench. Hexane (100 mL) was added to the reaction mixture and the solution was washed repeatedly with cold water (3 x 50 mL). The organic layer was dried over anhydrous Na_2SO_4 and the solvent was removed to give a solid residue, which was chromatographed over deactivated alumina (5% water). After elution of benzoDHP **36** (26 mg) by hexanes, the desired product **119** was eluted with dichloromethane : hexanes (1:1) to give a red crystalline product (135 mg, 78%), as a mixture of two isomers, mp 171-172 °C; ^{1}H NMR (CD_2Cl_2, 500 MHz) δ 8.85-8.79 (m, 4H, H-10,10',11,11'), 8.42 and 8.41 (d, J = 1.3 Hz, 2H, H-1,1'), 8.34 and 8.33 (d, J = 1.3 Hz, 2H, H-8,8'), 8.302 and 8.297 (d, J = 1.2 Hz, 2H, H-3,3'), 7.69-7.67 (m, 4H, H9,9',12,12'), 7.27 and 7.25 (d, J = 0.6 Hz, 2H, H-5,5'), 7.24 and 7.22 (d, J = 1.0 Hz, 2H, H-3,3'), 1.48 and 1.46 (s, 18H, 2,2'-C$(CH_3)_3$), 1.44 (s, 18H, 7,7'-C$(CH_3)_3$), -1.278, -1.284, -1.333, and -1.352 (12H, 12c,12c',12d,12d'-CH_3); ^{13}C NMR (CD_2Cl_2, 125.7 MHz) δ 200.79 and 200.73 (CO), 149.93 and 149.85 (C-7,7'), 145.97 (C-2,2'), 140.95 and 140.77 (C-3a,3a'), 137.61 and 137.57 (C-12b,12b'/12e,12e'), 137.36 (C-5a,5a'), 135.26 (C-12e,12e'/12b,12b'), 132.49 and 132.34 (C-4,4'), 130.15 (C-12f,12f'), 129.79 (C-12a,12a'), 127.00 (C-10,10'/11,11'), 126.67 (C-11,11'/10,10'), 125.35 (C-9,9'/12,12'),

125.05 (C-12,12'/9,9'), 121.93 and 121.90 (C-5,5'), 120.72 and 120.70 (C-6,6'), 118.35 and 118.33 (C-8,8'), 117.78 and 117.74 (C-1,1',3,3'), 37.17 and 37.16 (12c,12c'-$\underline{C}H_3$), 36.56 (2,2'-$\underline{C}(CH_3)_3$), 35.85 (7,7'-$\underline{C}(CH_3)_3$), 35.77 and 35.76 (C-12d,12d'), 30.88 and 30.87 (7,7'-C($\underline{C}H_3)_3$), 30.81 (2,2'-C($\underline{C}H_3)_3$), 18.18, 18.04 and 18.00 (12c,12c',12d,12d'-$\underline{C}H_3$); IR (thin film on NaCl) 3057, 2962, 2924, 2865, 1642, 1476, 1465, 1371, 1361, 1256, 873, 755 cm^{-1}; UV-Vis (cyclohexane) λ_{max} (ε_{max}) nm 311 (29,500), 325 (30,200), 339 (31,500), 407 (51,100), 514 (10,900); EI MS *m*/*z* 815 (M^+), 799 (M^+-O), 743 (M^+-$C(CH_3)_3$-CH_3), 538, 482; HRMS calcd for $C_{61}H_{66}O$: 814.5114, found: 814.5104.

The CPD forms (two isomers) for 119:

The opening of **119** followed the general procedures for photo opening and closing described above.

^{1}H NMR (THF-d8, 300 MHz) δ 7.69-7.65 (m, 2H), 7.60-7.50 (m, 2H), 7.43-7.38 (m, 4H), 7.32-7.28 (m, 2H), 7.16-7.09 (m, 2H), 6.96-6.94 (m, 2H), 6.89-6.83 (m, 2H), 6.80-6.71 (m, 2H), 1.27 and 1.26 (s, 21 H total), 1.21 and 1.19 (s, 18H), 1.17 (s, 3H), 0.58 (s, 3H); ^{13}C NMR (THF-d8, 75.0MHz) δ 196.95 (CO), 152.28, 151.39, 151.12, 151.04, 147.15, 145.06, 144.79, 144.57, 143.95, 142.56, 141.94, 141.81, 141.69, 140.90, 140.77, 140.39, 139.15, 138.84, 137.20, 137.14, 136.56, 130.57, 130.35, 129.69, 129.60, 129.41, 129.29, 129.23, 129.19, 125.72, 125.61, 124.56, 123.99, 35.12, 34.95, 34.86, 31.78, 31.75, 31.66, 30.81, 19.79, 19.53, 19.50.

4-Carboethoxy-2,7-di-*tert*-butyl-*trans*-10b,10c-dimethyl-10b,10c-dihydropyrene 120

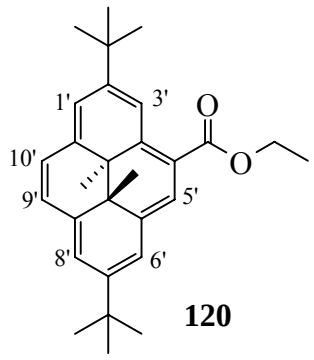

120

n-BuLi (1.0 mL of 1.6M solution in hexane, 1.6 mmol) was added to a solution of bromo-DHP **109** (656 mg, 1.55 mmol) in THF (100 mL) at -78 °C under argon. The color of the solution changed from green to dark green instantaneously. The cooling bath was removed after 3 minutes, and then the solution was stirred at room temperature for a further 5 minutes and then ethyl chloroformate (1.0 mL of 2 M solution in dry THF, 2.0 mmol) was added by syringe. The resulting mixture was stirred at 20°C for 1 h. Methanol (1 mL) was then added and the stirring was continued for another 10 min. Hexane (200 mL) was then added and the solution was washed well with cold water. The organic layer was then dried over anhydrous Na_2SO_4 and evaporated to give a solid residue, which was chromatographed over silica gel (60-200 mesh, deactivated with 5% water). Hexane eluted the parent DHP **35** (50 mg), and then dichloromethane:hexanes (2:1) eluted the product **120** as a green crystals (560 mg, 87%), mp 162-163 °C; ^{1}H NMR δ 9.90 (d, J = 1.1 Hz, 1H, H-3), 9.14 (s, 1H, H-5), 8.64 (s, 1H, H-6), 8.56 (s, 2H, H-1,8), 8.53 (AB, J = 7.9 Hz, 1H, H-9), 8.46 (AB, J = 7.9 Hz, 1H, H-10), 4.634 and 4.643 (dq each, J = 10.8, 7.2 Hz, 2H, C$\underline{H}_2$CH$_3$), 1.71 (s, 9H, 2-C(CH$_3$)$_3$), 1.67 (s, 9H, 7-C(CH$_3$)$_3$), 1.61 (t, J = 7.2 Hz, 3H, CH$_2$C$\underline{H}_3$), -3.93 (s, 3H, 10c-CH$_3$), -3.94 (s, 3H, 10b-CH$_3$), ^{13}C NMR δ 169.09 (CO), 150.08 (C-7), 146.02 (C-2), 139.91 (C-10a), 137.55 (C-3a), 136.69 (C-8a), 134.82

(C-5a), 125.25 (C-9), 124.83 (C-5), 123.54 (C-6), 123.15 (C-8), 121.40 (C-1), 119.95 (C-3), 118.70 (C-4), 61.04 ($\underline{C}H_2CH_3$), 36.81 (2-$\underline{C}(CH_3)_3$), 36.10 (7-$\underline{C}(CH_3)_3$), 32.13 (2-C($\underline{C}H_3)_3$), 32.08 (7-C($\underline{C}H_3)_3$), 31.35 (C-10b), 29.23 (C-10c), 15.11 (10b/10c-$\underline{C}H_3$), 14.94 ($CH_2\underline{C}H_3$), 14.63 (10c/10b-$\underline{C}H_3$); IR (film) ν 1698, 1595, 1455, 1384, 1233, 1215, 885, 739, 674 cm^{-1}; EI MS *m/z* 416 (M^+); HRMS calcd for $C_{29}H_{36}O_2$: 416.2715, found: 416.2711; Anal. Calcd for $C_{29}H_{36}O_2$: C, 83.61%; H, 8.71%; Found: C, 83.75%; H, 8.72%.

4-Carboethoxy-2,7-di-*tert*-butyl-*trans*-12c,12d-dimethyl-12c,12d-dihydrobenzo[e]pyrene 121

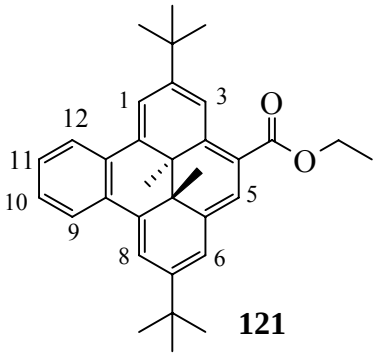

121

n-BuLi (0.2 mL of 2.2 M solution in hexane, 0.44 mmol) was added to a solution of bromo-BDHP **111** (200 mg, 0.42 mmol) in THF (100 mL) at -78 °C under argon. The color of the solution changed from green to dark green quickly. The cooling bath was removed after 3 min and the solution was stirred at 20°C for a further 5 min and then ethyl chloroformate (0.22 mL of 2 M solution in dry THF, 0.44 mmol) was added by syringe. The mixture was then stirred at 20°C for 1 h. Methanol (1 mL) was then added and the stirring was continued for 10 min. Hexane (200 mL) was then added and the solution was washed well with cold water. The organic layer was then dried over anhydrous Na_2SO_4 and evaporated to give a solid residue, which was chromatographed

over silica gel (60-200 mesh, deactivated with 5% water). Hexane eluted the parent benzodihydropyrene **36** (~15 mg) and then dichloromethane:hexanes (2:1) eluted the desired product **121** as dark purple crystals (150 mg, 80%), mp 173-174 °C; ^{1}H NMR ($CDCl_3$, 500 MHz) δ 8.84 (d, *J* = 1.3 Hz, 1H, H-3), 8.75-8.71 (m, 2H, H-9,12) 8.32 (d, *J* = 1.3 Hz, 1H, H-1), 8.25 (d, *J* = 1.3 Hz, 1H, H-8), 7.67 (d, *J* = 0.9 Hz, 1H, H-5), 7.66-7.60 (m, 2H, H-10,11), 7.38 (~t, *J* = ~1.1 Hz, 1H, H-6), 4.46 and 4.45 (dq each, *J* = 10.7, 7.2 Hz, 2H total, C$\underline{H}_2$CH$_3$), 1.53 (s, 9H, 2-C(CH$_3$)$_3$), 1.49 (t, *J* = 7.2 Hz, 3H, CH$_2$C$\underline{H}_3$), 1.48 (s, 9H, 7-C(CH$_3$)$_3$), -1.42 (s, 3H, 12d-CH$_3$), -1.47 (s, 3H, 12c-CH$_3$), ^{13}C NMR δ 168.04 (CO), 150.57 (C-2), 145.05 (C-7), 144.33 (C-3a), 138.36 (C-12b), 136.85 (C-12e), 134.64 (C-5a), 129.92 (C-12f), 129.28 (C-12a), 126.78 and 126.25 (C-10,11), 124.96 (C-12), 124.58 (C-9), 121.43 (C-5), 120.72 (C-6), 119.63 (C-4), 118.05 (C-8), 117.56 (C-3), 116.96 (C-1), 60.77 ($\underline{C}$H$_2$CH$_3$), 37.69 (C-12c), 36.49 (7-$\underline{C}$(CH$_3$)$_3$), 35.54 (2-$\underline{C}$(CH$_3$)$_3$), 34.99 (C-12d), 30.78 and 30.76 (2,7-C($\underline{C}$H$_3$)$_3$), 18.24 (12d-$\underline{C}$H$_3$), 17.66 (12c-$\underline{C}$H$_3$), 14.80 (CH$_2\underline{C}$H$_3$); IR (film) ν 1702, 1698, 1694, 1619, 1475, 1368, 1251, 1222, 1203, 1164, 908, 755, 733 cm^{-1}; EI MS *m*/*z* 466 (M$^+$); HRMS calcd for $C_{33}H_{38}O_2$: 466.2872, found: 466.2865.

[4-(2,7-Di-*tert*-Butyl-*trans*-12c, 12d-dimethyl-12c,12d-benzo-[e]-dihydropyrenyl)] [4'-(2',7'-di-*tert*-Butyl-*trans*-10b',10c'-dimethyl-10b',10c'-dihydropyrenyl)] ketone 122

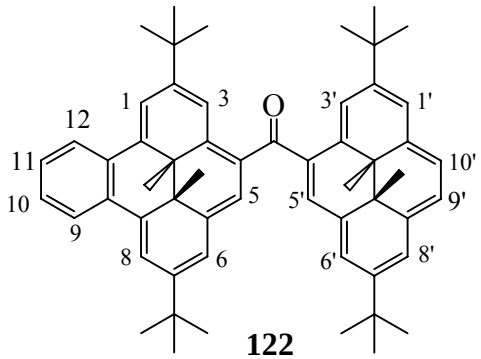

122

n-BuLi (0.24 mmol, 0.11 mL of 2.2 M solution in hexane) was added by syringe at -78 °C to a stirred solution of bromo-BDHP **111** (100 mg, 0.21 mmol) in THF (100 mL) under argon. The red color of the solution darkened instantaneously. The cooling bath was removed and the solution was stirred at room temperature for 10 minutes. The solution was cooled to -78 °C again and DHPCOOEt **120** solution (85 mg in 10 mL THF, 0.20 mmol) was quickly added through an addition funnel. The resulted mixture was stirred at -78 °C for 20 minutes and then warmed up to 20 °C for 1 h and 50 °C for 1h. Methanol (1 mL) was added and the solution was filtered through celite. Then solvent was removed to give a reddish brown solid, which was chromatographed on silica gel (5% water deactivated) with hexane / CH_2Cl_2 (3:1). Eluted first was BDHP **36** (10 mg) and then product **122** as a reddish brown solid (120 mg, 77 %), a mixture of two isomers, mp 132-133 °C; ^{1}H NMR (CD_2Cl_2, 500 MHz) δ 9.51 and 9.50 (d, J = 1.3 Hz, 1H, H-3'), 8.86 to 8.82 (m, 2H, H-9,12), 8.67 (s, 1H, H-1'), 8.640 and 8.627 (s, 1H, H-5'), 8.624 (s, 1H , H-8), 8.59 (AB, J = 7.9 Hz, 1H, H-9'), 8.56 (AB, J = 7.9 Hz, 1H, H-10'), 8.46 and 8.45 (s, 1H, H-6'), 8.428 and 8.421 (s, 1H, H-1), 8.35 (s, 1H, H-8), 8.310 and 8.304 (d, J

= 1.2 Hz, 1H, H-3), 7.72 to 7.67 (m, 2H, H-10,11), 7.24 and 7.23 (s, 1H, H-5), 7.15 (s, 1H, H-6), 1.69 and 1.68 (s, 9H, 2'-C(CH_3)$_3$), 1.62 an 1.61 (s, 9H, 7'-C(CH_3)$_3$), 1.420, 1.414, 1.412, 1.409 (s, 18H, 2, 7-C(CH_3)$_3$)), -1.175 and -1.183 (s, 3H, 12c-CH_3), -1.240 and -1.264 (s, 3H, 12d-CH_3), -3.755 and -3.757 (s, 3H, 10b'-CH_3), -3.78 and -3.80 (s, 3H, 10c'-CH_3); ^{13}C NMR (CD_2Cl_2, 125.7 MHz) δ 202.07 and 201.79 (CO), 149.99 and 149.91 (C-2'), 149.57 (C-2/7), 146.75 (C-7'), 145.95 (C-7/2), 140.75 and 140.64 (C-3a), 139.55 and 139.51 (C-10a'), 137.44 (C-12b), 137.28 and 137.24 (C-8a'), 137.17 (C-5a or C-12e), 136.20 and 136.12 (C-3a'), 135.26 (C-5a'), 135.21 (C-12e/5a), 133.34 and 133.24 (C-4), 132.35 and 132.29 (C-4'), 130.16 (C-12f), 129.80 (C-12a), 126.98, 126.67 (C-10,11), 125.36, 125.26 (C-9,12), 125.12 (C-9'), 125.08 (C-5'), 124.15 (C-10'), 123.44 (C-6'), 123.33 and 123.27 (C-8'), 122.40 (C-5), 122.06 and 122.03 (C-1'), 120.68 (C-6), 120.35 and 120.20 (C-3'), 118.32 (C-8), 117.93 (C-3), 117.78 (C-1), 37.20 and 37.18 (C-12c), 36.96 (2'-C(CH_3)$_3$), 36.49 (2-C(CH_3)$_3$), 36.36 (7'-C(CH_3)$_3$), 35.82 (C-12d and 7-C(CH_3)$_3$), 32.18 (2'-C(CH_3)$_3$), 32.11 (7'-C(CH_3)$_3$), 31.25 and 31.22 (C-10b'), 30.83 and 30.79 (2, 7-C(CH_3)$_3$), 29.98 (C-10c'), 18.23 and 18.06 (12c, 12d-CH_3), 15.19, 15.13 and 15.08 (10b', 10c'-CH_3); IR (thin film on NaCl plate) 3044, 2962, 2866, 1644, 1463, 1361, 1255, 1199, 887, 739 cm^{-1}; UV (cyclohexane) λ_{max} (ε_{max}) nm 345 (51,500), 405 (44,000), 493 (12,200), 660 (2,3000); EI MS *m*/*z* 764 (M^+), 749 (M^+-CH_3), 693 (MH^+-CH_3-C(CH_3)$_3$); HRMS calcd for $C_{57}H_{64}O$: 764.4957, found: 764.4985.

Open-closed forms (two isomers) 122'

The opening of **122** followed the general procedures for photo opening and closing described above.

^{1}H NMR (THF-d8, 300MHz) δ 9.39 and 9.33 (s, 1H total), 8.74 and 8.68 (s, 1H total), 8.66 (s, 1H), 8.60 and 8.58 (s, 1H), 8.53 (broad) and 8.52 (s, 2H), 8.50 (s, 1H); 7.70-7.66 (m, 1H), 7.59-7.52 (m, 2H), 7.49-7.30 (m, 2H), 7.16-7.13 (m, 1H), 7.03-7.02 (m 1H), 6.91-6.77 (m, 1H), 6.74-6.71 (m, 1H), 1.74 (s, 9H), 1.63 and 1.62 (s, 9H total), 1.35 and 1.33 (s, 12H total), 0.93 and 0.79 (s, 9H total).

Open form (two sides opened) 122" (two isomers):

^{1}H NMR (THF-d8, 300 MHz) δ 7.67-7.47 (m, 2H), 7.41-7.34 (m, 2H), 7.31-7.23 (m, 2H), 7.17-7.04 (m, 2H), 6.89-6.87 (m, 2H), 6.83-6.78 (m. 2H), 6.71-6.64 (m, 2H), 6.48-6.24 (two AB patterns for two isomers from H1',2', total 2H, 6.46 and 6.41, AB, *J* = 11.2; 6.30 and 6.27, AB *J* = 10.4 Hz), 1.51-0.52 (48H, all methyls and t-butyls); ^{13}C NMR (THF-d8, 75.0 MHz) δ 152.41, 152.03, 151.31, 151.18, 150.92, 147.69, 147.05, 144.71, 144.45, 142.63, 142.18, 141.73, 140.74, 139.14, 138.78, 138.05, 137.22, 136.45, 133.87, 133.66, 133.23, 130.49, 130.21, 129.60, 129.51, 129.44, 129.28, 129.13, 129.04, 125.76, 125.56, 125.35, 124.89, 124.82, 124.40, 124.14, 123.92, 123.78, 123.92, 35.00, 34.76, 32.30, 32.10, 31.67, 31.55, 30.70, 20.20, 19.93, 19.87, 19.74, 19.70, 19.50, 19.41, 19.27.

Bis-4, 4′-(2,7-di-*tert*-butyl-*trans*-10b, 10c-dimethyl-dihydropyrenyl) methane 123

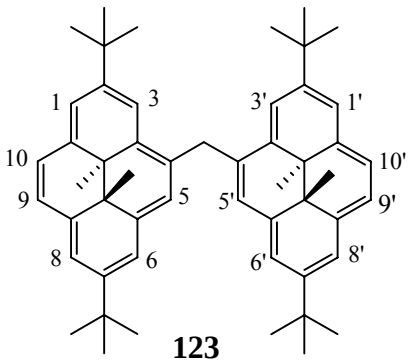

123

Method A: alcohol **116** (50 mg, 0.07 mmol) was added a suspension of $NaBH_4$ (5.5 mg, 0. 15 mmol) in dry THF (50 mL) under argon. The mixture was cooled to 0 °C and then BF_3·OEt_2 (270 μL, containing BF_3 48% ~52% by wt, ~2.2 mmol) was added dropwise. The ice bath was removed and then the mixture was allowed to stir for a further 2 h at room temperature (20 °C). Hexane (100 mL) was added to the reaction mixture and the solution was washed well with cold water (4 x 50 mL), dried over anhydrous Na_2SO_4 and evaporated to give a green crystalline solid. The solid was chromatographed over deactivated alumina (5% water) with hexane as eluant to yield the desired product **123** as a green crystalline solid (42 mg, 86 %).

Method B: alcohol **116** (50 mg, 0.07 mmol), cyclohexene (10 mL, mmol), Pd/C (15 mg), $AlCl_3$ (25 mg, mmol) and dry THF (50 mL) were refluxed for 36 h under argon. Hexane (100 mL) was added to the reaction mixture, which was filtered through Celite and washed by THF: hexanes 1:1 until the color is diminished. The solvent was removed by a rotary evaporator to give a green crystalline solid. The solid was chromatographed over deactivated alumina (5% water) with hexane as eluant to yield the desired product as a mixture of two isomers as a green crystalline solid (39 mg, 80 %), mp 198-199 °C; ^{1}H NMR ($CDCl_3$, 500 MHz) δ 9.042 and 9.035 (d, *J* = Hz, 2H, H-3,3'), 8.60 and 8.59 (s, 2H, H-5,5'), 8.408 and 8.405 (s, 2H, H-8,8'), 8.39 and 8.38 (d, *J* = 0.7 Hz, 2H, H-1,1'), 8.32-8.31 (6H, H-6,6',9,9',10,10'), 5.96(**123A**) (s, CH_2, **123A**), 6.01 and 5.91 (both AB, *J* = 15.5 Hz, CH_2, **123B**), 1.601 and 1.597 (s, 18H, 7,7'-$C(CH_3)_3$), 1.49 and 1.48 (s, 18H, 2,2'-$C(CH_3)_3$), -3.939, -3.944, -3.948 and -3.975 (12H, CH_3); ^{13}C NMR (C_6D_6, 125.7 MHz) δ 145.83 (C-7,7'), 144.98 and 144.94 (C-2,2'), 137.12, 137.00, 136.80 and 136.77 (C-5a,5a',8a,8a',10a,10a'), 133.90 (C-4,4'), 133.24 and 133.17 (C-3a,3a'), 126.21 and

126.16 (C-5,5'), 122.86 and 122.84 (C-10,10'), 122.50 (C-9,9'), 120.80 and 120.78 (C-1,1'), 120.51 (C-6,6'), 123.35 (C-8,8'), 118.11 (C-3,3'), 38.70 and 38.50 ($\underline{C}H_2$), 36.26 (2,2'-$\underline{C}(CH_3)_3$), 36.07 (7,7'-$\underline{C}(CH_3)_3$), 32.20 (2,2'-C($\underline{C}H_3)_3$), 32.09 (7,7'-C($\underline{C}H_3)_3$), 30.47 and 30.45 (C-10b,10b'), 30.09 and 30.08 (C-10c,10c'), 14.99, 14.69 and 14.65 (10b,10b',10c,10c'-CH_3); IR (thin film on NaCl) 3036, 2962, 2923, 2904, 2865, 1596, 1460, 1360, 1231, 884, 740, 671 cm^{-1}; UV-Vis (cyclohexane) λ_{max} (ε_{max}) nm 343 (11,500), 393 (5,500), 483 (1,700), 651 (200); EI MS *m*/*z* 701 (M^+), 686 (M^+-CH_3), 671 (M^+-2CH_3), 598 (M^+-2C$(CH_3)_3$-2CH_3), 327, 285; HRMS calcd for $C_{53}H_{64}$: 700.5008, found: 700.5004.

Bis-4, 4′-(2,7-di-tert-butyl-*trans*-12c, 12d-dimethyl-12c,12d-benzo-[e]-dihydropyrene) methane 124

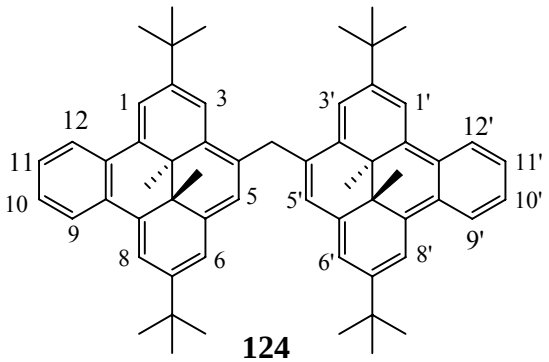

124

Bis-benzoDHP **119** (40 mg, 0.048 mmol) was added to the suspension of $NaBH_4$ (7.0 mg, 0.19 mmol) in dry THF (20 mL) under argon. The mixture was cooled to 0 °C and then $BF_3{\cdot}OEt_2$ (200 μL, containing BF_3 48% ~52% by wt, 1.6 mmol) was added drop wise. The ice bath was removed and then the mixture was allowed to stir for further 2 h at room temperature (20 °C). Hexane (50 mL) was added to the reaction mixture and the solution was washed well with cold water (4 x 30 mL), dried over anhydrous Na_2SO_4 and

evaporated to give the dark red crystalline solid, which was chromatographed over deactivated alumina (5% water) with hexane. The desired product **124** was obtained a mixture of isomers as a dark red crystalline solid (14.6 mg, 74 %), mp 128-129 °C; ^{1}H NMR (C_6D_6, 500 MHz) δ 8.81-8.75 (m, 4H, H-9,12,9',12'), 8.44(**124A**) and 8.41(**124B**) (d, *J* = 1.1 Hz, 2H, H-1,1'), 8.37(**124A**) and 8.36(**124B**) (d, *J* = 1.3 Hz, 2H, H-8, 8'), 8.13(**124A**) and 8.09(**124B**) (d, *J* = 1.1 Hz, 2H, H-3,3'), 7.50-7.47 (m, 4H, H-10,11,10',11'), 7.46(**124A**) and 7.43(**124B**) (s, 2H, H-5,5'), 7.36(**124A**) and 7.35(**124B**) (s, 2H, H-6,6'), 4.83 (s, CH_2, **124A**), 5.00 and 4.64 (both AB, *J*= 15.3 Hz, CH_2 **124AB**), 1.44(**124A**) and 1.42(**124B**) (s, 18H, 2,2'-C(CH_3)$_3$), 1.33(**124A**) and 1.32(**124B**) (s, 18H, 7,7'-C(CH_3)$_3$), -1.13(**124B**), -1.16(**124B**), and -1.17(**124A**), -1.19(**124A**) (s, 12H, CH_3); ^{13}C NMR (C_6D_6, 125.7 MHz) δ 145.05 (C-7, 7'), 144.56(**124B**) and 144.50(**124A**) (C-2,2'), 138.95 (C-5a,5a'), 136.22(**124B**) and 136.14(**124A**) (C-12b,12b'), 136.05(**124B**) and 136.04(**124A**) (C-12e,12e'), 133.26(**124A**) and 133.09(**124B**) (C-3a,3a'), 132.19(**124B**) and 132.13(**124B**) (C-4,4'), 130.40 (C-12a,12a'), 130.19 (C-12f,12f'), 126.57 and 126.53 (C-10,11,10',11'), 126.28(**124B**) and 126.23(**124A**) (C-5,5'), 125.47 and 125.33 (C-9,12,9',12'), 120.67(**124A**) and 120.62(**124B**) (C-6,6'), 117.64(**124A**) and 117.61(**124B**) (C-1,1'), 117.60(**124B**) and 117.56(**124A**) (C-8,8'), 116.87(**124A**) and 116.72(**124B**) (C-3,3'), 37.01, 36.52 and 36.45 (C-12c,12c',12d,12d'), 36.26(**124A**) and 36.24(**124B**) (2,2'-<u>C</u>(CH_3)$_3$), 35.72(**124A**) and 35.709(**124B**) (7,7'-<u>C</u>(CH_3)$_3$), 35.49 (<u>C</u>H_2), 31.31(**124A**) and 31.29(**124B**) (2,2'-C(<u>C</u>H_3)$_3$), 30.98(**124B**) and 30.96(**124A**) (7,7'-C(<u>C</u>H_3)$_3$), 18.48, 18.38 and 18.33 (12c,12c'12d,12d'-<u>C</u>H_3); IR (thin film on NaCl) 3061, 2962, 2922, 2865, 1617, 1474, 1366, 1258, 754 cm^{-1}; UV (cyclohexane) λ_{max} (ε_{max}) nm 311(35,700), 324 (35,800), 341 (35,600), 379 (36,900, shoulder), 398 (47,800), 510

(10,300); EI MS *m*/*z* 801 (M^+), 786 (M^+-CH_3); HRMS calcd for $C_{61}H_{68}$: 800.5321, found: 800.5317.

Open forms (two isomers) 124":

The opening of **124** followed the general procedures for photo opening and closing described above.

^{1}H NMR (Acetone-d6, 300 MHz) δ 7.66-7.56 (m, 4H), 7.38-7.36 (m, 4H), 7.20-7.18 (m, 2H), 6.89-6.74 (m, 6H), 6.59 and 6.56 (s, 2H total, from two isomers), 4.34 and 3.68 (both AB, J = 14.7 Hz, CH_2 in unsymmetrical isomer), 4.15 (s, CH_2 in symmetrical isomer), 1.33 (s, 6H, CH_3), 1.29 (s, 6H, CH_3),1.24 and 1.23 (s, 18H, $C(CH_3)_3$), 1.22 (s, 18H, $C(CH_3)_3$); ^{13}C NMR (acetone-d6, 75.0 MHz) δ (note: some peaks may come from different isomers) 150.80, 150.78, 144.86, 144.73, 143.50, 143.27, 140.91, 140.62, 140.47, 140.42, 139.96, 139.91, 138.80, 138.74, 130.61, 130.52, 129.45, 129.38, 129.36, 129.30, 129.03, 128.95, 128.75, 128.66, 128.59, 123.89, 123.77, 123.36, 122.67, 105.59, 34.72, 34.54, 31.79, 31.57, 19.15, 18.70.

1-[4'-(2',7'-di-*tert*-Butyl-*trans*-10b',10c'-dimethyl-10b',10c'-dihydropyrenyl)]
2-[4'-(2',7'-bis-(tert-butyl)-12c', 12d'-dimethyl-12c',12d'-benzo-[e]-dihydropyrenyl)]
acetylene 130

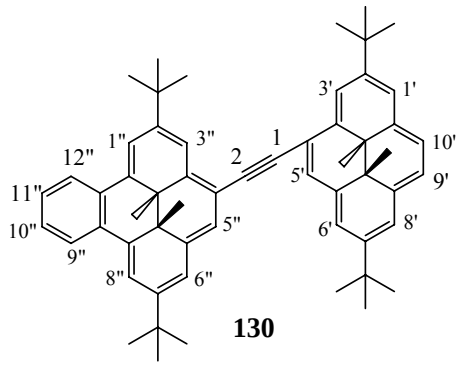

130

All the solvents were purged with argon before use. 4-iodo-dihydropyrene **129** (220 mg, 0.47 mmol), tetrakis-(triphenylphosphine) palladium(0) (22 mg, 0.02 mmol), cuprous iodide (5 mg, 0.025 mmol), KI (30 mg, 0.18 mmol), THF (3 mL) and di-isopropylamine (3 mL) were added to a two neck flask with stir bar under argon. After the resulting mixture was warmed to 60 °C. A solution of 4-ethynyl-benzo[e]dihydropyrene **128** (160 mg, 0.38 mmol) in THF: di-isopropylamine (1:1, 5 mL) was then added very slowly over one hour. The reaction mixture was stirred for a further 12 h under argon and then was cooled to room temperature, poured into hexanes (150 mL) and washed with water (4x50 mL). The organic phase was separated, and evaporated to give brown solid, which was chromatographed on silica gel using hexanes:benzene 9:1 as eluant. Eluted first was the unreacted iodo-DHP **129** (35 mg) followed by the desired product **130** as a redish brown crystalline solid (170 mg, 59%). Eluted last was the homo-coupling product **126** as red crystalline solid (80 mg, 27%).

Compound **130**: mp 206-208 °C; ^{1}H NMR ($CDCl_3$, 500 MHz) δ 9.25 (s, 1H, H-3'), 8.79-8.74 (m, 2H, H-9", 12"), 8.74 (s, 1H, H-5'), 8.55 (d, *J* = 1.0 Hz, 1H, H-1'), 8.52 (s, 1H, H-6'), 8.51 (s, 1H, H-8'), 8.44 (s, 2H, H-9',10'), 8.37 (s, 1H, H-3"), 8.36 (s, 1H, H-1"), 8.27 (d, *J* = 0.9 Hz, 1H, H-8"), 7.66-7.62 (m, 2H, H-10",11"), 7.54 (s, 1H, H-5"), 7.46 (s, 1H, H-6"), 1.78 (s, 9H, 2'-$C(CH_3)_3$), 1.70 (s, 9H, 7'-$C(CH_3)_3$), 1.64 (s, 9H, 2"-$C(CH_3)_3$), 1.53 (s, 9H, 7"-$C(CH_3)_3$), -1.285, -1.291, -1.303 and -1.309 (s, 6H total, 12c",12d"-CH_3), -3.77 and -3.78 (6H total, 10b',10c'-CH_3); ^{13}C NMR ($CDCl_3$, 125.7 MHz) δ 147.25 (C-2'), 147.06 (C-2"), 146.48 (C-7'), 145.48 (C-7"), 141.19 (C-3a"), 138.44 (C-10d'), 138.14 (C-5a"/12b"/12e"), 137.36 and 137.29 (C-10a', 3a'), 136.78 (C-5a"/12b"/12e"), 136.30 (C-5a'), 135.33 (C-5a"/12b"/12e"), 129.70 and 129.62 (C-

12a",12f"), 126.35 and 126.26 (C-10",11"), 125.89 (C-5'), 124.86 and 124.77 (C-9",12"), 123.97 and 123.61 (C-9',10'), 123.72 (C-5"), 121.89 (C-8'), 121.64 (C-1'), 120.99 (C-6'), 120.19 (C-3'), 119.61 (C-6"), 119.07 (C-3"), 117.57 (C-1",8"), 115.39 (C-4'), 114.34 (C-4"), 96.24 (C-2), 95.77 (C-1), 36.98 (C-12c"), 36.55 (2'-$\underline{C}(CH_3)_3$), 36.20 (2"-$\underline{C}(CH_3)_3$), 36.16 (7'-$\underline{C}(CH_3)_3$), 35.72 (7-$\underline{C}(CH_3)_3$), 35.68 (C-12d), 32.31 (2'-C($\underline{C}H_3)_3$), 32.13 (2-C($\underline{C}H_3)_3$), 31.04 (7'-C($\underline{C}H_3)_3$), 30.82 (7"-C($\underline{C}H_3)_3$, 10b'), 29.97 (C-10c'), 18.33 (12c",12d"-$\underline{C}H_3$), 15.37 and 14.97 (10b', 10c'-$\underline{C}H_3$); IR (Thin film on NaCl plate) 3034, 2962, 2923, 2866, 2178 (weak), 1596, 1475, 1462, 1361, 1256, 885, 755 cm^{-1}; UV-Vis (cyclohexane) λ_{max} (ε_{max}) nm 280 (15,100), 345 (58,000), 425 (69,400), 670 (3,000); LSIMS *m/z* 760.4 (M^+), 745.4 (M^+- CH_3), 730.3 (M^+-2CH_3), 715.3 (M^+-3CH_3); Anal. calcd for $C_{58}H_{64}$: C, 91.52%; H, 8.48; found: C, 91.48; H, 8.52.

Tetracarbonyl iron adduct 151

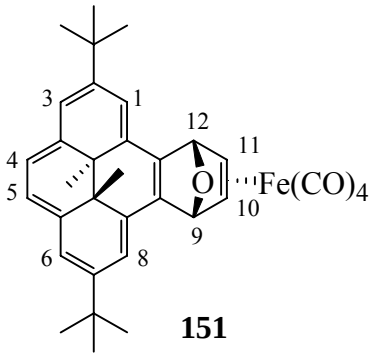

151

A solution of adduct **149** (100 mg, 0.243 mmol) and $Fe_2(CO)_9$ (200 mg, 0.548 mmol) in dry benzene (15 mL) was stirred under argon at 20 °C in the dark for 18 h. The mixture was then filtered directly through a column of Si gel (10 cm) using benzene as eluant. The intense reddish-green solution was evaporated in the dark, and the residue was chromatographed on Si gel using hexane as eluant. The first red band yielded 20 mg

(21%) of benzannulene **36** as red crystals. The second grass green band yielded 78 mg (60%) of complex **151**, mp ~60 °C (dec. color changed to reddish); ^{1}H NMR (C_6D_6, 500 MHz) δ 8.31 (d, *J* = 1.4 Hz, 2H, H-3,6), 8.26 (d, *J* = 1.4 Hz, 2H, H-1,8), 8.21 (s, 2H, H-4,5), 5.97 and 5.91 (s, 1H each, H-9,12), 3.29 (d, *J* = 5.1 Hz, 1H, H-10/11), 3.04 (d, *J* = 5.1 Hz, 1H, H-11/10), 1.61 and 1.60 (s, 9H each, $C(CH_3)_3$); -3.01 and -3.17 (s, 3H each, internal CH_3); ^{13}C NMR (C_6D_6, 125.7 MHz) δ 211.2 (CO), 146.4 and 146.2 (C-7/2), 138.2 and 138.1 (C-3a/5a), 136.2 and 136.1 (C-12a/12f), 128.7 and 128.2 (C-12b/12e), 125.6 and 125.5 (C-4/5), 122.4 and 122.3 (C-3/6), 116.1 and 115.5 (C-1/8), 81.43 and 81.38 (C-9/12), 59.6 and 59.5 (C-10/11), 36.4 and 36.3 (2, 7-$\underline{C}(CH_3)_3$), 34.0 and 32.4 (C-12c/12d), 32.3 and 32.1 (2,7-C($\underline{C}H_3)_3$), 17.0 and 15.4 (12c,12d-$\underline{C}H_3$); UV-vis (cyclohexane) λ_{max} (ε_{max}) nm 361 (60,500), 387 (44,700), 453 (7,340), 467 (7,000), 528 (394), 577 (425), 641 (816); IR (KBr) 2082, 2021, 1991, 1968, 885, 655, 626, 605 cm^{-1}; (CH_2Cl_2 solution) 2083, 2008, 1976 (shoulder) cm^{-1}; LSI MS *m*/*z* 578.1 (M^+); HRMS calcd for $C_{34}H_{34}O_5Fe$ 578.1756, found 578.1754.

2,7-Di-*tert*-butyl-*trans*-12c, 12d-dimethyl-12c,12d-benzo[e]dihydro-pyrene-[12b, 1, 2, 3-η^4]-tricarbonyl iron(0) and 2,7-di-*tert*-butyl-*trans*-12c, 12d-dimethyl-12c,12d-benzo[e]dihydropyrene-bis-[12b, 1, 2, 3-η^4], -[6, 7, 8, 12e-η^4]-tricarbonyl iron(0) 152, 153

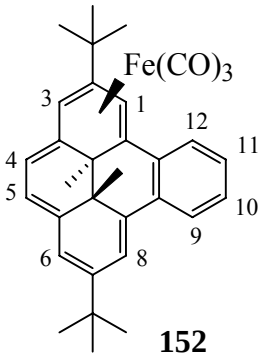

152

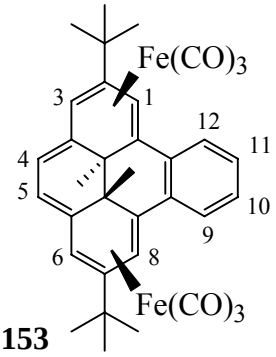

153

A solution of adduct **149** (600 mg, 1.46 mmol) and $Fe_2(CO)_9$ (1.15 g, 3.21 mmol) in dry benzene (50 mL) was stirred under argon at reflux in the dark for 2 h. After cooling, the mixture was filtered through Al_2O_3 (10 cm) using additional benzene (100 mL) as eluant. The intense red solution was evaporated in the dark. The solid was re-extracted with benzene (100 mL), and the solution was re-evaporated in the dark. The resulting red residue was chromatographed over Si gel using hexane as eluant. The first red band yielded 402 mg (70%) of benzannulene **36** as red crystals. The second dark green band yielded 77 mg (10%) of mono(tricarbonyliron) benzannnulene complex **152**. The third orange band yielded 118 mg (12%) of bis(tricarbonyliron) benzannnulene complex **153**. The fourth dark green band yielded 12 mg (1.5%) of tetracarbonyl iron complex **151**.

Complex **152**: mp 192-193 °C; ^{1}H NMR (C_6D_6, 500 MHz) δ 7.41 (dd, $J_{9,10}$ = 8.0 Hz, $J_{9,11}$ = 1.4 Hz, 1H, H-9), 7.19 (dd, $J_{12,11}$ = 8.1 Hz, $J_{12,10}$ = 1.3 Hz, 1H, H-12), 6.97 (td, $J_{11,12}$ = 8.1 Hz, $J_{11,10}$ = 7.0 Hz, $J_{11,9}$ = 1.4 Hz, 1H, H-11), 6.91 (td, $J_{10,9}$ = 8.0 Hz, $J_{10,11}$ = 7.3 Hz, $J_{10,12}$ = 1.3 Hz,, 1H, H-10), 6.38 (d, J = 1.2 Hz, 1H, H-8), 5.73 (s, 1H, H-6), 5.58

(d, $J_{1,3}$ = 1.4 Hz, 1H, H-1), 5.29 (dd, $J_{5,4}$ = 5.7 Hz, J = 0.7 Hz, 1H, H-5), 5.11 (d, $J_{4,5}$ = 5.7 Hz, 1H, H-4), 3.67 (d, $J_{3,1}$ = 1.4 Hz, 1H, H-3), 2.47 (s, 3H, 12d-CH_3), 2.01 (s, 3H, 12c-CH_3), 1.10 (s, 9H, 2-C(CH_3)$_3$), 1.03 (s, 9H, 7-C(CH_3)$_3$); ^{13}C NMR (C_6D_6, 125.7 MHz) δ 212.3 (CO), 145.9 (C-7), 144.3 (C-5a), 144.2 (C-3a), 140.9 (C-12e), 136.4 (C-12a), 134.6 (C-12f), 128.3 (C-11), 127.3 (C-10), 126.4 (C-12), 125.1 (C-9), 121.3 (C-5) 121.2 (C-6), 117.8 (C-8), 112.7 (C-4), 108.5 (C-2), 80.7 (C-1), 78.6 (C-12b), 64.1 (C-3), 44.4 (C-12c), 43.7 (C-12d), 34.8 (7-C(CH_3)$_3$), 34.3 (2-C(CH_3)$_3$), 30.5 (2-C(CH_3)$_3$), 29.3 (7-C(CH_3)$_3$), 27.5 (12c-CH_3), 27.1 (12d-CH_3); IR (KBr) 2032, 1977, 1954, 761, 611, 599, 552 cm^{-1}; (CH_2Cl_2 solution) 2032, 1972, 1962 cm^{-1}; UV-vis (cyclohexane) λ_{max} (ε_{max}) nm 323 (30 600), 420 sh (~8000), 500-600 tail (~700); EI-MS m/z 534 (M^+). Anal. calcd for $C_{33}H_{34}O_3Fe$: C, 74.16; H, 6.41. Found: C, 74.20; H, 6.59.

Complex **153**: mp 203 °C (dec); ^{1}H NMR (C_6D_6, 500 MHz) δ 7.40 (dd, $J_{12,11}$ = 7.8 Hz, $J_{12,10}$ = 1.4 Hz, 1H, H-9), 7.27 (dd, $J_{9,10}$ = 8.1 Hz, $J_{9,11}$ = 1.2 Hz, 1H, H-12), 7.07 (ddd, $J_{10,9}$ = 8.1 Hz, $J_{10,11}$ = 7.2 Hz, $J_{10,12}$ = 1.4 Hz,, 1H, H-10), 6.97 (ddd, $J_{11,12}$ = 7.8 Hz, $J_{11,10}$ = 7.2 Hz, $J_{11,9}$ = 1.2 Hz, 1H, H-11), 5.54 (dd, $J_{4,5}$ = 5.3 Hz, $J_{4,5}$ = 0.5 Hz, 1H, H-5), 5.52 (d, J = 1.6 Hz, 1H, H-1), 5.47 (dd, $J_{5,4}$ = 5.3 Hz, J = 0.5 Hz, 1H, H-4), 5.00 (d, J = 1.8 Hz, H-8), 3.89 (d, J = 1.4 Hz, 1H, H-3), 3.78 (d, J = 1.3 Hz, 1H, H-6), 1.67 (s, 3H, 12d-CH_3), 1.12 (s, 9H, 2-C(CH_3)$_3$), 1.02 (s, 9H, 7-C(CH_3)$_3$), 0.20 (s, 3H, 12c-CH_3); ^{13}C NMR (C_6D_6, 125.7 MHz) δ 214.7 and 212.8 (CO), 146.4 (C-3a), 145.3 (C-5a), 139.4 (C-12f), 138.8 (C-12a), 129.1 (C-9), 128.5 (C-11), 127.6 (C-10), 126.1 (C-12), 116.0 (C-5), 113.6 (C-4), 108.9 (C-2), 103.5 (C-7), 101.3 (C-12e), 86.3 (C-8), 79.02 (C-1) 79.00 (C-12b), 63.9 (C-6), 62.9 (C-3), 43.2 (C-12c), 42.4 (C-12d), 34.5 (7-C(CH_3)$_3$), 34.3 (2-C(CH_3)$_3$), 30.8 (12d-CH_3), 30.50 (2-C(CH_3)$_3$), 30.48 (7-C(CH_3)$_3$), 26.5 (12c-CH_3); IR

(KBr) 2032, 2025, 1956, 618, 600 cm^{-1}; (CH_2Cl_2 solution) 2037, 2027, 1963 cm^{-1}; UV-vis (cyclohexane) λ_{max} (ε_{max}) nm 302 (20 300), 343 (20 000), ~470 sh (~4000), tail to 600 (~200); EI-MS *m*/*z* 674 (M^+). Anal. calcd for $C_{36}H_{34}O_6Fe_2$: C, 64.12; H, 5.08. Found: C, 63.85; H, 5.08.

References:

1. Faraday, M. *Phil. Trans. Roy. London*, **1825**, 440-466.
2. Mitscherlin, E. *Ann. Phys.* **1833**, *115*, 440
3. Kekule, A. *Bull. Soc. Chim. Fr*. **1865**, *3*, 98.
4. a) Hückel, E. *Z. Physik*, **1931**, *70*, 204-286. b) *ibid* **1931**, *72*, 310.
5. (a) Breslow, R. *Chem. Eng. News*, **1965**, 90-99. (b) Breslow, R. *Acc.Chem. Res*. **1973**, *6*, 393-398.
6. Watts, L.; Fitzpatrick, J. D.; Pettit, R. *J. Am. Chem. Soc*. **1965**, *87*, 3253-3254.
7. (a) Kennedy, R. D.; Lloyd, D.; McNab, H. *J. Chem. Soc. Perkin Trans. 1,* **2002**, 1601-1621. (b) Sondheimer, F. *Acc. Chem. Res*. **1972**, *5*, 81-91.
8. Nakagawa, M. *Pure Appl. Chem*. **1975**, *44*, 885-924.
9. Boekelheide, V.; Phillips, J.B. *Proc. Natl. Acad. Sci. USA*, **1964**, *54*, 550-552.
10. Vogel, E.; Boll, W. A.; *Angew. Chem. Int. Ed. Engl*. **1964**, *3*, 642-643.
11. Streitweiser, A. *Molecular Orbital Theory for Organic Chemists*; John Wiley & sons Inc. New York, **1961**, p117-135.
12. (a) Randic, M. *Chem. Phys. Lett*. **1976**, *38*, 68-70. (b) Randic, M. *J. Am. Chem. Soc.* **1977**, *99*, 444-450. (c) Randic, M. *Tetrahedron*, **1977**, *33*, 1905-1920.
13. Diedrich, F.; Rubin, Y. *Angew. Chem. Int. Ed. Engl*. **1992**, *31*, 1101-1123.
14. a) Tsefrikas, V. M.; Scott, L. T. *Chem. Rev*. **2006**, *106*, 4868-4884. b) Scott, L. T.; Boorum, M. M.; McMahon, B. J.; Hagen, S.; Mack, J.; Blank, J.; Wegner, H.; de Meijere, A. *Science* **2002**, *295*, 1500-1053.
15. Gross, J.; Harder, G.; Vogtle, F. *Angew. Chem. Int. Ed. Engl*. **1995**, *34*, 481-483.

16. (a) Tobe, Y.; Matsumoto, H.; Naemura, K.; Achiba, Y.; Wakabayashi, T. *Angew. Chem. Int. Ed. Engl*. **1996**, *35*, 1800-1802. (b) Tobe, Y.; Fuji, T.; Matsumoto, H.; Naemura, K.; Achiba, Y.; Wakabayashi, T. *J. Am. Chem. Soc*. **1996**, *118*, 2758-2759.

17. Breslow, R.; Ryan, G. *J. Am. Chem. Soc.* **1967**, *89*, 3073-3075.

18. Benson, R. C.; Flygare, W. H.; Oda, M.; Breslow, R. *J. Am. Chem. Soc.* **1973**, *95*, 2772–2777.

19. Dahn, H.; Ung-Truong, M. N. *Helv. Chim. Acta*, **1987**, *70*, 2130–2136.

20. Paquette, L. A.; Watson, T. J.; Friedrich, D.; Bishop, R.; Bacque, E. *J. Org. Chem.* **1994**, *59*, 5700–5707.

21. Garbisch, E. W.; Sprecher, R. F. *J. Am. Chem. Soc.* **1969**, *91*, 6785–6800.

22. (*a*) Baron, P. A.; Brown, R. D.; Burden, F. R.; Domaille, P. J.; Kent, J. E. *J. Mol. Spectrosc.* **1972**, *43*, 401–410; (*b*) Replogle, E. S.; Trucks, G. W.; Staley, S. W. *J. Phys. Chem.* **1991**, *95*, 6908–6912. (c) Najafian, K.; Schleyer, P. V. R. and Tidwell, T. *Org. Biomol. Chem.* **2003**, *1*, 3410-3417.

23. (*a*) Havenith, R. W. A.; Fowler, P. W.; Steiner, E. *J. Chem. Soc. Perkin Trans. 2* **2002**, 502–507; (*b*) Stepien, B. T.; Krygowski, T. M.; Cyranski, M. K. *J. Org. Chem.* **2002**, *67*, 5987–5992.

24. Bauder, A.; Keller, C.; and Neuenschwander, M. *J. Mol. Spectrosc.* **1976**, *63*, 281-287.

25. Leroy, G.; Jaspers, S. *J. Chim. Phys*. **1967**, *64*, 463-478.

26. Mitchell, R.H.; Williams, R.V.; Mahadevan, R.; Lai, Y.H.; Dingle, T.W. *J. Am. Chem. Soc*. **1982**, *104*, 2571-2578.

27. Mitchell, R.H.; Iyer, V.S.; Khalifa, N.; Mahadevan, R.; Venugopalan, S.; Weerawarna, S.A.; Zhou, P. *J. Am. Chem. Soc*. **1995**, *117*, 1514-1532.

28. Pauling, L. *J. Chem. Phys*. **1936**, *4*, 674-677.

29. Elvidge, J. A.; Jackman, L. M. *J. Chem. Soc.* **1961**, 859-865.

30. Haigh, C. W.; Mallion, R.B. *Mol. Phys*. **1970,** *18*, 737-750.

31. Mitchell, R. H.; Klopfenstein, C.E.; Boekelheide, V. *J. Am. Chem. Soc*. **1969**, *91*, 4931-4932.

32. Vogel, E.; Konigshofen, H.; Mullen, k.; Oth, J.F.M. *Angew. Chem. Int. Ed. Engl.* **1974**, *13*, 281-283.

33. Vogler, H. *J. Am. Chem. Soc.* **1978**, *100*, 7464-7500.

34. Memory, J. D.; Wilson, N. K. *NMR of Aromatic Compounds*, John Wiley & Sons, New York, p30-33, **1982**.

35. Laszlo, P.; Stang, P. *Organic Spectroscopy: Principles and Applications* Harper & Row, New York, NewYork, **1971**.

36. Pouchert, C.J.; Behnke, J. *The Aldrich Library of ^{13}C and ^{1}H FT NMR Spectra*, Ed. 1; Vol. III; Aldrich Chemical Company, Milwaukee, **1993**.

37. Haddon, R. C. *J. Am. Chem. Soc.* **1979**, *101*, 1722-1728.

38. a) Aihara, J. *Bull. Chem. Soc. Jpn*. **1980**, *53*, 1163-1164. b) Verbruggen, A. *Bull. Soc. Chim. Belg*. **1982**, *91*, 865-868. c) Hess, B.A. Jr.; Schaad, L.J.; Agranat, F. *J. Am. Chem. Soc.* **1978**, *100*, 5268-5271.

39. Cremer, D.; Günther, H. *Liebigs. Ann. Chem*. **1972**, *763*, 87-108.

40. Mitchell, R.H.; Iyer, V.S.; Khalifa, N.; Mahadevan, R.; Venugopalan, S.; Weerawarna, S. A.; Zhou, P. *J. Am. Chem. Soc.* **1995**, *117*, 1514-1532.

41. Williams, R.V.; Edwards, W.D.; Vij, A.; Tolbert, R.W.; Mitchell, R.H. *J. Org. Chem.* **1998**, *63,* 3125-3127.

42. Mitchell, R. H. *Chem. Rev*. **2001**, *101*, 1301-1315.

43. Mitchell, R. H.; Ward, T. R. *Tetrahedron,* **2001**, *57*, 3689-3695.

44. Tashiro, M.; Yamato, T. *J. Am. Chem. Soc.* **1982**, *104*, 3701-3707.

45. Mitchell, R. H.; Fan, W.; Lau, D. Y.; Berg, D. J. *J. Org. Chem*. **2004**, *69*, 549-554.

46. a) Nicolaou, K. C.; Zhong, Y. L.; Baran, P. S. *J. Am. Chem. Soc.* **2000**, *122*, 7596-7597. b) Nicolaou, K. C.; Gray, D. L. F.; Montagnon, T.; Harrison, S. T. *Angew. Chem. Int. Ed*. **2002**, *41(6)*, 996-1000. c) Nicolaou, K. C.; Montagnon, T.; Baran, P. S. *Angew. Chem. Int. Ed*. **2002**, *41(8)*, 1386-1389.

47. Engman, L. *J. Org. Chem*. **1988**, *53*, 4031-4037.

48. Houllemare, D.; Ponthieux, S.; Outurquin, F.; Paulmier, C. *Synthesis*, **1997**, 101-106.

49. (a) Sharpless, K. B.; Lauer, R. F.; Teranishi, A. Y. *J. Am. Chem. Soc*. **1973**, *95*, 6137-6139. (b) Reich, H. J.; Reich, I. L.; Renga, J. M. *J. Am. Chem. Soc*. **1973**, *95*, 5813-5815.

50. a) Tebbe, F. N.; Parshall, G. W. and Reddy, G. S. *J. Am. Chem. Soc.* **1978**, *100*, 3611-3613. b) Pine, H. S.; Shen, S. G. and Hoang, H. *Synthesis*, **1991**, 165-167.

51. a) Peterson D. J. *J. Org. Chem.* **1968**, *33*, 780-784. b) Ager, D. J. *Synthesis*, **1984,** 384-398. c) Peterson D. J. *J. Org. Chem.* **1973**, *38*, 2664-2669.

52. Chajara, K. and Ottosson, H. *Tetrahedron Let.* **2004**, *45*, 6741-6744.

53. (a) Shimizu, S.; Shirakawa, S.; Suzuki, T. and Sasaki, Y. *Tetrahedron*, **2001**, *57*, 6169-6173. (b) Alper, H and Laycock, D. E. *Synthesis*, **1980**, 799-800.

54. (a) Mitchell, R. H.; Brkic, Z.; Berg, D. J.; Barclay, T. M. *J. Am. Chem. Soc.* **2002**, *124*, 11983-11988. (b) Williams, R. V.; Armantrout, J. R.; Twamley, B.; Mitchell, R. H.; Ward, T. R.; Bandyopadhyay, S. *J. Am. Chem. Soc.* **2002**, *124*, 13495-13505. (c) Kimball, D. B.; Haley, M. M.; Mitchell, R. H.; Ward, T. R.; Bandyopadhyay, S.; Williams, R. V.; Armantrout, J. R. *J. Org. Chem.* **2002**, *67*, 8798-8811.

55. Scott, L. T.; Kirms, M. A.; Gunther, H.; Puttkamer, H. *J. Am. Chem. Soc*. **1983**, *105*, 1372-1373.

56. a) Mitchell, R. H.; Williams, R. V.; Mahadevan, R.; Lai, Y. H.; Dingle, T. W. *J. Am. Chem. Soc.* **1982**, *104*, 2571-2578. (b) Mitchell, R. H.; Chen, Y.; Khalifa, N.; Zhou, P. *J. Am. Chem. Soc*. **1998**, *120*, 1785-1794.

57. Mitchell, R. H.; Khalifa, N. A.; Dingle, T. W. *J. Am. Chem. Soc*. **1991**, *113*, 6696-6697.

58. Günther, H.; Shyoukh, A.; Cremer, D.; Frisch, K. H. *Liebigs. Ann. Chem*. **1978**, 150-164.

59. (a) Mitchell, R. H.; Boekelheide, V. *J. Chem. Soc. Chem. Commun.* **1970**, 1557-1558. (b) Mitchell, R. H.; Zhou, P. *Angew. Chem. Int. Ed. Engl.* **1991**, *30*, 1013-1015.

60. (a) Schleyer, P. v. R.; Maerker, C.; Dransfeld, A.; Jiao, H.; van Eikema Hommes, N. J. R. *J. Am. Chem. Soc.* **1996**, *118*, 6317-6318. (b) Cyranski, M.; Krygowski, T.; Wisiorowski, M.; Hommes, N.; Schleyer, P. v. R. *Angew. Chem. Int. Ed.* **1998**, *37*, 177-180.

61. *Jaguar 4.0*; Schrodinger, Inc.: Portland, OR, 1991-2000.

62. Frisch, M. J.; Trucks, G. W.; Schlegel, H. B.; Gill, P. M. W.; Johnson, B. G.; Robb, M. A.; Cheeseman, J. R.; Keith, T.; Petersson, G. A.; Montgomery, J. A.; Raghavachari, K.; Al-Laham, M. A.; Zakrzewski, V. G.; Ortiz, J. V.; Foresman, J. B.; Cioslowski, J.; Stefanov, B. B.; Nanayakkara, A.; Challacombe, M.; Peng, C. Y.; Ayala, P. Y.; Chen, W.; Wong, M. W.; Andres, J. L.; Replogle, E. S.; Gomperts, R.; Martin, R. L.; Fox, D. J.; Binkley, J. S.; Defrees, D. J.; Baker, J.; Stewart, J. P.; Head-Gordon, M.; Gonzalez, C.; Pople, J. A. *Gaussian 94*, Revision E.2; Gaussian, Inc.: Pittsburgh, PA, 1995.

63. Farrugia, L. J. *J. Appl. Crystallogr*. **1997**, *30*, 565-565.

64. Fan, W. *PhD Thesis*; University of Victoria: Victoria, B.C. Canada, **2005**.

65. ΔΣ = (average long bond (Å)) - (average short bond (Å)). See Mitchell, R. H.; Chen, Y.; Iyer, V. S.; Lau, D. Y.; Baldridge, K. K.; Siegel, J. S. *J. Am. Chem. Soc*. **1996**, *118*, 2907-2911.

66. Forsyth, D. A.; Sebag, A. B. *J. Am. Chem. Soc*. **1997**, *119*, 9483-9494.

67. Bouas-Laurent, H.; Dürr, H. *Pure Appl. Chem.* **2001**, *73*, 639-665.

68. *Photochromism, Molecules and Systems*, Chapter 1, Dürr, H. Eds. Dürr, H. and Bouas-Lauret, H. Elsevier, Amsterdam, **1990**, p1-14.

69. Irie, M. *Chem. Rev*. **2000**, *100*, 1685-1716.

70. a) Balzani, V.; Scandola, F. *Supramolecular Photochemistry*, Horwood, Chichester, **1991**, chapter 7. b) *Photochromism, Molecules and Systems,* Chapter 4, Rau, H. Eds.: Durr, H. and Bouas – Laurent, H. Elsevier, Amsterdam, **1990**, p165-192. c) Kumar, G.S.; Neckers, D.C. *Chem. Rev*. **1989**, *89*, 1915-1925. d) Shinkai, S.; Manabe, O. *Top. Curr. Chem.* **1984**, *121*, 67-104. e) Malkin, S.;

Fischer, E. *J. Phys. Chem*. **1962**, *66*, 2482-2486. f) Zimmerman, G.; Chow, L.Y.; Paik, U.J. *J. Chem. Phys*. **1958**, *80*, 3528-3531. g) Fischer, E.; Frei,Y. *J. Chem. Phys*. **1957**, *27*, 328-330.

71. a) Berkovic, G.; Krongauz, V.; Weiss, V. *Chem, Rev*. **2000**, *100*, 1741-1753. b) Bercovici, T.; Fischer, E. *J. Am. Chem. Soc.* **1964**, *86*, 5687-5688. c) Hirshberg, Y. *J. Am. Chem. Soc.* **1956**, *78*, 2304-2312.

72. a) Stobbe, H. *Ber. Dtsch. Chem. Ges*. **1905**, *38*, 3673-3682. b) Heller, H.G. *IEE Proc*. **1983**, *130*, Pt. I, 209-211. c) Yokoyama, Y. *Chem. Rev*. **2000**, *100*, 1717-1739.

73. a) Irie, M.; Mohri, M. *J. Org. Chem.* **1988**, *53*, 803-808.

74. a) Henry, A. J. *J. Chem. Soc*. **1946**, 1156-1164. b) Beveridge, D.J.; Jaffe, H. H. *J. Am. Chem. Soc.* **1965**, *87*, 5340-5346. c) Dyck, R.H.; McClure, D.S. *J. Chem. Phys*. **1962**, *36*, 2326-2345. d) Muszkat, K.A.; Fischer, E. *J.Chem. Soc. (B)* **1967**, 662-678. e) Gegiou, D.; Muszkat, K.A.; Fischer, E. *J. Am. Chem. Soc.* **1968**, *90*, 3907-3918.

75. (a) Feringa, B. L.; Jager, W. F.; de Lange, B. *J. Chem. Soc. Chem. Commun.* **1993**, 288-290. (b) Wiel, M. K. J.; Van Delden, R. A.; Meetsman, A.; Feringa, B. L. *J. Am. Chem. Soc*. **2003**, *125*, 15076-15086.

76. a) Waldeck, D. H. *Chem. Rev*. **1991**, 415. b) *Photochromism, Molecules and Systems,* Saltiel, J.; Sun, Y.-P. Chapter 3, Eds.: Dürr, H. and Bouas – Laurent, H. Elsevier, Amsterdam, **1990**, p64-164. c) Mallory, F.B.; Mallory, C.W. *Org. React*. **1984**, *30*, 1.

77. a) Brown, G.H. *Photochromism*, John Wiley & Sons; New York; **1971**, p98-99, p440-444, p569-578. b) Bouas – Laurent, H.; Dürr, H. *Pure appl. Chem.* **2001**, *73(4)*, 639-665.

78. a) Woodward, R.B.; Hoffmann, R. *Angew. Chem. Int. Ed. Engl.* **1969**, *8*, 781-853. b) Maeda, K.; Chinone, A.; Hyashi, T. *Bull. Chem. Soc. Jpn*. **1970**, *43*, 1431-1434.

79. Blattmann, H.R.; Schmidt, W. *Tetrahedron* **1970**, *26*, 5885-5899.

80. Sheepwash, M. L.; Mitchell, R. H.; Bohne, C. *J. Am. Chem. Soc.* **2002**, *124*, 4693-4700.

81. Blattmann, H. R.; Meuche, D.; Heilbronner, E.; Molyneux, R. J.; Boekelheide, V. *J. Am. Chem. Soc.* **1965**, *87*, 130-131.

82. Murakami, S.; Tsutsui, T.; Saito, S.; Yamato, T.; Tashiro, M. *Nippon Kagukukai Shi*, **1988**, 221-229.

83. Mitchell, R. H.; Iyer, V. S.; Mahadevan, R.; Venugopalan, S.; Zhou, P. *J. Org. Chem.* **1996**, *61*, 5116-5120.

84. Mitchell, R.H.; Iyer, V.S.; Khalifa, N.; Mahadevan, R.; Venugopalan, S.; Weerawarna, S. A.; Zhou, P. *J. Am. Chem. Soc.* **1995**, *117*, 1514-1532.

85. Mitchell, R. H. *Eur. J. Org. Chem.* **1999**, 2695-2703.

86. Mitchell, R.H.; Ward, T.R.; Chen, Y.; Wang, Y.; Weerawarna, S. A.; Dibble, P. W.; Marsella, M. J.; Almutairi, A; Wang, Z.Q. *J. Am. Chem. Soc.* **2003**, *125*, 2974-2988.

87. Sheepwash, M. *PhD Thesis*; University of Victoria: Victoria, B.C. Canada, **2002**.

88. Mitchell, R. H.; Chen, Y.; *Tetrahedron Lett.* **1996**, *37*, 5239-5242.

89. Mitchell, R.H.; Ward, T.R. *Tetrahedron* **2001**, *57*, 3689-3695.

90. Mitchell, R. H.; Ward, T. R.; Wang, Y.; Dibble, P. W. *J. Am. Chem. Soc.* **1999**, *121*, 2601-2602.

91. Wang, Y. *PhD Thesis*; University of Victoria: Victoria, B.C. Canada, **2003**.

92. (a) Mitchell, R. H.; Bandyopadhyay, S.; *Org. Lett.* **2004**, *6*, 1729-1732. (b) Bandyopadhyay, S. *Ph. D. Thesis*; University of Victoria: Victoria, B.C. Canada, **2004**.

93. Peters, A.; Branda, N. R. *Adv. Mater. Opt. Electron*. **2000**, *10*, 245-249.

94. a) Kaieda, T.; Kobatake, S.; Miyasaka, H.; Murakami, M.; Iwai, N.; Nagata, Y.; Itaya, A.; Irie. M. *J. Am. Chem. Soc.* **2002**, *124*, 2015–2024. b) Yagi, K.; Irie. M. *Chem. Lett.* **2003**, *32*, 848–849. c) Peters, A.; Branda, N. R. *Adv. Mater. Opt. Electron*. **2000**, 245-249.

95. Kobatake, S.; Irie. M. *Tetrahedron*, **2003**, *59*, 8359-8364.

96. Phillips, J. B.; Molyneux, R. J.; Sturm, E.; Boekelheide, V. *J. Am. Chem. Soc.* **1967**, *89*, 1704-1709.

97. Miyazawa, A.; Yamato, T.; Tashiro, M. *J. Org. Chem.* **1991**, *56*, 1334-1337.

98. Pettit, G. R.; Green, B.; Hofer, P.; Ayres, D. C.; Pauwels, P. J. S. *Proc. Chem. Soc*. **1962**, *86*, 357-360.

99. (a) Gribble, G. W.; Leese, R. M. and Evans, B. E. *Synthesis*, **1977**, 172-175. (b) Ketcha, D. M.; Gribble, G. W. *J. Org. Chem*. **1985**, *50*, 5451-5457.

100. Olah, G. A.; Surya Prakash, G. K. *Synthesis*, **1978**, 397-398.

101. Baltzly, R. and Buck, J.S. *J. Am. Chem. Soc.* 1943, **65**, 1984-1992.

102. Cerfontain, H.; Koeberg-Telder, A.; Bakker, B. H.; Mitchell, R. H. and Tashiro, M. *Liebigs Ann. Recueil*, **1997**, 873-878.

103. Carey, F. A.; Sundberg, R.J. *Advanced Organic Chemistry, Part A: Structure and Mechanism.* Third Ed. Plenum Press, New York, **1990**.

104. Mitchell, R. H.; Brkic, Z.; Sauro, V. A.; Berg, D. J. *J. Am. Chem. Soc.* **2003**, *125*, 7581-7585.

105. Fan, W.; Berg, D. J.; Mitchell, R. H. and Barclay, T. M. *Organometallics*, **2007**, *26*, 4562-4567.

106. Bond, A.; Bottrill, M.; Green, M.; Welch, A. J. *J. Chem. Soc. Dalton Trans* **1977**, 2372-2381.

107. Manuel, T. A. *Inorg. Chem*. **1964**, *3*, 1794-1796.

108. Bauer, R. A.; Fisher, E. O.; Kreiter, C. G. *J. Organomet. Chem*. **1970**, *24*, 737-751.

109. Harper, R. J. *U.S. Patent* 3,073,855 (Jan. 15, 1963) (assigned to the Ethyl Corporation).

110. a) Lombardo, L.; Wege, D.; Wilkinson, S. P. *Aust. J. Chem*. **1974**, *27*, 143-152. b) Lokshin, B. V.; Klemenkova, Z. S.; Rybin, L. V.; Aleksanyan, V. T. *Izvestiya Akademii Nauk SSSR, Seriya Khimicheskaya* **1981**, *5*, 989-996. [CAN 95:123168, AN 1981:523168]. c) Bachler, V.; Grevels, F-W.; Kerpen, K.; Olbrich, G.; Schaffner, K. *Organometallics* **2003**, *22*, 1696-1711. d) Davidson, G. *Inorg. Chim. Acta* **1969**, *3*, 596-600.

111. Spartan 06, V1.0.2, 2006, Wavefunction, Inc, Irvine, CA 92612.

112. a) Haddon, R. C.; Scott, L. T. *Pure Appl. Chem.* **1986**, *58*, 137-142. b) Mitchell, R. H. *Adv. Theor. Int. Molec.* Edited by R.P. Thummel, JAI Press, **1989**, Volume 1, p135-199.

113. Deeming, A. J. *Comprehensive Organometallic Chemistry*, Pergamon Press Ltd, **1982**, Editors, Wilkson, G. Sir, Stone, G. A.; Abel, E. W. Vol. 4, Chapter 31.3, 377.

114. a) Albright, J. O.; Brown, L.D.; Datta, S.; Kouba, J.K.; Wreford, S. S. *J. Am. Chem. Soc*. **1977**, *99*, 5518-5519. b) Albright, J. O.; Datta, S.; Dezube, B.; Kouba, J.K.; Marynick, D. S.; Wreford, S. S.; Foxman, B. M. *J. Am. Chem. Soc*. **1979**, *101*, 611-619. c) Gladfelter, W. L.; Hull, J. W. *Organometallics* **1984**, *3*, 605-613. d) Schaufele, H.; Hu, D.; Pritzkow, H.; Zenneck, U. *Organometallics* **1989**, *8*, 396-401.

115. Mills, O.S.; Robinson, G. *Acta Cryst.* **1963**, *16*, 758-761.

116. Cotton, F. A.; Troup, J. M. *J. Organomet. Chem*. **1981**, *212*, 411-418.

117. Cotton, F. A.; Day, V. W.; Frenz, B. A.; Hardcastle, K. I.; Troup, J. M. *J. Am. Chem. Soc.* **1973**, *95,* 4522-4528.

118. a) Stegemann, J.; Lindner, H. J. *J. Organomet. Chem*. **1979**, *166*, 223-231. b) Müllen, K.; Allison, N. T.; Lex, J.; Schmickler, H.; Vogel, E. *Tetrahedron* **1987**, *43*, 3225-3236.

119. The $Fe(CPDHP)_2$ and Ferrocenyl substituted BenzoDHP complexes do not photoopen under similar conditions.

Appendices

Note: The x in ln(x) is defined in Section 2.4.3 (p127) as mole fraction.

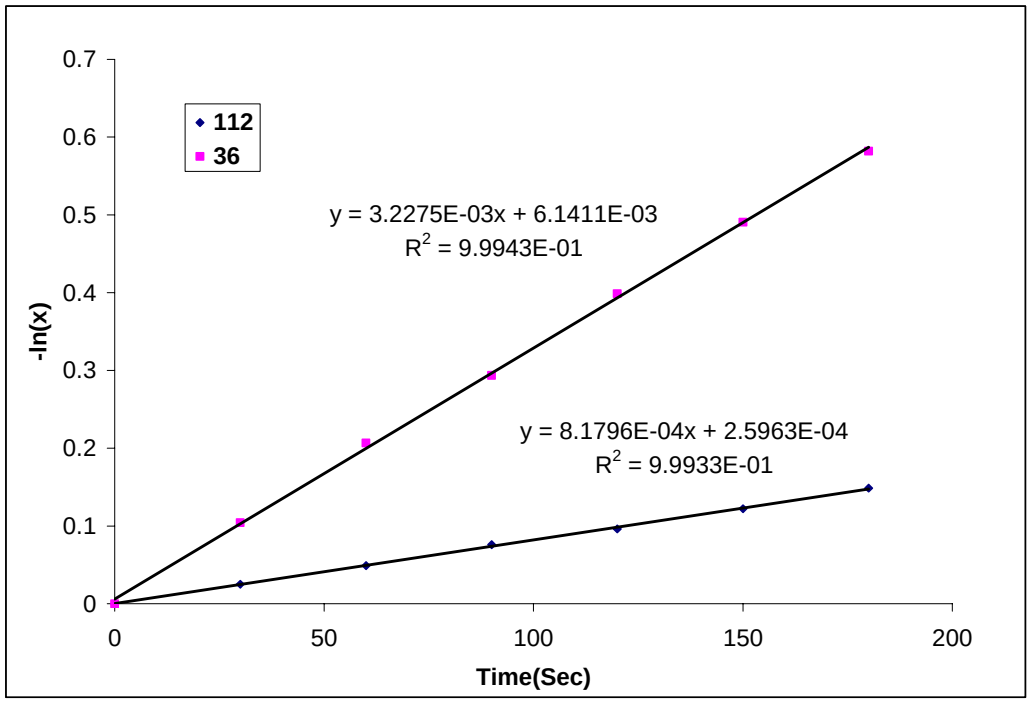

Figure A.1. Relative pseudo-first order rate constants of photo opening (>490 nm) for **112** comparing to **36**.

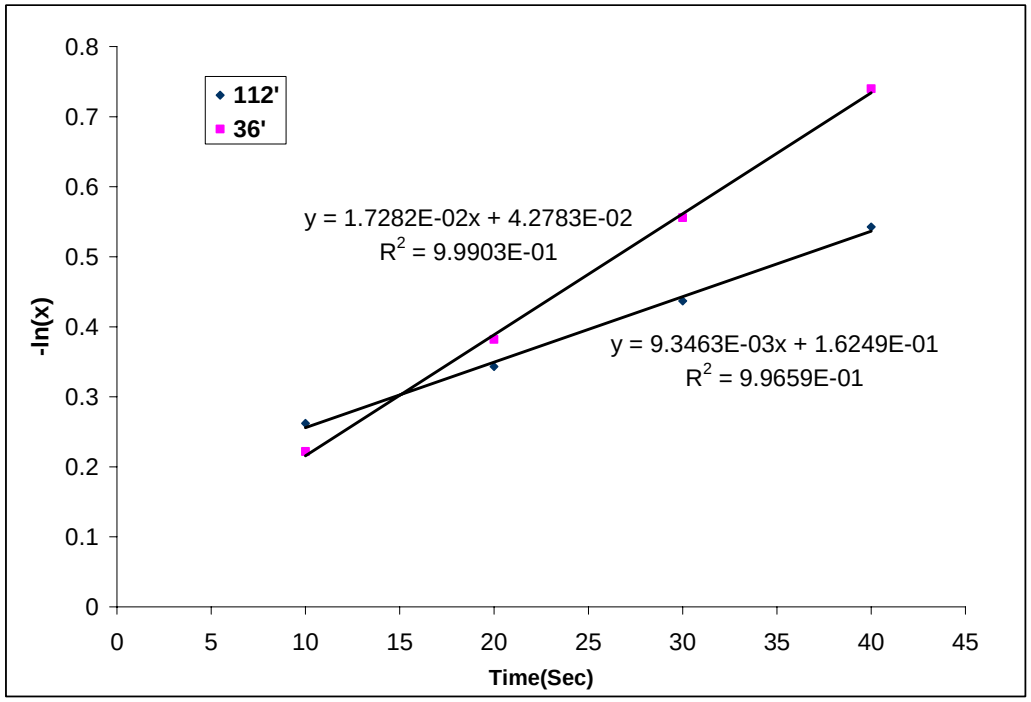

Figure A.2. Relative pseudo-first order rate constants of photo closing (250 nm) for **112'** comparing to **36'**.

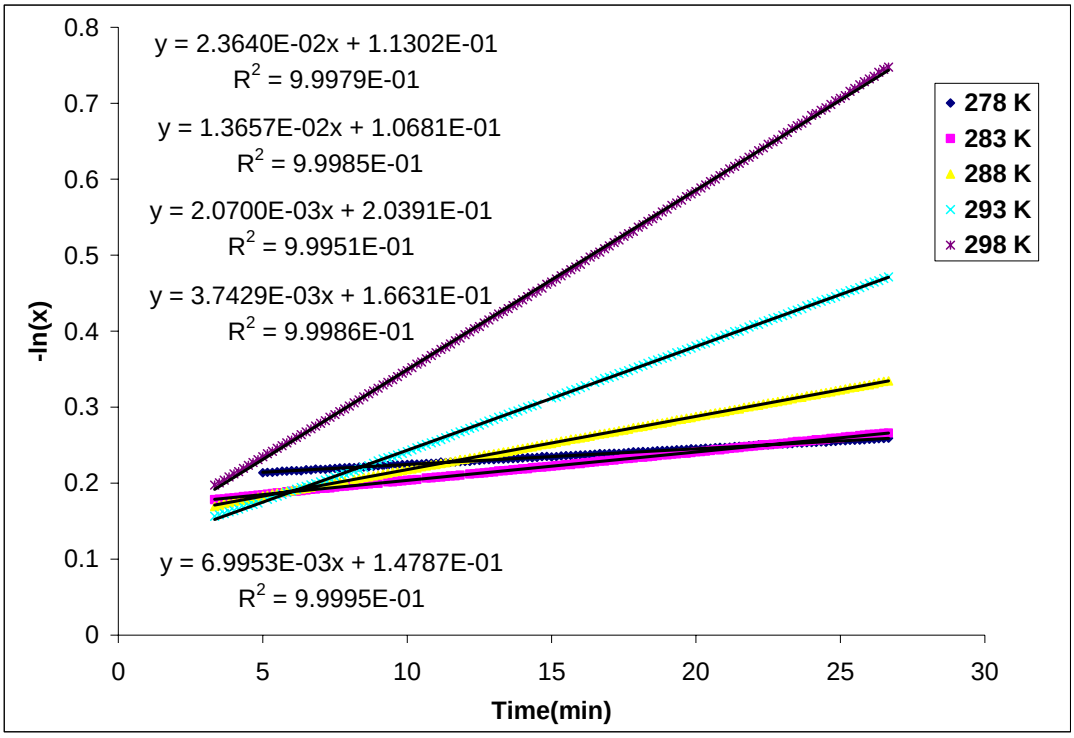

Figure A.3. Rate constants for the thermal return of **112'** in cyclohexane followed by UV-vis spectroscopy

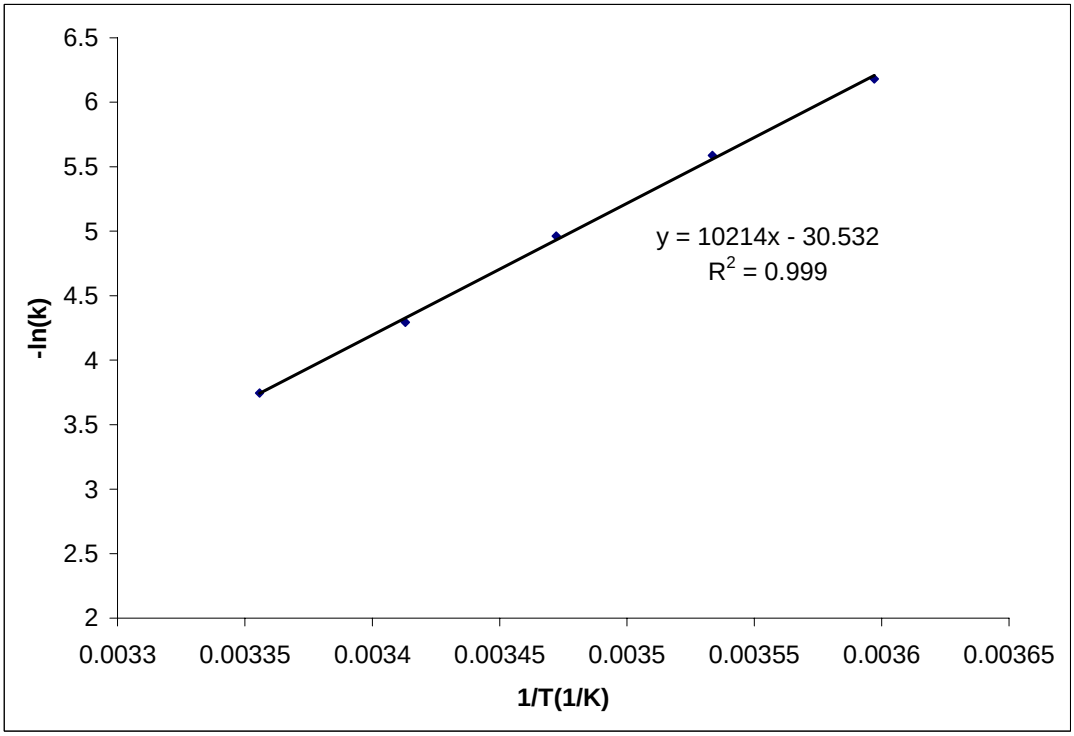

Figure A.4. The Arrhenius plot for **112'**.

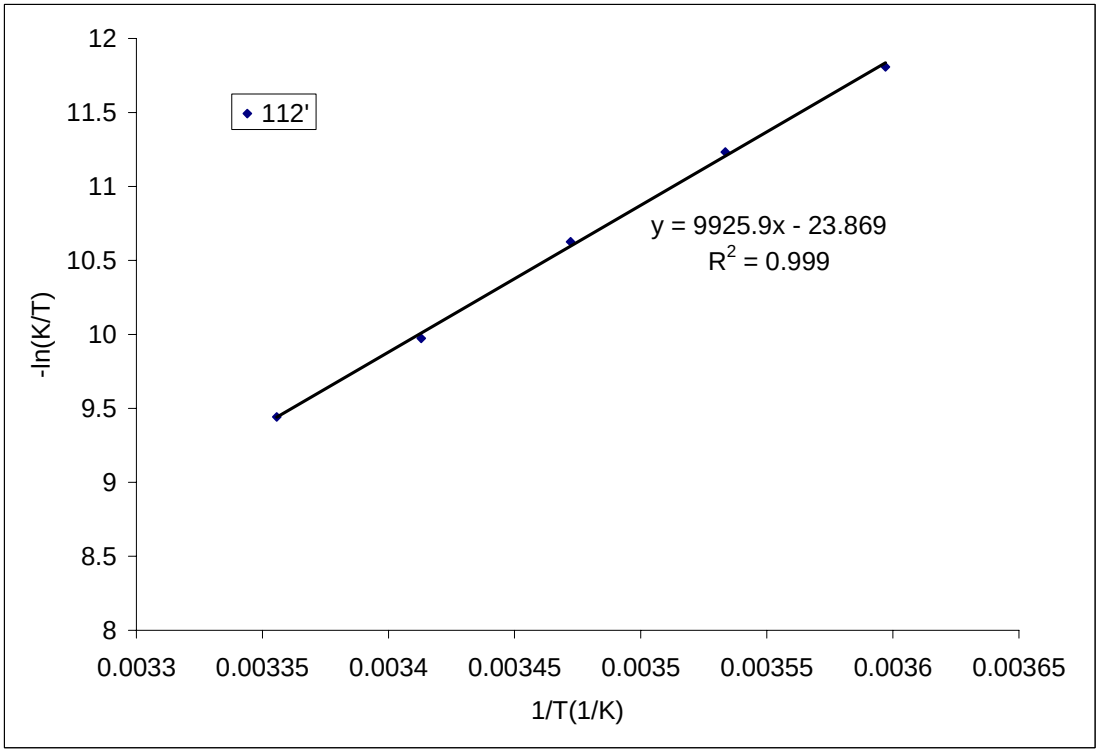

Figure A.5. The Eyring plot for **112'**.

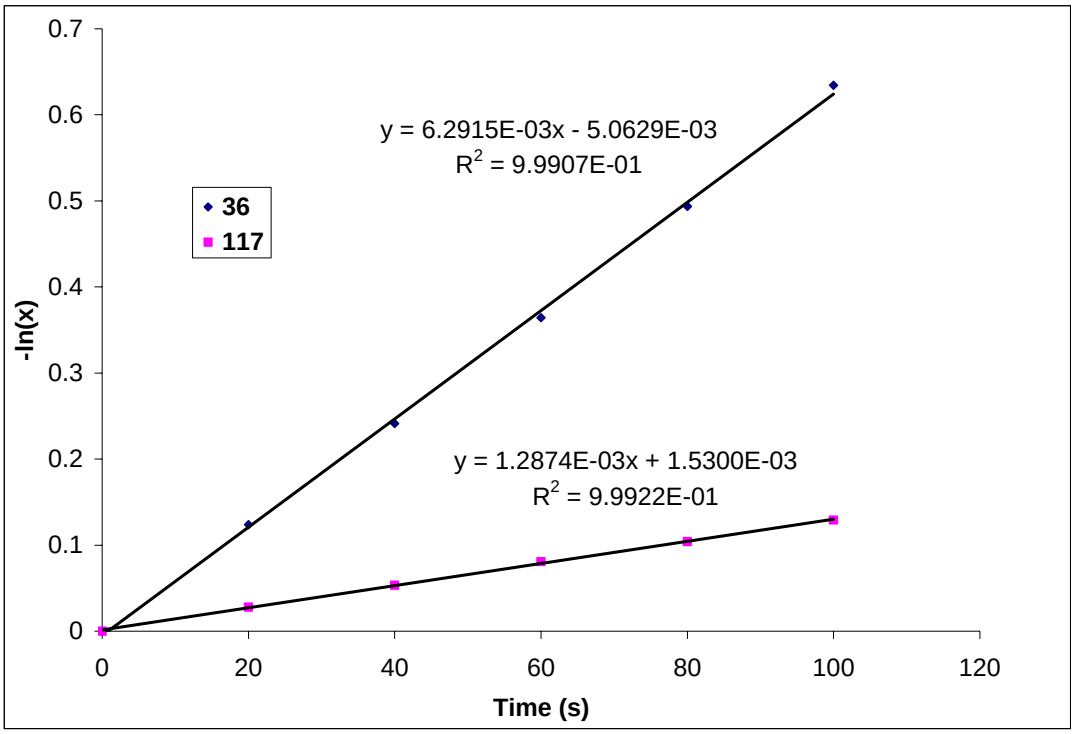

Figure A.6. Relative pseudo-first order rate constants of photo opening (>490 nm) for **117** comparing to **36**.

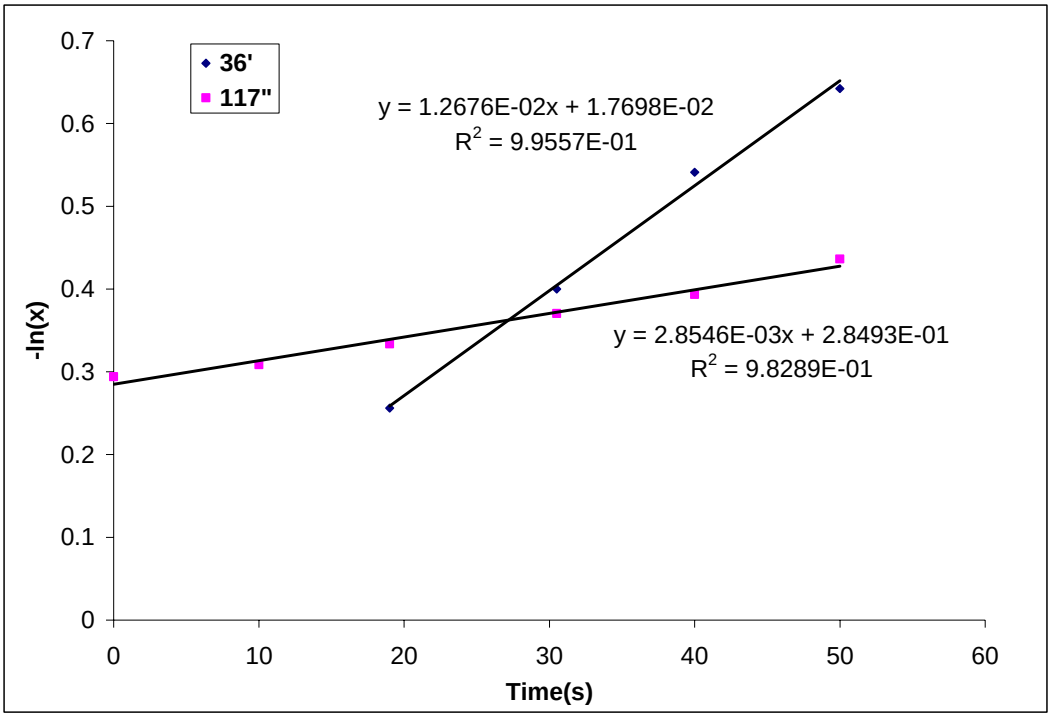

Figure A.7. Relative pseudo-first order rate constants of photo closing (250 nm) for **117'** comparing to **36'**.

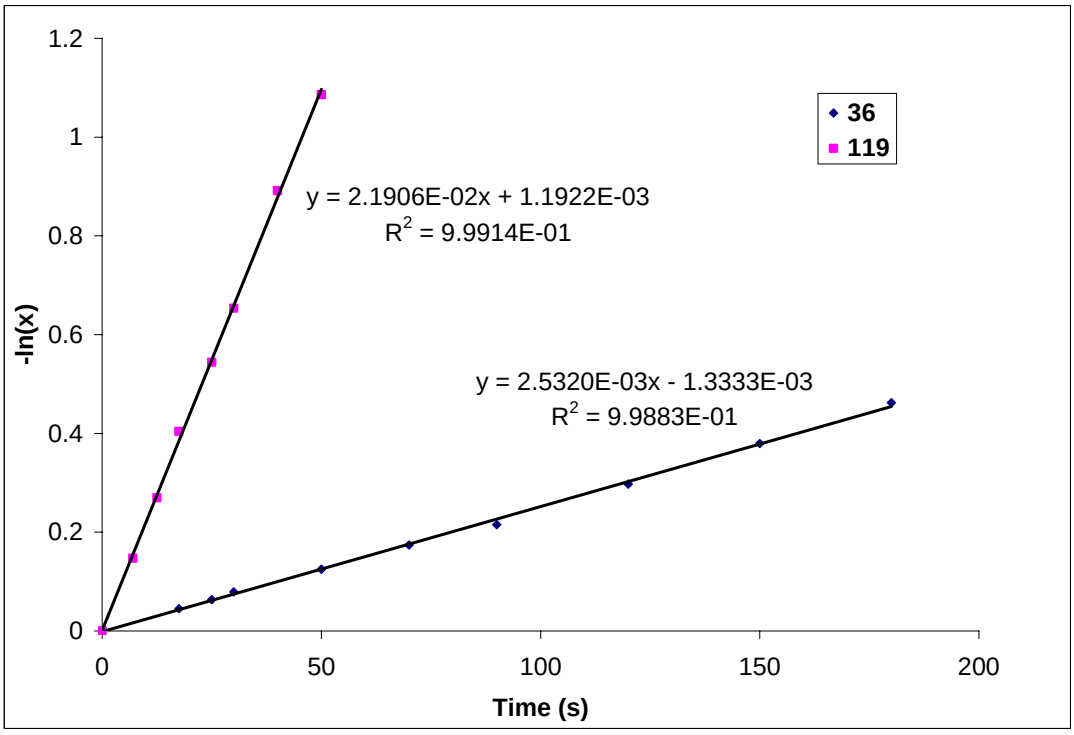

Figure A.8. Relative pseudo-first order rate constants of photo opening (>490 nm) for **118** comparing to **36**..

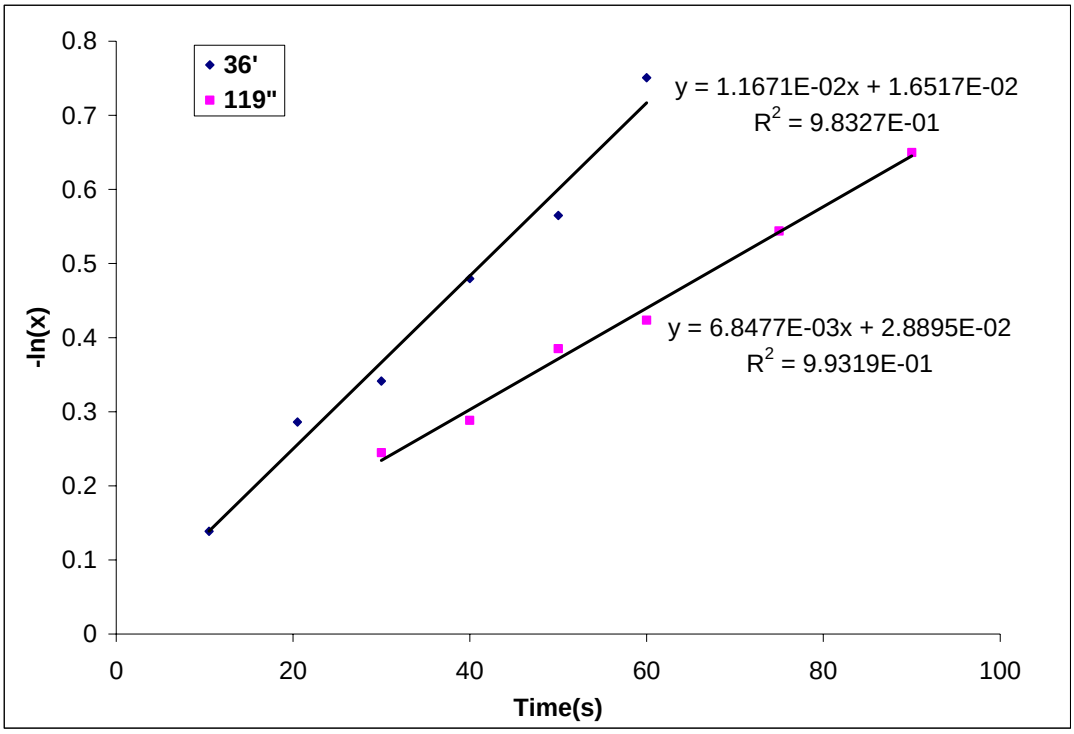

Figure A.9. Relative pseudo-first order rate constants of photo closing (250 nm) for **112'** comparing to **36'**.

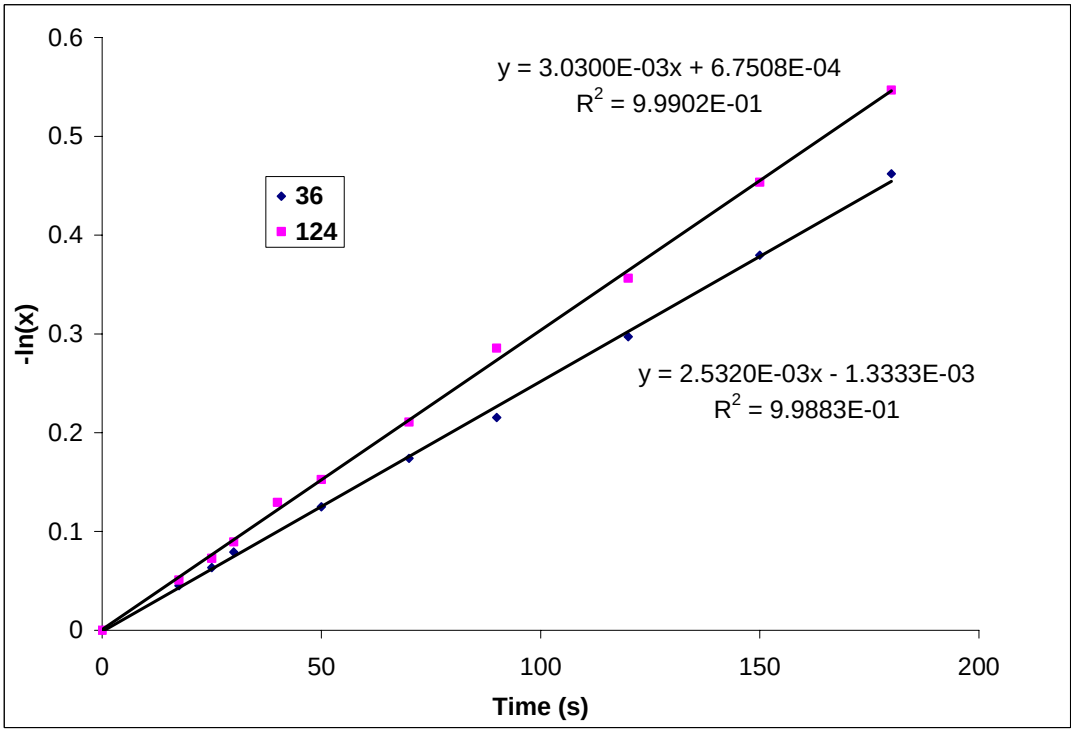

Figure A.10. Relative pseudo-first order rate constants of photo opening (>490 nm) for **124** comparing to **36**.

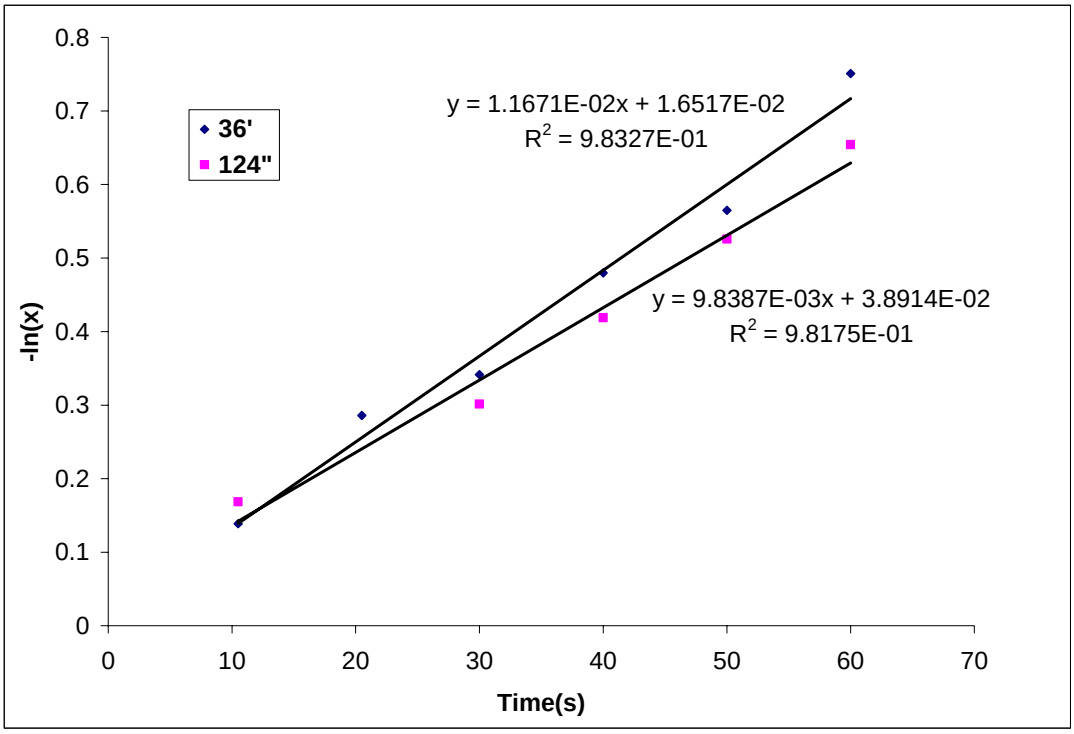

Figure A.11. Relative pseudo-first order rate constants of photo closing (250 nm) for **112'** comparing to **36'**.

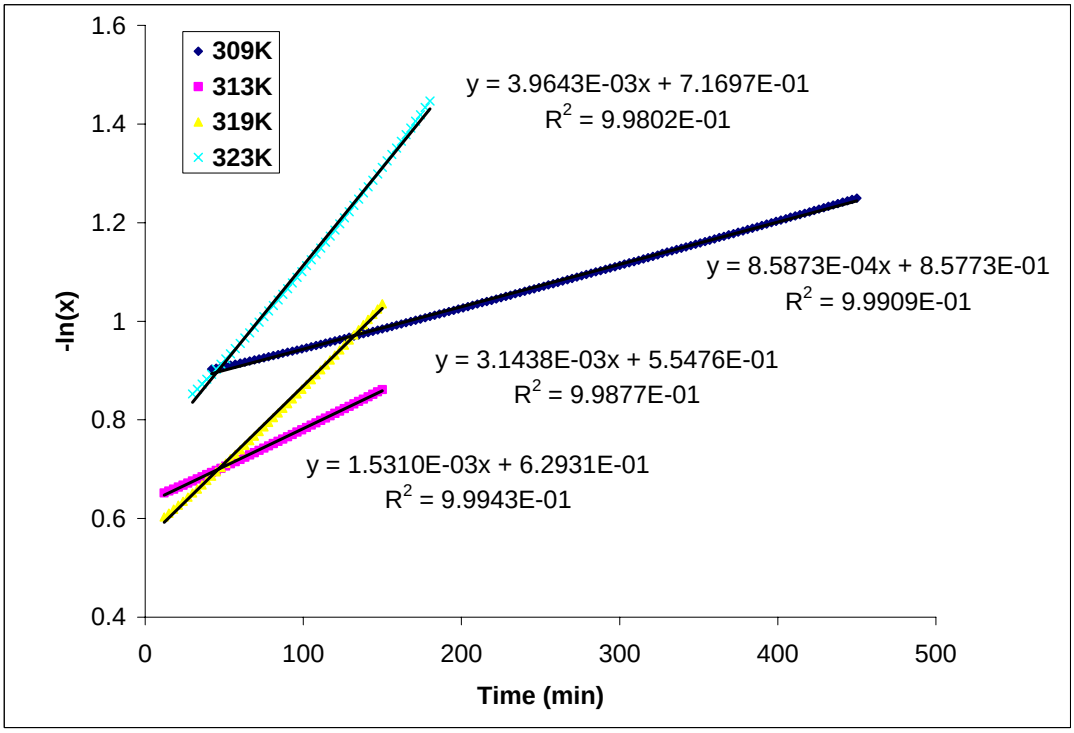

Figure A.12. Rate constants for the thermal return of **117"** in cyclohexane followed by UV-vis spectoscopy

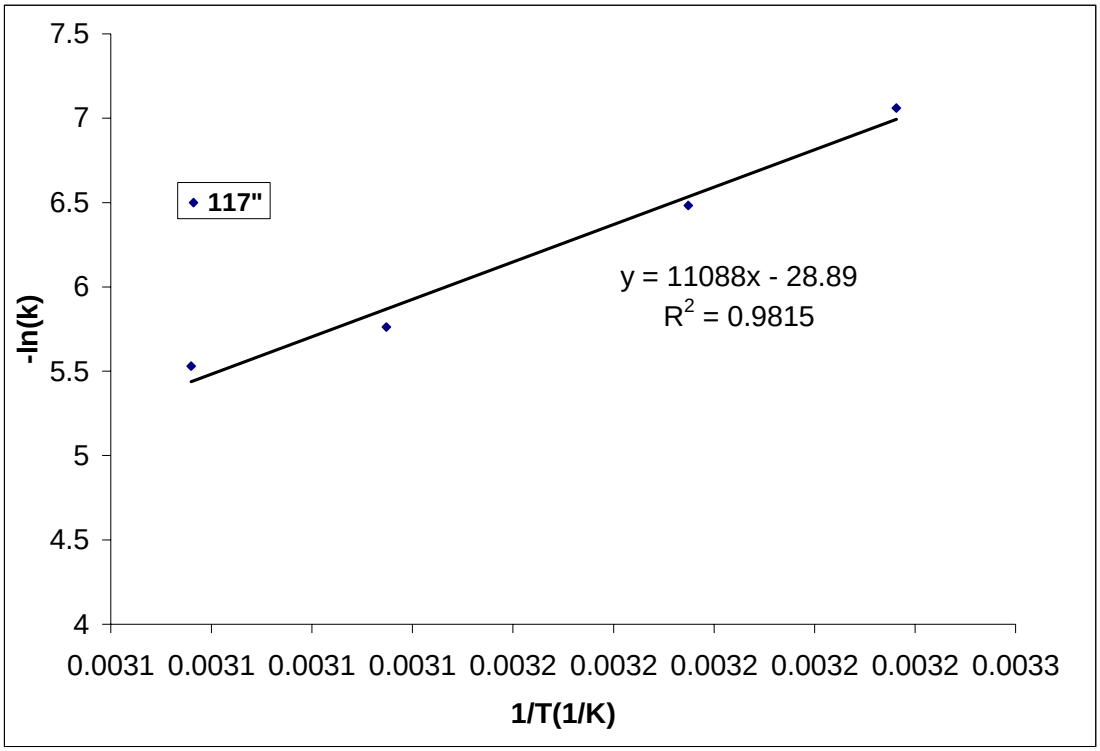

Figure A.13. The Arrhenius plot for **117”**.

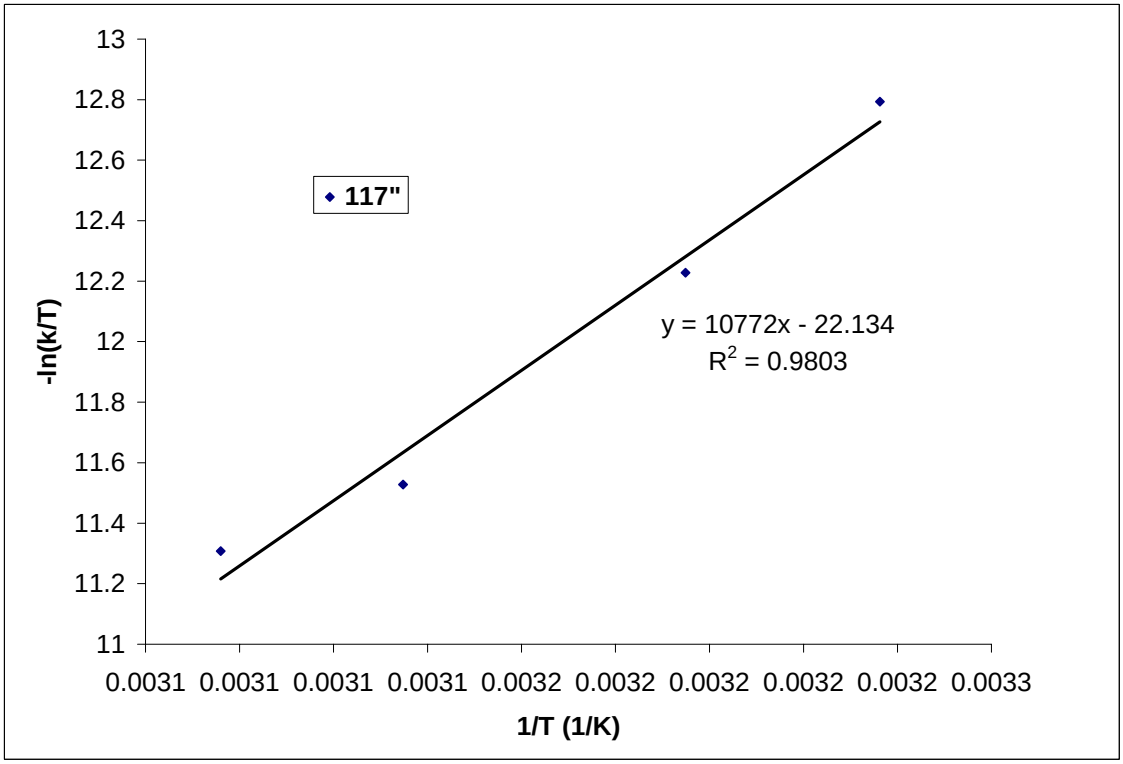

Figure A.14. The Eyring plot for **117”**.

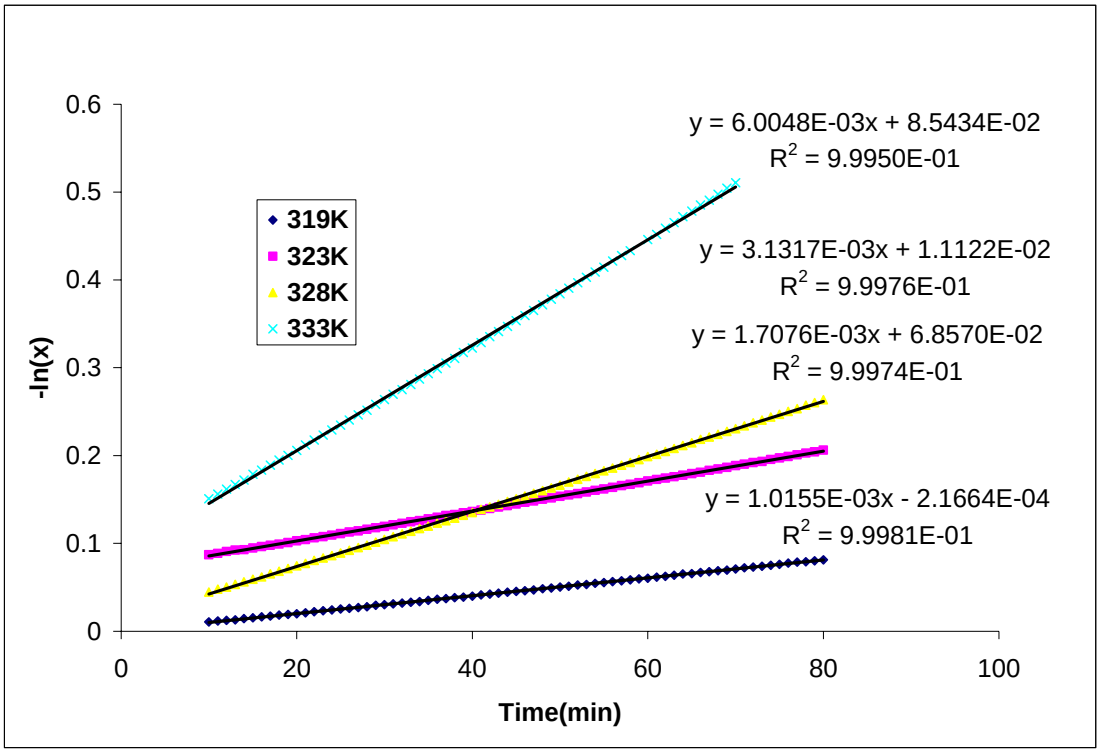

Figure A.15. Rate constants for the thermal return of **119"** in cyclohexane followed by UV-vis spectroscopy

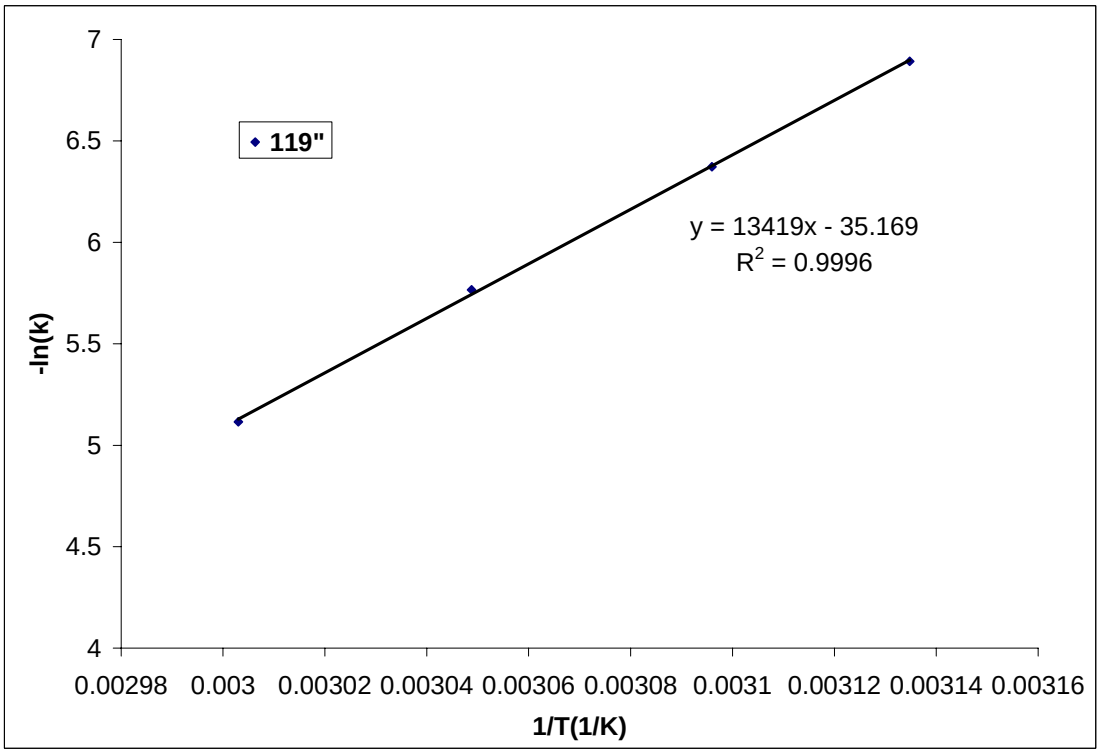

Figure A.16. The Arrhenius plot for **119"**.

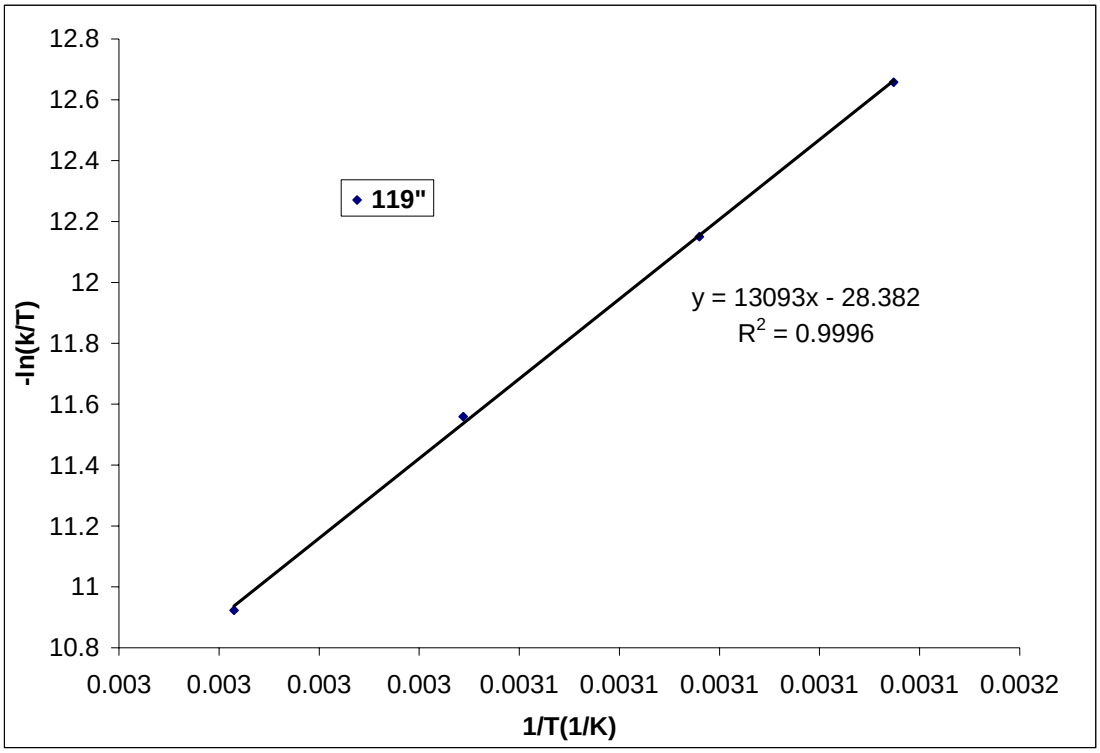

Figure A.17. The Eyring plot for **119"**.

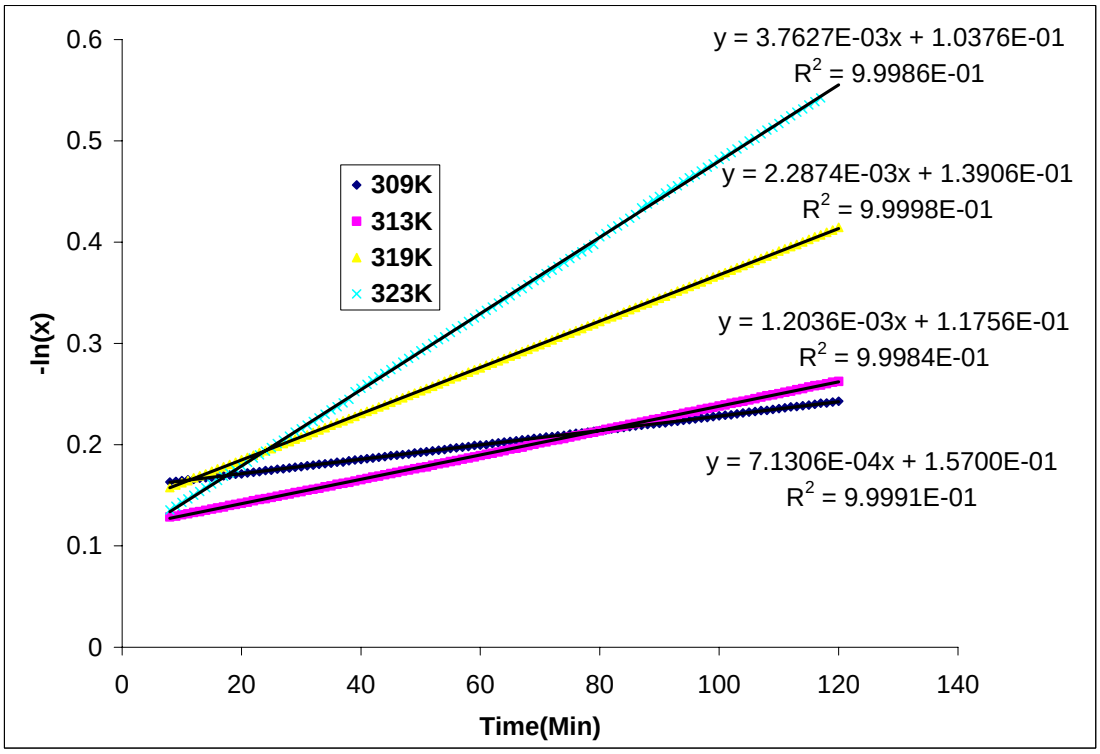

Figure A.18. Rate constants for the thermal return of **124"** in cyclohexane followed by UV-vis spectroscopy

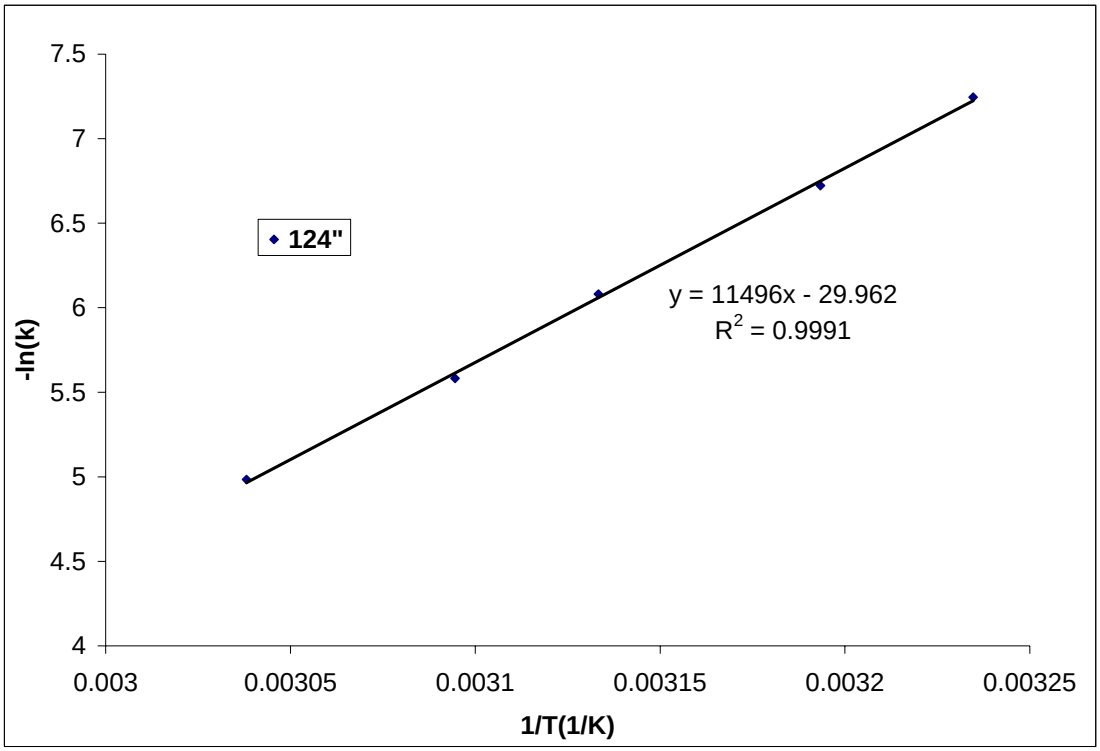

Figure A.19. The Arrhenius plot for **124”**.

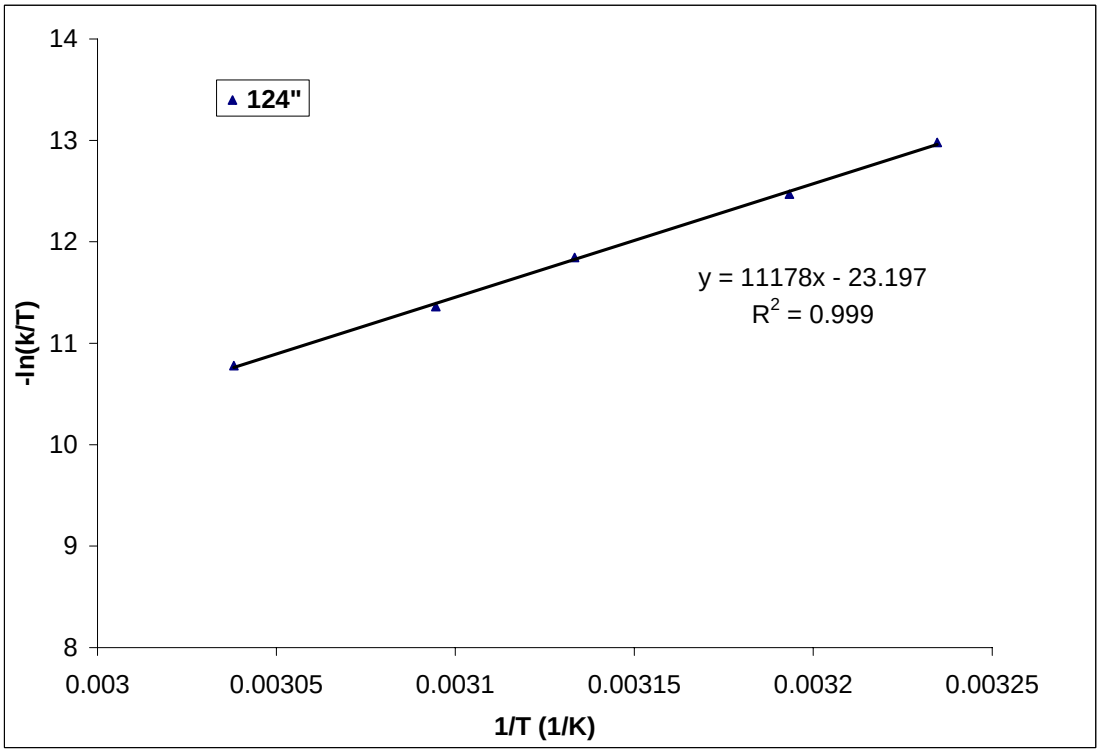

Figure A.20. The Eyring plot for **124”**.

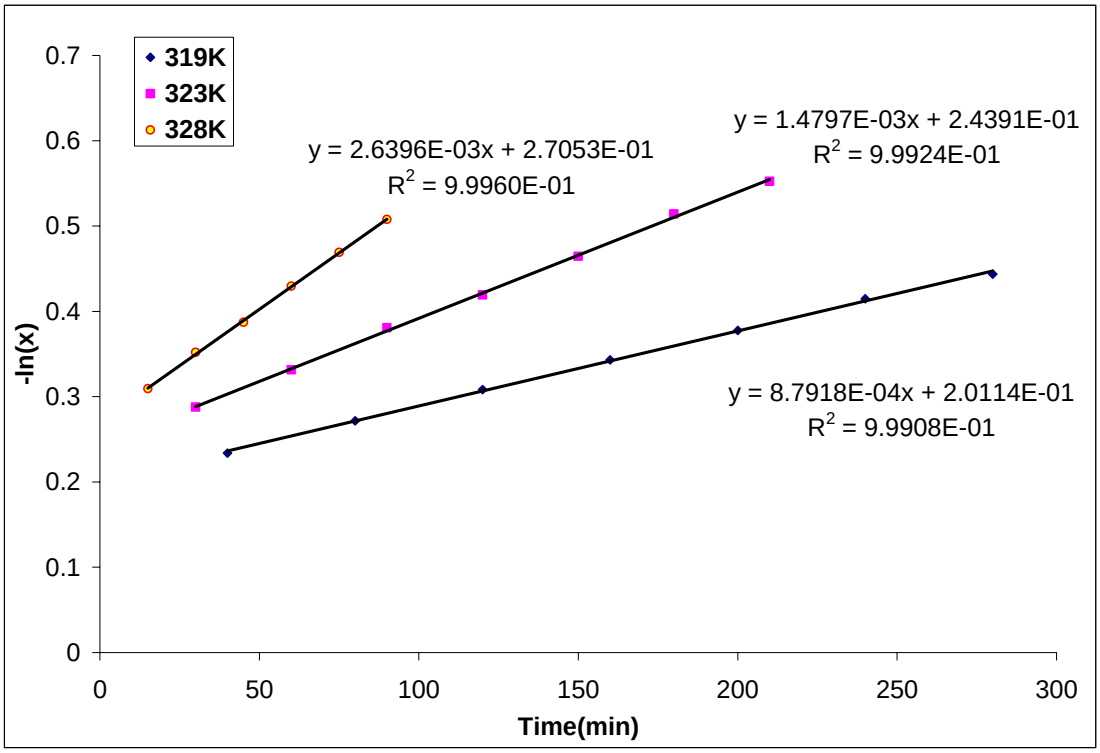

Figure A.21. Rate constants for the thermal return of **122'** on BDHP side in C_6D_6 followed by ^{1}H-NMR spectroscopy

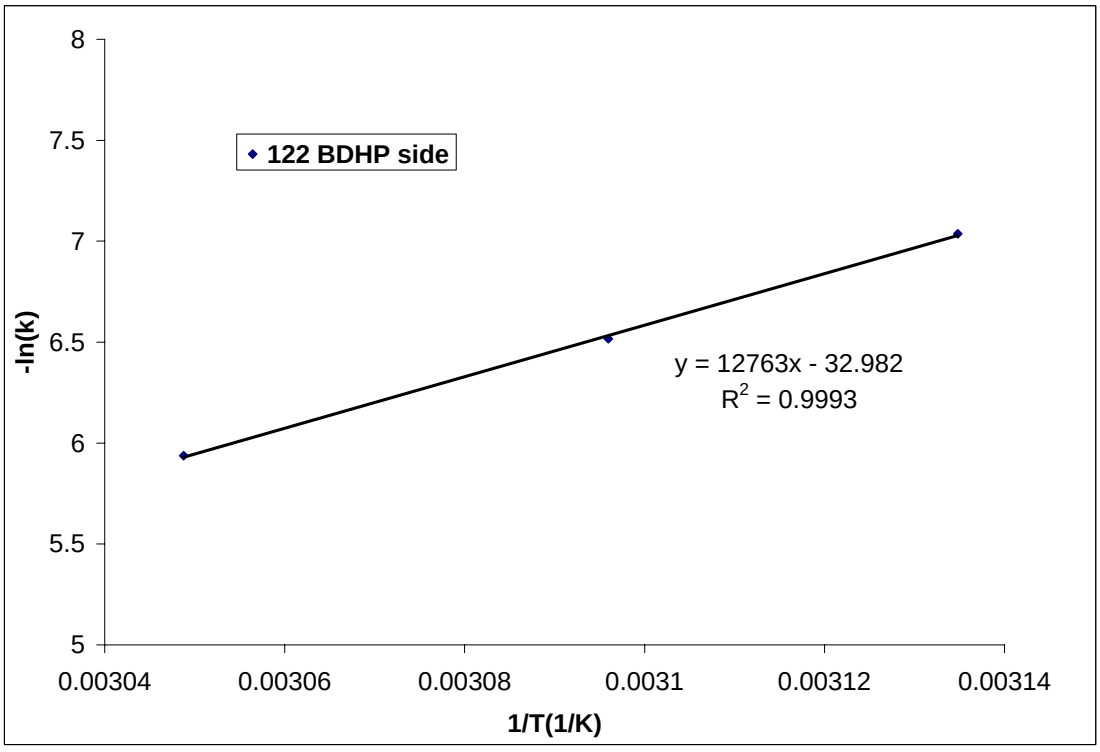

Figure A.22. The Arrhenius plot for **122'** BDHP side.

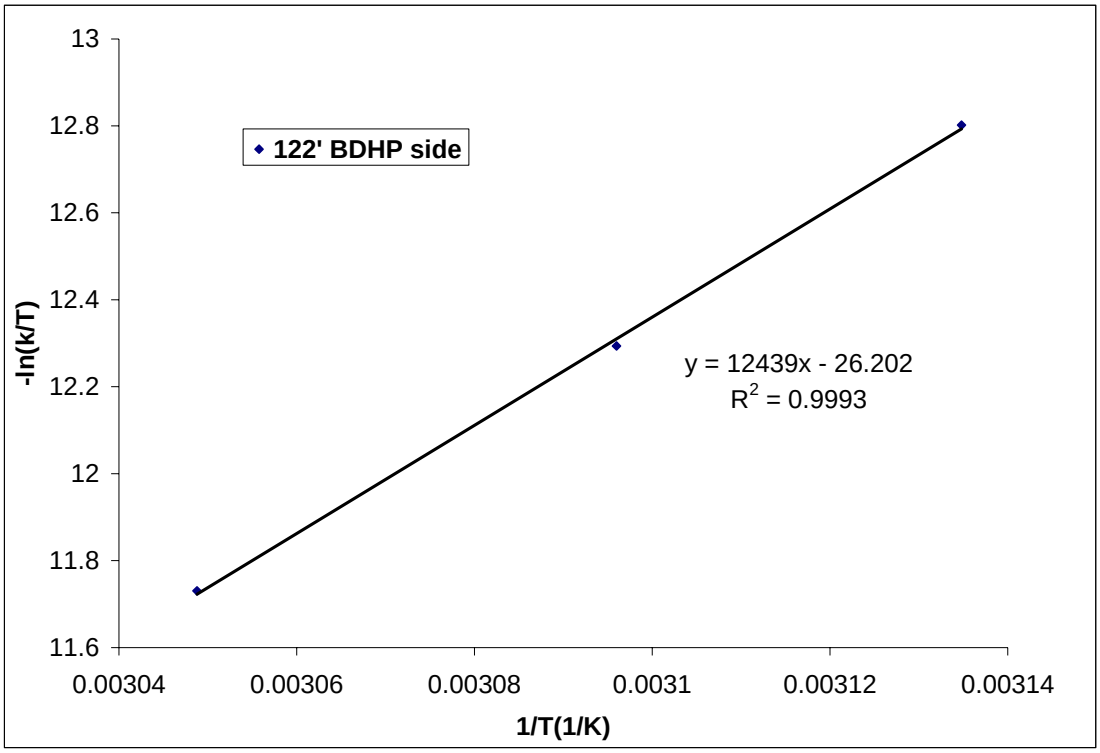

Figure A.23. The Eyring plot for **122'** BDHP side.

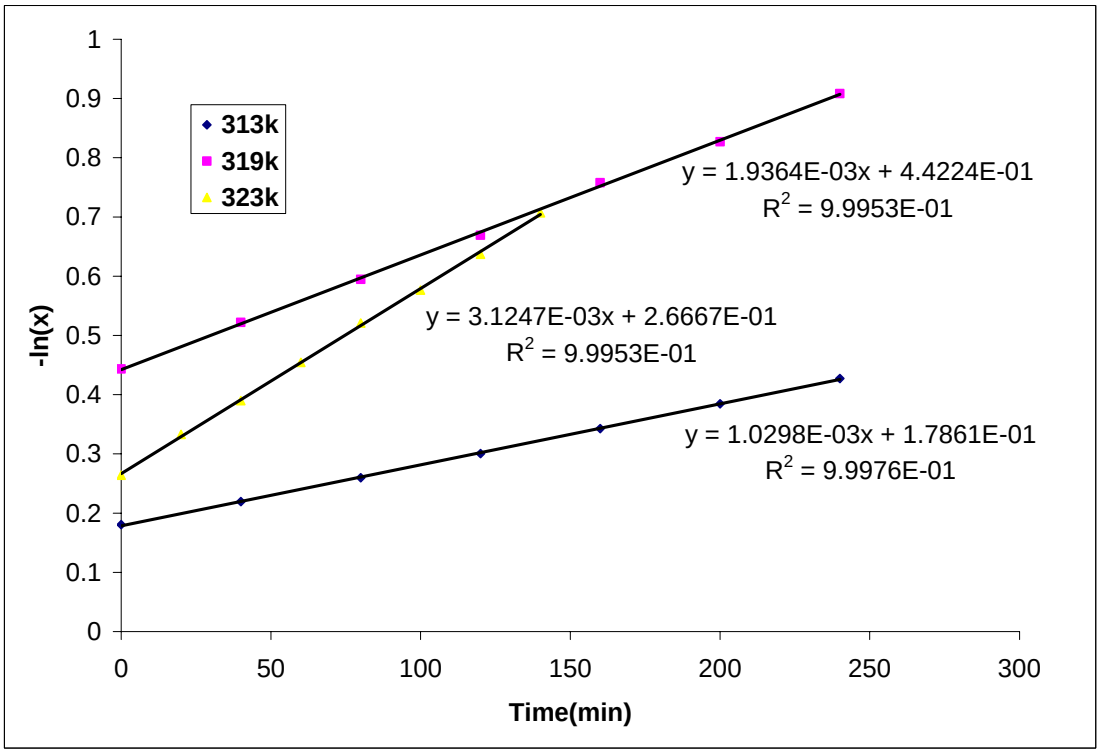

Figure A.24. Rate constants for the thermal return of **122"** on DHP side in C_6D_6 followed by ^{1}H-NMR spectroscopy

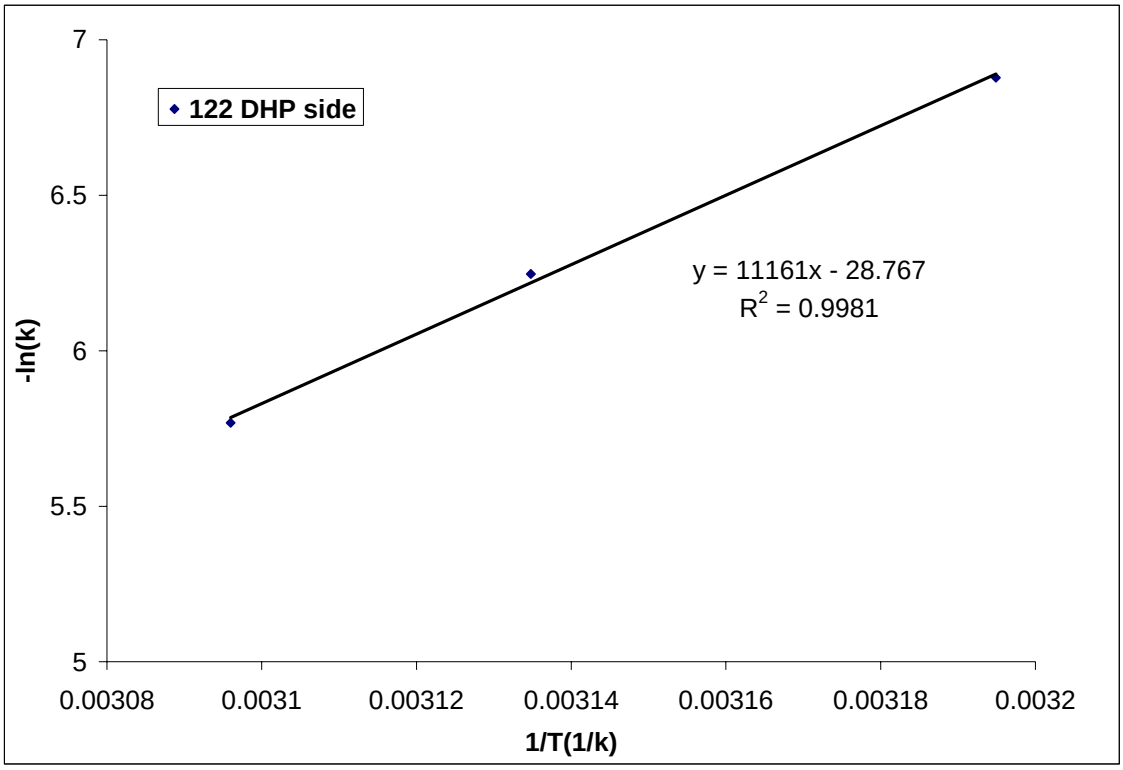

Figure A.25. The Arrhenius plot for **122** on DHP side.

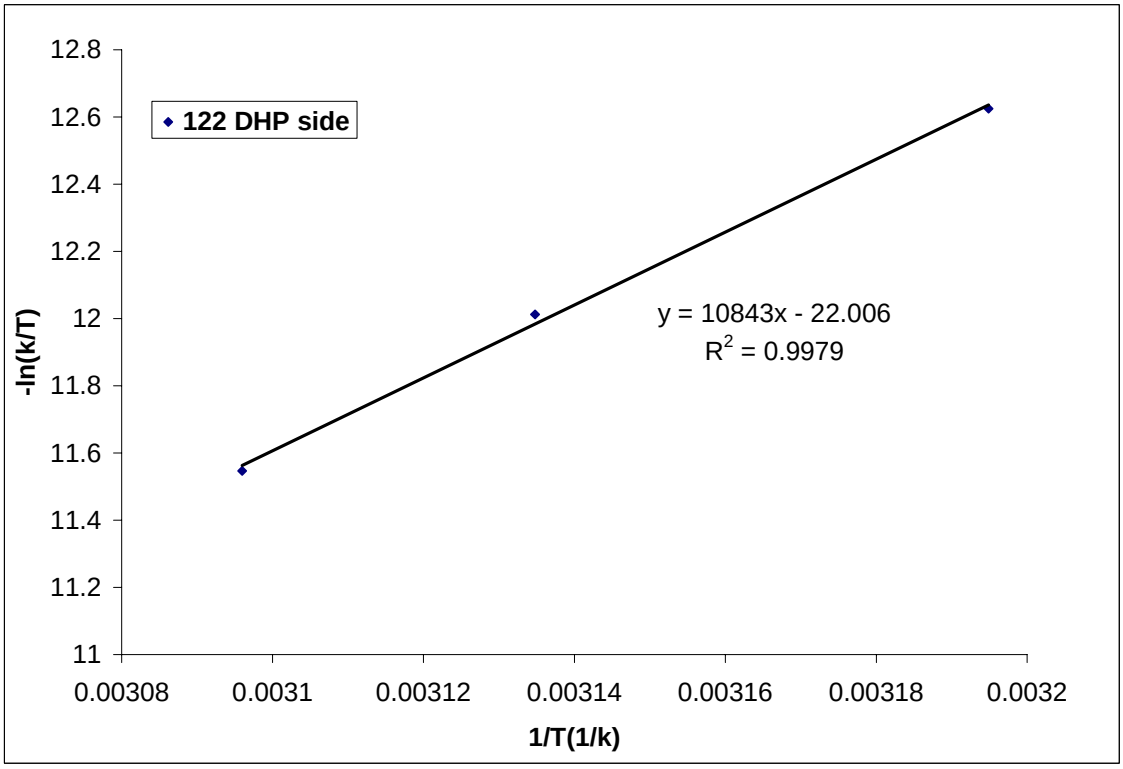

Figure A.26. The Eyring plot for **122** on DHP side.

Table A.1. Atomic coordinates (x 10^4) and equivalent isotropic displacement parameters ($Å^2$x 10^3) for cyclopentanone fused DHP **43**. U(eq) is defined as one third of the trace of the orthogonalized U^{ij} tensor.

	x	y	z	U(eq)
C(1)	-650(3)	2332(3)	871(2)	22(1)
C(2)	127(3)	2936(3)	193(3)	24(1)
C(3)	1413(3)	3996(3)	658(2)	24(1)
C(4)	2264(3)	4577(3)	-14(3)	25(1)
C(5)	3529(3)	5641(3)	495(3)	24(1)
C(6)	4081(3)	6113(3)	1663(2)	21(1)
C(7)	5313(3)	7232(3)	2229(3)	25(1)
C(8)	5824(3)	7744(3)	3420(3)	26(1)
C(9)	5051(3)	7122(3)	4121(3)	22(1)
C(10)	3818(3)	6004(3)	3654(2)	22(1)
C(11)	2984(3)	5406(3)	4331(2)	18(1)
C(12)	3307(3)	5812(3)	5634(2)	24(1)
C(13)	2106(3)	4790(3)	5895(2)	23(1)
C(14)	1116(3)	3894(3)	4748(2)	21(1)
C(15)	1721(3)	4321(3)	3815(2)	19(1)
C(16)	1122(3)	3827(3)	2631(2)	19(1)
C(17)	-111(3)	2767(3)	2076(2)	22(1)
C(22)	-2092(3)	1208(3)	371(2)	24(1)
C(23)	-3254(3)	1808(3)	1044(3)	29(1)
C(24)	-2021(3)	-125(3)	554(3)	35(1)
C(25)	-2515(3)	792(3)	-950(3)	35(1)
C(26)	7119(3)	9043(3)	3962(3)	28(1)
C(27)	8423(3)	8741(3)	3319(3)	35(1)
C(28)	6737(3)	10292(3)	3805(3)	32(1)
C(29)	7554(3)	9481(3)	5284(3)	38(1)
C(18A)	1786(4)	4745(4)	1981(3)	21(1)
C(19A)	1140(4)	6047(4)	2405(3)	21(1)
C(20A)	3434(4)	5216(4)	2305(3)	21(1)
C(21A)	4073(4)	3918(4)	1902(3)	21(1)
O(1A)	7(2)	2993(2)	4631(2)	28(1)
C(18B)	2252(16)	4270(17)	1923(13)	21(1)

C(19B)	3339(16)	3300(16)	1742(13)	21(1)
C(20B)	2973(16)	5808(17)	2557(13)	21(1)
C(21B)	1925(15)	6741(16)	2755(13)	21(1)
O(1B)	4291(17)	6690(20)	6322(17)	28(1)

Table A.2. Bond lengths [Å] and angles [°] for cyclopentanone fused DHP **43**.

C(1)-C(2)	1.389(4)	C(14)-C(15)	1.492(4)
C(1)-C(17)	1.422(4)	C(14)-H(14A)	0.9559
C(1)-C(22)	1.539(4)	C(14)-H(14B)	0.9603
C(2)-C(3)	1.400(4)	C(15)-C(16)	1.404(4)
C(2)-H(2A)	0.9500	C(16)-C(17)	1.378(4)
C(3)-C(4)	1.404(4)	C(16)-C(18B)	1.531(14)
C(3)-C(18A)	1.506(5)	C(16)-C(18A)	1.544(4)
C(3)-C(18B)	1.630(15)	C(17)-H(17A)	0.9500
C(4)-C(5)	1.393(4)	C(22)-C(23)	1.533(4)
C(4)-H(4A)	0.9500	C(22)-C(25)	1.535(4)
C(5)-C(6)	1.376(4)	C(22)-C(24)	1.540(4)
C(5)-H(5A)	0.9500	C(23)-H(23A)	0.9800
C(6)-C(7)	1.407(4)	C(23)-H(23B)	0.9800
C(6)-C(20A)	1.516(4)	C(23)-H(23C)	0.9800
C(6)-C(20B)	1.641(14)	C(24)-H(24A)	0.9800
C(7)-C(8)	1.388(4)	C(24)-H(24B)	0.9800
C(7)-H(7A)	0.9500	C(24)-H(24C)	0.9800
C(8)-C(9)	1.421(4)	C(25)-H(25A)	0.9800
C(8)-C(26)	1.539(4)	C(25)-H(25B)	0.9800
C(9)-C(10)	1.395(4)	C(25)-H(25C)	0.9800
C(9)-H(9A)	0.9500	C(26)-C(29)	1.534(4)
C(10)-C(11)	1.411(4)	C(26)-C(28)	1.541(4)
C(10)-C(20B)	1.480(14)	C(26)-C(27)	1.546(4)
C(10)-C(20A)	1.539(5)	C(27)-H(27A)	0.9800
C(11)-C(15)	1.403(4)	C(27)-H(27B)	0.9800
C(11)-C(12)	1.503(4)	C(27)-H(27C)	0.9800
C(12)-O(1B)	1.195(11)	C(28)-H(28A)	0.9800
C(12)-C(13)	1.537(4)	C(28)-H(28B)	0.9800
C(12)-H(12A)	1.0656	C(28)-H(28C)	0.9800
C(12)-H(12B)	1.0690	C(29)-H(29A)	0.9800
C(13)-C(14)	1.513(4)	C(29)-H(29B)	0.9800
C(13)-H(13A)	0.9900	C(29)-H(29C)	0.9800
C(13)-H(13B)	0.9900	C(18A)-C(20A)	1.547(5)
C(14)-O(1A)	1.226(3)	C(18A)-C(19A)	1.565(5)

C(19A)-H(19A)	0.9800
C(19A)-H(19B)	0.9800
C(19A)-H(19C)	0.9800
C(20A)-C(21A)	1.558(5)
C(21A)-H(21A)	0.9800
C(21A)-H(21B)	0.9800
C(21A)-H(21C)	0.9800
O(1A)-H(14A)	1.0110
O(1A)-H(14B)	1.0417
C(18B)-C(20B)	1.49(2)
C(18B)-C(19B)	1.60(2)
C(19B)-H(19D)	0.9800
C(19B)-H(19E)	0.9800
C(19B)-H(19F)	0.9800
C(20B)-C(21B)	1.54(2)
C(21B)-H(21D)	0.9800
C(21B)-H(21E)	0.9800
C(21B)-H(21F)	0.9800
O(1B)-H(12A)	1.0350
O(1B)-H(12B)	1.0989

C(2)-C(1)-C(17)	119.4(2)
C(2)-C(1)-C(22)	122.5(3)
C(17)-C(1)-C(22)	118.1(2)
C(1)-C(2)-C(3)	122.6(3)
C(1)-C(2)-H(2A)	118.7
C(3)-C(2)-H(2A)	118.7
C(2)-C(3)-C(4)	124.1(3)
C(2)-C(3)-C(18A)	118.3(3)
C(4)-C(3)-C(18A)	116.7(3)
C(2)-C(3)-C(18B)	119.3(5)
C(4)-C(3)-C(18B)	114.0(5)
C(5)-C(4)-C(3)	121.8(3)
C(5)-C(4)-H(4A)	119.1
C(3)-C(4)-H(4A)	119.1
C(6)-C(5)-C(4)	122.4(3)
C(6)-C(5)-H(5A)	118.8
C(4)-C(5)-H(5A)	118.8
C(5)-C(6)-C(7)	124.3(2)
C(5)-C(6)-C(20A)	116.4(3)
C(7)-C(6)-C(20A)	118.7(3)
C(5)-C(6)-C(20B)	117.2(6)
C(7)-C(6)-C(20B)	114.3(6)
C(8)-C(7)-C(6)	123.9(3)
C(8)-C(7)-H(7A)	118.1
C(6)-C(7)-H(7A)	118.1
C(7)-C(8)-C(9)	118.5(3)
C(7)-C(8)-C(26)	119.3(2)
C(9)-C(8)-C(26)	122.0(3)
C(10)-C(9)-C(8)	122.7(3)
C(10)-C(9)-H(9A)	118.7
C(8)-C(9)-H(9A)	118.7
C(9)-C(10)-C(11)	124.3(3)
C(9)-C(10)-C(20B)	118.5(6)
C(11)-C(10)-C(20B)	112.2(6)
C(9)-C(10)-C(20A)	119.1(3)
C(11)-C(10)-C(20A)	116.1(2)
C(15)-C(11)-C(10)	121.5(3)
C(15)-C(11)-C(12)	112.4(2)
C(10)-C(11)-C(12)	126.1(2)
O(1B)-C(12)-C(11)	128.9(10)
O(1B)-C(12)-C(13)	126.7(10)
C(11)-C(12)-C(13)	104.4(2)
O(1B)-C(12)-H(12A)	54.1
C(11)-C(12)-H(12A)	113.9
C(13)-C(12)-H(12A)	110.1
O(1B)-C(12)-H(12B)	57.7
C(11)-C(12)-H(12B)	109.9
C(13)-C(12)-H(12B)	106.2
H(12A)-C(12)-H(12B)	111.8
C(14)-C(13)-C(12)	106.8(2)
C(14)-C(13)-H(13A)	110.4

C(12)-C(13)-H(13A)	110.4	H(23B)-C(23)-H(23C)	109.5
C(14)-C(13)-H(13B)	110.4	C(22)-C(24)-H(24A)	109.5
C(12)-C(13)-H(13B)	110.4	C(22)-C(24)-H(24B)	109.5
H(13A)-C(13)-H(13B)	108.6	H(24A)-C(24)-H(24B)	109.5
O(1A)-C(14)-C(15)	127.1(3)	C(22)-C(24)-H(24C)	109.5
O(1A)-C(14)-C(13)	125.1(2)	H(24A)-C(24)-H(24C)	109.5
C(15)-C(14)-C(13)	107.8(2)	H(24B)-C(24)-H(24C)	109.5
O(1A)-C(14)-H(14A)	53.5	C(22)-C(25)-H(25A)	109.5
C(15)-C(14)-H(14A)	110.0	C(22)-C(25)-H(25B)	109.5
C(13)-C(14)-H(14A)	110.3	H(25A)-C(25)-H(25B)	109.5
O(1A)-C(14)-H(14B)	55.3	C(22)-C(25)-H(25C)	109.5
C(15)-C(14)-H(14B)	109.6	H(25A)-C(25)-H(25C)	109.5
C(13)-C(14)-H(14B)	110.3	H(25B)-C(25)-H(25C)	109.5
H(14A)-C(14)-H(14B)	108.7	C(29)-C(26)-C(8)	113.1(2)
C(11)-C(15)-C(16)	123.7(2)	C(29)-C(26)-C(28)	108.0(3)
C(11)-C(15)-C(14)	108.5(2)	C(8)-C(26)-C(28)	108.7(2)
C(16)-C(15)-C(14)	127.7(2)	C(29)-C(26)-C(27)	108.2(2)
C(17)-C(16)-C(15)	126.3(2)	C(8)-C(26)-C(27)	110.0(3)
C(17)-C(16)-C(18B)	121.2(6)	C(28)-C(26)-C(27)	108.8(2)
C(15)-C(16)-C(18B)	109.8(6)	C(26)-C(27)-H(27A)	109.5
C(17)-C(16)-C(18A)	117.9(3)	C(26)-C(27)-H(27B)	109.5
C(15)-C(16)-C(18A)	114.9(2)	H(27A)-C(27)-H(27B)	109.5
C(16)-C(17)-C(1)	122.8(2)	C(26)-C(27)-H(27C)	109.5
C(16)-C(17)-H(17A)	118.6	H(27A)-C(27)-H(27C)	109.5
C(1)-C(17)-H(17A)	118.6	H(27B)-C(27)-H(27C)	109.5
C(23)-C(22)-C(25)	108.5(2)	C(26)-C(28)-H(28A)	109.5
C(23)-C(22)-C(1)	108.3(2)	C(26)-C(28)-H(28B)	109.5
C(25)-C(22)-C(1)	112.6(2)	H(28A)-C(28)-H(28B)	109.5
C(23)-C(22)-C(24)	108.9(2)	C(26)-C(28)-H(28C)	109.5
C(25)-C(22)-C(24)	108.6(2)	H(28A)-C(28)-H(28C)	109.5
C(1)-C(22)-C(24)	109.9(2)	H(28B)-C(28)-H(28C)	109.5
C(22)-C(23)-H(23A)	109.5	C(26)-C(29)-H(29A)	109.5
C(22)-C(23)-H(23B)	109.5	C(26)-C(29)-H(29B)	109.5
H(23A)-C(23)-H(23B)	109.5	H(29A)-C(29)-H(29B)	109.5
C(22)-C(23)-H(23C)	109.5	C(26)-C(29)-H(29C)	109.5
H(23A)-C(23)-H(23C)	109.5	H(29A)-C(29)-H(29C)	109.5

H(29B)-C(29)-H(29C)	109.5	C(18B)-C(19B)-H(19D)	109.5
C(3)-C(18A)-C(16)	113.0(3)	C(18B)-C(19B)-H(19E)	109.5
C(3)-C(18A)-C(20A)	109.1(3)	H(19D)-C(19B)-H(19E)	109.5
C(16)-C(18A)-C(20A)	109.5(3)	C(18B)-C(19B)-H(19F)	109.5
C(3)-C(18A)-C(19A)	108.0(3)	H(19D)-C(19B)-H(19F)	109.5
C(16)-C(18A)-C(19A)	106.2(3)	H(19E)-C(19B)-H(19F)	109.5
C(20A)-C(18A)-C(19A)	111.0(3)	C(10)-C(20B)-C(18B)	107.3(11)
C(6)-C(20A)-C(10)	112.3(3)	C(10)-C(20B)-C(21B)	114.2(12)
C(6)-C(20A)-C(18A)	109.4(3)	C(18B)-C(20B)-C(21B)	113.0(13)
C(10)-C(20A)-C(18A)	109.3(3)	C(10)-C(20B)-C(6)	108.7(9)
C(6)-C(20A)-C(21A)	107.0(3)	C(18B)-C(20B)-C(6)	103.2(11)
C(10)-C(20A)-C(21A)	107.9(3)	C(21B)-C(20B)-C(6)	109.8(10)
C(18A)-C(20A)-C(21A)	110.9(3)	C(20B)-C(21B)-H(21D)	109.5
C(14)-O(1A)-H(14A)	49.4	C(20B)-C(21B)-H(21E)	109.5
C(14)-O(1A)-H(14B)	49.3	H(21D)-C(21B)-H(21E)	109.5
H(14A)-O(1A)-H(14B)	98.7	C(20B)-C(21B)-H(21F)	109.5
C(20B)-C(18B)-C(16)	109.6(11)	H(21D)-C(21B)-H(21F)	109.5
C(20B)-C(18B)-C(19B)	113.0(13)	H(21E)-C(21B)-H(21F)	109.5
C(16)-C(18B)-C(19B)	107.4(11)	C(12)-O(1B)-H(12A)	56.5
C(20B)-C(18B)-C(3)	108.7(11)	C(12)-O(1B)-H(12B)	55.4
C(16)-C(18B)-C(3)	107.1(9)	H(12A)-O(1B)-H(12B)	111.8
C(19B)-C(18B)-C(3)	110.8(10)		

Table A.3. Anisotropic displacement parameters ($Å^2 x\ 10^3$) for cyclopentanone fused DHP **43**. The anisotropic displacement factor exponent takes the form: $-2\pi^2[\ h^2\ a^{*2}U^{11} + ... + 2\ h\ k\ a^*\ b^*\ U^{12}\ ]$

	U^{11}	U^{22}	U^{33}	U^{23}	U^{13}	U^{12}
C(1)	14(2)	26(2)	28(2)	12(1)	7(1)	5(1)
C(2)	18(2)	34(2)	23(2)	14(1)	6(1)	3(1)
C(3)	20(2)	33(2)	23(2)	16(1)	8(1)	4(1)
C(4)	22(2)	36(2)	25(2)	20(2)	11(1)	7(1)
C(5)	16(2)	31(2)	33(2)	22(2)	12(1)	5(1)
C(6)	13(2)	31(2)	30(2)	22(1)	10(1)	7(1)
C(7)	17(2)	33(2)	35(2)	24(2)	13(1)	5(1)
C(8)	16(2)	29(2)	38(2)	20(2)	6(1)	4(1)
C(9)	14(2)	29(2)	26(2)	16(1)	2(1)	3(1)
C(10)	13(2)	30(2)	28(2)	18(1)	4(1)	4(1)
C(11)	13(1)	23(2)	24(2)	14(1)	5(1)	7(1)
C(12)	20(2)	30(2)	25(2)	16(1)	9(1)	4(1)
C(13)	19(2)	32(2)	26(2)	21(1)	11(1)	7(1)
C(14)	16(2)	27(2)	28(2)	18(1)	9(1)	5(1)
C(15)	12(2)	24(2)	28(2)	16(1)	8(1)	6(1)
C(16)	12(2)	24(2)	26(2)	15(1)	10(1)	6(1)
C(17)	12(2)	29(2)	32(2)	20(1)	12(1)	7(1)
C(22)	14(2)	29(2)	29(2)	15(1)	5(1)	0(1)
C(23)	10(2)	40(2)	37(2)	18(2)	5(1)	0(1)
C(24)	20(2)	32(2)	52(2)	23(2)	5(2)	-4(1)
C(25)	23(2)	39(2)	35(2)	16(2)	5(1)	-5(1)
C(26)	14(2)	29(2)	43(2)	21(2)	6(1)	-2(1)
C(27)	10(2)	39(2)	61(2)	30(2)	8(2)	0(1)
C(28)	13(2)	32(2)	52(2)	20(2)	8(1)	-1(1)
C(29)	18(2)	39(2)	51(2)	21(2)	0(2)	-6(1)
C(18A)	13(1)	30(1)	26(1)	19(1)	9(1)	5(1)
C(19A)	13(1)	30(1)	26(1)	19(1)	9(1)	5(1)
C(20A)	13(1)	30(1)	26(1)	19(1)	9(1)	5(1)
C(21A)	13(1)	30(1)	26(1)	19(1)	9(1)	5(1)
O(1A)	18(1)	42(1)	29(1)	25(1)	7(1)	-4(1)
C(18B)	13(1)	30(1)	26(1)	19(1)	9(1)	5(1)

C(19B)	13(1)	30(1)	26(1)	19(1)	9(1)	5(1)
C(20B)	13(1)	30(1)	26(1)	19(1)	9(1)	5(1)
C(21B)	13(1)	30(1)	26(1)	19(1)	9(1)	5(1)
O(1B)	18(1)	42(1)	29(1)	25(1)	7(1)	-4(1)

Table A. 4. Hydrogen coordinates (x 10^4) and isotropic displacement parameters ($Å^2$x 10^3) for cyclopentanone fused DHP **43**.

	x	y	z	U(eq)
H(2A)	-227	2617	-618	29
H(4A)	1970	4235	-838	30
H(5A)	4029	6055	19	28
H(7A)	5825	7664	1769	30
H(9A)	5387	7482	4939	26
H(13A)	2511	4189	6186	28
H(13B)	1579	5322	6505	28
H(17A)	-623	2307	2518	26
H(23A)	-3247	2704	994	44
H(23B)	-3064	1966	1873	44
H(23C)	-4193	1138	693	44
H(24A)	-1329	-554	83	52
H(24B)	-2968	-800	305	52
H(24C)	-1721	131	1391	52
H(25A)	-2628	1619	-1073	52
H(25B)	-3421	55	-1231	52
H(25C)	-1766	437	-1390	52
H(27A)	8716	7990	3459	52
H(27B)	9218	9598	3622	52
H(27C)	8162	8443	2470	52
H(28A)	5903	10484	4200	49
H(28B)	6513	10057	2962	49
H(28C)	7551	11129	4153	49
H(29A)	7793	8697	5407	57
H(29B)	6756	9725	5714	57
H(29C)	8389	10301	5578	57
H(12A)	3316	6875	6167	31
H(12B)	4283	5582	5820	31
H(19A)	1572	6695	2052	31
H(19B)	1341	6535	3267	31

H(19C)	102	5727	2162	31
H(21A)	3834	3392	1044	31
H(21B)	3672	3304	2294	31
H(21C)	5117	4241	2114	31
H(14A)	178	4034	4826	31
H(14B)	1051	2913	4534	31
H(19D)	3994	3638	2474	31
H(19E)	3890	3346	1104	31
H(19F)	2798	2323	1536	31
H(21D)	1184	6462	3196	31
H(21E)	1477	6624	1989	31
H(21F)	2448	7731	3204	31

Table A.5. Atomic coordinates (x 10^4) and equivalent isotropic displacement parameters ($Å^2$x 10^3) for cyclopentadienone fused DHP **46**. U(eq) is defined as one third of the trace of the orthogonalized U^{ij} tensor.

	x	y	z	U(eq)
C(1)	5103(1)	2768(4)	874(1)	32(1)
C(2)	3702(1)	2578(4)	319(1)	33(1)
C(3)	4060(2)	5965(4)	840(1)	36(1)
C(4)	4124(1)	3477(3)	850(1)	25(1)
C(5)	3664(1)	2642(3)	1362(1)	21(1)
C(6)	2917(1)	1380(3)	1333(1)	22(1)
C(7)	2494(1)	637(3)	1810(1)	19(1)
C(8)	1730(1)	-565(3)	1817(1)	22(1)
C(9)	1175(1)	-1442(4)	1353(1)	28(1)
C(10)	465(1)	-2696(3)	1611(1)	26(1)
C(11)	566(1)	-2625(3)	2160(1)	22(1)
C(12)	1341(1)	-1295(3)	2317(1)	21(1)
C(13)	1678(1)	-758(3)	2827(1)	22(1)
C(14)	1365(1)	-1520(3)	3333(1)	21(1)
C(15)	1763(1)	-1003(3)	3827(1)	21(1)
C(16)	1463(1)	-1918(4)	4377(1)	27(1)
C(17)	651(2)	-3370(4)	4314(1)	36(1)
C(18)	2232(2)	-3240(4)	4634(1)	36(1)
C(19)	1228(1)	-29(4)	4760(1)	31(1)
C(20)	2526(1)	392(3)	3832(1)	24(1)
C(21)	2882(1)	1220(3)	3372(1)	21(1)
C(22)	3653(1)	2552(3)	3372(1)	25(1)
C(23)	4025(1)	3243(3)	2899(1)	24(1)
C(24)	3682(1)	2614(3)	2371(1)	21(1)
C(25)	4025(1)	3280(3)	1890(1)	21(1)
C(26A)	3003(2)	771(5)	2361(1)	19(1)
C(27A)	3519(2)	-1401(5)	2422(1)	19(1)
C(28A)	2355(2)	1099(5)	2833(1)	19(1)
C(29A)	1849(2)	3248(5)	2776(1)	19(1)
O(1A)	1271(1)	-1193(3)	860(1)	37(1)

C(26B)	2713(5)	1738(13)	2355(3)	24(1)
C(27B)	2048(4)	3646(11)	2420(3)	24(1)
C(28B)	2653(5)	170(13)	2828(3)	24(1)
C(29B)	3336(4)	-1743(11)	2759(3)	24(1)
O(1B)	99(10)	-3520(30)	2467(5)	37(1)

Table A.6. Bond lengths [Å] and angles [°] for cyclopentadienone fused DHP **46**.

C(1)-C(4)	1.542(3)	C(14)-C(15)	1.370(3)
C(1)-H(1A)	0.9800	C(14)-H(14)	0.9500
C(1)-H(1B)	0.9800	C(15)-C(20)	1.439(3)
C(1)-H(1C)	0.9800	C(15)-C(16)	1.536(3)
C(2)-C(4)	1.532(3)	C(16)-C(17)	1.524(3)
C(2)-H(2A)	0.9800	C(16)-C(18)	1.539(3)
C(2)-H(2B)	0.9800	C(16)-C(19)	1.542(3)
C(2)-H(2C)	0.9800	C(17)-H(17A)	0.9800
C(3)-C(4)	1.539(3)	C(17)-H(17B)	0.9800
C(3)-H(3A)	0.9800	C(17)-H(17C)	0.9800
C(3)-H(3B)	0.9800	C(18)-H(18A)	0.9800
C(3)-H(3C)	0.9800	C(18)-H(18B)	0.9800
C(4)-C(5)	1.534(3)	C(18)-H(18C)	0.9800
C(5)-C(6)	1.372(3)	C(19)-H(19A)	0.9800
C(5)-C(25)	1.440(3)	C(19)-H(19B)	0.9800
C(6)-C(7)	1.419(3)	C(19)-H(19C)	0.9800
C(6)-H(6)	0.9500	C(20)-C(21)	1.357(3)
C(7)-C(8)	1.372(3)	C(20)-H(20)	0.9500
C(7)-C(26B)	1.520(7)	C(21)-C(22)	1.426(3)
C(7)-C(26A)	1.533(4)	C(21)-C(28B)	1.510(7)
C(8)-C(12)	1.439(3)	C(21)-C(28A)	1.522(4)
C(8)-C(9)	1.493(3)	C(22)-C(23)	1.366(3)
C(9)-O(1A)	1.225(3)	C(22)-H(22)	0.9500
C(9)-C(10)	1.477(3)	C(23)-C(24)	1.430(3)
C(9)-H(9)	0.9678	C(23)-H(23)	0.9500
C(10)-C(11)	1.345(3)	C(24)-C(25)	1.359(3)
C(10)-H(10)	0.9500	C(24)-C(26A)	1.531(4)
C(11)-O(1B)	1.180(5)	C(24)-C(26B)	1.560(7)
C(11)-C(12)	1.472(3)	C(25)-H(25)	0.9500
C(11)-H(11)	0.9653	C(26A)-C(28A)	1.544(4)
C(12)-C(13)	1.373(3)	C(26A)-C(27A)	1.555(4)
C(13)-C(14)	1.413(3)	C(27A)-H(27A)	0.9800
C(13)-C(28A)	1.536(4)	C(27A)-H(27B)	0.9800
C(13)-C(28B)	1.580(7)	C(27A)-H(27C)	0.9800

C(28A)-C(29A)	1.536(4)	C(5)-C(4)-C(3)	108.59(18)
C(29A)-H(29A)	0.9800	C(2)-C(4)-C(1)	107.83(18)
C(29A)-H(29B)	0.9800	C(5)-C(4)-C(1)	109.16(17)
C(29A)-H(29C)	0.9800	C(3)-C(4)-C(1)	110.08(18)
O(1A)-H(9)	0.2576	C(6)-C(5)-C(25)	119.49(18)
C(26B)-C(28B)	1.511(10)	C(6)-C(5)-C(4)	122.60(18)
C(26B)-C(27B)	1.559(10)	C(25)-C(5)-C(4)	117.88(17)
C(27B)-H(27D)	0.9800	C(5)-C(6)-C(7)	121.95(18)
C(27B)-H(27E)	0.9800	C(5)-C(6)-H(6)	119.0
C(27B)-H(27F)	0.9800	C(7)-C(6)-H(6)	119.0
C(28B)-C(29B)	1.580(10)	C(8)-C(7)-C(6)	125.62(18)
C(29B)-H(29D)	0.9800	C(8)-C(7)-C(26B)	113.2(3)
C(29B)-H(29E)	0.9800	C(6)-C(7)-C(26B)	118.7(3)
C(29B)-H(29F)	0.9800	C(8)-C(7)-C(26A)	114.86(19)
O(1B)-H(11)	0.2155	C(6)-C(7)-C(26A)	118.38(18)
		C(7)-C(8)-C(12)	122.88(18)
C(4)-C(1)-H(1A)	109.5	C(7)-C(8)-C(9)	129.96(18)
C(4)-C(1)-H(1B)	109.5	C(12)-C(8)-C(9)	107.11(17)
H(1A)-C(1)-H(1B)	109.5	O(1A)-C(9)-C(10)	126.2(2)
C(4)-C(1)-H(1C)	109.5	O(1A)-C(9)-C(8)	128.3(2)
H(1A)-C(1)-H(1C)	109.5	C(10)-C(9)-C(8)	105.46(17)
H(1B)-C(1)-H(1C)	109.5	C(10)-C(9)-H(9)	127.3
C(4)-C(2)-H(2A)	109.5	C(8)-C(9)-H(9)	127.2
C(4)-C(2)-H(2B)	109.5	C(11)-C(10)-C(9)	110.07(18)
H(2A)-C(2)-H(2B)	109.5	C(11)-C(10)-H(10)	125.0
C(4)-C(2)-H(2C)	109.5	C(9)-C(10)-H(10)	125.0
H(2A)-C(2)-H(2C)	109.5	O(1B)-C(11)-C(10)	124.3(8)
H(2B)-C(2)-H(2C)	109.5	O(1B)-C(11)-C(12)	125.5(8)
C(4)-C(3)-H(3A)	109.5	C(10)-C(11)-C(12)	110.18(18)
C(4)-C(3)-H(3B)	109.5	C(10)-C(11)-H(11)	124.9
H(3A)-C(3)-H(3B)	109.5	C(12)-C(11)-H(11)	124.9
C(4)-C(3)-H(3C)	109.5	C(13)-C(12)-C(8)	122.80(17)
H(3A)-C(3)-H(3C)	109.5	C(13)-C(12)-C(11)	130.02(18)
H(3B)-C(3)-H(3C)	109.5	C(8)-C(12)-C(11)	107.18(17)
C(2)-C(4)-C(5)	112.29(16)	C(12)-C(13)-C(14)	125.87(18)
C(2)-C(4)-C(3)	108.89(18)	C(12)-C(13)-C(28A)	114.77(19)

C(14)-C(13)-C(28A)	118.63(19)	C(20)-C(21)-C(22)	123.99(19)
C(12)-C(13)-C(28B)	114.3(3)	C(20)-C(21)-C(28B)	118.6(3)
C(14)-C(13)-C(28B)	117.0(3)	C(22)-C(21)-C(28B)	114.5(3)
C(15)-C(14)-C(13)	122.69(18)	C(20)-C(21)-C(28A)	119.18(19)
C(15)-C(14)-H(14)	118.7	C(22)-C(21)-C(28A)	115.86(19)
C(13)-C(14)-H(14)	118.7	C(23)-C(22)-C(21)	122.35(19)
C(14)-C(15)-C(20)	118.78(18)	C(23)-C(22)-H(22)	118.8
C(14)-C(15)-C(16)	123.35(18)	C(21)-C(22)-H(22)	118.8
C(20)-C(15)-C(16)	117.82(18)	C(22)-C(23)-C(24)	121.97(18)
C(17)-C(16)-C(15)	112.56(17)	C(22)-C(23)-H(23)	119.0
C(17)-C(16)-C(18)	109.00(19)	C(24)-C(23)-H(23)	119.0
C(15)-C(16)-C(18)	108.27(16)	C(25)-C(24)-C(23)	123.97(18)
C(17)-C(16)-C(19)	107.97(17)	C(25)-C(24)-C(26A)	118.8(2)
C(15)-C(16)-C(19)	109.25(17)	C(23)-C(24)-C(26A)	116.26(19)
C(18)-C(16)-C(19)	109.77(18)	C(25)-C(24)-C(26B)	117.5(3)
C(16)-C(17)-H(17A)	109.5	C(23)-C(24)-C(26B)	115.7(3)
C(16)-C(17)-H(17B)	109.5	C(24)-C(25)-C(5)	123.09(18)
H(17A)-C(17)-H(17B)	109.5	C(24)-C(25)-H(25)	118.5
C(16)-C(17)-H(17C)	109.5	C(5)-C(25)-H(25)	118.5
H(17A)-C(17)-H(17C)	109.5	C(24)-C(26A)-C(7)	112.0(2)
H(17B)-C(17)-H(17C)	109.5	C(24)-C(26A)-C(28A)	109.2(2)
C(16)-C(18)-H(18A)	109.5	C(7)-C(26A)-C(28A)	110.3(2)
C(16)-C(18)-H(18B)	109.5	C(24)-C(26A)-C(27A)	107.8(2)
H(18A)-C(18)-H(18B)	109.5	C(7)-C(26A)-C(27A)	106.0(2)
C(16)-C(18)-H(18C)	109.5	C(28A)-C(26A)-C(27A)	111.6(3)
H(18A)-C(18)-H(18C)	109.5	C(21)-C(28A)-C(29A)	106.5(2)
H(18B)-C(18)-H(18C)	109.5	C(21)-C(28A)-C(13)	112.1(2)
C(16)-C(19)-H(19A)	109.5	C(29A)-C(28A)-C(13)	108.3(2)
C(16)-C(19)-H(19B)	109.5	C(21)-C(28A)-C(26A)	108.9(2)
H(19A)-C(19)-H(19B)	109.5	C(29A)-C(28A)-C(26A)	111.7(3)
C(16)-C(19)-H(19C)	109.5	C(13)-C(28A)-C(26A)	109.3(2)
H(19A)-C(19)-H(19C)	109.5	C(28B)-C(26B)-C(7)	111.4(5)
H(19B)-C(19)-H(19C)	109.5	C(28B)-C(26B)-C(27B)	110.7(6)
C(21)-C(20)-C(15)	123.52(19)	C(7)-C(26B)-C(27B)	107.6(5)
C(21)-C(20)-H(20)	118.2	C(28B)-C(26B)-C(24)	106.1(5)
C(15)-C(20)-H(20)	118.2	C(7)-C(26B)-C(24)	111.1(5)

C(27B)-C(26B)-C(24)	110.0(5)
C(26B)-C(27B)-H(27D)	109.5
C(26B)-C(27B)-H(27E)	109.5
H(27D)-C(27B)-H(27E)	109.5
C(26B)-C(27B)-H(27F)	109.5
H(27D)-C(27B)-H(27F)	109.5
H(27E)-C(27B)-H(27F)	109.5
C(21)-C(28B)-C(26B)	112.3(5)
C(21)-C(28B)-C(29B)	106.2(5)
C(26B)-C(28B)-C(29B)	110.2(7)
C(21)-C(28B)-C(13)	110.4(5)
C(26B)-C(28B)-C(13)	107.8(5)
C(29B)-C(28B)-C(13)	109.9(5)
C(28B)-C(29B)-H(29D)	109.5
C(28B)-C(29B)-H(29E)	109.5
H(29D)-C(29B)-H(29E)	109.5
C(28B)-C(29B)-H(29F)	109.5
H(29D)-C(29B)-H(29F)	109.5
H(29E)-C(29B)-H(29F)	109.5

Table A.7. Anisotropic displacement parameters ($Å^2 x\ 10^3$) for cyclopentadienone fused DHP **46**. The anisotropic displacement factor exponent takes the form: $-2\pi^2[\ h^2\ a^{*2}U^{11} + ...\ + 2\ h\ k\ a^*\ b^*\ U^{12}\ ]$

	U^{11}	U^{22}	U^{33}	U^{23}	U^{13}	U^{12}
C(1)	25(1)	47(1)	24(1)	4(1)	7(1)	-3(1)
C(2)	30(1)	47(1)	21(1)	6(1)	4(1)	-8(1)
C(3)	45(1)	33(1)	29(1)	11(1)	4(1)	-3(1)
C(4)	24(1)	30(1)	22(1)	5(1)	2(1)	-4(1)
C(5)	18(1)	24(1)	21(1)	3(1)	1(1)	2(1)
C(6)	24(1)	25(1)	16(1)	2(1)	-1(1)	3(1)
C(7)	18(1)	20(1)	20(1)	0(1)	1(1)	1(1)
C(8)	22(1)	25(1)	20(1)	1(1)	1(1)	2(1)
C(9)	26(1)	37(1)	20(1)	-3(1)	0(1)	-4(1)
C(10)	21(1)	29(1)	28(1)	-5(1)	-4(1)	-5(1)
C(11)	17(1)	23(1)	26(1)	1(1)	1(1)	0(1)
C(12)	16(1)	20(1)	26(1)	1(1)	3(1)	0(1)
C(13)	18(1)	25(1)	22(1)	1(1)	2(1)	-2(1)
C(14)	18(1)	20(1)	25(1)	1(1)	4(1)	-1(1)
C(15)	21(1)	23(1)	20(1)	1(1)	4(1)	4(1)
C(16)	29(1)	32(1)	20(1)	4(1)	6(1)	2(1)
C(17)	43(1)	42(1)	23(1)	4(1)	11(1)	-11(1)
C(18)	43(1)	43(1)	23(1)	14(1)	8(1)	8(1)
C(19)	30(1)	40(1)	22(1)	2(1)	7(1)	0(1)
C(20)	23(1)	32(1)	18(1)	-2(1)	-1(1)	3(1)
C(21)	20(1)	21(1)	21(1)	2(1)	0(1)	2(1)
C(22)	23(1)	34(1)	18(1)	-2(1)	-3(1)	-2(1)
C(23)	19(1)	27(1)	25(1)	0(1)	-2(1)	-3(1)
C(24)	16(1)	25(1)	22(1)	2(1)	1(1)	-1(1)
C(25)	15(1)	21(1)	27(1)	2(1)	1(1)	-2(1)
C(26A)	18(1)	21(1)	19(1)	2(1)	2(1)	1(1)
C(27A)	18(1)	21(1)	19(1)	2(1)	2(1)	1(1)
C(28A)	18(1)	21(1)	19(1)	2(1)	2(1)	1(1)
C(29A)	18(1)	21(1)	19(1)	2(1)	2(1)	1(1)
O(1A)	31(1)	63(1)	16(1)	-6(1)	2(1)	-15(1)
C(26B)	22(2)	25(2)	24(2)	1(2)	-2(2)	-4(2)

C(27B)	22(2)	25(2)	24(2)	1(2)	-2(2)	-4(2)
C(28B)	22(2)	25(2)	24(2)	1(2)	-2(2)	-4(2)
C(29B)	22(2)	25(2)	24(2)	1(2)	-2(2)	-4(2)
O(1B)	31(1)	63(1)	16(1)	-6(1)	2(1)	-15(1)

Table A.8. Hydrogen coordinates (x 10^4) and isotropic displacement parameters ($Å^2$x 10^3) for cyclopentadienone fused DHP **46**.

	x	y	z	U(eq)
H(1A)	5136	1182	878	48
H(1B)	5391	3344	1208	48
H(1C)	5403	3326	552	48
H(2A)	3742	993	321	49
H(2B)	4016	3152	4	49
H(2C)	3079	3013	293	49
H(3A)	4350	6521	514	53
H(3B)	4354	6558	1170	53
H(3C)	3436	6400	830	53
H(6)	2675	992	983	26
H(10)	5	-3444	1417	32
H(14)	857	-2427	3330	25
H(17A)	164	-2552	4139	54
H(17B)	474	-3870	4676	54
H(17C)	793	-4623	4086	54
H(18A)	2377	-4442	4389	54
H(18B)	2056	-3817	4989	54
H(18C)	2751	-2305	4686	54
H(19A)	1742	931	4807	46
H(19B)	1065	-604	5118	46
H(19C)	730	788	4599	46
H(20)	2796	753	4177	29
H(22)	3917	2975	3714	30
H(23)	4527	4169	2922	29
H(25)	4525	4211	1903	25
H(27A)	3915	-1570	2113	29
H(27B)	3098	-2609	2424	29
H(27C)	3868	-1392	2766	29
H(29A)	1441	3395	3079	29
H(29B)	1513	3265	2426	29

H(29C)	2270	4456	2785	29
H(11)	185	-3342	2415	44
H(27D)	2116	4679	2119	35
H(27E)	2168	4378	2771	35
H(27F)	1442	3080	2412	35
H(29D)	3938	-1153	2750	35
H(29E)	3201	-2516	2416	35
H(29F)	3293	-2745	3069	35
H(9)	1261	-1231	965	44

Table A.9. Atomic coordinates (x 10^4) and equivalent isotropic displacement parameters ($Å^2$x 10^3) for **152**. U(eq) is defined as one third of the trace of the orthogonalized U^{ij} tensor.

	x	y	z	U(eq)
C(1)	10845(2)	11111(2)	1298(1)	26(1)
C(2)	10404(2)	9316(2)	976(1)	25(1)
C(3)	10699(2)	9789(2)	2210(1)	28(1)
C(4)	10143(2)	10140(2)	1509(1)	16(1)
C(5)	8684(2)	10289(2)	1622(1)	13(1)
C(6)	7765(2)	9518(2)	1501(1)	13(1)
C(7)	6488(2)	9662(2)	1758(1)	12(1)
C(8)	5451(2)	8905(2)	1613(1)	13(1)
C(9)	5484(2)	8286(2)	1026(1)	14(1)
C(10)	4563(2)	7548(2)	887(1)	17(1)
C(11)	3560(2)	7401(2)	1343(1)	19(1)
C(12)	3506(2)	7987(2)	1931(1)	17(1)
C(13)	4439(2)	8738(2)	2086(1)	13(1)
C(14)	4337(2)	9351(2)	2721(1)	13(1)
C(15)	3578(2)	9121(2)	3254(1)	14(1)
C(16)	3474(2)	9764(2)	3868(1)	14(1)
C(17)	4253(2)	10589(2)	3932(1)	15(1)
C(18)	5166(2)	10869(2)	3416(1)	14(1)
C(19)	6068(2)	11612(2)	3498(1)	16(1)
C(20)	7028(2)	11803(2)	2981(1)	15(1)
C(21)	7223(2)	11117(2)	2476(1)	13(1)
C(22)	8178(2)	11196(2)	1942(1)	14(1)
C(23)	6456(2)	10142(2)	2473(1)	13(1)
C(24)	7129(2)	9383(2)	2985(1)	15(1)
C(25)	5069(2)	10349(2)	2717(1)	13(1)
C(26)	4264(2)	11073(2)	2251(1)	15(1)
C(27)	2504(2)	9444(2)	4411(1)	16(1)
C(28)	2572(2)	10127(2)	5048(1)	19(1)
C(29)	2782(2)	8342(2)	4640(1)	19(1)
C(30)	1120(2)	9511(2)	4097(1)	18(1)
C(31)	8151(2)	11703(2)	514(1)	18(1)

C(32)	6736(2)	10168(2)	207(1)	16(1)
C(33)	5850(2)	11688(2)	998(1)	21(1)
Fe(1)	7199(1)	10819(1)	990(1)	13(1)
O(1)	8691(2)	12308(1)	210(1)	26(1)
O(2)	6459(2)	9790(1)	-305(1)	23(1)
O(3)	5038(2)	12274(1)	936(1)	35(1)

Table A.10. Bond lengths [Å] and angles [°] for **152**.

C(1)-C(4)	1.529(3)	C(14)-C(25)	1.514(3)
C(1)-H(1A)	0.9800	C(15)-C(16)	1.469(3)
C(1)-H(1B)	0.9800	C(15)-H(15)	0.9500
C(1)-H(1C)	0.9800	C(16)-C(17)	1.355(3)
C(2)-C(4)	1.527(3)	C(16)-C(27)	1.528(3)
C(2)-H(2A)	0.9800	C(17)-C(18)	1.439(3)
C(2)-H(2B)	0.9800	C(17)-H(17)	0.9500
C(2)-H(2C)	0.9800	C(18)-C(19)	1.357(3)
C(3)-C(4)	1.538(3)	C(18)-C(25)	1.523(3)
C(3)-H(3A)	0.9800	C(19)-C(20)	1.449(3)
C(3)-H(3B)	0.9800	C(19)-H(19)	0.9500
C(3)-H(3C)	0.9800	C(20)-C(21)	1.353(3)
C(4)-C(5)	1.538(3)	C(20)-H(20)	0.9500
C(5)-C(6)	1.405(3)	C(21)-C(22)	1.450(3)
C(5)-C(22)	1.447(3)	C(21)-C(23)	1.506(3)
C(5)-Fe(1)	2.0641(19)	C(22)-H(22)	1.0184
C(6)-C(7)	1.431(3)	C(23)-C(25)	1.541(3)
C(6)-Fe(1)	2.0574(19)	C(23)-C(24)	1.561(3)
C(6)-H(6)	0.9500	C(24)-H(24A)	0.9800
C(7)-C(8)	1.484(3)	C(24)-H(24B)	0.9800
C(7)-C(23)	1.527(3)	C(24)-H(24C)	0.9800
C(7)-Fe(1)	2.2650(19)	C(25)-C(26)	1.544(3)
C(8)-C(9)	1.404(3)	C(26)-H(26A)	0.9800
C(8)-C(13)	1.423(3)	C(26)-H(26B)	0.9800
C(9)-C(10)	1.381(3)	C(26)-H(26C)	0.9800
C(9)-H(9)	0.9500	C(27)-C(28)	1.531(3)
C(10)-C(11)	1.391(3)	C(27)-C(29)	1.540(3)
C(10)-H(10)	0.9500	C(27)-C(30)	1.543(3)
C(11)-C(12)	1.380(3)	C(28)-H(28A)	0.9800
C(11)-H(11)	0.9500	C(28)-H(28B)	0.9800
C(12)-C(13)	1.407(3)	C(28)-H(28C)	0.9800
C(12)-H(12)	0.9500	C(29)-H(29A)	0.9800
C(13)-C(14)	1.480(3)	C(29)-H(29B)	0.9800
C(14)-C(15)	1.347(3)	C(29)-H(29C)	0.9800

C(30)-H(30A)	0.9800	C(22)-C(5)-C(4)	121.98(17)
C(30)-H(30B)	0.9800	C(6)-C(5)-Fe(1)	69.81(11)
C(30)-H(30C)	0.9800	C(22)-C(5)-Fe(1)	73.01(11)
C(31)-O(1)	1.143(3)	C(4)-C(5)-Fe(1)	132.44(13)
C(31)-Fe(1)	1.792(2)	C(5)-C(6)-C(7)	117.93(18)
C(32)-O(2)	1.144(3)	C(5)-C(6)-Fe(1)	70.32(11)
C(32)-Fe(1)	1.803(2)	C(7)-C(6)-Fe(1)	78.73(11)
C(33)-O(3)	1.143(3)	C(5)-C(6)-H(6)	121.0
C(33)-Fe(1)	1.800(2)	C(7)-C(6)-H(6)	121.0
		Fe(1)-C(6)-H(6)	121.1
C(4)-C(1)-H(1A)	109.5	C(6)-C(7)-C(8)	120.66(17)
C(4)-C(1)-H(1B)	109.5	C(6)-C(7)-C(23)	114.27(16)
H(1A)-C(1)-H(1B)	109.5	C(8)-C(7)-C(23)	114.83(16)
C(4)-C(1)-H(1C)	109.5	C(6)-C(7)-Fe(1)	62.98(10)
H(1A)-C(1)-H(1C)	109.5	C(8)-C(7)-Fe(1)	124.60(13)
H(1B)-C(1)-H(1C)	109.5	C(23)-C(7)-Fe(1)	109.64(12)
C(4)-C(2)-H(2A)	109.5	C(9)-C(8)-C(13)	117.84(18)
C(4)-C(2)-H(2B)	109.5	C(9)-C(8)-C(7)	120.89(18)
H(2A)-C(2)-H(2B)	109.5	C(13)-C(8)-C(7)	121.16(17)
C(4)-C(2)-H(2C)	109.5	C(10)-C(9)-C(8)	122.59(18)
H(2A)-C(2)-H(2C)	109.5	C(10)-C(9)-H(9)	118.7
H(2B)-C(2)-H(2C)	109.5	C(8)-C(9)-H(9)	118.7
C(4)-C(3)-H(3A)	109.5	C(9)-C(10)-C(11)	119.37(19)
C(4)-C(3)-H(3B)	109.5	C(9)-C(10)-H(10)	120.3
H(3A)-C(3)-H(3B)	109.5	C(11)-C(10)-H(10)	120.3
C(4)-C(3)-H(3C)	109.5	C(12)-C(11)-C(10)	119.65(19)
H(3A)-C(3)-H(3C)	109.5	C(12)-C(11)-H(11)	120.2
H(3B)-C(3)-H(3C)	109.5	C(10)-C(11)-H(11)	120.2
C(2)-C(4)-C(1)	108.56(18)	C(11)-C(12)-C(13)	122.00(19)
C(2)-C(4)-C(5)	112.02(17)	C(11)-C(12)-H(12)	119.0
C(1)-C(4)-C(5)	113.71(17)	C(13)-C(12)-H(12)	119.0
C(2)-C(4)-C(3)	108.73(19)	C(12)-C(13)-C(8)	118.53(18)
C(1)-C(4)-C(3)	108.58(18)	C(12)-C(13)-C(14)	120.04(18)
C(5)-C(4)-C(3)	105.06(16)	C(8)-C(13)-C(14)	121.42(17)
C(6)-C(5)-C(22)	114.73(17)	C(15)-C(14)-C(13)	124.95(18)
C(6)-C(5)-C(4)	122.86(18)	C(15)-C(14)-C(25)	119.85(18)

C(13)-C(14)-C(25)	114.97(17)	H(24B)-C(24)-H(24C)	109.5
C(14)-C(15)-C(16)	123.35(18)	C(14)-C(25)-C(18)	113.99(16)
C(14)-C(15)-H(15)	118.3	C(14)-C(25)-C(23)	108.38(16)
C(16)-C(15)-H(15)	118.3	C(18)-C(25)-C(23)	108.07(16)
C(17)-C(16)-C(15)	118.86(18)	C(14)-C(25)-C(26)	106.02(16)
C(17)-C(16)-C(27)	123.58(18)	C(18)-C(25)-C(26)	105.73(16)
C(15)-C(16)-C(27)	117.54(17)	C(23)-C(25)-C(26)	114.81(16)
C(16)-C(17)-C(18)	122.42(18)	C(25)-C(26)-H(26A)	109.5
C(16)-C(17)-H(17)	118.8	C(25)-C(26)-H(26B)	109.5
C(18)-C(17)-H(17)	118.8	H(26A)-C(26)-H(26B)	109.5
C(19)-C(18)-C(17)	123.97(19)	C(25)-C(26)-H(26C)	109.5
C(19)-C(18)-C(25)	117.42(18)	H(26A)-C(26)-H(26C)	109.5
C(17)-C(18)-C(25)	118.50(17)	H(26B)-C(26)-H(26C)	109.5
C(18)-C(19)-C(20)	121.37(18)	C(16)-C(27)-C(28)	112.19(17)
C(18)-C(19)-H(19)	119.3	C(16)-C(27)-C(29)	109.74(16)
C(20)-C(19)-H(19)	119.3	C(28)-C(27)-C(29)	108.25(17)
C(21)-C(20)-C(19)	120.23(18)	C(16)-C(27)-C(30)	108.98(16)
C(21)-C(20)-H(20)	119.9	C(28)-C(27)-C(30)	108.17(17)
C(19)-C(20)-H(20)	119.9	C(29)-C(27)-C(30)	109.47(17)
C(20)-C(21)-C(22)	125.90(18)	C(27)-C(28)-H(28A)	109.5
C(20)-C(21)-C(23)	118.94(18)	C(27)-C(28)-H(28B)	109.5
C(22)-C(21)-C(23)	115.05(17)	H(28A)-C(28)-H(28B)	109.5
C(5)-C(22)-C(21)	120.37(18)	C(27)-C(28)-H(28C)	109.5
C(5)-C(22)-H(22)	112.9	H(28A)-C(28)-H(28C)	109.5
C(21)-C(22)-H(22)	113.9	H(28B)-C(28)-H(28C)	109.5
C(21)-C(23)-C(7)	109.46(16)	C(27)-C(29)-H(29A)	109.5
C(21)-C(23)-C(25)	109.87(16)	C(27)-C(29)-H(29B)	109.5
C(7)-C(23)-C(25)	113.04(16)	H(29A)-C(29)-H(29B)	109.5
C(21)-C(23)-C(24)	108.37(16)	C(27)-C(29)-H(29C)	109.5
C(7)-C(23)-C(24)	107.36(15)	H(29A)-C(29)-H(29C)	109.5
C(25)-C(23)-C(24)	108.62(16)	H(29B)-C(29)-H(29C)	109.5
C(23)-C(24)-H(24A)	109.5	C(27)-C(30)-H(30A)	109.5
C(23)-C(24)-H(24B)	109.5	C(27)-C(30)-H(30B)	109.5
H(24A)-C(24)-H(24B)	109.5	H(30A)-C(30)-H(30B)	109.5
C(23)-C(24)-H(24C)	109.5	C(27)-C(30)-H(30C)	109.5
H(24A)-C(24)-H(24C)	109.5	H(30A)-C(30)-H(30C)	109.5

H(30B)-C(30)-H(30C)	109.5
O(1)-C(31)-Fe(1)	175.50(19)
O(2)-C(32)-Fe(1)	177.09(18)
O(3)-C(33)-Fe(1)	172.61(19)
C(31)-Fe(1)-C(33)	91.48(9)
C(31)-Fe(1)-C(32)	90.57(9)
C(33)-Fe(1)-C(32)	96.80(10)
C(31)-Fe(1)-C(6)	129.45(9)
C(33)-Fe(1)-C(6)	137.31(9)
C(32)-Fe(1)-C(6)	94.56(8)
C(31)-Fe(1)-C(5)	96.75(9)
C(33)-Fe(1)-C(5)	140.62(9)
C(32)-Fe(1)-C(5)	121.44(9)
C(6)-Fe(1)-C(5)	39.87(8)
C(31)-Fe(1)-C(7)	164.77(8)
C(33)-Fe(1)-C(7)	99.18(8)
C(32)-Fe(1)-C(7)	98.86(8)
C(6)-Fe(1)-C(7)	38.30(7)
C(5)-Fe(1)-C(7)	68.13(7)

Table A. 11. Anisotropic displacement parameters ($Å^2 x\ 10^3$) for **152**. The anisotropic displacement factor exponent takes the form: $-2\pi^2[\ h^2\ a^{*2}U^{11} + ...\ + 2\ h\ k\ a^*\ b^*\ U^{12}\ ]$

	U^{11}	U^{22}	U^{33}	U^{23}	U^{13}	U^{12}
C(1)	13(1)	24(1)	42(1)	3(1)	4(1)	-3(1)
C(2)	15(1)	28(1)	33(1)	-8(1)	8(1)	-1(1)
C(3)	14(1)	44(2)	26(1)	7(1)	-1(1)	4(1)
C(4)	12(1)	18(1)	18(1)	1(1)	1(1)	-1(1)
C(5)	12(1)	18(1)	9(1)	5(1)	0(1)	4(1)
C(6)	16(1)	12(1)	10(1)	2(1)	-1(1)	4(1)
C(7)	14(1)	10(1)	13(1)	2(1)	-1(1)	1(1)
C(8)	11(1)	11(1)	15(1)	1(1)	-2(1)	3(1)
C(9)	14(1)	14(1)	15(1)	0(1)	0(1)	0(1)
C(10)	20(1)	15(1)	17(1)	-3(1)	-1(1)	0(1)
C(11)	16(1)	16(1)	25(1)	-4(1)	-1(1)	-5(1)
C(12)	13(1)	17(1)	20(1)	-2(1)	4(1)	-2(1)
C(13)	12(1)	12(1)	15(1)	0(1)	-1(1)	2(1)
C(14)	10(1)	13(1)	17(1)	-1(1)	-2(1)	1(1)
C(15)	13(1)	11(1)	18(1)	0(1)	-2(1)	0(1)
C(16)	11(1)	16(1)	14(1)	1(1)	-1(1)	3(1)
C(17)	15(1)	15(1)	13(1)	-2(1)	0(1)	4(1)
C(18)	13(1)	13(1)	15(1)	-2(1)	0(1)	3(1)
C(19)	18(1)	15(1)	14(1)	-4(1)	0(1)	1(1)
C(20)	15(1)	12(1)	19(1)	-1(1)	-1(1)	-3(1)
C(21)	11(1)	14(1)	14(1)	0(1)	-3(1)	-1(1)
C(22)	13(1)	14(1)	16(1)	0(1)	-2(1)	-3(1)
C(23)	12(1)	13(1)	14(1)	0(1)	0(1)	0(1)
C(24)	15(1)	16(1)	14(1)	-1(1)	-1(1)	0(1)
C(25)	12(1)	13(1)	14(1)	-1(1)	1(1)	0(1)
C(26)	14(1)	15(1)	18(1)	0(1)	1(1)	2(1)
C(27)	14(1)	18(1)	15(1)	0(1)	1(1)	1(1)
C(28)	18(1)	23(1)	17(1)	-1(1)	5(1)	-1(1)
C(29)	19(1)	20(1)	19(1)	2(1)	4(1)	2(1)
C(30)	14(1)	19(1)	21(1)	2(1)	2(1)	1(1)
C(31)	18(1)	18(1)	19(1)	0(1)	-3(1)	2(1)

C(32)	13(1)	17(1)	19(1)	4(1)	2(1)	1(1)
C(33)	25(1)	22(1)	16(1)	4(1)	5(1)	2(1)
Fe(1)	12(1)	12(1)	13(1)	1(1)	0(1)	1(1)
O(1)	27(1)	23(1)	27(1)	9(1)	3(1)	-4(1)
O(2)	25(1)	28(1)	17(1)	-3(1)	-1(1)	-5(1)
O(3)	36(1)	34(1)	35(1)	14(1)	12(1)	21(1)

Table A. 12. Hydrogen coordinates (x 10^4) and isotropic displacement parameters ($Å^2$x 10^{-3}) for **152**.

	x	y	z	U(eq)
H(1A)	11780	10982	1290	39
H(1B)	10667	11652	1629	39
H(1C)	10538	11320	839	39
H(2A)	9966	9493	540	38
H(2B)	10074	8662	1140	38
H(2C)	11339	9263	906	38
H(3A)	11639	9700	2180	42
H(3B)	10300	9141	2337	42
H(3C)	10512	10302	2560	42
H(6)	7984	8918	1256	15
H(9)	6166	8379	712	17
H(10)	4614	7144	483	20
H(11)	2916	6900	1251	23
H(12)	2819	7879	2240	20
H(15)	3084	8511	3232	17
H(17)	4194	10999	4333	18
H(19)	6069	12016	3904	19
H(20)	7523	12412	2998	19
H(22)	8873	11731	2037	17
H(24A)	8044	9310	2869	22
H(24B)	6699	8720	2952	22
H(24C)	7065	9644	3455	22
H(26A)	4186	10784	1787	23
H(26B)	4697	11735	2230	23
H(26C)	3398	11158	2441	23
H(28A)	3451	10108	5248	29
H(28B)	1955	9883	5387	29
H(28C)	2353	10827	4916	29
H(29A)	2638	7881	4249	29
H(29B)	2200	8157	5011	29

H(29C)	3684	8287	4804	29
H(30A)	943	10212	3952	26
H(30B)	492	9307	4442	26
H(30C)	1046	9058	3698	26

Table A.13. Atomic coordinates (x 10^4) and equivalent isotropic displacement parameters ($Å^2$x 10^3) for **153**. U(eq) is defined as one third of the trace of the orthogonalized U^{ij} tensor.

	x	y	z	U(eq)
C(1)	4561(2)	-370(1)	2961(1)	25(1)
C(2)	3709(2)	-1356(1)	3445(1)	26(1)
C(3)	4657(2)	-639(2)	4156(1)	28(1)
C(4)	4066(1)	-600(1)	3565(1)	18(1)
C(5)	3408(1)	-48(1)	3753(1)	15(1)
C(6)	2798(1)	-210(1)	4231(1)	14(1)
C(7)	2297(1)	371(1)	4464(1)	15(1)
C(8)	1615(1)	239(1)	4938(1)	13(1)
C(9)	1240(1)	-443(1)	4977(1)	16(1)
C(10)	660(1)	-611(1)	5447(1)	17(1)
C(11)	430(1)	-88(1)	5902(1)	18(1)
C(12)	781(1)	594(1)	5873(1)	16(1)
C(13)	1371(1)	777(1)	5403(1)	13(1)
C(14)	1782(1)	1501(1)	5418(1)	13(1)
C(15)	2124(1)	1743(1)	6021(1)	14(1)
C(16)	2502(1)	2438(1)	6052(1)	15(1)
C(17)	2497(2)	2813(1)	5427(1)	17(1)
C(18)	2674(1)	2388(1)	4837(1)	16(1)
C(19)	3244(1)	2531(1)	4374(1)	14(1)
C(20)	3462(1)	1988(1)	3886(1)	14(1)
C(21)	3224(1)	1290(1)	3963(1)	16(1)
C(22)	3396(1)	691(1)	3523(1)	16(1)
C(23)	2767(1)	1078(1)	4580(1)	15(1)
C(24)	3402(1)	947(1)	5136(1)	15(1)
C(25)	2178(1)	1701(1)	4768(1)	15(1)
C(26)	1545(1)	1831(1)	4213(1)	16(1)
C(27)	2972(2)	2690(1)	6661(1)	20(1)
C(28)	3853(2)	2410(2)	6586(2)	40(1)
C(29)	2992(2)	3516(2)	6723(1)	30(1)
C(30)	2599(2)	2384(2)	7292(1)	28(1)
C(31)	2532(2)	-146(1)	2553(1)	18(1)

C(32)	1518(2)	-615(1)	3385(1)	19(1)
C(33)	1550(2)	803(1)	3067(1)	22(1)
C(34)	476(2)	2545(1)	5226(1)	22(1)
C(35)	676(2)	2333(1)	6526(1)	20(1)
C(36)	1198(2)	3507(1)	5979(1)	27(1)
Fe(1)	2250(1)	115(1)	3367(1)	14(1)
Fe(2)	1293(1)	2562(1)	5819(1)	15(1)
O(1)	2680(1)	-301(1)	2021(1)	27(1)
O(2)	1059(1)	-1083(1)	3358(1)	27(1)
O(3)	1085(1)	1172(1)	2815(1)	30(1)
O(4)	-85(1)	2540(1)	4889(1)	34(1)
O(5)	290(1)	2226(1)	6982(1)	30(1)
O(6)	1121(1)	4118(1)	6058(1)	44(1)

Table A.14. Bond lengths [Å] and angles [°] for **153**.

C(1)-C(4)	1.531(3)	C(14)-C(25)	1.517(3)
C(1)-H(1A)	0.9800	C(14)-Fe(2)	2.262(2)
C(1)-H(1B)	0.9800	C(15)-C(16)	1.422(3)
C(1)-H(1C)	0.9800	C(15)-Fe(2)	2.068(2)
C(2)-C(4)	1.529(3)	C(15)-H(15)	0.9500
C(2)-H(2A)	0.9800	C(16)-C(17)	1.448(3)
C(2)-H(2B)	0.9800	C(16)-C(27)	1.530(3)
C(2)-H(2C)	0.9800	C(16)-Fe(2)	2.039(2)
C(3)-C(4)	1.542(3)	C(17)-C(18)	1.461(3)
C(3)-H(3A)	0.9800	C(17)-Fe(2)	2.167(2)
C(3)-H(3B)	0.9800	C(17)-H(17)	0.9500
C(3)-H(3C)	0.9800	C(18)-C(19)	1.349(3)
C(4)-C(5)	1.528(3)	C(18)-C(25)	1.509(3)
C(5)-C(6)	1.422(3)	C(19)-C(20)	1.455(3)
C(5)-C(22)	1.440(3)	C(19)-H(19)	0.9500
C(5)-Fe(1)	2.065(2)	C(20)-C(21)	1.351(3)
C(6)-C(7)	1.427(3)	C(20)-H(20)	0.9500
C(6)-Fe(1)	2.059(2)	C(21)-C(22)	1.449(3)
C(6)-H(6)	0.9500	C(21)-C(23)	1.511(3)
C(7)-C(8)	1.491(3)	C(22)-Fe(1)	2.171(2)
C(7)-C(23)	1.530(3)	C(22)-H(22)	0.9500
C(7)-Fe(1)	2.282(2)	C(23)-C(25)	1.545(3)
C(8)-C(9)	1.400(3)	C(23)-C(24)	1.553(3)
C(8)-C(13)	1.426(3)	C(24)-H(24A)	0.9800
C(9)-C(10)	1.379(3)	C(24)-H(24B)	0.9800
C(9)-H(9)	0.9500	C(24)-H(24C)	0.9800
C(10)-C(11)	1.389(3)	C(25)-C(26)	1.547(3)
C(10)-H(10)	0.9500	C(26)-H(26A)	0.9800
C(11)-C(12)	1.382(3)	C(26)-H(26B)	0.9800
C(11)-H(11)	0.9500	C(26)-H(26C)	0.9800
C(12)-C(13)	1.398(3)	C(27)-C(30)	1.527(3)
C(12)-H(12)	0.9500	C(27)-C(29)	1.528(4)
C(13)-C(14)	1.493(3)	C(27)-C(28)	1.534(4)
C(14)-C(15)	1.420(3)	C(28)-H(28A)	0.9800

C(28)-H(28B)	0.9800	C(4)-C(3)-H(3C)	109.5
C(28)-H(28C)	0.9800	H(3A)-C(3)-H(3C)	109.5
C(29)-H(29A)	0.9800	H(3B)-C(3)-H(3C)	109.5
C(29)-H(29B)	0.9800	C(5)-C(4)-C(2)	112.4(2)
C(29)-H(29C)	0.9800	C(5)-C(4)-C(1)	112.7(2)
C(30)-H(30A)	0.9800	C(2)-C(4)-C(1)	108.9(2)
C(30)-H(30B)	0.9800	C(5)-C(4)-C(3)	105.85(19)
C(30)-H(30C)	0.9800	C(2)-C(4)-C(3)	108.7(2)
C(31)-O(1)	1.145(3)	C(1)-C(4)-C(3)	108.1(2)
C(31)-Fe(1)	1.786(2)	C(6)-C(5)-C(22)	114.3(2)
C(32)-O(2)	1.143(3)	C(6)-C(5)-C(4)	121.5(2)
C(32)-Fe(1)	1.798(3)	C(22)-C(5)-C(4)	123.9(2)
C(33)-O(3)	1.141(3)	C(6)-C(5)-Fe(1)	69.61(13)
C(33)-Fe(1)	1.810(3)	C(22)-C(5)-Fe(1)	74.13(13)
C(34)-O(4)	1.142(3)	C(4)-C(5)-Fe(1)	129.99(16)
C(34)-Fe(2)	1.796(3)	C(5)-C(6)-C(7)	118.0(2)
C(35)-O(5)	1.139(3)	C(5)-C(6)-Fe(1)	70.08(13)
C(35)-Fe(2)	1.805(3)	C(7)-C(6)-Fe(1)	79.49(13)
C(36)-O(6)	1.144(3)	C(5)-C(6)-H(6)	121.0
C(36)-Fe(2)	1.780(3)	C(7)-C(6)-H(6)	121.0
		Fe(1)-C(6)-H(6)	120.5
C(4)-C(1)-H(1A)	109.5	C(6)-C(7)-C(8)	121.3(2)
C(4)-C(1)-H(1B)	109.5	C(6)-C(7)-C(23)	113.78(19)
H(1A)-C(1)-H(1B)	109.5	C(8)-C(7)-C(23)	114.36(19)
C(4)-C(1)-H(1C)	109.5	C(6)-C(7)-Fe(1)	62.55(12)
H(1A)-C(1)-H(1C)	109.5	C(8)-C(7)-Fe(1)	125.03(15)
H(1B)-C(1)-H(1C)	109.5	C(23)-C(7)-Fe(1)	110.08(14)
C(4)-C(2)-H(2A)	109.5	C(9)-C(8)-C(13)	117.7(2)
C(4)-C(2)-H(2B)	109.5	C(9)-C(8)-C(7)	120.5(2)
H(2A)-C(2)-H(2B)	109.5	C(13)-C(8)-C(7)	121.5(2)
C(4)-C(2)-H(2C)	109.5	C(10)-C(9)-C(8)	122.6(2)
H(2A)-C(2)-H(2C)	109.5	C(10)-C(9)-H(9)	118.7
H(2B)-C(2)-H(2C)	109.5	C(8)-C(9)-H(9)	118.7
C(4)-C(3)-H(3A)	109.5	C(9)-C(10)-C(11)	119.5(2)
C(4)-C(3)-H(3B)	109.5	C(9)-C(10)-H(10)	120.2
H(3A)-C(3)-H(3B)	109.5	C(11)-C(10)-H(10)	120.2

C(12)-C(11)-C(10)	119.4(2)	C(18)-C(19)-C(20)	120.7(2)
C(12)-C(11)-H(11)	120.3	C(18)-C(19)-H(19)	119.6
C(10)-C(11)-H(11)	120.3	C(20)-C(19)-H(19)	119.6
C(11)-C(12)-C(13)	122.2(2)	C(21)-C(20)-C(19)	120.4(2)
C(11)-C(12)-H(12)	118.9	C(21)-C(20)-H(20)	119.8
C(13)-C(12)-H(12)	118.9	C(19)-C(20)-H(20)	119.8
C(12)-C(13)-C(8)	118.6(2)	C(20)-C(21)-C(22)	126.7(2)
C(12)-C(13)-C(14)	120.6(2)	C(20)-C(21)-C(23)	118.9(2)
C(8)-C(13)-C(14)	120.66(19)	C(22)-C(21)-C(23)	114.33(19)
C(15)-C(14)-C(13)	118.31(19)	C(5)-C(22)-C(21)	121.4(2)
C(15)-C(14)-C(25)	120.66(19)	C(5)-C(22)-Fe(1)	66.22(12)
C(13)-C(14)-C(25)	112.96(18)	C(21)-C(22)-Fe(1)	107.20(15)
C(15)-C(14)-Fe(2)	63.60(12)	C(5)-C(22)-H(22)	119.3
C(13)-C(14)-Fe(2)	128.46(15)	C(21)-C(22)-H(22)	119.3
C(25)-C(14)-Fe(2)	104.72(14)	Fe(1)-C(22)-H(22)	96.3
C(14)-C(15)-C(16)	119.4(2)	C(21)-C(23)-C(7)	109.80(18)
C(14)-C(15)-Fe(2)	78.44(13)	C(21)-C(23)-C(25)	108.65(18)
C(16)-C(15)-Fe(2)	68.64(13)	C(7)-C(23)-C(25)	111.05(18)
C(14)-C(15)-H(15)	120.3	C(21)-C(23)-C(24)	108.54(18)
C(16)-C(15)-H(15)	120.3	C(7)-C(23)-C(24)	108.31(18)
Fe(2)-C(15)-H(15)	124.0	C(25)-C(23)-C(24)	110.46(18)
C(15)-C(16)-C(17)	112.8(2)	C(23)-C(24)-H(24A)	109.5
C(15)-C(16)-C(27)	121.8(2)	C(23)-C(24)-H(24B)	109.5
C(17)-C(16)-C(27)	124.7(2)	H(24A)-C(24)-H(24B)	109.5
C(15)-C(16)-Fe(2)	70.86(13)	C(23)-C(24)-H(24C)	109.5
C(17)-C(16)-Fe(2)	74.69(14)	H(24A)-C(24)-H(24C)	109.5
C(27)-C(16)-Fe(2)	129.67(16)	H(24B)-C(24)-H(24C)	109.5
C(16)-C(17)-C(18)	117.7(2)	C(18)-C(25)-C(14)	110.52(18)
C(16)-C(17)-Fe(2)	65.18(13)	C(18)-C(25)-C(23)	108.27(18)
C(18)-C(17)-Fe(2)	111.54(16)	C(14)-C(25)-C(23)	107.44(18)
C(16)-C(17)-H(17)	121.1	C(18)-C(25)-C(26)	107.24(18)
C(18)-C(17)-H(17)	121.1	C(14)-C(25)-C(26)	112.89(18)
Fe(2)-C(17)-H(17)	92.9	C(23)-C(25)-C(26)	110.42(18)
C(19)-C(18)-C(17)	127.3(2)	C(25)-C(26)-H(26A)	109.5
C(19)-C(18)-C(25)	117.9(2)	C(25)-C(26)-H(26B)	109.5
C(17)-C(18)-C(25)	114.8(2)	H(26A)-C(26)-H(26B)	109.5

C(25)-C(26)-H(26C)	109.5	C(31)-Fe(1)-C(6)	126.97(10)
H(26A)-C(26)-H(26C)	109.5	C(32)-Fe(1)-C(6)	93.02(10)
H(26B)-C(26)-H(26C)	109.5	C(33)-Fe(1)-C(6)	139.85(10)
C(30)-C(27)-C(29)	107.9(2)	C(31)-Fe(1)-C(5)	94.49(10)
C(30)-C(27)-C(16)	111.7(2)	C(32)-Fe(1)-C(5)	119.31(10)
C(29)-C(27)-C(16)	112.4(2)	C(33)-Fe(1)-C(5)	143.65(10)
C(30)-C(27)-C(28)	109.4(2)	C(6)-Fe(1)-C(5)	40.32(9)
C(29)-C(27)-C(28)	108.9(2)	C(31)-Fe(1)-C(22)	92.59(10)
C(16)-C(27)-C(28)	106.5(2)	C(32)-Fe(1)-C(22)	158.95(10)
C(27)-C(28)-H(28A)	109.5	C(33)-Fe(1)-C(22)	104.43(10)
C(27)-C(28)-H(28B)	109.5	C(6)-Fe(1)-C(22)	69.22(9)
H(28A)-C(28)-H(28B)	109.5	C(5)-Fe(1)-C(22)	39.64(9)
C(27)-C(28)-H(28C)	109.5	C(31)-Fe(1)-C(7)	162.64(10)
H(28A)-C(28)-H(28C)	109.5	C(32)-Fe(1)-C(7)	99.03(9)
H(28B)-C(28)-H(28C)	109.5	C(33)-Fe(1)-C(7)	101.92(9)
C(27)-C(29)-H(29A)	109.5	C(6)-Fe(1)-C(7)	37.96(9)
C(27)-C(29)-H(29B)	109.5	C(5)-Fe(1)-C(7)	68.15(8)
H(29A)-C(29)-H(29B)	109.5	C(22)-Fe(1)-C(7)	74.22(8)
C(27)-C(29)-H(29C)	109.5	C(36)-Fe(2)-C(34)	94.28(12)
H(29A)-C(29)-H(29C)	109.5	C(36)-Fe(2)-C(35)	91.93(12)
H(29B)-C(29)-H(29C)	109.5	C(34)-Fe(2)-C(35)	96.76(11)
C(27)-C(30)-H(30A)	109.5	C(36)-Fe(2)-C(16)	98.72(11)
C(27)-C(30)-H(30B)	109.5	C(34)-Fe(2)-C(16)	150.54(10)
H(30A)-C(30)-H(30B)	109.5	C(35)-Fe(2)-C(16)	109.03(10)
C(27)-C(30)-H(30C)	109.5	C(36)-Fe(2)-C(15)	137.31(11)
H(30A)-C(30)-H(30C)	109.5	C(34)-Fe(2)-C(15)	127.33(10)
H(30B)-C(30)-H(30C)	109.5	C(35)-Fe(2)-C(15)	92.05(10)
O(1)-C(31)-Fe(1)	176.9(2)	C(16)-Fe(2)-C(15)	40.49(9)
O(2)-C(32)-Fe(1)	176.0(2)	C(36)-Fe(2)-C(17)	86.42(11)
O(3)-C(33)-Fe(1)	171.1(2)	C(34)-Fe(2)-C(17)	115.34(10)
O(4)-C(34)-Fe(2)	174.8(2)	C(35)-Fe(2)-C(17)	147.90(10)
O(5)-C(35)-Fe(2)	176.4(2)	C(16)-Fe(2)-C(17)	40.14(9)
O(6)-C(36)-Fe(2)	177.3(3)	C(15)-Fe(2)-C(17)	68.69(9)
C(31)-Fe(1)-C(32)	89.31(10)	C(36)-Fe(2)-C(14)	160.51(11)
C(31)-Fe(1)-C(33)	92.15(11)	C(34)-Fe(2)-C(14)	90.24(10)
C(32)-Fe(1)-C(33)	96.44(11)	C(35)-Fe(2)-C(14)	106.37(10)

C(16)-Fe(2)-C(14)	69.35(8)
C(15)-Fe(2)-C(14)	37.96(8)
C(17)-Fe(2)-C(14)	74.54(8)

Table A.15. Anisotropic displacement parameters ($Å^2 x\ 10^3$) for **153**. The anisotropic displacement factor exponent takes the form: $-2\pi^2[\ h^2\ a^{*2}U^{11} + ...\ + 2\ h\ k\ a^*\ b^*\ U^{12}\ ]$

	U^{11}	U^{22}	U^{33}	U^{23}	U^{13}	U^{12}
C(1)	25(1)	26(1)	24(1)	0(1)	9(1)	6(1)
C(2)	24(1)	18(1)	36(2)	-4(1)	2(1)	6(1)
C(3)	22(1)	38(2)	26(1)	-3(1)	-4(1)	8(1)
C(4)	17(1)	19(1)	18(1)	-2(1)	-1(1)	1(1)
C(5)	13(1)	18(1)	14(1)	-3(1)	-3(1)	-2(1)
C(6)	16(1)	13(1)	12(1)	0(1)	-4(1)	-2(1)
C(7)	18(1)	14(1)	14(1)	1(1)	-1(1)	-2(1)
C(8)	13(1)	13(1)	13(1)	2(1)	-4(1)	0(1)
C(9)	18(1)	15(1)	16(1)	-1(1)	-2(1)	0(1)
C(10)	15(1)	14(1)	21(1)	5(1)	-4(1)	-4(1)
C(11)	15(1)	21(1)	19(1)	4(1)	2(1)	-2(1)
C(12)	15(1)	18(1)	16(1)	0(1)	1(1)	1(1)
C(13)	11(1)	15(1)	12(1)	2(1)	-3(1)	1(1)
C(14)	12(1)	13(1)	15(1)	0(1)	2(1)	1(1)
C(15)	11(1)	16(1)	15(1)	1(1)	1(1)	3(1)
C(16)	13(1)	16(1)	16(1)	-3(1)	2(1)	1(1)
C(17)	20(1)	12(1)	17(1)	-2(1)	3(1)	-1(1)
C(18)	18(1)	13(1)	15(1)	-1(1)	-2(1)	-2(1)
C(19)	16(1)	11(1)	15(1)	2(1)	-2(1)	-2(1)
C(20)	13(1)	18(1)	12(1)	2(1)	0(1)	0(1)
C(21)	15(1)	17(1)	14(1)	0(1)	0(1)	0(1)
C(22)	18(1)	18(1)	12(1)	0(1)	2(1)	-3(1)
C(23)	15(1)	16(1)	14(1)	-1(1)	0(1)	-1(1)
C(24)	13(1)	17(1)	16(1)	1(1)	-2(1)	-1(1)
C(25)	16(1)	15(1)	14(1)	0(1)	1(1)	-2(1)
C(26)	15(1)	17(1)	17(1)	4(1)	-2(1)	0(1)
C(27)	20(1)	23(1)	16(1)	-4(1)	-1(1)	-2(1)
C(28)	24(2)	64(2)	32(2)	-19(2)	-9(1)	7(1)
C(29)	44(2)	27(1)	20(1)	-5(1)	-3(1)	-15(1)
C(30)	36(2)	31(1)	16(1)	-1(1)	-3(1)	-9(1)
C(31)	19(1)	13(1)	22(1)	-1(1)	-2(1)	1(1)

C(32)	19(1)	25(1)	13(1)	2(1)	-1(1)	1(1)
C(33)	28(1)	22(1)	15(1)	-1(1)	2(1)	1(1)
C(34)	23(1)	21(1)	21(1)	1(1)	2(1)	3(1)
C(35)	18(1)	21(1)	23(1)	-2(1)	-2(1)	5(1)
C(36)	26(1)	23(1)	33(1)	-4(1)	-1(1)	2(1)
Fe(1)	16(1)	13(1)	13(1)	0(1)	1(1)	1(1)
Fe(2)	17(1)	13(1)	15(1)	0(1)	0(1)	2(1)
O(1)	39(1)	23(1)	18(1)	-5(1)	3(1)	3(1)
O(2)	26(1)	28(1)	26(1)	1(1)	-5(1)	-10(1)
O(3)	36(1)	31(1)	23(1)	0(1)	-7(1)	14(1)
O(4)	22(1)	51(1)	27(1)	-4(1)	-6(1)	8(1)
O(5)	25(1)	38(1)	25(1)	-1(1)	8(1)	0(1)
O(6)	47(1)	19(1)	66(2)	-10(1)	-5(1)	8(1)

Table A.16. Hydrogen coordinates (x 10^4) and isotropic displacement parameters ($Å^2$x 10^{-3}) for **153**.

	x	y	z	U(eq)
H(1A)	4190	-303	2587	37
H(1B)	4966	-746	2856	37
H(1C)	4845	88	3053	37
H(2A)	3383	-1505	3826	39
H(2B)	4157	-1703	3376	39
H(2C)	3358	-1345	3053	39
H(3A)	4886	-156	4241	43
H(3B)	5102	-979	4058	43
H(3C)	4357	-806	4545	43
H(6)	2725	-690	4390	17
H(9)	1392	-805	4667	19
H(10)	420	-1080	5458	20
H(11)	36	-198	6231	22
H(12)	616	951	6183	20
H(15)	2101	1443	6400	17
H(17)	2382	3317	5401	20
H(19)	3506	2992	4367	17
H(20)	3774	2124	3511	17
H(22)	3504	788	3072	19
H(24A)	3836	624	4977	23
H(24B)	3128	723	5514	23
H(24C)	3644	1412	5270	23
H(26A)	1266	2295	4286	24
H(26B)	1139	1438	4215	24
H(26C)	1827	1841	3788	24
H(28A)	3849	1878	6573	60
H(28B)	4184	2574	6959	60
H(28C)	4089	2597	6177	60
H(29A)	3207	3727	6316	45
H(29B)	3346	3654	7092	45

H(29C)	2435	3698	6802	45
H(30A)	2020	2524	7319	41
H(30B)	2895	2579	7672	41
H(30C)	2644	1854	7289	41

Vita

Surname: Zhang Given Name: Rui

Place of Birth: Chongqing, P. R. China

Educational Institutions Attended:

University of Science and Technology of China (USTC) 1988 – 1993

Nanyang Technological University, Singapore (NTU) 1998 – 2001

Degrees Awarded:

M.Sc.	NTU	2001
B.Sc.	USTC	1993

Fellowships and Awards

1. Dr. Julius F. Schleicher Merit Graduate Student Award, *University of Victoria*, **2005/2006**.
2. Scholarship, *Nanyang Technological University, Singapore*, **1998-2001**.
3. Visiting Scholarship, *Lee's Foundation, Singapore*, **2000**.
4. Excellent worker, *Chenguang Research Institute of Chemical Industry (**Chenguang**), China*, **1997**.

Publications

1. Zhang, R.; Zhong, H.-J. * "Study on the preparation and catalytic activity of polymer supported sulphonium compounds as phase-transfer catalyst." *Journal of University of Science and Technology of China,* **1995**, *25(1)*, 102-107.

2. Han, J.; Zhi, Y. G.; Zhang L. F.*; Zhang R. and Yan, Y. K.* "A practical synthesis of 3-oximido-substituted-1,5-diazacycloheptane dihydrochloride." *Chemical Research in Chinese Universities*, **2001**, *17 (4)*, 415-419.

3. Fan, W.; Zhang, R.; Leong, W. K. and Yan, Y. K.* "Reactions of the complexes $[Re_2(CO)_9(\eta^1\text{-P–P})]$ (P–P=$Ph_2P(CH_2)_nPPh_2$, n=1–6) with Me_3NO: formation of close-bridged complexes $[Re_2(CO)_8(\mu\text{-P–P})]$ and phosphine oxide complexes $[Re_2(CO)_9\{P\text{–}P(O)\}]$." *Inorg. Chim. Acta.* **2004**, *357(9)*, 2441-2450.

4. Zhang, R.; Kee, C. L.; Leong, W. K. and Yan, Y. K.* "Oxalate-bridged dirhenium(I) hexacarbonyl complexes: synthesis, reactions, and crystal structures." *J. Organomet. Chem.* **2004**, *689(17)*, 2837-2844.

5. Fan, W.; Zhang, R.; Leong, W. K.; Chu, C. K. and Yan, Y. K.* "Rhenium carbonyl complexes with monodentate-coordinated diphosphines: activation of terminal phosphino groups towards amine-oxide oxidation." *J. Organomet. Chem.* **2005**, *690(16)*, 3765-3773.

6. Mitchell, R. H.*; Zhang, R.; Fan, W.; and Berg. D. J. "Measuring Antiaromaticity by an Analysis of Ring Current and Coupling Constant changes in a Cyclopentadienone-Fused Dihydropyrene." *J. Am. Chem. Soc.* **2005**, *127(46)*, 16251-16254.

7. Zhang, R.; Fan, W.; Twanley, B; Berg, D.* and Mitchell, R. H.* "The Synthesis and Structures of Dimethyldihydropyrene Iron Carbonyl Complexes." *Organometallics*, **2007**, *26(8)*, 1888-1894.

Presentations

1. Zhang, R. and Mitchell, R. H. "Syntheses, ^{1}H NMR and photochromic properties of Modified Dimethyldihydropyrenes." 90th Conference of the Canada Society for Chemistry, Winnipeg, Manitobga, Canada. ORP. 633, **May. 2007**.
2. Zhang, R. and Mitchell, R. H. "Syntheses, ^{1}H NMR and photochromic properties of Modified Dimethyldihydropyrenes." 89th Conference of the Canada Society for Chemistry, Halifax, Nova Scotia, Canada. ORP. 1082, **May. 2006**.
3. Zhang, R. and Mitchell, R. H. "Multiple photochromic Switching of Dihydropyrene." The 11th International Symposium on Novel Aromatic Compounds, St John's, Newfoundland, Canada. Poster 248, **Aug. 2005**.
4. Zhang, R. and Mitchell, R. H. "Modifying the photochromic switching of dihydropyrenes with metals and substiuents." 39th IUPAC Congress and 86th Conference of the Canada Society for Chemistry, Ottawa, Ontraio, Canada. OR. 12. Poster 093, **Aug. 2003**.